



SERGE BERTHIER

IRIDESCENCES

The Physical Colors of Insects



Springer



Iridescences

Serge Berthier

Iridescences

The Physical Colors of Insects

Serge Berthier
Institut des Nano-Sciences de Paris
UMR CNRS - Université Pierre et Marie Curie
Université Denis Diderot
4 Place Jussieu
Paris, 75252
France

Translator

Capucine Lafait
7 Rue Christian Dewet
Paris, 75012
France

Library of Congress Control Number: 2006925252

ISBN-10: 0-387-34119-6 e-ISBN-10: 0-387-34120-X
ISBN-13: 978-0-387-34119-4 e-ISBN-13: 978-0-387-34120-0

Printed on acid-free paper.

© 2007 Springer Science+Business Media, LLC

All rights reserved. This work may not be translated or copied in whole or in part without the written permission of the publisher (Springer Science+Business Media, LLC, 233 Spring Street, New York, NY 10013, USA), except for brief excerpts in connection with reviews or scholarly analysis. Use in connection with any form of information storage and retrieval, electronic adaptation, computer software, or by similar or dissimilar methodology now known or hereafter developed is forbidden.

The use in this publication of trade names, trademarks, service marks, and similar terms, even if they are not identified as such, is not to be taken as an expression of opinion as to whether or not they are subject to proprietary rights.

9 8 7 6 5 4 3 2 1

springer.com

About the Author

Serge Berthier teaches physics at the Denis Diderot-Paris 7 University and researches biologic structures, colors and biomimetism at the Institut des NanoSciences de Paris (Pierre and Marie Curie-Paris 6 University and CNRS). He teaches solid state optics in the *post-graduate* degree “Optics and Material” and the post-graduate research degree “Optics and Photonic” for the Denis Diderot University. He also teaches electromagnetism and laser physics to undergraduates at the Paris-Jussieu Institut of Technology.

Foreword

Here is a book to recommend for various reasons. First of all, let us note that the first chapter introduces the reader into a reflection on the physical explanation of an observation. The origin of butterfly colors has interested a great physics experimenter, A.A. Michelson, Nobel Prize in 1907, thought it proceeded from selective reflection over butterfly wings and defended this idea during his whole life. The book he wrote in 1927 at the age of 75 and which contains all of the conclusions of his work, ends with a chapter entitled “metallic colors of birds and insects”. At the same time, another great physicist, Lord Raleigh, claimed that observed colors were caused by light interferences. How is it possible to defend two different explanations for similar observations? Simply because the knowledge of the objects observed was inappropriate. Here is a simple case which shows how a scientific explanation can evolve with the knowledge of the object observed.

S. Berthier’s book beautifully shows that it is possible to teach physics in relation with biology, which makes the latter certainly more attracting and lively. One is here offered an optics course through a treatise on Lepidoptera and Coleopteron colors. This shows that it is possible to teach physics in a “painless” way.

Lastly, the conclusion underlines that the study of butterfly iridescence entice researchers to find ways to apply the same principles to textiles. It also highlights that Butterflies and Cincidelidae’s properties could be used to ensure the identification and protection of bank notes.

As founder of the laboratory in which S. Berthier works, I am very happy and proud to present this book. Its author has a gift for pedagogy and this book is fascinating at all levels. It should interest young people, as young as high school seniors, but also every people who likes to learn and understand nature further. This book succeeds in being concise and clear, but also in making one marvel. It is also a step forward as concerns pluridisciplinarity. I wish that it is successful, as it deserves, and I congratulate the author.

Florin Abeles
Professor Emeritus of Pierre et Marie University, Paris.

Acknowledgments

Part of this book is a new, improved, and substantially modified version of the first book, *Butterfly Colors or the Imperative Beauty*. I won't mention again all the people who contributed to the first book. They will recognize their contribution in the present work that made up *Imperative Beauty* and was the basis of *Iridescence*. I would like to thank them once again, the pupils, students, and teachers who gave a reason for being to these publications. I thank my colleague and friend Michel Perreau for his uncompromising correcting of the first book and making pertinent remarks about the present book, which were very useful to me.

Other people took over, furthering and widening the scope of the first exploratory work. A schoolboy also whose stay was too short: Antoine Baillet. Thank you, my dear Antoine! Spadework, exalting at first but also quite laborious, was performed joyfully and contentedly by Aurélie Tournie and Marius Knoch, students at the Institut Universitaire de technologie (IUT) Paris-Jussieu, and Mathieu Gueguen at IUT of Annecy. They made a great number of the most beautiful of the photonic microscopy photos presented here. I thank them for their patience and congratulate them for succeeding in conciliating scientific rigor and artistic sensitivity.

Postgraduate students focused more on applications. Passing from quality to quantity does not always prove uplifting. If their conclusions have only a small place in the present book, they still made the latter possible in terms of logistics. Thanks to Jean Druille and Loic Ledernez, students of the Optics and Materials Master at the University Denis Diderot in Paris.

We aimed at widening the scope of the study of iridescence beyond physics and butterflies in the present publication, which is beyond our qualifications. That is why we relied on the work of specialists, especially Pr. Henri Descimon, of Marseille University, on pigments. He also provided us with a certain number of photos illustrating his conclusions. I want to respectfully thank him.

I would also like to thank my friend Emanuel Fritsch of the Institut des Matériaux de Nantes for photos of opals, as well as Philippe Lalanne of the Institut d'Optique d'Orsay, my colleague of the Optics and Photonic post-graduate degree, for the calculations of electromagnetic fields diffracted by the *Morphos*.

These research works were performed at the “color and biomimetism” group of the Laboratoire d'Optique des Solides—Université Pierre et Marie Curie, Paris. I thank all the staff of the laboratory, beginning with its director, Jacques Lafait, for his unbreakable support. Some people directly contributed to this work, like Claude Sella, who suggested I should use ionic thinning on elytrons, thus allowing me to distinguish “in relief” chitin sticks. These elytrons had first undergone optical polishing in our crystallography workshop in Michelle Jacquet's expert hands, who I friendly thank. A special thanks to Eric Charron, who performed spectogoniometric measurements and established *Morphos* diffraction maps, as well as to those who patiently and kindly tried to pacify my relationship with computers and get me out of the incredible messes I get myself in: Claude Naud and Gérard Vuye.

viii Acknowledgments

Most of the scanning electron microscopy photos were taken by Stéphane Borensztein at the Laboratoire de Physique des Liquides et Électrochimie at the University Pierre and Marie Curie. Transmission electronic or photonic microscopy sections of scales and alary membranes were made at the Laboratoire de Biologie Marine at the same university. Thanks to Jean-Pierre Lechair and Ghislaine Frébourg for welcoming me and for their beautiful work.

I was about to forget my friend and official supplier of butterflies and other insects, Claude Nature. You can go to his shop 6, rue des Chantiers in the 5th in Paris to get a good dose of marvel and good spirits.

Lastly, authors are unbearable persons. Thanks to my children, Valérian and Juliette, for putting up with my unavailability and sudden changes of moods with so much kindness and humor. Annie Fontaine had her share, and in addition, she patiently and rigorously—and tactfully, authors being touchy persons—corrected proofs. Thank you for the warmth and tenderness you gave me.

Contents

1 Iridescence	1
About the Book	5
2 Why Colors	7
Variations in Colors	9
Colors: Another Classification	10
Mimicry	10
3 Lepidoptera Description and Scales of Observation	14
Outlining a Classification	14
Summary Description of Butterflies	15
Description of the Wings	20
4 Coleoptera Description and Observation Scales	40
Coleoptera	40
5 Changing Colors: Structures or Pigments?	49
A Few Basic Experiments	49
Pigments	49
A Few General Principles	52
Changing Colors	54
6 Physical Colors, Chemical Colors Basics of Solid State Optics	56
Light—Matter Interaction, Polarization, and Optical Index	56
Structural Origin of Colors; What Kind of Logic for Structures?	65
7 1-Dimensional Structures: Interferences	68
Theory Recalls	68
Type Butterflies with Convex Structures	72
Dispersion and Polarization	77
Colored Effects	77
Concave Structures: <i>Papilio and Cincidelae</i>	78
<i>Papilionidae</i> : Solid/Gas Structures	78
<i>Cicindelidae</i> : Solid/Solid Structures	82
<i>Cetonia</i> : Circular Polarization	82

8	2-Dimensional Structures: Interferences and Diffraction	86
	Theory Recalls.....	86
	Type Butterflies with 2-Dimensional Structures	88
	Structures of Wings and Scales.....	92
	Dispersion and Polarization	98
	Evolution of the Structures.....	104
	Polarization Effects	105
9	3-Dimensional Structures: Crystalline Diffraction	112
	Theory Recalls.....	112
	Polarization Effects	114
	Insects and Photonic Crystals	115
10	Amorphous Structures: Scattering	117
	Theoretical Recalls	117
	Type Butterflies with Scattering Structures.....	123
11	Pigments and Pigmentary Colors	127
	Selective Absorption and Colors of Pigments	127
12	Thermoregulation and Spectral Selectivity	135
	Imperatives	135
	Energetic Balance.....	136
13	Vision and Colorimetry	142
	Color Perception.....	142
	Sources and Illuminants.....	143
	Colorimetry Notions	144
	Butterfly Vision	146
	Conclusion	151
	Subject Index	157
	General Index	158

Iridescence

Solid state physics is traditionally classified among hard sciences, in the literal sense by students and in the figurative sense by the Academy. To introduce the study of optical properties of butterfly wings is, at best, mere wandering and at worst, provocation. Since I have started this research, I have been told so many times, though always politely, that in accordance with the current symbolism of butterflies, I was flitting around. Yet, butterflies have not always stood for inconsistency, futility and banter! This view appeared as late as in the 17th century and applies to diurnal butterflies only. Moths are not luckier though. In his introduction to devotion life (1608), Saint-François de Sales, a connoisseur, immortalizes the symbolism of moths:

“As the small butterfly perceiving the candlelight goes towards it in a peculiar manner to see if it is as soft as it is beautiful, and hurried by his fantasy, never stops unless it gets lost on its first attempt: so the young heart goes for voluptuous flames.”

The Ancients had a completely different view, which is more relevant to the purpose of this book: “The butterfly embodies immortality of the human being.” In Greek, the word “psyche” designates both the human soul and the butterfly. Metamorphosis, the mysterious and obscure passage from earth to ether, offers a simple symbolism to the first Christians who adopted it.

But let us come back to earth for a moment, and return temporarily to physics. One of the most fascinating aspects of butterfly colors, in addition to their infinite diversity, is certainly the metallic and changing aspect of some

species, mostly tropical. Coleoptera and even certain birds can actually surpass them as far as this aspect is concerned. It is iridescence, an inappropriate term in French, yet a last allusion to the Ancients and the messenger of the Olympic gods, the winged goddess Iris draped in her rainbow. From the very end of the 19th century, iridescence started to intrigue scholars: biologists of course, who gave the name of the goddess to a great number of species presenting the quality—which we tried to illustrate in this book—but also physicists. If artists would then stick to a frivolous symbolism, things were much less easy on the other side! On one side the poet:

*Naître avec le printemps, mourir avec les roses,
Sur l’aile du zéphyr nager dans un ciel pur
Balancé sur le sein des fleurs à peine écloses,
S’enivrer de parfums, de lumière et d’azur,
Secouant, jeune encore, la poudre de ses ailes,
S’envoler comme un souffle aux voûtes éternelles;
Voilà du papillon le destin enchanté!
Il ressemble au désir qui jamais ne se pose
Et sans se satisfaire, effleurant toute chose
Retourne enfin au ciel chercher la volupté.*

—Lamartine, *Nouvelles méditations poétiques*

*To be borne with the spring, and die with roses,
On zephyr wings to swim in a clear sky
Rocked in the hearts of blooming flowers,
To get drunk on fragrances, on light and azure,
Flapping the dust out of its new borne wings,
To fly like a breath to the eternal skies,
Here is the enchanted fate of the butterfly!
It is like desire which never rests,
And never contented, always fleeting
At last goes back to the sky to find delight.*

—Lamartine, *New poetic meditations*



Figure 1.1. Representation of soul holding fruit of paradise. Roman catacombs at Domitille, second or third century (after a Charbonneau-Lassay drawing: The Christ bestiary).

And on the other side, questions: Why these colors? And how such colors? Then, of course, things started to take a turn for the worse. The cacophony of the “homo technicus” is opposed to Lamartine’s almost immortal verses.

Here is what professor R.W. Wood said in 1919 concerning the structural origin of certain colors, clearly separated from pigmentary colors:

“Not only are the existing theories inadequate to explain the phenomena but these (colors) cannot be explained by any of the common laws of optics with which we are familiar.” (Phil. Mag., London, 38 (1919) 98)

And we must admit that the controversy that opposed two physicists who were among the greatest of the time could puzzle people and make them cautious. Let us start with Michelson himself, the first American to be



Figure 1.2. The butterfly cherub by William Bouguereau: “It looks like desire . . .”

awarded the Nobel Prize in science (1907). President of the American Association for the Advancement of Science and soon president of the National Academy of Sciences, his position made him somehow haughty:

“It is somewhat surprising to find that the contrary view [he was a passionate advocate of the theory of selective reflection, which will be mentioned later on] is still held by eminent naturalists and it is hoped that further evidences here presented may serve to emphasize the distinction between metallic or surface colors and the

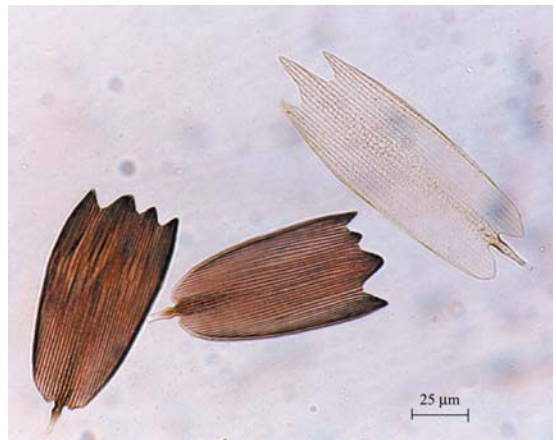


Figure 1.3. Scales of the dorsal side of *Morpho godarti*. Picture obtained by transmission photon microscopy. Each scale is about 200 μm long by 50 μm wide. One can distinguish the main longitudinal striae network and, in places, the transversal counter-striae network.

remaining classes of colors: interferences, diffraction . . ." (Phil. Mag. 21 (1911) 554)

From the other side of the Atlantic Ocean, another famous name, Lord Raleigh (4th baron), president of the Royal Institution and professor at the Imperial College of London, and advocate of the interferential approach, replied:

"It is singular that the explanation of some of the most striking and beautiful of optical phenomena should be still matters of controversy!" (Phil. Mag. 37 (1919) 98)

In order to understand how great physicists can have quarreled over such a subject, let us remember that at the turn of the 20th century, the only means of observation available was traditional photonic microscopy, which was indeed unable to resolve structures capable of creating such colors, whatever they were. The image it could give of a scale resembled the one depicted above, and originated many a mistake. One can clearly distinguish longitudinal striae—and even a square pattern sometimes—which immediately reminds one of a grating. Hence the hypotheses of diffraction that were made at a certain time. Two types of experimental approaches were then considered and two factions emerged opposing the different protagonists of the controversy.

One faction was headed by Michelson and included those who think that colors result from absorption and selective reflection of a metallic type. In almost all of their papers, they refer to thin films of aniline or cyanine. The first consequence of which is that it is not necessary to carry a minute observation of scales, since the atomic or molecular origin of the

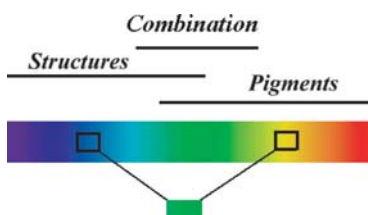


Figure 1.4. Structures and pigments share the visible spectrum for the production of colors among butterflies. Green, in the middle of the spectrum, often results from combined effects. This gives the process a large flexibility and allows a cheap adaptability.

colors rules out any kind of visualization. The problem can only be addressed through optical measurements of the whole wing as it enables us to track down the nature and structure of its components. This faction is mainly composed of physicists, like B. Walter, and Biedermann, a biologist who will later side with Raleigh. Michelson based his theory on measurements of polarization of light reflected by the wing under various angles of incidence (ellipsometric measurements, as one would call them nowadays) very similar to those obtained on thin films of aniline, or magenta. This was a forceful argument, which has yet to be turned back.

In the other faction were the defenders of structural origin. In this faction, Lord Raleigh and numerous biologists attempted to make out this structure. It is to them that we owe extremely precise microscopic observations and outstanding drawings of the scales of a great number of butterflies and of sections that they did thanks to rather rudimentary microtomes. The weightier argument in favor of the "thin film" hypothesis as defended by Lord Raleigh—which we will fully illustrate in this book—is the alteration or even the total disappearance of colors when scales are immersed in a liquid with an adequate optical index. This implies that the structure responsible for colors remains "open," enabling the liquid to penetrate it. This was not easily conceivable, but it excluded the hypothesis of selective reflection—which, on the contrary, would imply even brighter colors in this case. It is quite hard to understand how physicists like Michelson and Walter could have neglected this question. Another physical source of colors, among which sky—studied by Lord Raleigh the father—is a familiar example is the selective scattering by small particles in numerous living beings—(feathers of certain birds, muzzle of mandrills, human iris, and so on). Tyndall observed this as early as the late 19th century (1873), and so did Madoul in 1903. When these particles are small enough, they only scatter the shortest wavelengths—purple and blue—the longest being transmitted and eventually absorbed by deep layers. This is the case of many *Lycaenidae*, one of the rare

examples of blue butterflies living under our tempered climate. When larger, the particles scatter longer wavelengths and we obtain the white of the *Pieridae*.

Those physical phenomena generally cause “cold” colors, or high energy colors, ranging from near ultra-violet to blue-green, while pigments usually create “hot” colors, from red to yellow. Indeed, blue pigments are rare in the animal world: there is a carotenoid in the shells of some crustaceans, like lobster, while haemocyanin is quite widespread among mollusks, crustaceans and arachnids. As we will see in the chapter on pigments, the scarcity of blue pigments in the animal world can easily be understood. Basic organic molecules that compose blue pigments naturally absorb in the ultra-violet, the violet, and the blue, making them appear as complementary colors: red, orange, and yellow. However, there are no clear reasons why structural colors remain confined to violet and blue. We are forced to notice that in this case, exceptions still exist, but they are very few. Nevertheless, this splitting of the visible spectrum, in addition to the fact that it offers great saving of means, enables—as we will see—the creation of composed colors, of mixed origin, one of the compounds of which (physical) is iridescent and the other –(pigmentary) is not. This results in remarkable and subtle colored variations.

Even if it is long, difficult, and incomplete, the study of pigments has apparently been an easier task for the scientist—and not for the butterfly. The chemical analysis requirements are decreasing but still involve a substantial quantity of material. The total of the scales of a big *Pieridae* does not weigh more than one to two milligrams, from which the pigment only represents a small percentage. So, not surprisingly, it required some 215,000 butterflies in 1925 to extract . . . 39 grams of pigment.

We have just briefly exposed the different means used by butterflies to adorn themselves with such wonderful colors, and conversely, to make themselves invisible to our eyes. So butterflies actually use all the processes of color creation that are available to living beings. They are barred from some other sources, essentially colors created by the crystalline field

(the majority of semi-precious stones) or inter or intra-band transitions of crystalline material (for example, metals and semiconductors). If effects like camouflage are obviously useful, we can wonder why a butterfly develops very loud motifs or colors. Butterflies belong to the class of insects, which entails two important consequences. First, because of their position in the food chain, they undergo great selective pressure. Second, thanks to their short life span and high reproductive rate, they can rapidly evolve. Colors are, of course, only a small element of the gear that butterflies develop throughout their fight for life. One still remains fascinated by the ingenuity that they show in this domain, and even more in the extraordinary saving of means to develop their various tricks. Indeed, if through our scientific approach, we distinguished the main coloration processes, no butterfly actually uses one to the exclusion of another! The effects are almost always combined in order to obtain, with only a few basic elements, the infinite palette of colors that one can observe. Why develop a green pigment when it is possible to obtain the color by mixing an interferential blue or a blue of scattering with a pigmentary yellow, a very common melanin? In the same way, *Morphos*, the undisputed champions of interferential colors, distinguish themselves by combining pigments that form a background more or less opaque and accentuating or, on the contrary, diminishing the their vividness, sometimes even annihilating it by curving its wings, in order to obtain the dull blue of a mere *Argus*?

Butterflies are often considered to be the standard bearers of insects, decried creatures that sometimes provoke brutal reactions among us. Butterflies, at least diurnal species, are exempted because of their evanescent beauty. The color and the texture of their wings, which remind us of the most precious fabric, play an important role in our infatuation. It is actually to answer the questions of a renowned textile manufacturer that this research project was launched at the Laboratoire d'Optique des Solides of the Université Pierre and Marie Curie in Paris. How can one manufacture, without using any pigment,

a colored fiber to create fabric and garments with the same iridescence as butterflies? We had just entered a fascinating and extraordinarily complex world. Yet, the richness of the explanations was as fascinating and other potential applications were found, which were even more astonishing. I will mention these “biomimetic” applications of butterflies in the correspondent chapters, which will lead us quite far from the little flitting butterfly, so dear to Lamartine.

About the Book

I tried to write this book so that it could be read at different levels or at various speeds to enable everyone to get something out of it. This book is for numerous audiences, including the following: students who often tackle in a disorganized manner the various subjects gathered here; physicists or engineers striving for original structures and new applications; and biologists to whom, as I am not a biologist, I have no pretense of teaching anything but to whom I would like to remind or to put together some notions of physics that may be somehow distant. This book is also for the inquiring mind or the artist who would like to go a little beyond fascination. This book falls into three parts that are not necessarily related. The main theme—color—is extremely rich and complex as it relates to a variety of fields.

When one has seen a butterfly eaten by a bird and another butterfly remain perfectly invisible to the brushing wings of the same bird, the reason for being of those colors, so beautiful and loud at the same time, cannot but appeal to us. That is why I decided to start this book by trying to answer this question. Even before describing the orders that concern us here—Lepidoptera and Coleoptera—I want to address this question because the question goes far beyond the classification of insects. In this part, I evoke color as part of the defensive gear of insects and generally present the various types of mimicry principles. The next two chapters, structured along the same line, mention a certain number of elements, which we all know more or less about: the life cy-

cles, wings, and structures of butterflies and Coleoptera. If, once hatched, the imago keeps its colors and motifs forever, the latter undergoes changes at some crucial stages of the insect life. These critical stages will be described in those chapters. I focused on the scales and cuticles of the insects where colors primarily dwell. In this part, I presented—quite synthetically given their diversity and with a great number of illustrations—the arrangements, shapes, and fine structures of the scales. The colors of insects are changing in many ways. They are iridescent of course, in that they change according to the point of view or lighting: that is the subject of the present book. But they can also change under natural or artificial constraints. Even if this is never the case with butterflies and hardly ever the case for Coleoptera, I found it important to shortly mention the structures that enable this changing in colors. The study of material known as X-chromes, which can change colors under a constraint X, represents a very active field for civil and military research. I also present several structural principles and some simple experiments to determine the origin of colors in insects.



Figure 1.5. Iris, gods messenger. Spreading her scarf, she makes appear the rainbows (detail, Louvre Museum). Inset: *Aparaturia iris*, the changing Great Mars. One of the rare iridescent blue butterflies in our countries.

Whatever its origin, color results from an interaction between light and matter. This interaction, addressed in Chapter 6, is the part that is the most distant from the view of the “little butterfly.” In addition to an inevitably superficial presentation of notions of solid state optics and index of material, I draw a panorama of the effects of polarization of light and of their treatments. If insects are vividly colored animals, they also behave as polarizers. Polarization is a chromatic character that we are not sensitive to and can originate interesting discoveries and applications. This chapter is certainly the most complex of the book and if the reader avoids it at his first reading, he will still have a good understanding of the book. Such a reader will be able to come back to it afterwards if certain exposed phenomena stimulates his curiosity enough that the equations don't scare him anymore.

The gratification for such an effort can be found in the third main part, which describes the various types of colors produced by the insect, phenomenon by phenomenon. Each of them is illustrated at all different scales by one or several type-species that uses it primarily. For some of the species and for the requirements of certain specific studies, the descrip-

tion and modeling might sometimes seem too detailed. If the results only concern specialists, it will still provide the inquiring mind with an idea of the secrets of nature and the extent of knowledge available, partly unexplored.

Still in this part on electromagnetic properties of insects, a chapter is dedicated to the radiation qualities of wings. Here, we reach the limits of the study since radiations are not comprised in the colored spectrum but in the infrared. Color is nevertheless related to this problem as it directly affects the absorption of solar energy by dark butterflies, or its reflection towards the body by light-colored butterflies.

Lastly, as a counterpart of the first chapter on the reason of colors and after this long development on their physical and chemical origins, the book ends with a chapter dealing with colorimetry: how to name a color, measure it, and how humans and butterflies perceive it.

This book will have achieved its purpose if it can stimulate the reader's desire to understand the reason of being of those colors and how they are produced. The reason why is a fascinating subject. As far as the how is concerned, one should just imagine that an equation can be beautiful too.

Why Colors

Very few species in the animal world have such diversified colored motifs—as much in the pattern as in the colors themselves—as butterflies. These remarkable variations are the mere counterpart of the infinite diversity of biotypes. Biotypes in which adult butterflies must within a short period of time reproduce, feed, and eat without being eaten. This equates to three imperatives: to move, to recognize, and to escape predators.

To Move

Imagos feed mostly on nectar, a mix of water and simple sugars that specific flowers produce, which butterflies must recognize and approach. They must fly to feed but also to seek partners and reproduce.

To Recognize

Let us imagine a “triangle of senses,” the three angles that represent of the main sensorial stimuli: olfactory, visual, and auditory. On this triangle, butterflies would, contrary to the majority of their predators, be situated on the chemical/ visual base. Butterflies are known to be quite sensitive to odors and pheromones. But the chemical messages conceal numerous disadvantages: Their dynamic and variability are limited and they depend on uncertain exterior conditions such as wind. Optical recognition is therefore vital and very well developed.

To Escape Predators

Lepidoptera have no system of active defense but their predators are many and fearsome: They are mostly birds, reptiles (chameleons, lizards, and the like), batrachians, spiders, and other insects (for example, mantids) against

which the best trick is total immobility, which drives us back to the first imperative.

In order to comply with the three imperatives that can be contradictory, butterflies have developed an amazing palette of processes, among which color, or more generally optics, play an essential and sometimes primary part. As we will see later on, pigments spring from preexisting metabolic compounds. They are often toxic and stocked—we are tempted to say “for lack of anything better”—in wings, which are dry organs where toxic compounds cannot cause any harm.

Coloration, and thus the pigmentary function, is a secondary consequence of the properties of those compounds. Yet, it still plays an important part in the vital processes listed above. All of them are closely linked, even when we try to study them separately.

Butterflies have to fly in order to feed and to reproduce. To reproduce they must make themselves recognizable, hence make themselves visible. These two vital activities make them easy targets for predators. What role can coloration play in the strategies designed to conciliate the two contradictory activities? This role obviously depends on the ecologic context of butterflies and predators, which must trap the butterfly next to one of the three angles.

To Display

A great number of butterflies are not palatable, either because of their repelling taste or because they represent a danger for predators (toxicity). Thus, it is in the interest of these species to show it and deliver a clear message to predators. That is why warning colors can be loud and intense.

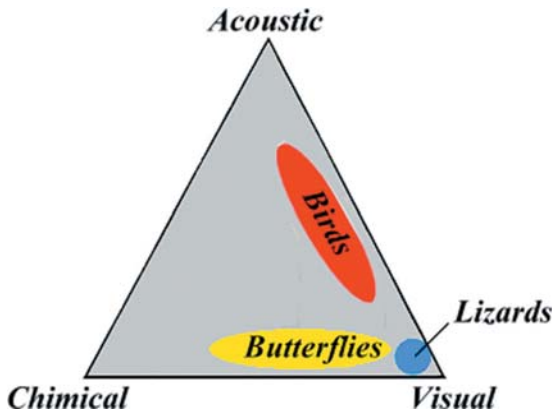


Figure 2.1. Relative part of sensorial channels among butterflies, birds, lizards. Butterflies remain mainly close to the visual point of the chemical/visual baseline and relatively close to the lizard domain. Under the strict point of view of safety, their interest will be to go further and develop chemical systems for communication and recognition. Many of them do it, but none can avoid optical signals. What is lost concerning safety is compensated by a much more efficient sexual recognition or a better management of thermal flux. Tactile channels have been neglected here.

They can play a part in sexual recognition too. Other perfectly edible butterflies may also try to enjoy the protection provided by such colors. This process of real or faked warning through colors represents a defense strategy, mimicry, that is developed by butterflies in particular.

To Hide

Butterflies perfected the art of visual camouflage, which is, by the way, widespread in the animal world. Visual camouflage is particularly used by animals at rest. Only a specific part of the animal is affected: one face, generally the ventral side, or one pair of wings (the anterior ones that overlap the posterior ones at rest). In this way, visual camouflage is compatible with the effects of mimicry as mentioned earlier.

To Pick Up

Diurnal butterflies are heterotherm insects, which means that they get a relatively important part of their energy from the environment. But, they are quite poor navigators. The results

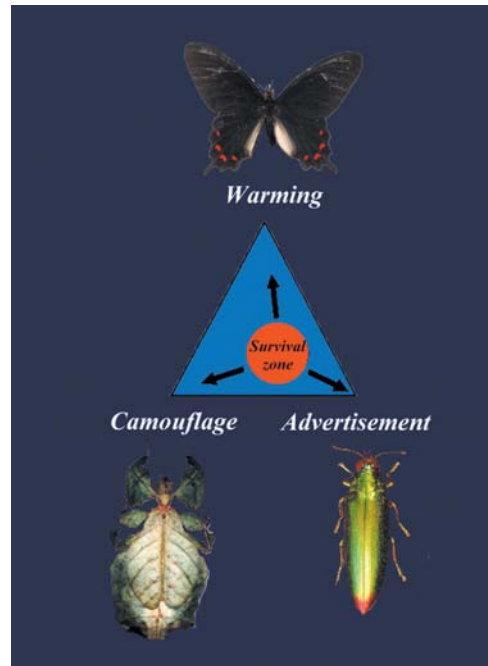


Figure 2.2. In a given place, a butterfly must be able both to hide for escaping from its predators and to display its specific characteristics, sexual or not, in order to: (i) ensure its reproduction; (ii) push back predators; and (iii) collect the exact amount of solar radiation indispensable to give it the energy for taking off. These requirements are often contradictory and the insect has to discover an optimal balance between these three constraints, the relative amount of which can change. Other complementary strategies using nonvisual techniques can be used.

are limited and the generated efforts, especially to get off, are substantial.

In order to get off, the average temperature at their thorax, where the extensors and abductors of the wings are situated, must be over 36°C. The energy required to reach such a temperature is often superior to the ecologic context. It can be produced partly through an endogeneous way by muscles and through an exogeneous one by picking up solar energy directly onto the body, onto the wings if they absorb all or part of the solar spectrum, or onto the body after reflection on wings (for white wings). Besides, butterflies are incapable of flying, or even surviving, if their interior temperature goes over 40°C. The surplus of energy generated during the flight must be eliminated

through convection or radiation. The energetic balance essentially depends on the coloration of the wings and their radiative properties.

The markings of a butterfly proceed from a subtle balance between those three main “attractors:” perfect camouflage (to escape from predators), maximum coloration (for recognition or warning), and the absence of color, black (to pick up as much solar energy as possible).

Variations in Colors

Variations in colors within a species are widespread. They often proceed from specific ecologic conditions, but may also be accidental. In most of these latter cases, it is related to melanism phenomena that can result in the insect turning totally black.



Figure 2.3. Industrial melanism in *Biston betularia*. Melanic forms were rare in the past because they were more often exposed to predators by their optical contrast on the light bark of birch trees. Nowadays, they are preponderant, due to the darkening of birch trees under the effects of pollution. Recent efforts against pollution make the melanic light forms reappear, showing thus the dynamism and efficiency of adaptation.

The phenomenon is beautifully illustrated by the case of a Phalaenae: *Biston betularia*. Most of adults as well as heterocercs are active only at dusk and settle on various supports—branches, trunks, and so on—with their wings wide open. In the early 19th century, while the species was only known to be light-colored, some totally dark specimens started to appear around Manchester. The phenomenon spread rapidly and in 1950, the dark species was in the majority in Eastern England as well as in the Glasgow and Newcastle areas; that is, the highly industrialized regions. That is why the phenomenon was called *industrial melanism*. We now know that this evolution was not caused by the ingestion of soot by caterpillars, as people thought at the time. It is indeed a consequence of natural selection, which favored the form that was best adapted to the environment. Before the industrial revolution, trees were covered with lichens on which the beige veins and white color of the light form of *Biston betularia* were perfectly invisible, whereas dark mutants were rapidly eliminated. When trunks started to turn black as a consequence of the soot released by manufactures and the disappearance of lichens, modalities reversed and the light form, which had thus become vulnerable, disappeared completely.



Figure 2.4. Example of procrystic colors. *Biston strataria* (5 cm). Here, as often, shades and chromatic motifs of the background are imitated.

This widely accepted interpretation corresponds to the decline of the dark form noticed over the last decades after anti-pollution measures were launched.

Colors: Another Classification

As regards selection, we can try to classify colors not according to their physical characteristics or physico-chemical origins, but to their role in the strategy for survival and development of a species. We can, as the English naturalist Alfred Russel Wallace did in the late 19th century, distinguish colors between those designed to warn and those for camouflage. The latter allow the insect to become invisible in its environment for defensive or offensive purposes. As we have seen, there is a price to pay, which is a decrease in mobility. On the contrary, warning colors, which are very loud a priori, are related to a real danger or a faked one from the viewpoint of predators. A few years later, Sir Edward B. Pulton offered another classification by distinguishing colors that deceive from those that don't. The latter warn against a real danger: toxicity, venom, spine, repelling taste... These colorations are called sematic colorations.

Deceiving colors, called *apetetic*, include all hiding or cryptic colors and warning colors faking a danger or pseudo-sematic. Each branch consists of other ramification depending on whether the insect carrying colors is a prey (procryptic) or a predator (anti-cryptic), whether it tries to repel (pseudoaposematic), or, on the contrary, to attract (pseudepise-matic). In this latter group, which is actually quite rare within the butterfly population, the widespread cases of "auto-mimicry," in which the motifs of a nonvital body part (like posterior wings) fake those of the vital part (the head or anterior wings): Those are called parase-matic colors.

While sematic colored butterflies, which have nothing to hide, have a wide range of colors and patterns, apathetic must resort to isochromy with their model or with a widespread element of their environment (homotypy) and to isomorphy, and even

isokinemy, that is the same mobility as their models. The objects that are the more often imitated are leaves and bark but also include lichens and bird excrements. We won't address the genesis of mimicry and camouflage; several theories were offered that involve natural selection in the origin, dynamic, and stability of the phenomenon. These questions are still unanswered today and we will only briefly set out the modalities of the main types of mimicry.

Mimicry

As is often the case, the fathers of important discoveries tend to remain unknown from the public, whereas their work comes at the right time to support great theories with a more universal impact. Henry Walter Bates, Fritz Müller, and on another hand, Charles Darwin, illustrate this.

H.W. Bates, an English naturalist and explorer, was born in Leicester in 1825 and died in London in 1892. He explored the Amazon valley for 11 years and came back with



Figure 2.5. W. Bates, lithography by W. Purkiss (1880). C. Hulton Picture Library.



Figure 2.6. F. Müller in Brazil in 1890.

14,712 species of insects, among which 8,000 were unknown and for this, the king awarded him £800! Even more than Bates, Fritz Müller is the scientist of the 19th century in all its glory. Born in Windischlölzlausen (Thuringe) in 1822, he had an extraordinary gift for languages and spoke Italian, Russian, Syrian, Arabic, English, and later, of course, Portuguese. He studied pharmacy, mathematics, zoology, and medicine at the same time. He was forced to flee his country because of commitments during the 1848 Revolution. His anticlerical and libertarian ideas were unacceptable in the then-intolerant Prussia. He exiled himself to Brazil where he settled down as a farmer and then as a mathematics teacher. Attached to the National Museum of Rio with the official title “traveling naturalist,” his great talent and his genius as a naturalist, his modern and precursory mind give him a place among the greatest. Darwin, who knew his subject and whom Müller’s observations provided with weighty arguments, predicted honor and recognition for his work . . . posthumously! Müller died in Blumenau, Brazil, in 1897 after a tormented and difficult life—he was in a constant battle

with the Church, he was kidnapped, and his family died—yet his life proved exceptionally rich.

Basic Principles of Mimicry

Mimicry is an intricate biologic phenomenon that aims at ensuring protection of the species against predators (repelling mimicry), which concerns Lepidoptera. Or it can also aim at providing the predator with an advantage over his preys (attracting mimicry). We will focus on the optical strategies involving colors in the first type only. Chemical or auditory actions can obtain similar effects. Mimicry involves at least three protagonists, among which the predator is either duped by the deceiving appearance of an eatable prey (Batesian mimicry) and the predator is thus described as an effective dupe,



Figure 2.7. Some classical examples of batesian mimicry . . . *Danaus chrysippus* (6 cm) non-edible (top left) and one of its numerous mimickers, *Hypolimnas missippus* (top right), *Tirumala limniace* (9 cm) (middle) and its mimicker, *Chilasa clytia* (10 cm) (bottom).

or it is warned against a real danger by means of a minimalist signal, like a color, common to different uneatable species (Müllerian mimicry). Here there is no deceiving in the proper sense, so the predator is described as an indifferent dupe. The two strategies require a geographical concordance of the various protagonists.

Batesian Mimicry

This is certainly one of the most remarkable protective strategies of Lepidoptera. Here, the mimic, an eatable butterfly, imitates the markings and flying manners of an uneatable insect for whatever reason: toxicity, repelling taste, or venom. This kind of mimicry can be both intra or inter order/group. Swamps—Hymenoptera—are often imitated by Lepidoptera. If it guarantees a relative immunity to the mimic, Batesian mimicry puts the model in danger and its efficiency depends on the ratio between the mimic population and the imitated one. Predators learn their lessons through successive successes (eatable insects) and failures (uneatable insects); if the proportion of the former outnumbered that of the latter, it

would annihilate the warning effect of sematic colorations of the latter. In this way, Batesian mimicry is similar to some parasitism from which a model can escape by changing its markings. This can lead to a parallel evolution of the mimic and the model, the latter becoming more and more different from the former, which, put in danger, always tries to resemble it.

Müllerian Mimicry

Species that are truly protected because they are uneatable or dangerous and present sematic colors are not *ipso facto* safe from predators. The danger here occurs during the learning stage of the predator, which associates an annoyance to a warning signal only after experimenting it many times. This is often deadly for a butterfly, yet the risk gets smaller according to the clarity and non-ambiguity of the message. The latter must be strong. As sematic colorations are loud, they should not be too many. Thus, protected species should always present the same markings to predators. Indeed, they reduce and share the chances of



Figure 2.8. Müllerian mimicry in *Heliconius* genus.



Figure 2.9. Examples of Müllerian mimicry. *Itulia hilione* (9 cm) (top), *Thyridia confusa* (9 cm) (bottom).

being eaten during the learning stage and accelerate it. This kind of association, known as Müllerian, pushes the limits of mimicry because it implies that everybody imitates everybody and so there are no definite models or mimics in the end. Furthermore, if any eatable intruder enters the association, as a result of hazard or Batesian mimicry, it reduces the impact of the message.

To end this chapter about the protective role of colors, let us mention Guillauminian associations[correct word?]*—*“les associations d’introuvables,” to take up Michel Boulard’s beautiful expression—which include sematic and procryptic colorations. The predator, attracted by the strong visual signal of its prey when it is flying, but frustrated when it becomes invisible at rest, eventually associates sematic colors not to an uneatable prey anymore, but to the absence of prey! The reverse strategy also exists with “blitz”



Figure 2.10. Guillauminian association, or “flash” color: *Catacolia ilia* (photo A.B. Klots).

colorations. Here, the spotted insect suddenly reveals the vivid colors of its posterior wings by getting off, deceiving the predator for a moment.

Throughout our summary description of those theories, we considered the pressure of predators as a sole and unique constraint. The logical consequence of this would be a great standardization of colors in a given geographical area, through Batesian, Müllerian, or any other mimicry, or even due to hazard. But the experience refutes this and one can observe in the same place butterflies from the same species, threatened by the same predators and all uneatable, presenting different markings. This also contradicts the Müllerian theory! One can also encounter cases of Batesian mimicry concerning one gender only or a species presenting polymorph mimicry, which is imitating various models. This is due to the other constraints that are as vital to the species or the insect as recognition of genders and thermal regulation. If one of them is slackened—because the species lives at the top or at the base of the canopy and therefore receives a different solar radiance, for instance—the whole balance is affected, either upset or displaced to another point, which is less of a constraint for the two others. New markings will then emerge.

3

Lepidoptera Description and Scales of Observation

Our present purpose is not to write a book on butterflies, but rather a book on their colors. It is still useful to begin by situating butterflies into classifications and review some general facts concerning their anatomy, development, and the structure of their wings.

Among insects, a group that already outweighs the animal world by its remarkable diversity, five orders outclass all of the others by the number of species composing them. Those are Coleoptera (300,000 species), Hymenoptera (250,000 species), Diptera and Hemiptera (150,000 to 200,000 species), and Lepidoptera with about 170,000 species. It is mere utopia to try to establish a comprehensive classification of such a huge number of species, all the more since only 5 to 20 percent—depending on orders—of the total have officially been described and studied.

The order of Lepidoptera comprises diurnal and nocturnal butterflies. The word derives from the Greek term *Lepidos* (scales) and *Pteris* (wings), and therefore means scaled wings or wings covered with scales. This is one of their main characteristics, and yet some of them only partially present scales while others are totally deprived of them.

The large majority of nocturnal butterflies and the total of the diurnal belong to the infraorder of Heteroneura, which means that they present different veins on their anterior and posterior wings (Figure 3.9). Homoneura consists of some primitive butterflies presenting the same veins on both wings. We will hardly mention them, as they have little or no coloring.

We can define other big groups that are related to the previous ones and usually commonly known as micro and macro Lepidoptera. The latter group is composed of the most developed diurnal and nocturnal butterflies, while former group includes the less developed and usually small nocturnal butterflies.

Outlining a Classification

Distinctions are sometimes more marked in English. Indeed, the word *butterflies* comprises all of Rhopalocera, the real diurnal butterflies, and *moths*, the Heterocera, mostly nocturnal butterflies with feathery or threadlike antennas. These terms designate some useful categories, the limits of which still remain blurry. However, they are quite acceptable for us.

Heteroneura are subdivided into a large number of “superfamilies,” which will not be described here. Indeed, the majority of butterflies presented in our study come from one superfamily only, the *Papilionoidea*, consisting of 14 families, with one well-known exception, the *Uranoidea*, illustrated by the famous *Uraniidae*. It is impossible to describe in a few lines insects as diverse as butterflies, which are adapted to almost all environments, and the size of which varies from 2 mm for the minuscule *Nepticulides* to more than 20 cm for the big *saturnides*. We will only briefly mention their development and characteristics. Butterflies appeared in the early Jurassic, 200 million years ago, and despite their apparent fragility,

they survived all the cataclysms that proved fatal to many a species.

Summary Description of Butterflies

The development of butterflies from egg to adulthood consists of four very different stages:

- The egg or embryonal stage.
- The caterpillar or larval stage, which is essentially a development stage.
- The chrysalis or pupa, which is a phase of reconstruction and differentiation of tissues.
- And at last, the imago (adult) butterfly, which is sexually mature and capable of flying.

We will describe those stages when they can influence the motifs and colorations of the mature insect, which concerns the larval and nymphal stages.

Caterpillar

Like the adult insect, the caterpillar consists of the head (which has five combined segments),

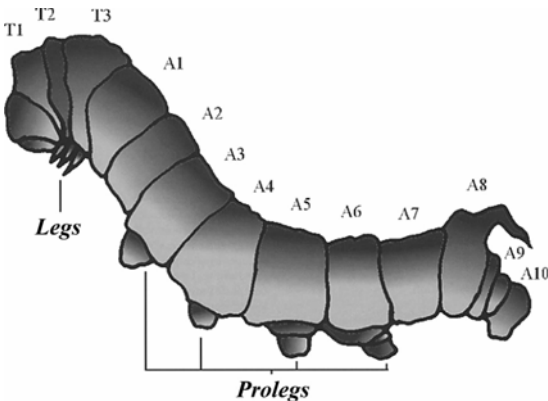


Figure 3.1. Schematic representation of a caterpillar highlighting the main anatomic parts—*Archerontia atropos*—the death's-head moth. A caterpillar can look quite different from one shedding to the other. More exposed than the imago because they move relatively little, caterpillars possess a substantial defense arsenal, mainly camouflage and mimicry/mimetism like the imago, but also chemical means.

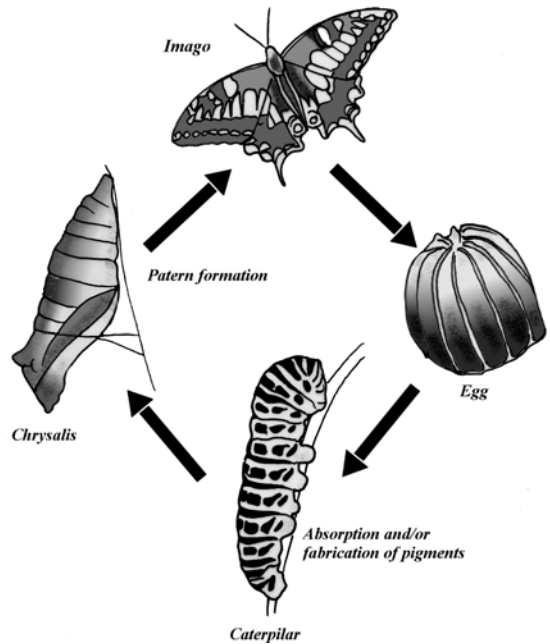


Figure 3.2. The life cycle of Lepidopteron. Here *Papilio machaon*. Certain stages of the butterfly life are particularly critical for its color.

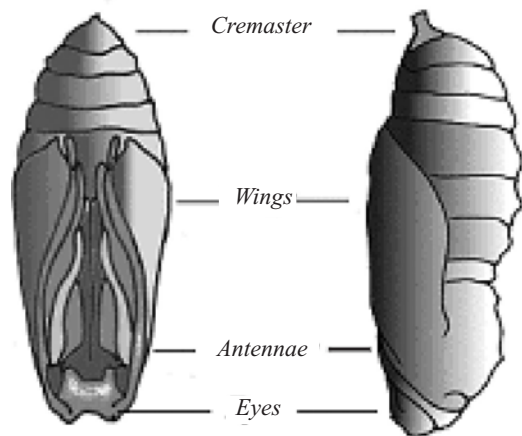


Figure 3.3. Schematic representation of a *Melitea phoeba* chrysalis—Japan. The Chrysalis is the first specialized stage of adulthood including all the future organs. Compound eyes are perceivable, while antennae, proboscis, wings and legs are along the body, distinguishable in relief. The external cuticle can be highly colored.

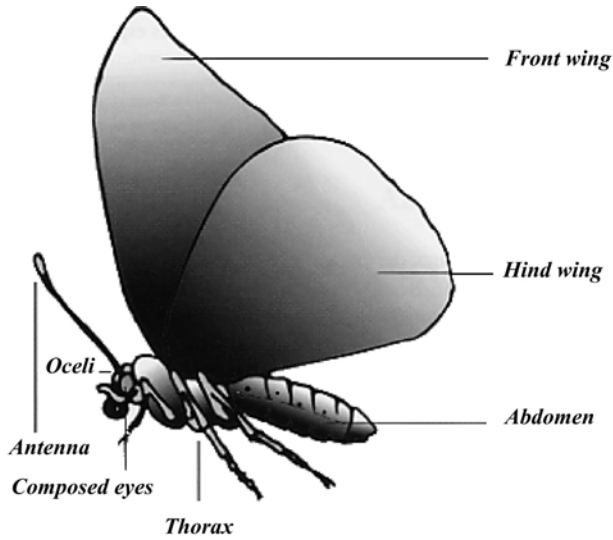
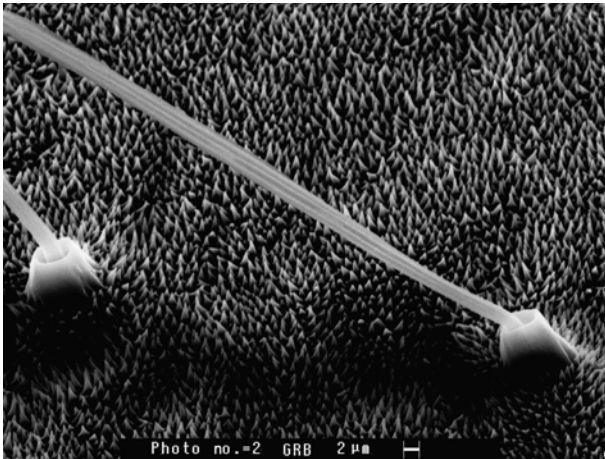
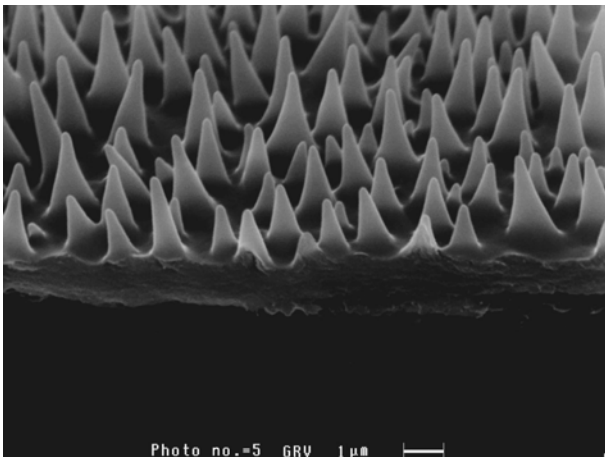


Figure 3.4. Schematic representation of a Rhopalocera. One can note on the head, under compound eyes, the folded labial palps and proboscis. Anterior legs are atrophied and thus unable to move among many Rhopalocera. Each of the first eight abdomen segments is equipped with a pair of respiratory stigmas. At the posterior end, the anus and reproductive organs (genitalia).



(a)



(b)

Figure 3.5. The structured membrane of *Grapium weiskei*—purple areas—top view on the left, and cross on the right. This structure is similar to that of green areas where a biliary pigment was found. The pigment is diffuse in both cleaved membranes, which are well visible on the picture.

Figure 3.6. *Morpho menelaus* alary membrane. Most of the scales were removed on both sides. One can distinguish the two membranes of the wing, and on the inferior membrane, the scales pedicels joined by a thin tracheole.

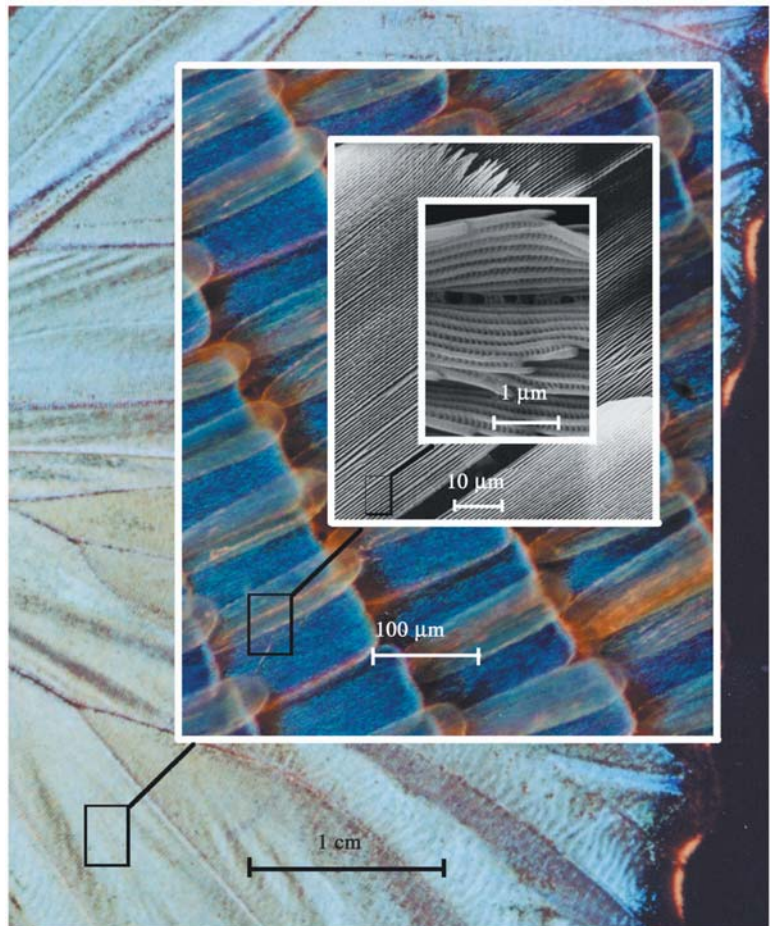
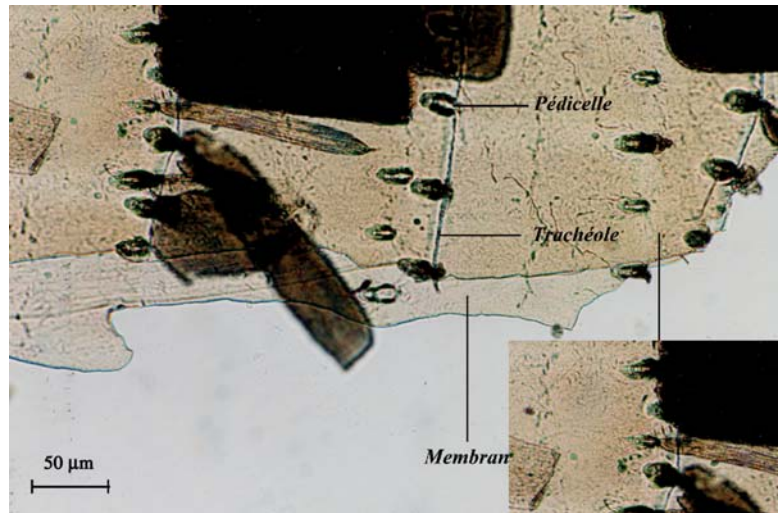


Figure 3.7. The different scales used to observe butterfly wings and their units of measure. The entire wing (5 cm), scales (100 μm), striae (10-1 μm) and striae fine structures (–1 μm–100 nm).

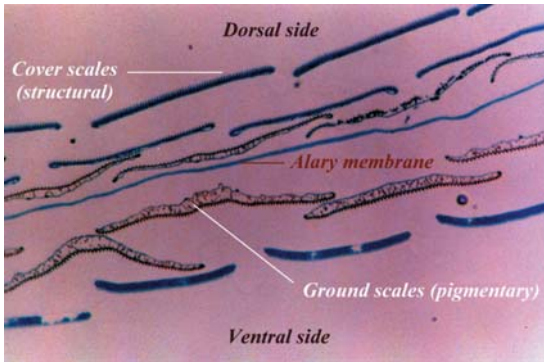


Figure 3.8. Optical microscope cross-section of an *Ornithoptera priamus poseidon* wing. The alary membrane is in the center, surrounded by the various layers of scales. The exterior scales here are the structural, while those closer to the center are pigmentary.

the thorax (which is composed of three segments, T1 to T3), and the abdomen (which is composed of ten segments, A1 to A10, that are not always distinguishable).

Each of the thoracic segments presents a pair of articulated legs composed of five segments and ended by a claw and which are distinct from pseudopods or membranous legs, which are not articulated and are situated on segments A3 to A6 on the abdomen. The latter end is a contractile sucker crowned with hooks. Pseudopods play a very important role in the mobility of the larva and are sometimes used

in the fixation of the chrysalis. The head is provided with a pair of small antennas, two single eyes situated on both sides of the head, and large mandibles. The larval stage is essentially a development stage consisting of successive shedding—between 3 to 7 times depending on species. Caterpillars primarily feed on plants and their digestive systems are capable of eliminating natural toxic substances or stocking them. Some of them can make pigments out of toxins, which are yet absent in adult insects, with the possible exception of some yellow or cream-colored vegetal flavones.

Chrysalis

The pupal stage, or chrysalis, is a stage of the adult state in which all of the future organs of the imago are already in place. Some of them can be perceived through the integument. We won't describe the nymphal diapause since it doesn't really concern us. However, a certain point directly concerns us. One can easily understand that it is during this stage of complete reorganization when the insect actually takes on its final form, that the patterns and colors of the wings of the imago are defined and that exterior constraints can change those plans. There are actually very few exchanges between the chrysalis, protected as it is by a quasi-waterproof integument, and the exterior.

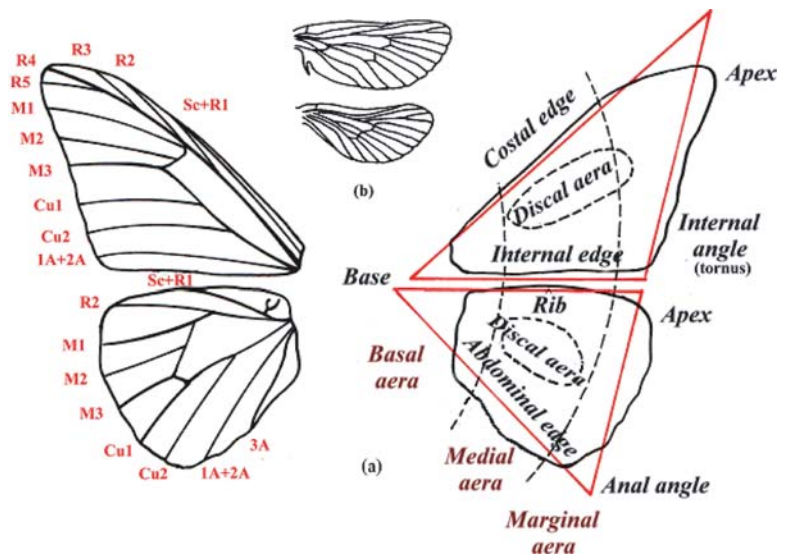


Figure 3.9. Heteroneura standard venation and nomenclature of the edges, angles, and of the main wing areas (a). In comparison, a schematic representation of an Homoneura venation (b).

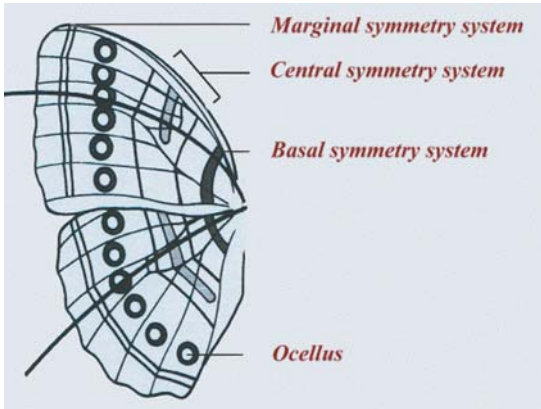


Figure 3.10. The basic Nymphaloid plane and the different symmetry systems—according to Siiffert, 1925.

The chrysalis does not feed nor does it excrete anything. Respiratory exchanges and evaporation are minimal. Only thermal variations and hygrometric, natural or experimental ones to a lesser extent—applied to definite stages of diapause—have an impact on the motifs and colors of the wings.

Moderate and prolonged thermal variations tend to bring out motifs, colors, and seasonal forms that are usually distinct within a same species (seasonal dimorphism). More spectacular modifications can be obtained experimentally by subjecting the chrysalis during the critical phase of the early nymphal stage to high variations in temperature. Even more interesting is that in 1933, a detailed stratification of the critical phase was established: an intervention altering the motifs during the first sub-phase, the structures and development of scales during the second sub-phase, and finally their pigmentation during the third one. Thus, according to species, the final aspect of the motifs and colors of the imago are defined during the second or third day after the chrysalis was formed.

Imago

The imago, the last stage in the development of the butterfly, essentially concerns reproduction. The imago is mobile and provided with all the organs necessary to recog-

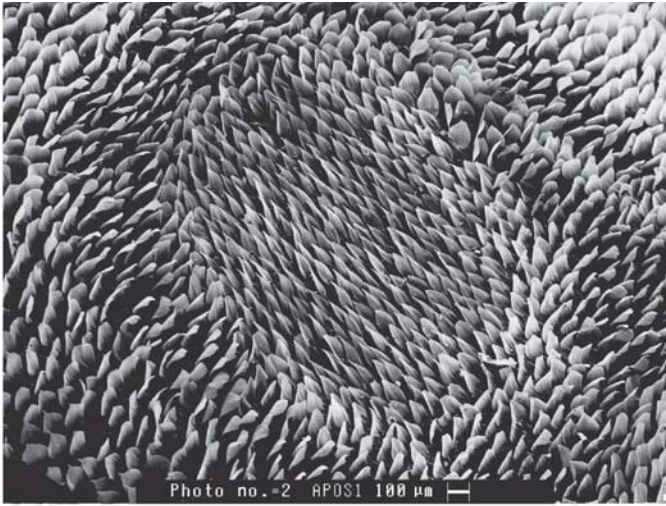
nize and encounter sexual partners. This is also the stage in which, through his search for food and partners, the insect is the most exposed to dangers.

Like the larva, the body of an adult butterfly comprises three distinct parts: head, thorax, and abdomen. Each part is covered with scales of various shapes and functions, most of which don't concern us. We will focus on the thorax and, to a lesser extent, the head and its two extraordinary composed eyes.

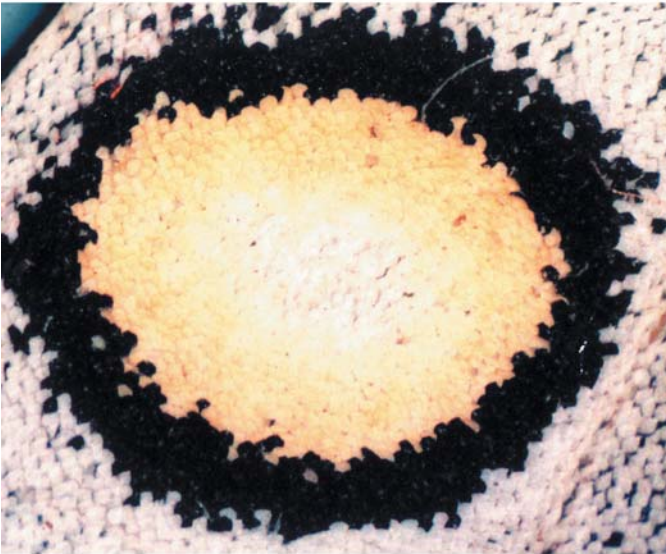
As in every insect (and their larva), the thorax is composed of three united segments to which the three pairs of legs are attached: prothorax, mesothorax, and metathorax. Anterior wings are already present in an embryonic state in the caterpillar and in an almost final state in the chrysalis. Anterior and posterior wings are linked with a passive device: the frenulum. The thorax also contains the muscular groups that are responsible for flying and walking.



Figure 3.11. Series of dislocations on the ventral side of a *Charaxes jasius* anterior wing.



(a)



(b)

Figure 3.12. Scanning electronic microscope image of *Parnassius apollo* ocellus. And its image by using a binocular lens glass at approximately the same magnification. One can note the scales' color variations as well as their corresponding structures.

Description of the Wings

We are going to describe the wing of the butterfly and its optical properties through two parallel yet opposite points of view. As we will see, we can distinguish five levels of observation or five magnifications, ranging from macroscopic scale, the whole wing measured in cm, to the molecular scale measured in nanometers (nm). Between the two and in descending order are the scale of scales—(roughly the

hundred of micrometers, μm), then that of striae (roughly micrometers), and lastly, that of the structure of striae or inter-striae spacing (from around 50 to 100 nanometers). Each scale corresponds to a specific means of observation and measurement, and also to its role in optical properties! It is logical to describe the anatomy of the wing by zooming in, from the macroscopic to the microscopic, each element characterizing one scale supporting its smaller components. As for optical properties, if the scale is



(a)



(b)



(c)

Figure 3.13. *Morpho godarti* ocelli, ventral side. On the left image, the ocellus is spherical and its concentric circles present the same thickness. On the right image, the ocellus, in the neighboring cell, starts elongating, the circle thickness increasing towards the wing apex—located on the right of the images. Blue scales, which are almost absent in the spherical ocellus, cover half of the central motif in the elongating ocellus. Generally confined in an alary cell, ocelli can sometimes substantially expand onto the neighboring cells (*Caligo idomeneus*).

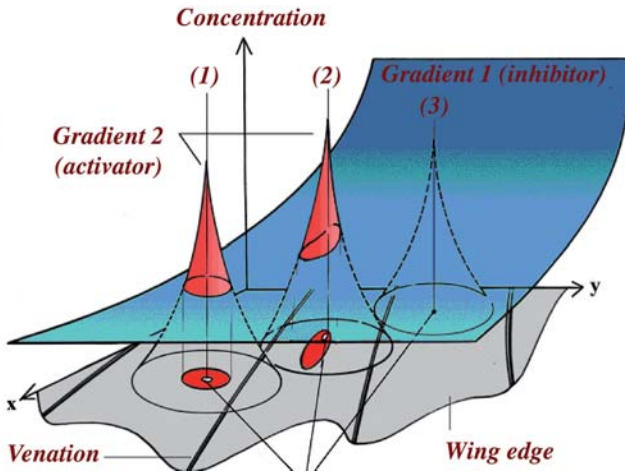


Figure 3.14. Circular and ellipsoidal ocelli formation process resulting from the combined action of two components. The inhibitor diffuses from the base to the periphery—on the front—whereas the activator diffuses from the foci. At the first focus, the inhibiting gradient is equal to zero, resulting in a circular ocellus. It is decreasing to a great extent at the second focus, leading to an ellipsoidal ocellus. Finally, the activator never reaches the critical concentration; therefore, the ocellus is not formed.

the same, we will study it in the opposite direction, in ascending order. Zooming out, color is created at the bottom of the scale and is modified at each rung to eventually obtain the final macroscopic effect.

Macroscopic Level: Structure of the Wings

Lepidoptera possess four membranous wings covered with relatively few veins in comparison to that of other insects. The wing venation characterizes species and thus allows one to classify species.

The wing consists of one double membrane, the two of which developed independently and united at the final formation stage of the wing. That is why the colors, motifs, and implantation of the scales of the ventral and dorsal sides of the wing are totally independent and often highly contrasted. Already developed in the chrysalis, the double membrane is covered by tracheas. During their development, the two membranes join each other and at the same time, are sclerotized along tracheas forming the veins, which continue to transport the nervous, gas, and haemolymph messages.

These membranes are the support of the scales, the surface on which colors mainly reside in Lepidoptera. Diffuse pigments can nevertheless be found on membranes, like that found with *Graphium* (see Chapter 11). In this specific case, the membrane consists of a

remarkable surface structure that scarcely affects coloration, but that slightly diffuses light and gives a pale, velvety aspect to these areas.

One can roughly imagine the wings of an “ideal” Lepidoptera as two triangles, the angles of which are more or less rounded off. The angles, sides, and main concentric areas have been designated with different names, which

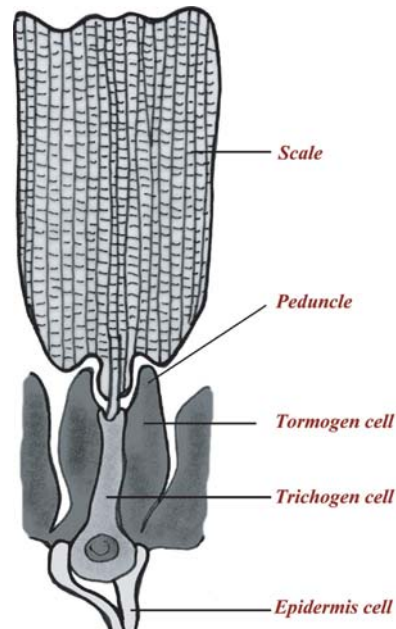


Figure 3.15. Schematic representation of a Lepidopteron scale.

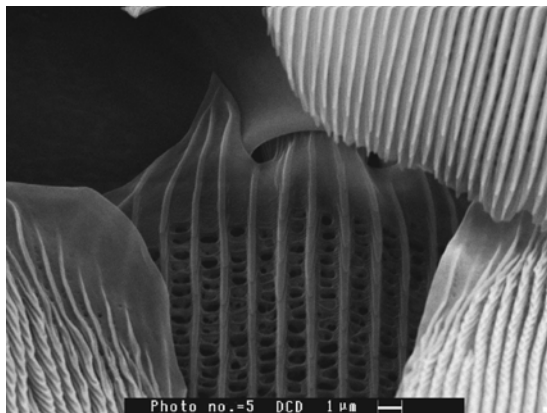


Figure 3.16. The base of a *Dixocopa chlotilda* scale showing the insertion of scales in the peduncle.

is quite convenient for the study of the wing (Figure 3.9.). We will only represent the principal divisions here, which is more than enough to illustrate our study.

The ratio between the size of the wings and that of the body is a critical parameter concerning the study of the flying process but also when it comes to thermal exchanges, which particularly concern us. This ratio is greatly reduced among species that present a high flying speed, like *Sphingidae* and substantial among *Nymphalidae*, which often glide.

The variations in shape and size of the wings between species and also within a given species between male and female, are innumerable, so that some of them can not rank in our diagram. They can present tails, sometimes very long, they can be oblong and without definite anal or internal angles, or they can even form narrow fringed lobes. Let us now mention the disparities that sometimes exist between males and females within one species. Whereas among numerous species, males are smaller than females, there are many contradictory cases of partial or total aptery affecting the latter only. Aptery can be found in specific biotypes (in an island environment) and protects the insect from being carried away towards the sea or away from the eggs by winds. All the transitions between well developed wings and completely atrophied ones exist, and even when there is the total absence of a pair of wings. We won't give a comprehensive description of the



(a)



(b)

Figure 3.17. Transmission photon microscope view of an isolated *Morpho menelaus* structural scale, top view. The scale presents a very geometric shape but is not perfectly plane. One can note the same iridescent effects, from blue to purple, as on the whole wing. Below, *Archeoprepona* pigmentary scale; striae are more spaced out, and the scale apex is characteristically multi-lobed.

various shapes of wings, which would go beyond our subject. Some will be included in our illustrations, thus outlining their extraordinary diversity.

As we have already said, the pattern of veins characterizes species. Several designation and numeration systems are available. We chose one only to situate more precisely measures. We chose, without any *a priori* on its relevance,

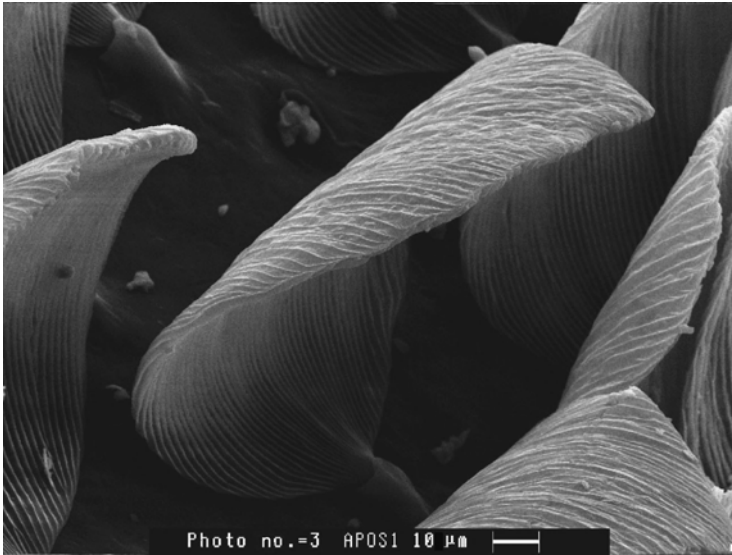


Figure 3.18. SEM view of *Parnassius apollon* scales. Located in a white area of the wing, these scales are little inclined on the membrane and strongly curved, thus revealing its two sides. The superior membrane is closely and regularly striated, whereas the inferior one, turning outward here, presents larger and less distinct structures.

Tillard's system, which is more adapted to designate triangles than the Anglo-Saxon numeration. The majority of secondary veins actually proceed from two main big veins, known as radial and cubital. Their subdivisions are numbered from the rear to the back. The previous ones are the subcostal, and those between the two medial and the following ones are the abdominal. The main veins are all oriented from the base towards the periphery of the wing, excepted for one transversal vein, the only one

joining the radial and the cubital, and from which proceed the medial ones: It is the discal crossvein. But of course, scarce are the butterflies that match this diagram, even without counting the supernumerary, merged, or subdivided veins...

The areas delimited by the pattern of veins and the edge of the wings, known as alary cells, are more important to us. They were named after their inferior vein, except for the triangular area delimited by the radial, cubital, and discal



Figure 3.19. SEM image of the end of a Pieridae androconia scale, *Pieris rapae*. These specialized scales give out pheromones. They are here spread all over the wing. Among many species, they form distinct bunches in a few specific places, like the abdomen extremity, or they can also be arranged in rows alternating with cover scales. Androconia scale cuticle presents numerous pores responsible for evaporation *secreta*.

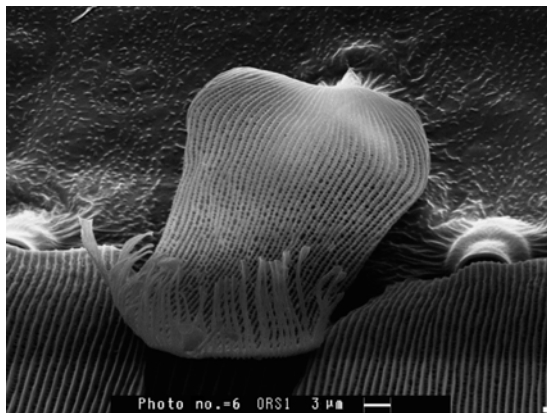
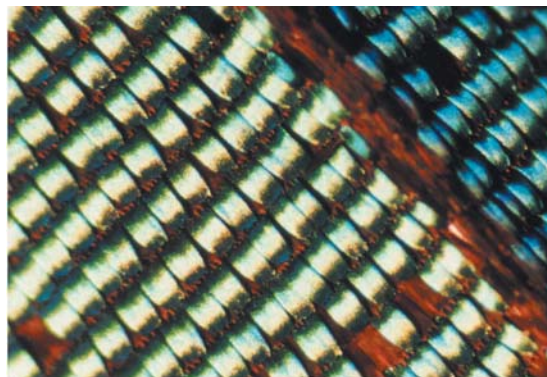
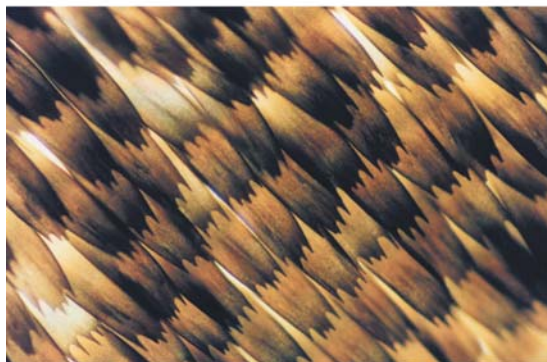


Figure 3.20. Androconia scale of *Hebonia glocippe* (Pieridae), surrounded by two typical scales—the superior row scales have been removed in order to expose the peduncles of the two scales types.



(a)



(b)

Figure 3.21. Shapes and arrangements characterizing structural and pigmentary scales—*Archaeoprepona*.

vein: the discal cell. Optical measures focus for the most part on the biggest areas, Cu1, Cu2, 1A, and the discal cell, as they are relatively flat and homogeneous.

Coloration and Motifs

Colored motifs on the wings are various: eye-spots, lines, simple or composed strips, ocelli that are spherical or not. They can be found on one side only, or on both. A perfect mess or a great uniformity, this apparent anarchy conceals a pattern, a general outline that is always more or less transcended from several simple geometrical transformations.

General outlines or basic sketches were developed by Schannitsal in 1924 and Siifert in 1925 concerning certain groups, such as the Nymphalidae, one of the very large families of butterflies.

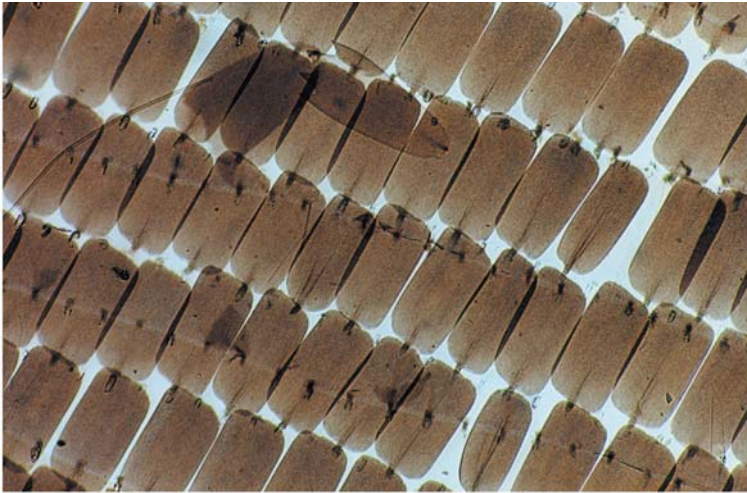
Here are the main characteristics of the sketch:

- The edges of the wing present a row of ocelli, a group of concentric circles, centered on the median axis of each cell.
- Symmetries in relation to median lines of anterior and posterior wings. The median line crosses several groups of colored strips in their middle, the main of which is situated in the center of the wing. The latter is the central system basing symmetry and includes in the middle a vividly colored strip: the discal spot. One can also find two eccentric systems of symmetry on the base and the periphery of the wing.

No butterfly species perfectly correspond to this sketch, yet all of them develop their particularities based on it. The most common and obvious transformations are pure and simple eliminations of all or part of its elements but also the contraction or dilatation of strips or ocelli and finally the dislocation, which means the displacement of a motif along the veins within a given area.

Formation of Chromatic Motifs

Chromatic motifs of butterflies' wings tend to be very intricate, spreading on several cells,



(a)



(b)

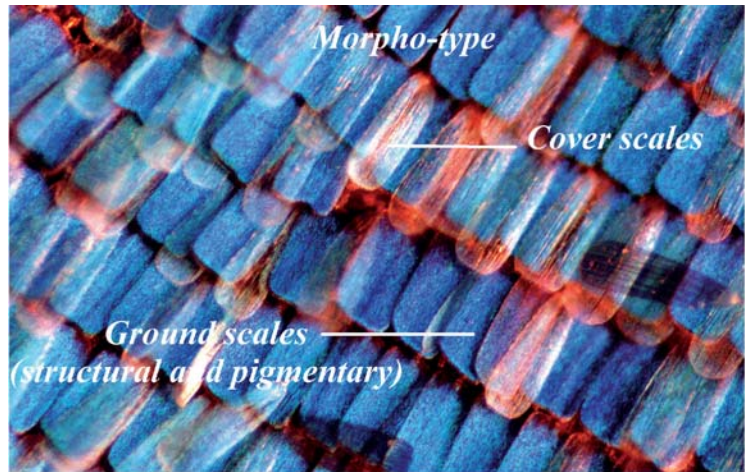
Figure 3.22. Transmission optical microscope image of *Morpho menelaus* dorsal side structural scales immersed in an index liquid. The ventral side scales have been removed, but cover scales, deprived of pigment, are visible. One can thus only perceive the brown pigments on the inferior sides of the structural scales.

even sometimes on the whole wing, and it proves quite difficult to experimentally determine its biogenetic origin. This is not the case where ocelli are concerned, which consist of relatively small motifs that are always precisely situated.

An ocellus is characterized by a specific pigmentation and an arrangement of the scales contrasting with its environment. The ocellus itself generally includes several colors, yet it does not affect the morphology of its scales. It is an established fact now that the arrangement of ocelli, which are always placed precisely

along the median axis of alary cells, depends on a specific property of the cells of the motif center. Known as the focus, it has been possible to experimentally shift this group of cells leading to the formation of an ocellus on the place of the shift, or to remove it, which brought about the complete disappearance of the ocellus. These experiments also establish a rather detailed chronology of the development of the ocellus and show that the motif is definite about three days after the wing has been totally pigmented, which occurs within the 24 hours before hatching.

Figure 3.23. The two arrangement types characterizing structural scales. Above, *Morpho*-type; structural scales form the under layer, the ground scales, so that cover scales are translucent. Below, the reverse situation in *Archaeoprepona*. Cover scales generate structural colors, whereas the ground scales—pigmentary—form an opaque screen that absorbs the light that has not been reflected by the cover scales.



(a)



(b)

The foci are thus a source of information indicating the place where the ocelli can develop. The geometry of the motifs of the ocellus can be explained by a double process of activator-inhibitory kind; this is the theory of the two gradients.

The focus diffuses a substance, an activator—the first gradient—leading to the synthesis of a dark melanin after its concentration has reached a critical limit. Under this limit, the scales synthesize another pigment, a yellow papiliochromis for instance. This limit may be determined by the presence of a second

substance, an inhibitory, which allows the synthesis of the melanin only when the concentration in the activator is superior to that of the melanin. The fact that the nonspherical or composed ocelli remain symmetrical in relation to the median line of the alary cell implies that the foci (or focus) of this second substance is situated at the base of the wings and that the inhibitory diffuses mostly towards the periphery—this is the second gradient.

The respective shapes of the two gradients allow us to reproduce most of the motifs thanks

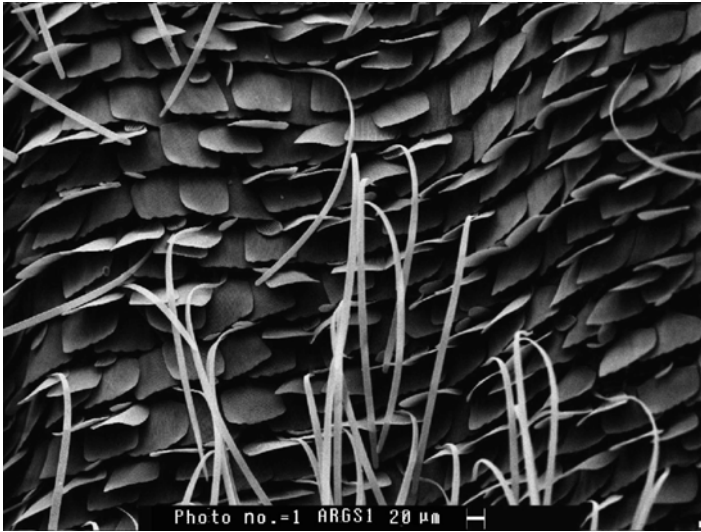


Figure 3.24. SEM image of the arrangement characterizing scales that produce color by scattering light. The disorganization doesn't affect the resulting color, which is rather lusterless. Overlapping rate is high. *Polyommatus icarus*.

to few parameters. An isotropic scattering from the foci would thus create circular motifs if the second gradient were absent (which entails a uniform concentration on the whole surface of the ocellus) and elliptic motifs if the gradient is strong with the main axis towards it.

It is quite possible, but not yet established, that the motifs of the symmetric systems are also related to rows of foci running across the wings from the edges to the interior and abdominal edges. As a plane wave can be split up into overlapped spherical waves, straight lines

here could result from the fusion of peripheral rings of large ocelli.

Gradients of activator and inhibitor concentration seem to be the key to the system of arrangement of the colored motifs of butterfly wings. However, the reality is obviously more complex and may imply more than two components (inhibitor of inhibitor) and saturation phenomena of one component with the emergence of a limit.

Finally, the detailed chronology of chemical reactions turning tyrosine into melanin or

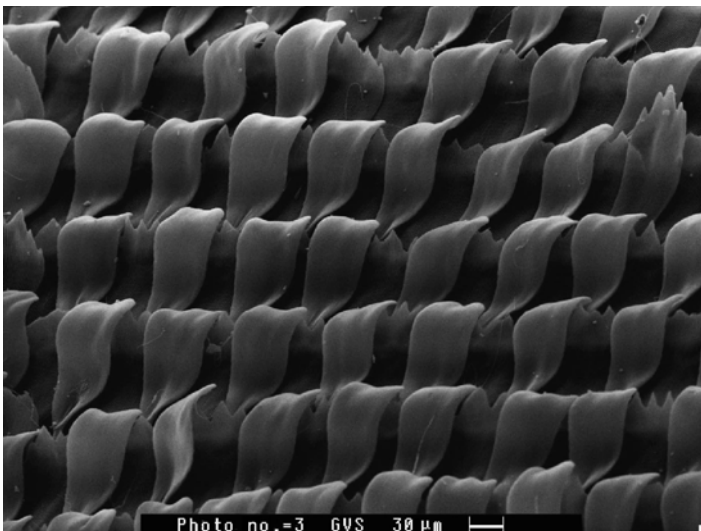


Figure 3.25. The colors produced by interference and diffraction require a very regular arrangement of the scales. SEM. *Ornithoptera priamus poseidon*.

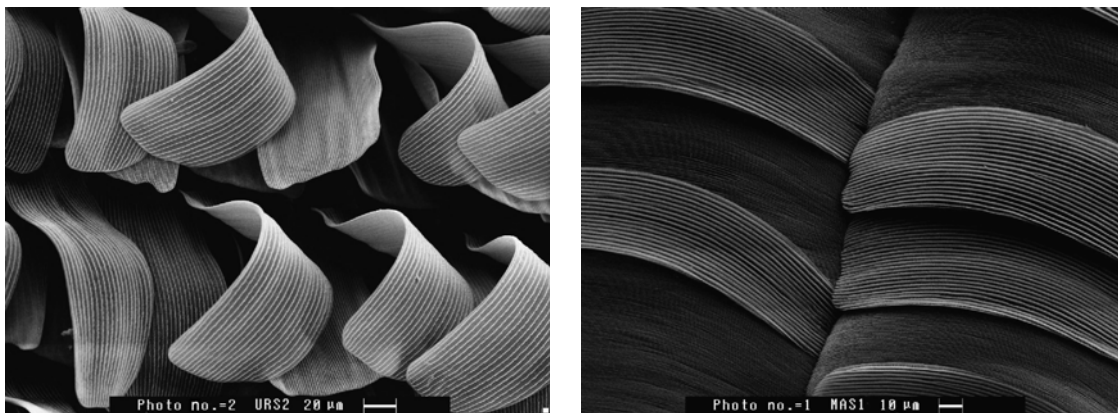


Figure 3.26. Iridescence effects can be substantially weakened by the scales geometry and arrangement. The most remarkable effect results from flat scales that are little or not at all covered by cover scales, like in *Morpho menelaus* or *Morpho cypris*. In *Morpho anaxibia*, on the right, structural scales are slightly convex—hardly affecting interferential effects—but are completely covered by highly scattering cover scales. Iridescence remains, yet the butterfly looks dull, compared to the bright *Urania Chrysidia madagascariensis*, the structural scales of which are highly curved but not covered—on the left.

papiliochromis represents a temporal indicator that could explain many details of the polychromatic structure in a given motif.

Scales: Structures and Morphologies

Nomenclature Attempt

If we focus on the scales covering wings, one should remember that the phaneres recover the whole of the body, including legs, head, and an-

tennas, where they play sensorial, respiratory, and odoriferous roles. To make our description more simple and before describing scales in detail, we would like to distinguish pigmentary scales and the colors they produce from the structural ones, the color of which primarily originates from physical effects related to the fine structure of the membranes. The caterpillar already shows embryonic wings as tiny spots. The imaginal discs split up into vesicles during

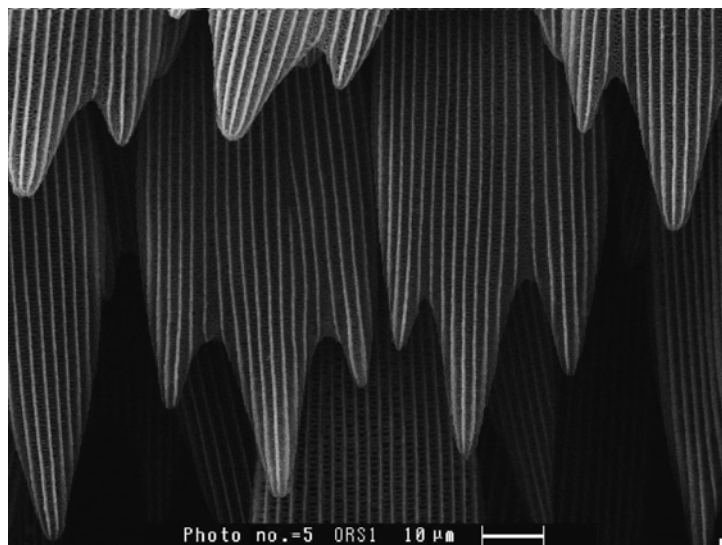


Figure 3.27. *Hebonia glaucippe vossi* Pieridae pigmentary scales. Pigmentary scales tend to be lanceolate or multi-lobed. Striae are big and regular.

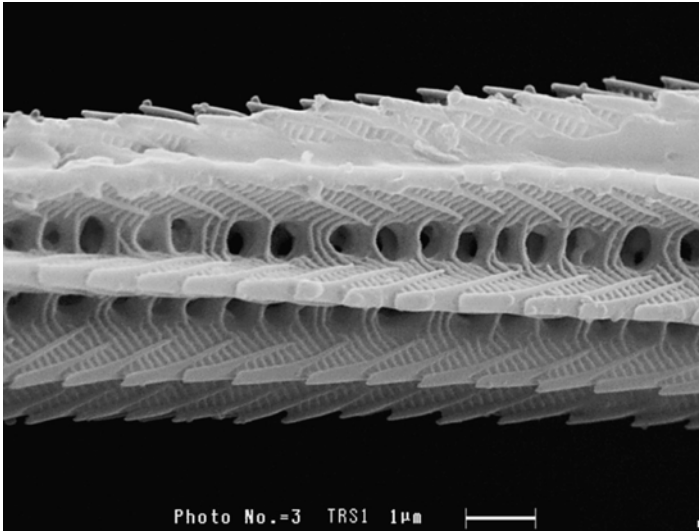


Figure 3.28. *Cithaeria menander* Pili-form scales. These very long scales that can be 1 mm long are often concentrated in certain places on the wing—basal and abdominal margins. They can also be scattered over the whole wing.

the successive shedding. At last, during the nymphal shedding, the latter evolve to form the pterotecae. Onto the folds of these future wings wrinkled up in the chrysalis, some cells differentiate turning into trichogenous cells on one hand and tormogenous on the other hand. The former will produce flattened and altered hair, scales, and the latter will create scales peduncle.

On the surface of the scales, an epicuticular skeleton will emerge that will produce the various structural systems generating physical colors. In the same time, pigments will be stocked into the epicuticle system or outside of it as ovoid granules.

The general morphology of the scales is as fascinatingly diverse as their roles are. We

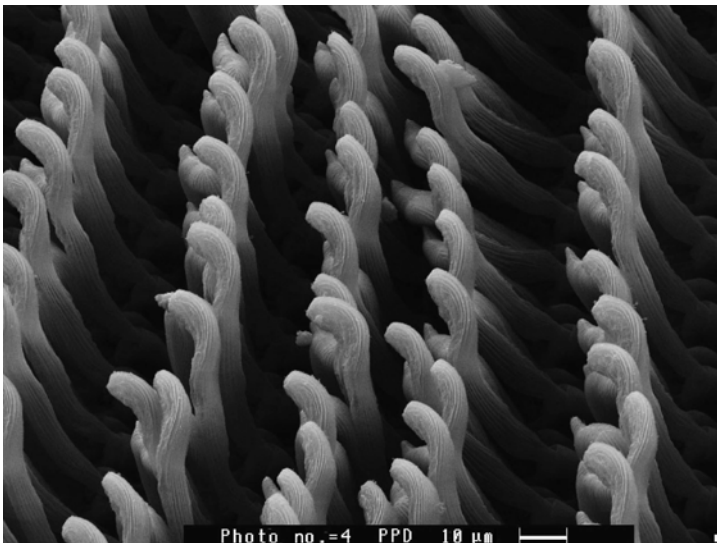
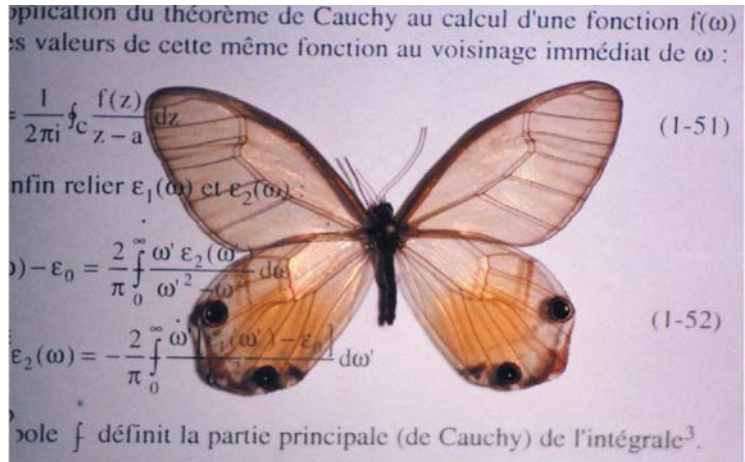
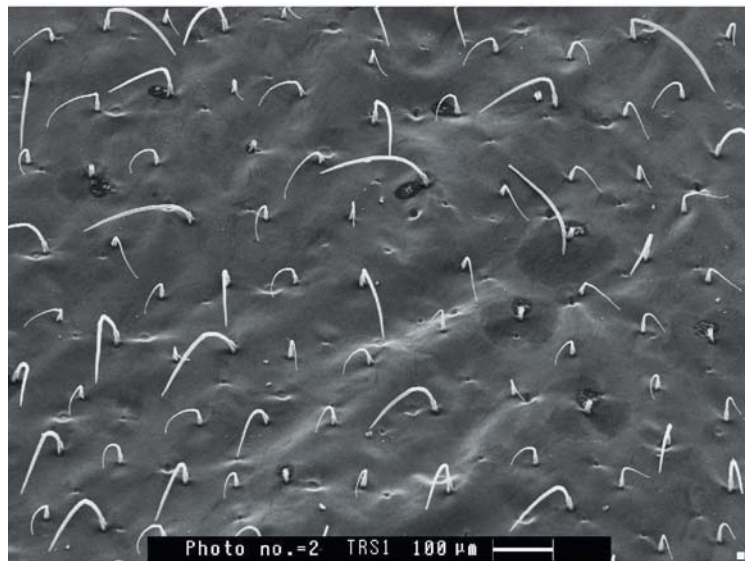


Figure 3.29. Pili-form scales of *Ornitoptera priamus* Poseidon.

Figure 3.30. Below: Over the whole anterior wings and most of the posterior, *Cithaeria menander* scales—6-cm long—are completely atrophied revealing the alary membrane, which is slightly pigmented and produces thin film interferences in places. The only characterizing element that the insect still presents is two big ocelles at the posterior wing ends and a wide scattering brown area. In the background, Kramers-Kronig relations that link the imaginary and the real part of the dielectric function of a material and are used to determine its optical index.



(a)



(b)

propose to give an outline of the former—which has never been completed—in order to establish the nomenclature.

The scales of Lepidoptera usually consist of two chitineou layers that form the limb. Facing the alary membrane, the inferior side is generally smooth or slightly undulating, whereas the superior side, which is turned outward, is thicker and shows a great diversity of structures. Almost all of the scales present a regular pattern of more or less spaced out longitudinal

striae that are visible through an optical microscope, and on other scales, a secondary pattern of transversal striae. Other, even smaller structures can be perceived that are shut in those patterns. The lamellae composing the two sides of a scale are joined inside by vertical trabeculae.

As we will see, scales are implanted in a more or less regular manner into the cuticle of the alary membrane, which is curved as a cupule with angular edges, the axis of which

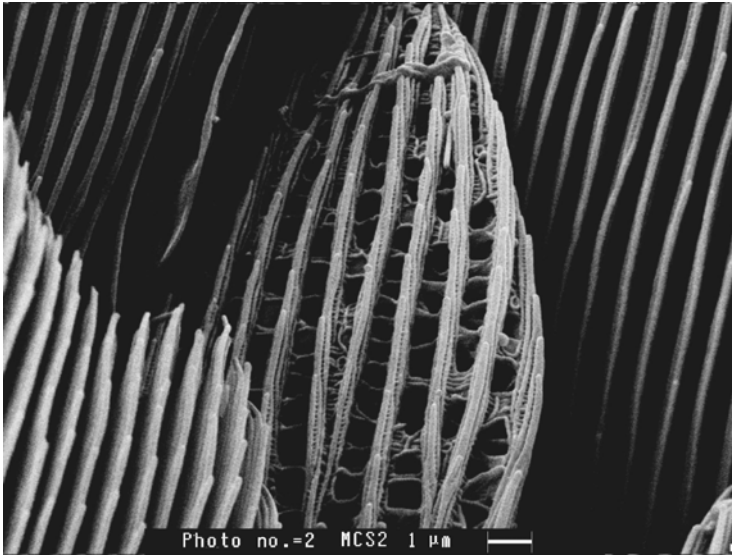


Figure 3.31. Thick and irregular striae of a *Morpho cypris* androconia.

inclines towards the apex of the wing. Scales present a great variety of shapes as shown by the illustrations in this book: flat, concave, undulating, threadlike, pilliform . . . These various shapes influence colors and must be considered when analyzing the colorimetry of the wing. Within a species, the shapes of scales greatly depend on their central or peripheral implantation on the wing, and also sometimes on the implantation of one single cell.

Peripheral scales are usually quite long, sometimes pilliform, but they can also be haphazardly scattered throughout the wing among the standard scales. The end of the limb can present extremely various shapes: curved, dense, or even filamentous.

Pigmentary or Structural

Scales are the center of colors among butterflies. We will first make a distinction concerning the origin of these colors.

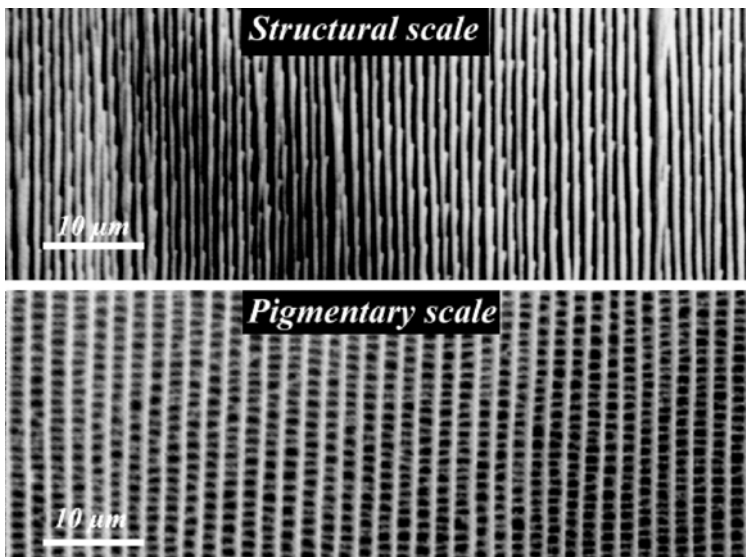


Figure 3.32. Grating of structural striae, above, and of pigmentary striae below—at the same magnification, by using SEM, *Morpho menelaus*. Structural striae, very dense, but also much higher than the pigmentary, can tilt and interweave in places.

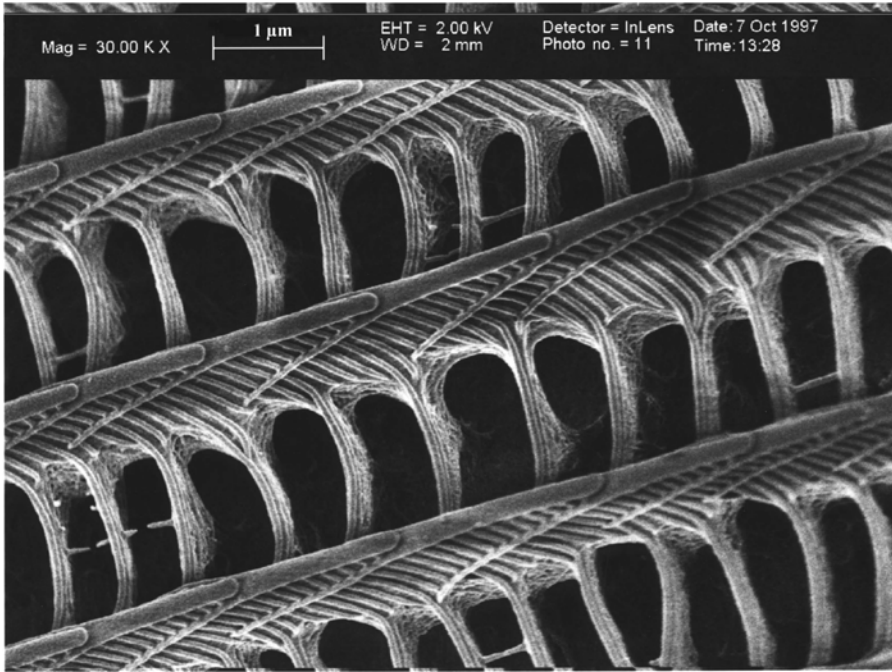


Figure 3.33. SEM image of a *Morpho menelaus* ventral side pigmentary scale. The key to Lepidopterons colors is concealed in this extraordinary and mysterious architecture. The various elements composing the thin structure of scales can all be seen here; keystone supporting striae, lamellae partially overlapping one another along striae and held by a very regular network of microtrabeculae. All scales, whether pigmentary or/and structural, use these elements to differentiate. Here, the pigment can be found in a diffuse state in the alary membrane scales, but it can also be found in others as small granules hanging from keystones. The lamellae, little developed here, don't take part in color. Color actually proceeds from the lamellae that are excessively long among certain structural scales—producing real multilayers, sometimes up to a dozen! Other structures can be contained in the scale thickness, thus not visible by using SEM.

A certain amount of scales are provided with more or less complex and regular structures on their external membrane or into the membrane itself. The standard dimension of those structures is comprised between a hundred and several hundred nanometers, which corre-

sponds to about a quarter of the visible wavelengths of the spectrum and leads to colored optical effects. These scales are designated as structural. Others, which don't tend to show such structures, have stocked a certain quantity of pigments, either in the constitutive material

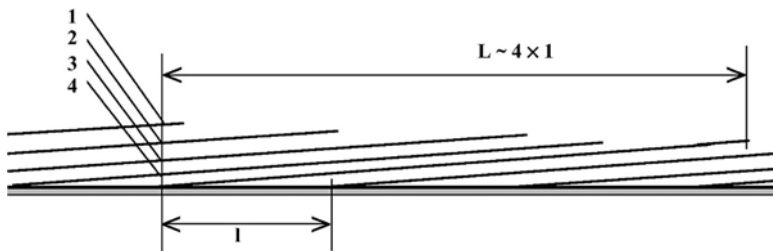


Figure 3.34. Scheme representing the arrangement of lamellae in striae. Lamellae are in equal number anywhere on the stria and form, with the scale superior membrane, an angle that can vary by around 10° according to species.

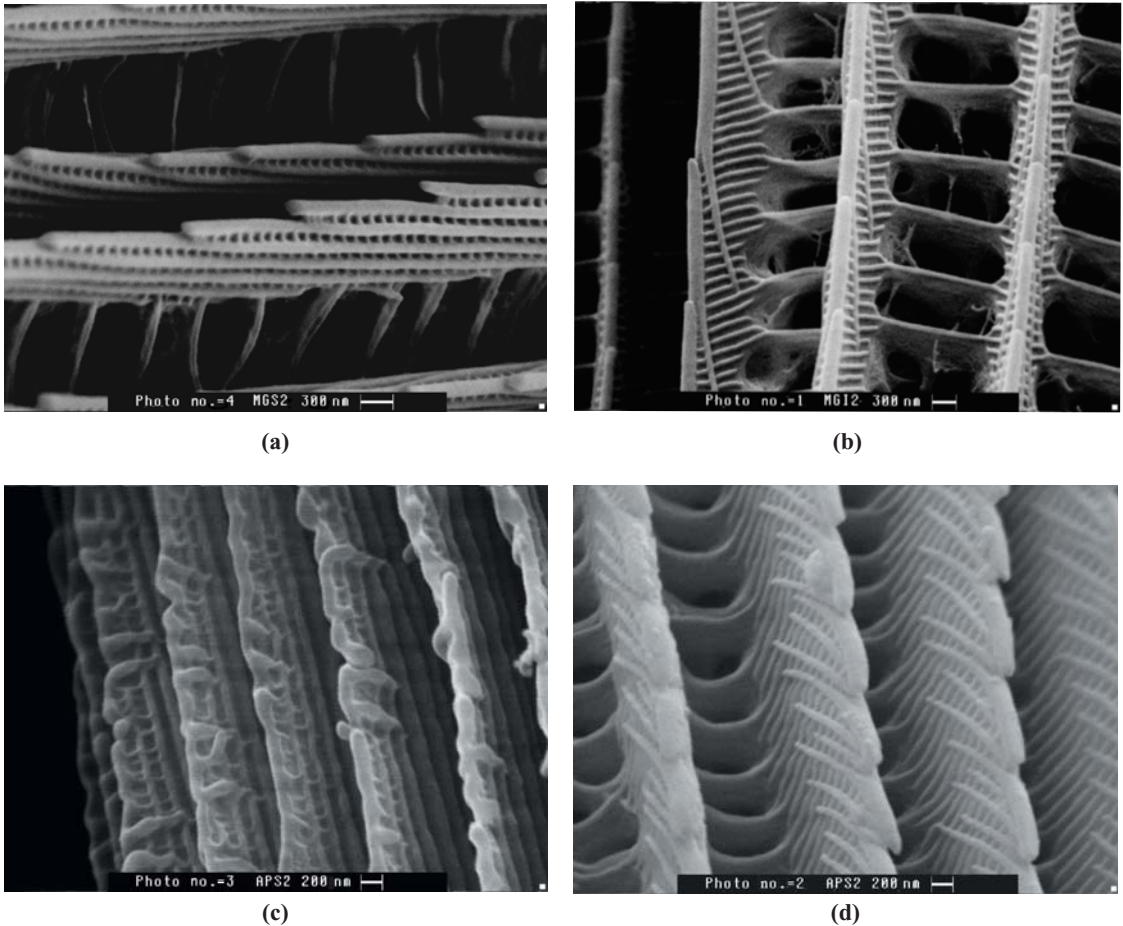


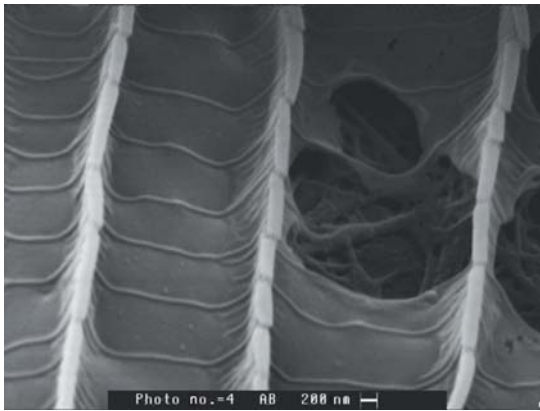
Figure 3.35. Diverse structures of striae. SEM view of *Morpho godarti* structural—above, on the left—and pigmentary striae—above, right. Structural striae here consist of five overlapping lamellae kept wide apart from the membrane by a system of long arches. Lamellae, their overall covered surface flattened, are almost cylindrical at their ends. They are linked to one another by a thin network of vertical ridges around a hundred nanometers apart. Pigmentary striae actually present the same structure, yet lamellae, very short, do not overlap. The widening main arches are present all along the inter-striae space, forming small compartments, in which granules of pigment can be found among some species. Reinforcement pieces are well developed. Below, *Archeoprepona* striae: pigmentary on the right and structural on the left. The general arrangement is roughly similar to that of Morphos, but the structural scales lamellae, which are cover scales here, are peculiarly distorted.

itself or externally as granules—these scales are pigmentary. The distinction is not always so definite though, and numerous structural scales can also include diffused pigments in their structures.

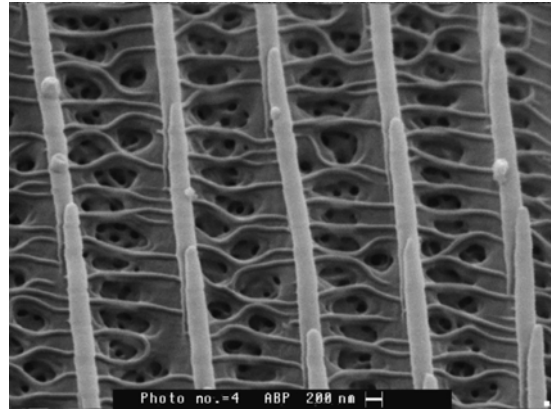
Structural scales generally show simple geometrical shapes that can efficiently recover without overlapping, whereas pigmen-

tary scales are often lobed and overlap on a significant part of their surface.

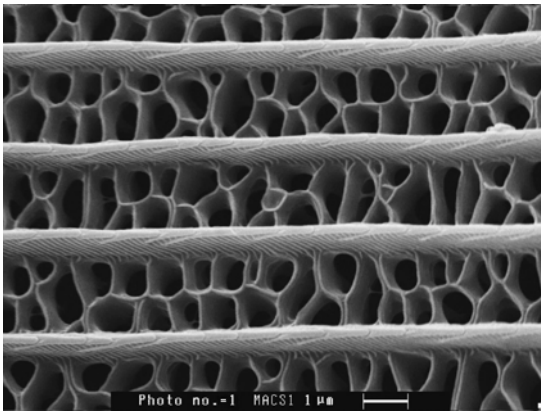
Among scales with a well-established role, we can mention the beautiful androconia, a characteristic of Lepidoptera. Aphrodisiac, these scales are often very long, sometimes ending in various capitate filaments or plumes. They are hollow and relate to a glandular cell



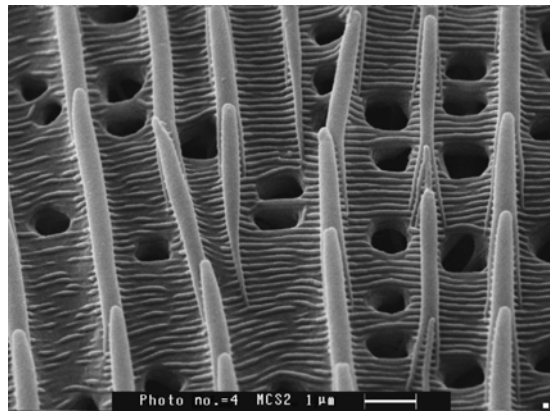
(a)



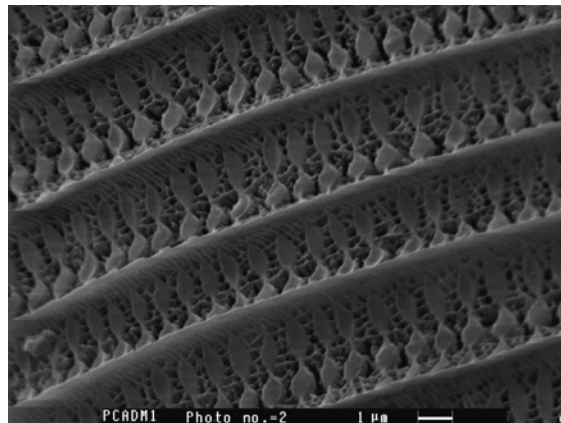
(b)



(c)



(d)



(e)

Figure 3.36. Various inter-striae spacings. From top to bottom and left to right, two views of *Polyommatus icarus*, and *Papilio machaon*, *Morpho cypris*, and *Catopsilia florella*.

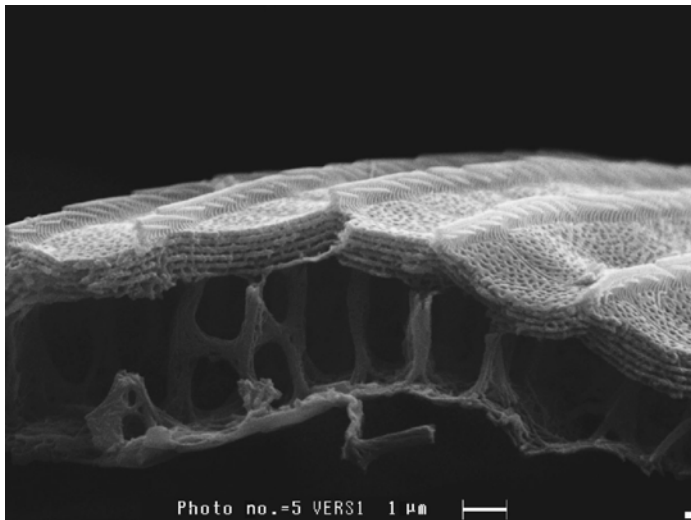


Figure 3.37. Multilayer structure of a *Procris statica* scale observed by SEM. The cross section of a scale cut through the middle reveals the main trabeculae joining the two membranes of the scales and the superior membrane multilayer structure. The structure consists in six very irregular chitinous layers that are alternated with constant spacing with a thick network of microtrabeculae. The exterior layer shows numerous alveolae. The penetration speed of diverse liquids in the structure proves to be high, suggesting that the other layers must contain alveolae as well.

the scented secretion of which goes through the cuticle and spreads its fragrance around the insect. Androconia can be either grouped in various spots on the wing, or scattered all over the surface between the cover scales.

Arrangement of the Scales

There is no characteristic arrangement of scales on the membrane. If in primitive groups scales are spread about without any apparent logic, they can—especially among the developed and vividly colored species that concern us—show a quasi crystalline-like arrangement. As we will see in our physical study of the optical properties of wings, the alary membrane only takes part in the infrared properties of the wing, and not in the visible coloration. Whatever their origin—physical or pigmentary—colors arise in the scales. An isolated scale includes all the effects of the whole wing. The way it is implanted and arranged among the other scales may greatly influence the final aspect.

With the exception of scattering, colors of a physical origin imply a great regularity of the structure, at the microscopic level as well as at the macroscopic, and the effect could be undermined, or even annihilated if scales were disorganized. That is why the structures, shapes, and implantation of iridescent scales show a rather strict order. They tend to be parallel to the membrane or slightly inclined, evenly

covering the latter by overlapping each other a little bit. Their shape is usually simple with regular or slightly dense edges.

As concerns physical colors, scales are often arranged in two layers: the under layer scales, known as ground scales and the outer ones, or cover scales on top, which are always very different in terms of shapes and structures. Depending on species, structural scales can either cover (*Archeoprepona*, *Uranidae* . . .) or line at the bottom (*Morpho*), but in the last case, the covering scale must be transparent or atrophied so that light can reach the structural scales. In the first case, the ground scales are often highly pigmented and form a dark screen against which other scales stand out. Ground and cover scales emerge alternatively along the same line, the ones covering the others, ground ones spreading almost over the whole surface without overlapping.

However, we will mention certain species of *Morpho* among which this distinction is not obvious anymore. While presenting structural colors, cover scales eventually slip between the ground scales. Covered with only one layer of iridescent scales, the butterfly is radiant. The two types of scales have almost similar shapes. However, if cover scales are composed of structures, they still aren't pigmentary. When immersed in a liquid of index, they disappear completely and only ground scales remain.

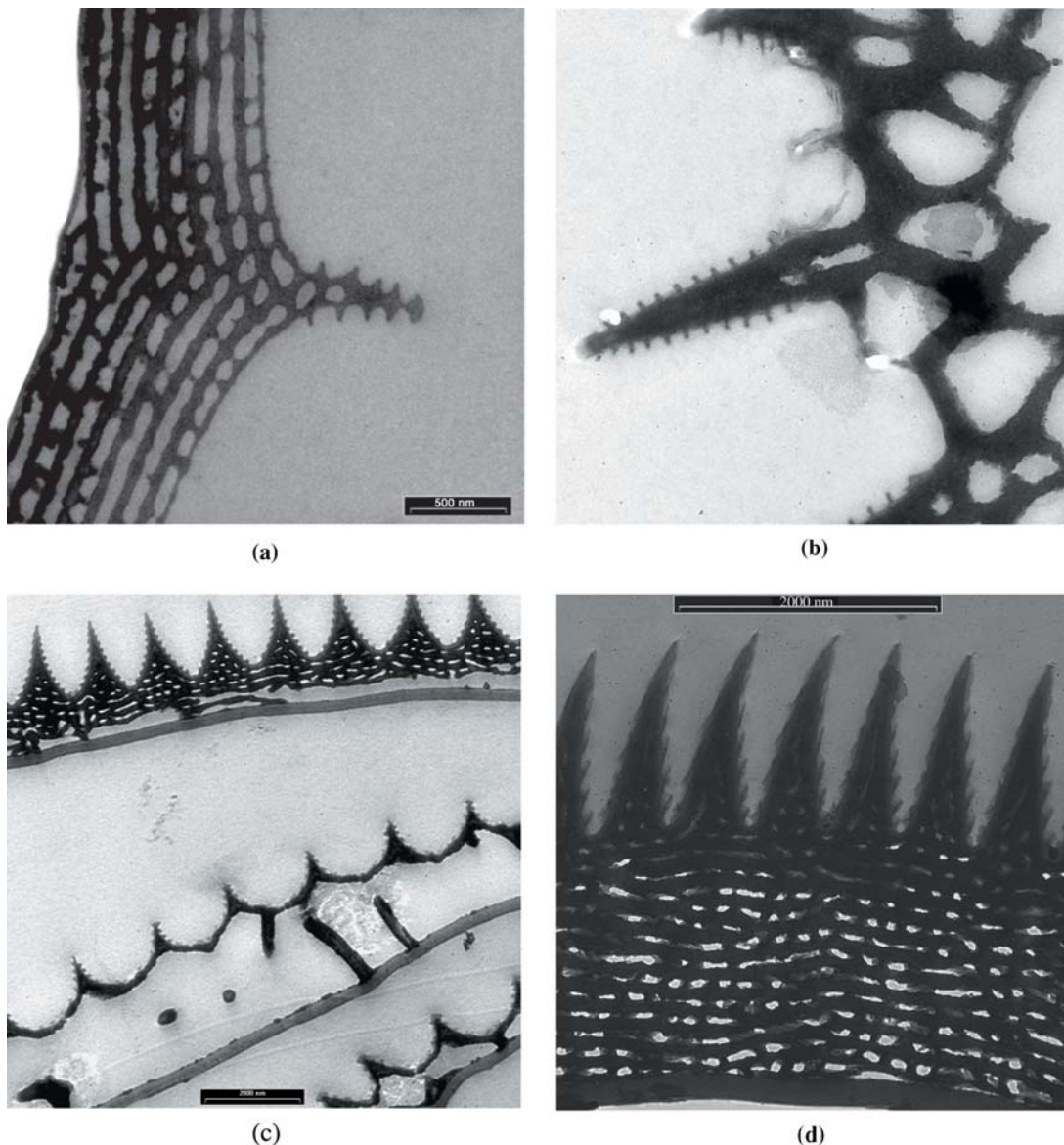


Figure 3.38. Several internal structures. From top to bottom and left to right;
 (a) *Papilio blumei*—a cover scale on a striae
 (b) The same butterfly—ground scales
 (c) *Ornithoptera priamus poseidon*—a cover scale on top of two ground scales
 (d) The same—another type of cover scales.

This is not the case for colors proceeding from a pigment or obtained by scattering. Those effects are not very sensitive to the incidence of light and don't require any specific arrangement. Scales can be more or less inclined on the membrane and show a great variety of shapes.

Shape of Scales

As we have already mentioned, scales present a wide range of different shapes and sizes, in relation to their roles (camouflage, aerodynamic, sexual, thermal regulation, hydrophoby...). The smaller ones measure less than a few microns, whereas the larger ones are several

hundred microns long. Either pigmentary or structural, almost all of them present on their superior side a pattern of longitudinal striae and also some other transversal structures, which we will describe in detail later. Here is the source of colors, which can still be greatly affected by the general shape of the scales. The pigmentary and physical effects are clearly distinguishable on flat or slightly curved scales. Structures are always situated on the superior face, while potential pigments are found on the inferior face or among the ground scales. The whole structural surface is exposed to radiance. But numerous scales include more complex sections (concave, convex, undulating, or twisted), which can lead to combined effects that resemble iridescence, without being iridescence *stricto sensu*. This is the case of certain concave structural scales, the apex of which is directed towards the exterior of the wing, thus revealing the inferior pigmented face of the scales, when observed from the apex towards the base. In this direction, they look matte and brown, whereas they turn iridescent in the opposite direction. According to this principle, scales presenting several undulations show from a distance successive bright stripes corresponding to the crests of the waves and dark stripes corresponding to the troughs, and thus create a changing combination thanks to the incidence of viewpoint. However, this is more the result of effects of geometry and shade than strictly iridescence.

The morphology of the scales has a great influence on the color of the wing, as well as its intensity, purity, and on optical effects in general. And yet, the diversity of geometries is such that it is impossible even to mention them. We will study in detail a few cases to convey this diversity.

Fine Structures; Striae and Interstriae Spacing

We have already mentioned the complex system of striae present on the superior surface of the scales. This characteristic is quasi general among Lepidoptera. Apart from a few rare specific scales, all of them include longitudinal

striae, in most cases parallel to their main axis—more rarely oblique or as a spiral—more or less thick, spaced, and easily distinguishable thanks to an optical microscope. Over the largest surface of the scales, striae tend to be parallel to each other, crossing the scale from one side to the other and regularly spaced, especially on the scales producing physical colors. On the contrary, they can be totally disorganized on some specialized scales like androconia.

The distance separating each main striae varies from 500 nm on certain structural scales, which corresponds to 2000 striae per mm, to more than 2 μm on pigmentary scales.

The thickness of striae also varies substantially. The highest ones can be as high as a micron (among *Morphos* for instance), but less than the hundred of nanometers. All striae share a rather simple structure, which each species will modify at will by developing or inhibiting certain elements, sometimes excessively.

Striae are composed of more or less long lamellae, arising at regular intervals on the superior membrane of the scale and overlapping like tiles. Lamellae are thus all inclined on the scale according to an angle of about 10° . The longer the lamellae are, the more they are to overlap. Hence, there are some cases where as much as 12 lamellae overlap. Their length is also remarkably constant and almost equal to a whole multiple of the interval between their bases, so that the number of layers is constant on every point of the stria.

The Interstriae Spacing

The diversity is as great concerning interstriae spacing. The latter plays a significant role especially among butterflies that diffuse light since it is there that structures take place. We will describe them fully in the chapter dedicated to scattering and will now only give an idea of their diversity. Let us mention that this area in the membrane often shows pores, which allow the gas exchanges with the interior of the scales.

Internal Structures of Scales

Always on the same scale, one can notice structures not in striae anymore, but in the superior membrane of the scale itself, for instance, among a whole family of Lepidoptera such as the *Urania*. The membrane is thus not composed of a single chitin layer anymore, but consists of overlapping layers, sometimes as many as six or seven, each measuring about a hundred nanometers and separated at constant intervals by microtrabeculae. These layers often contain numerous alveolae enabling gas or liquids to circulate in the system. The internal structures of the scales are extremely diverse, as illustrated by the series of sections in

Figure 3.28, examined with a transmission electron microscope. In a few rather simple cases, the structures that are optically active are situated in the membrane, as we have just seen with the *Uranidae*. However, these structures may be situated in the striae themselves and not in the supporting membrane. This arrangement resembles that of *Morphos*, yet here the stria doesn't form a surface structure by transforming itself, but it creates an internal architecture.

The two arrangements can be combined. Lastly, the membrane may also consist of a structure composed of alveolae, capable of producing colors through scattering.

4

Coleoptera Description and Observation Scales

Coleoptera represents an extraordinary order from every point of view and we will study it in detail. It is indeed the most important order in the animal world, including the biggest insects but especially the most colorful ones. Coleoptera appeared before Lepidoptera some 280 million years ago. They are characterized by sclerotic anterior wings: the elytrons. The latter are not involved in flying but form an extremely strong protective case (*koleos* in Greek) after which the group was named.

Coleoptera

As indicated by their name, Coleoptera are characterized by elytrons, anterior sclerotic wings that recover and protect the abdomen. Posterior wings are the only ones used for flying; they are membranous and folded both longitudinally and transversally under elytrons, which remain folded or half-open during flying.

Among many Coleoptera that lost the capacity of flying, posterior wings can be partly or totally atrophied. The order is divided into these suborders: archostemata, myxophaga, and adephaga, composed of the carnivorous Coleoptera including cicindelidae and polyphaga. They can be found in almost every environment, including running and sea waters.

The great variety of insect larvae is usually classified according to functional rather than phylogenetic criteria; hence the traditional distinction between polypod, oligopod, and apod larvae. The polypod larvae, like the

caterpillars, have legs and pseudopods, while oligopod ones are not provided with pseudopods, and apodes larvae at least, which are even completely deprived of any locomotive organs. Most of Coleoptera have oligopod (carabidae, scarabaeidae) or apod (scolytidae) larvae. These larvae undergo successive metamorphoses before reaching the nymphal stage.

If numerous Coleoptera are carnivorous and therefore possess strong mandibles, many have also developed some chemical protection, which make them repellent in terms of taste or often even toxic. Like butterflies, Coleoptera use Batesian and Müllerian mimicry, in which their extraordinary colors play a critical part, of course. We won't elaborate on the subject.

These colors generally recover the whole body, including legs, antennas . . . and they are particularly visible among elytrons. Among Coleoptera, the cuticle is an incredibly complex material that we will study later. Let us notice for now that, contrary to butterflies and even concerning physical colors, Coleoptera can present optical structures in their scales, inside of the wing itself and sometimes in both at the same time. This must be the price for the most beautiful colors existing in nature.

The Cuticle of Coleoptera

In order to address this second place where color can be found that is the "carapace" of Coleoptera, we must describe this extraordinary structure covering arthropods: the cuticle.



Figure 4.1. *Campsosternus* head. Colors are interferential.

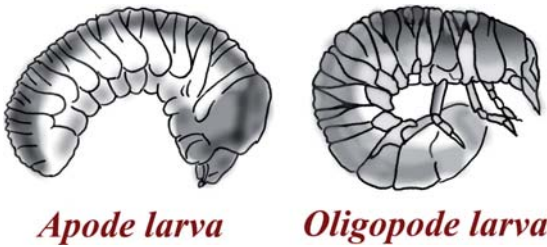


Figure 4.2. Diverse Coleopterons larvae. (a) *Scolytidae* apode larva. (b) *Scarabaedidae* ligopod larva (according to Chu, 1949).

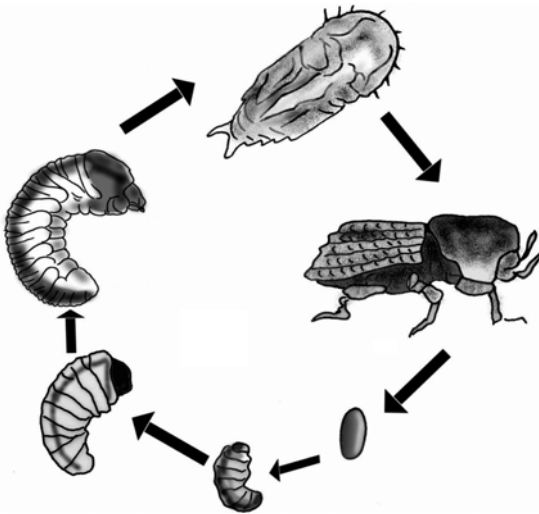


Figure 4.3. The life cycle of a Coleopteron with apode larva. The latter undergoes several sheddings before the final nymphal stage (according to Gullan et al., 2000).

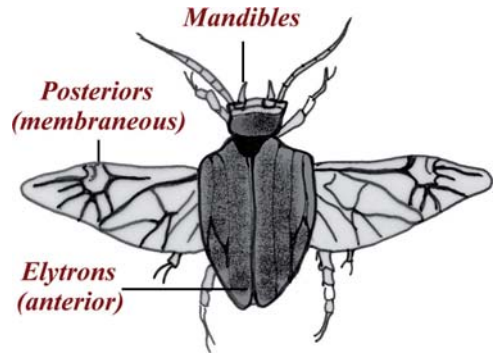


Figure 4.4. Schematic representation of a flying Coleopteron. The general outline is similar to that of butterflies. Anterior wings, which are very atrophied and after which the group was named, remain half open or folded during flight and kept together by a coopting device. Venation is roughly similar yet more complex than among Lepidopterons.

This highly complicated integument plays a major role in the success of insects. It both supports and protects the insect, providing muscles with bases and regulating liquid and gas exchanges with the environment. It is also the center of the magnificent colors that some Coleoptera sometimes show, making them look like exquisite pieces of jewelry. This last aspect particularly interests us, that is why we will examine this structure in detail. Like among Lepidoptera, this structure is sometimes covered by scales that can totally or partially generate colors themselves or modify those produced by the supporting structure.

Most of the scales of Coleoptera are thick and without surface structures. However, others are covered in protuberances measuring some hundreds of nanometers that diffuse light and break the shine of the scales. Scales broken after freezing show an almost perfect crystalline structure, which as we will see, originates diffractive phenomena resulting in extraordinary effects of color.

Structure of the Cuticle

The cuticle is a complex system of various layers in which one can distinguish two main parts: a thin external layer known as epicuticle and a thicker internal one covering the epidermis, called the procuticle. The two big layers, and especially the first one, are also divided

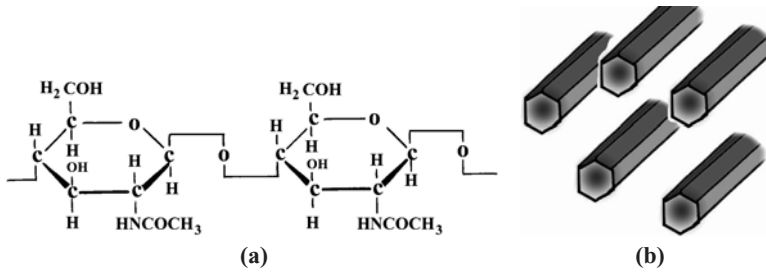


Figure 4.5. Chitin at various magnifications. (a) Two monomers of the molecule (b) The microfibrils arrangements of molecule groups.

into many sub-layers that can individually play a part in the coloration of the elytron thanks to their structures.

We won't elaborate on this subdivision, the classification of which hasn't been established yet, but we will study one of the components that play an essential role in the elytron color: chitin.

The chitin molecule is a polysaccharide with a structure similar to vegetal cellulose. It is a long chain composed of monomers of N-acetylglucosamine. About twenty in total, these molecules form two or three rows, thus creating almost crystalline sticks: the microfibrils. The latter are coated with a proteinic matrix

and oriented parallel to the epicuticle, forming layers that produce lamellae by superposing. It is this system of lamellae that originates the numerous optical phenomena resulting in the physical colors of Coleoptera.

At this point, helicoid arrangement can occur. This is a most peculiar and characteristic phenomenon providing arthropods with unique properties of circular polarization.

Helicoidal Structure

In the exocuticle, layers are parallel to each other, whereas each microfibril turns following a relatively constant angle, which results in a helicoid structure similar to that of some liquid

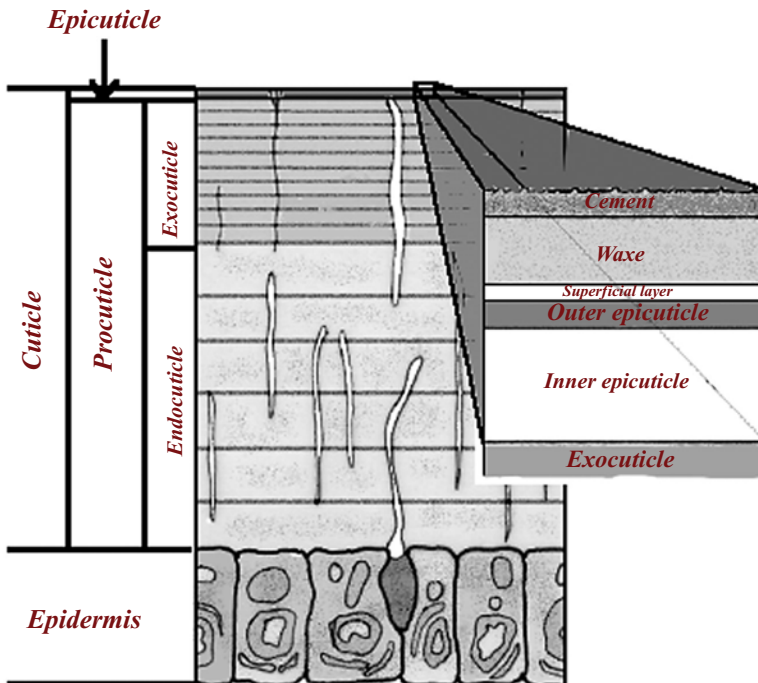
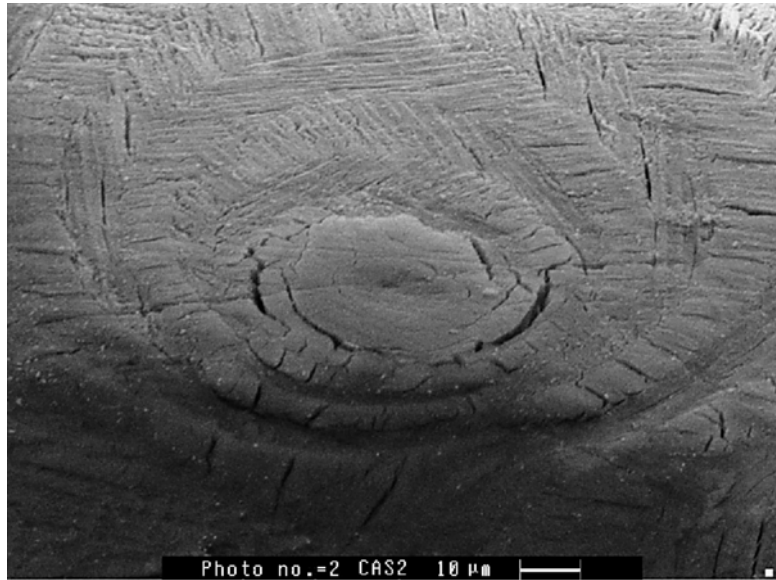


Figure 4.6. The main subdivisions of arthropodes cuticle. Divided between endocuticle and exocuticle, the procuticle lies on the epidermis cells and is covered by a very fine epicuticle. Numerous ducts and canaliculi run across the whole.

Figure 4.7. SEM image of an helicoidal structure in the caside cuticle. The elytron underwent an optical polishing at a circular alveola, followed by an ion etching revealing the orientations of leaves in each layer.



crystals in the cholesteric phase. Yves Bouligand is the first who demonstrated it concerning seashells and later, Neville demonstrated it concerning insects. The oblique section of such a structure shows a puzzling arrangement of arches, a result of this helicoid piling according to Bouligand.

One can also notice it on a section of the tubercles or concavities in the elytron. The layers thus look like concentric circular bands in which fibrilles are all parallel to each other.

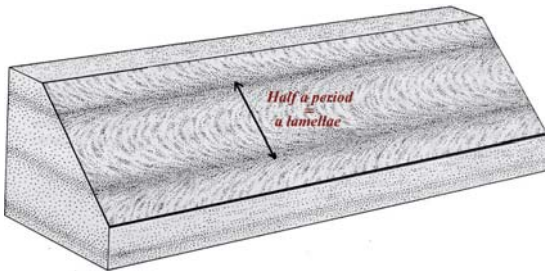


Figure 4.8. A cross section through the endocuticle points out arched structures characterizing cholesteric-type arrangement. Lamellae are formed by a 180° rotation of sticks.

The analogy with the cholesteric phase of liquid crystals may be fortuitous, yet the formalism elaborated by Fridel will allow us to briefly study the phenomenon.

This phase appears with molecules known as chirals, which means that their image cannot be superposed in a mirror. This is the case of every organic molecule including at least one asymmetrical carbon with four different groups. The main physical result of this characteristic, called chirality, is an optical activity, which entails that the direction of the light polarization

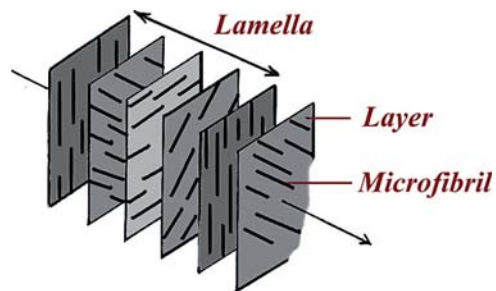


Figure 4.9. In a cholesteric stage as in the cuticle in Coleopterons, the director orientation regularly varies along the axis. A period shows up when the elements underwent a 180° rotation, determining thus a lamella.

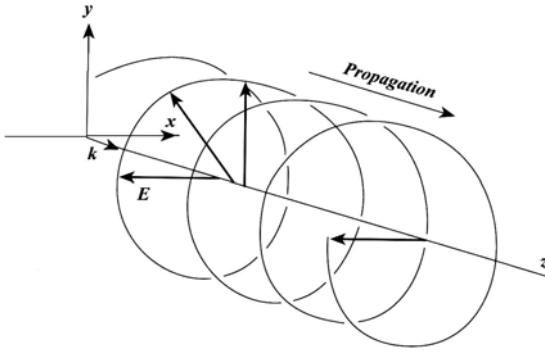


Figure 4.10. When entering the cuticle, the polarization direction of a polarized wave rotates according to the medium director.

rotates when crossing such a medium, with the associated interference phenomena.

In each plane and because of their elongated shape, molecules present a well-specified orientation, called *director*. In the cholesteric phase like in the endocuticle, the orientation varies from one plane to the next one, constantly revolving around an axis perpendicular to the molecules.

This rotation is known as *twist*. Among insects, it goes clockwise from the viewpoint of an observer looking at a point. The characteristic length on which the director undergoes a rotation of 2π is called period of the *cholesteric* and forms two lamellae in the cuticle.

Every layer actually behaves like a uniaxial anisotropic medium with a slow axis parallel to molecules and a quick perpendicular axis. These two axes regularly revolve layer by layer when light enters the cuticle, which then behaves, if the step is of an appropriate size, as a multilayer generating interferential colors. This rotation of the index also gives an optical activity to the whole, making the direction of polarization of the wave revolve in the same way and with the same step.

The epicuticle is also overlapped to this already quite complex structure. The former can include a single-multilayer structure consisting of isotropic lamellae—in which no fibrillary structure has been established. It sometimes also originates interferences, often combined

with phenomena of polarization by reflection caused by the carvings and alveoles sometimes adorning the surface.

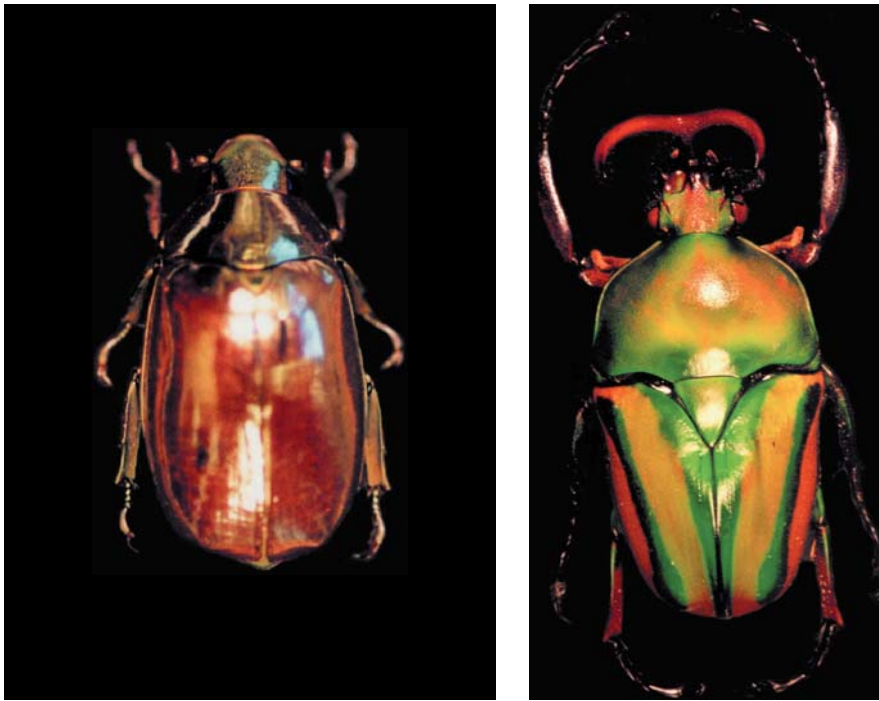
Cuticle and Scales

The color of Coleoptera originates from the cuticle or, as we have seen, from the scales covering it. The structures that can be found are very different and produce various colored effects, which cover a larger part of the spectrum than the colors of butterflies. We will overview those different structures.

When color comes from a structure included in the cuticle, the surface itself is only involved in the spatial scattering of light. One can find almost any kind of surface structures, from the perfectly smooth surfaces of *cetonia aurata* and other scarabs to the alveolar surfaces of cincidelidae, or hillocky ones of cassidae, or even longhorn beetles . . . In almost every case, color is interferential but the colored effect is modified by the surface structure, which can scatter color and thus decrease its brightness, on the one hand, and mix the different shades, thus undermining the spectral purity, on the other hand. These surface structures show diverse sizes, ranging from a millimeter among cassidae for instance . . . to about ten micrometers among cincidelidae.

In any case, the hierarchy of the scales of sizes and colored effects of Coleoptera is quite similar to that of butterflies. Like among cincidelidae as represented on the next page, the elytron, which is rather dull, possesses an alveolar structure. When examined with a photonic microscope, the alveoles, measuring about ten microns, look extremely colorful with chroma covering the whole spectrum, from the red to the blue with green as a predominant color. This proceeds from a pointillist effect. A cross-section reveals the multi-layer structure that produces the color. We will see in the chapter on interferences that the basin shape introduces, on a smaller scale, a chromatic component and generate polarization effects.

Among many species on the contrary, the cuticle doesn't produce any physical color but



(a)

(b)



(c)

Figure 4.11. Views of the surface structures of elytrons at different scales. Millimetric alveolae in a cassida: below. In the center, the slightly depolished surface of a Scarabeide *Eudicella graffi*. Left, *Plusiotis cupreomaiginata* smooth surface.

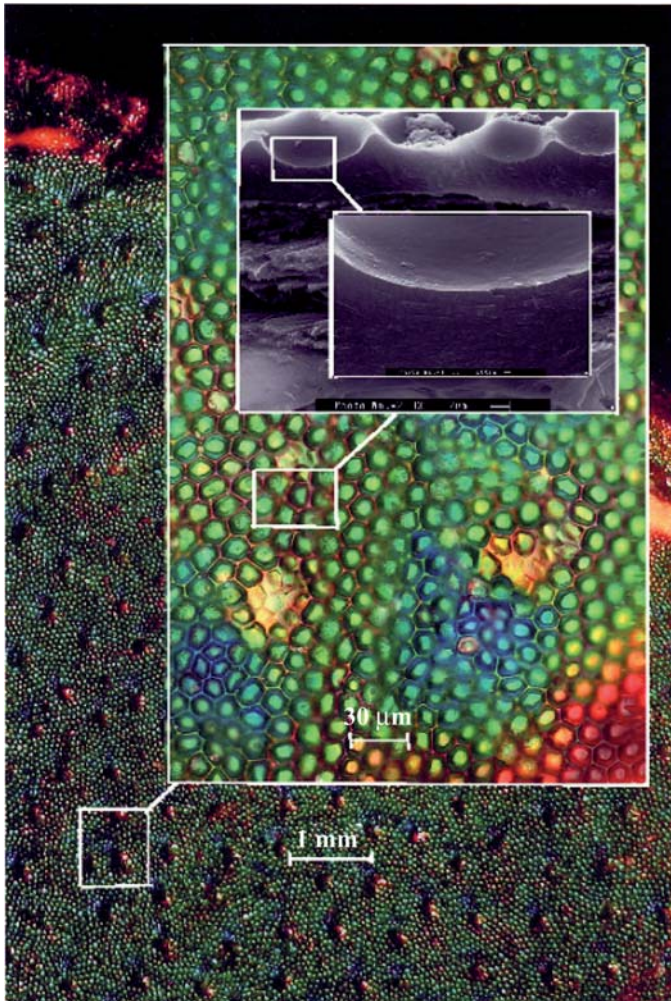


Figure 4.12. Coleopteron—*Cincidela campestris*—at different magnifications, from the elytron to the external epicuticle.

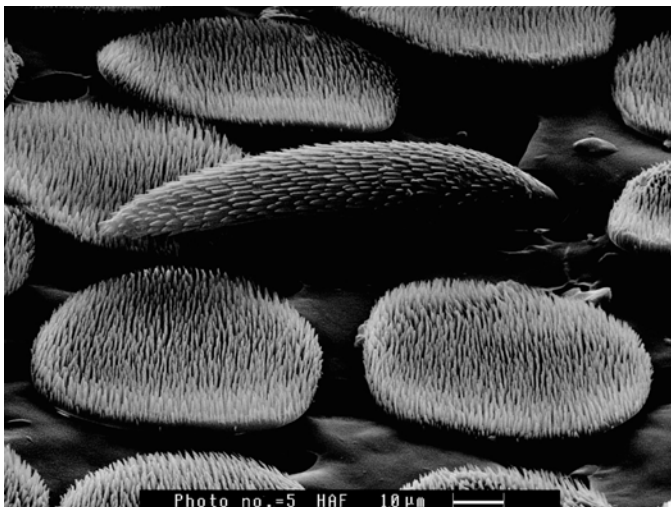
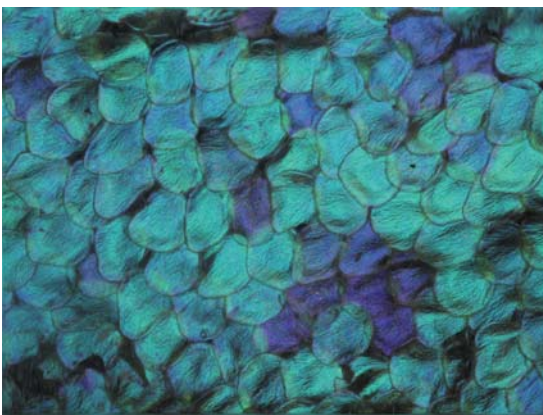
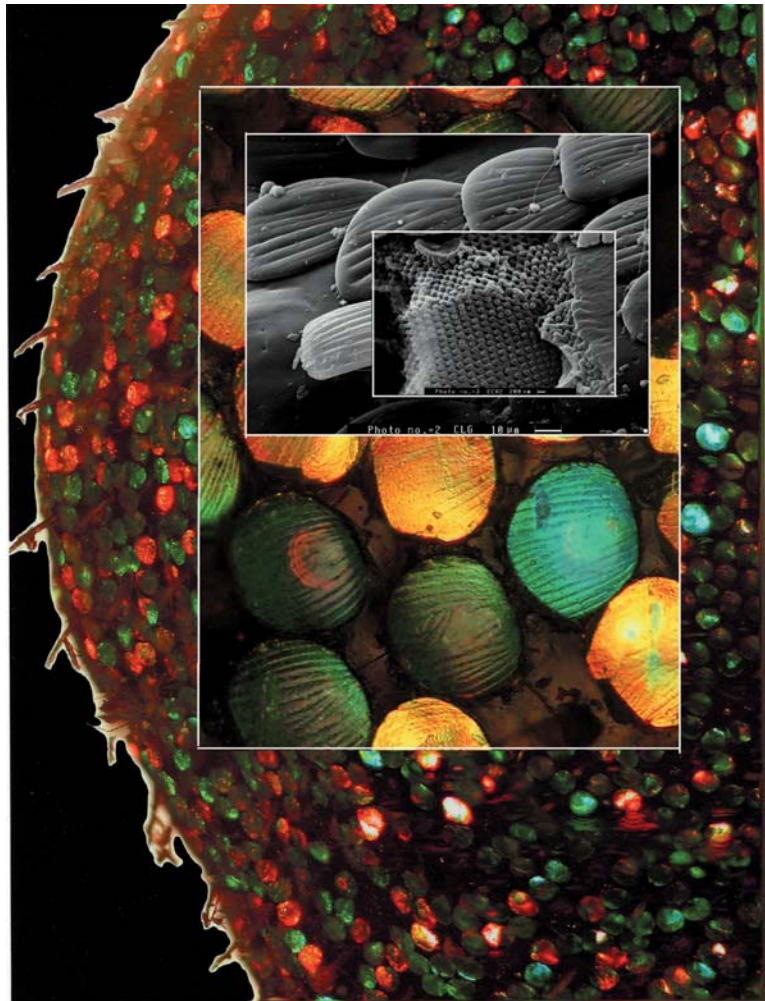
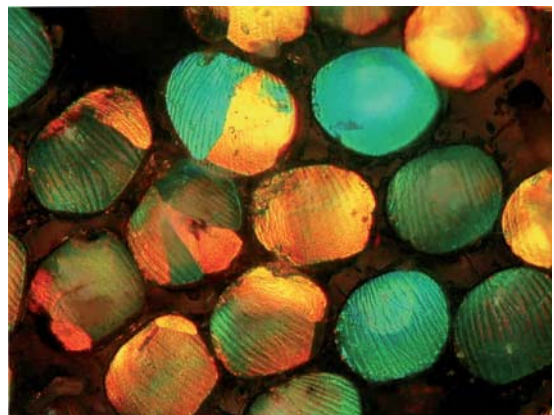


Figure 4.13. The lined scales of *Hoplia argentea*.

Figure 4.14. Coleopteron with scales—*Curculionidae*—at different magnifications. The bulk scales (massive) only partially cover the elytron. A broken scale reveals the crystalline structure, the base of diffraction phenomena generating colors.



(a)



(b)

Figure 4.15. Various arrangements of Coleopteron scales. Above, fish-type arrangement: *Hoplia cerulea* C. Scales overlap to a large extent. Below, scales are more scattered, like pebbles: *Curculionidae*.

is covered with scales like Lepidoptera. Their structure is nevertheless quite different since we always find the same internal crystalline organization, which is rare among butterflies. There are numerous families of Coleoptera provided with colored scales. The principal one is the *Curculionidae*, which includes our dear and rather dull weevils, but also the Scarabeidae and especially *cetonia*, well known for their extraordinary metallic shine.

Contrary to Lepidoptera, scales are generally arranged without apparent order and often scattered, discovering most of the underlying

cuticle. However, there are cases presenting a "fish type" arrangement in which thin and flat scales overlap.

With a few exceptions of the latter kind, the scales of Coleoptera are thick, hard, circular, and convex. They are usually flattened against the elytron, making it difficult to perceive the peduncle. Their external surface is the more often loosely folded. However, it can be covered with tiny nipples resembling those of the corneal lens of ommatidium (compound eyes of many butterflies), where they can play the same role of antireflecting layer.

Changing Colors: Structures or Pigments?

A Few Basic Experiments

If, as we have seen in the introduction, the pigmentary or structural origin of the colors of Lepidoptera was established a long ago, the classification of a given butterfly in one of the two categories has not been as easy and remains blurry today. This is generally due to the combination of structural and pigmentary effects, but also to the multiplicity of structural effects. Let us make a list of the phenomena as the biologist H. Onslow, for instance, would present them in the early century.

Pigments

Like those used by painters, pigments work by selectively absorbing a certain range of wavelengths. Observed in transmission—which is rare because they are usually opaque—the pigmented objects show the complementary color of the dominant that has been absorbed. This becomes more complicated with reflection as we will see, since it involves the phenomenon of selective reflection, which scarcely leads to pigmentary coloration. Fluorescence phenomena also belong to this category.

On a regular basis, the absorption peaks of the pigments are wide, resulting in not very pure colors. Furthermore, they are often associated with scattering structures that break specular reflections, making them look rather matte. There are many exceptions in which very bright colors derive from a pigment, as has been established. This is the case of *Lycaena phlaeas*, the *small copper* of our mountains,

which shows a surprising metallic aspect, the pigment of which has recently been isolated. The electron microscope reveals an arrangement of rather similar scales relatively raised at the apex, which contributes to the resulting iridescence strictly due to a geometric effect.

The scales themselves present no structure capable of producing such brightness. The wonderful *Ornithoptera priamus poseidon* offers a similar case. Its bright yellow glint apparently does not result from any structure of a surface or volume.

Concerning structures, the phenomena of diffraction, refraction, interferences, and scattering were commonly distinguished, whereas they are not fundamentally different and it is not easy to separate them. All proceed from the diffraction of an electromagnetic wave by an obstacle. Their difference is more due to the geometry and arrangement of the obstacles than to physics itself. It is nevertheless more convenient to first study them separately, even if we will later mention them all together.

In order to explain the metallic and iridescent colors among certain insects, four categories have been established:

- The diffraction of the wave by a grating type periodic structure
- Light interferences on the surface of thin single-layer or multilayer films
- Light refraction caused by prismatic structures
- The selective scattering of low (blue) wavelength by particles or cavities smaller than the wavelength



Figure 5.1. Iridescence effects in *Lycaena phlaeas*, illumination coming from the right.

In the following chapters, we will first focus on each of these phenomena by studying specific butterfly wings that show one of these phenomena predominantly. However, such phenomenon seems to be always combined with others, which is why we will then mention the combinations of the phenomena, which will ruin our illusory yet convenient distinctions.

It is in many instances convenient to distinguish between pigmentary and structural colors. There are two methods to do so: either removing the pigment by dipping the wings into various solvents, or removing the structure—from the optical point of view—by dipping it into a liquid of optical index exactly equal to

that of the material constituting the structure. When pigments are dissolved, the color vanishes irreversibly, and one must check that the scale structure hasn't been altered during this rather aggressive process. When the origin is structural, the process is reversible. As the liquid evaporates, the wing retrieves its initial color. The process can also be partial; if the index of the liquid is different from that of the structure, the color is modified. This implies that the structure is open and somehow lets the liquid penetrate it and then get out. We will mention the possible consequences of such a treatment on a pigmented surface in our study of pigments.

We will illustrate our point with the 2-dimensional structures of a *Morpho* type. Their big size offers a better support for study and they show the most spectacular effects. Besides, the structure of iridescent scales among *Morphos* is very open, allowing index liquids to rapidly circulate. We will see in the chapter on interferential phenomena that for a given configuration, a minimum occurs in the reflectance, hence the extinction of the corresponding color, for each wavelength such that:

$$k\lambda_{\min} = 2ne \cos \theta_r \quad (5-1)$$

where “n” is the layer index, “e” its thickness, “k” an integer, and θ_r the refraction angle.

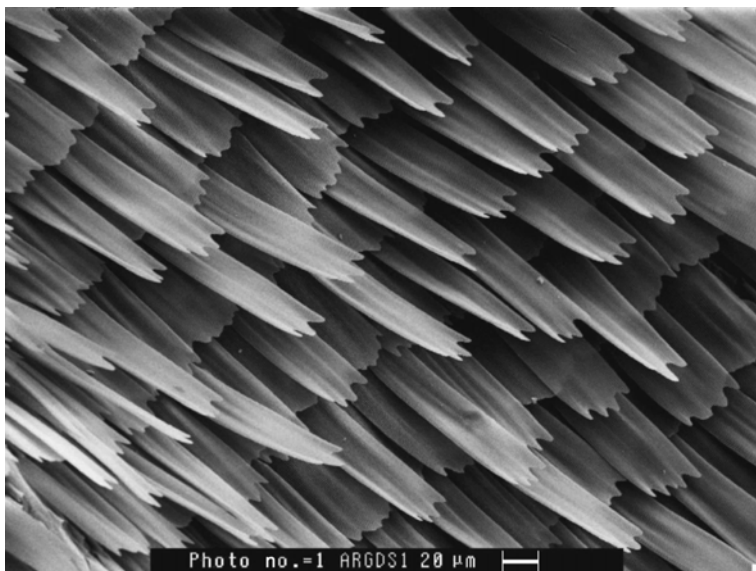


Figure 5.2. SEM view of *Lycaena phlaeas* scales. Cover and ground scales show different lengths, but similar thin structures.



Figure 5.3. Colors variations in *Morpho menelaus*, the scales of which are highly pigmented. When the matching of indices is reached, it turns almost black.

Under a given incidence, the reflected wavelength, and so the observed color, depends on the product of the layer thickness and with its optical index, and can therefore vary by

changing one of these parameters. Let us begin with the index variations.

An increase in the index of one of the components of the multilayer obtained by dipping an insect into a liquid with an increasing index leads to a shift of the dominant color towards the high wavelengths (blue \rightarrow green \rightarrow yellow \rightarrow red) but also to a decrease of the reflectance (or increase of the transmittance) resulting in the disappearance of red colors. When indices are equal, interference and thus color disappear and the wing becomes transparent. If such a structure is laid on a pigmentary motif or background, those only will be visible.

Other elements can also help us. The modification of colors under various index liquids certainly provides the most convincing test. However, it is little selective and doesn't allow one to distinguish between the different structural origins of colors. As thin layer interferences are concerned, the position of reflection maxima and thus the resulting color not only depends on the refraction index of the various layers, but also on their thickness. The same effects can be observed (yet they are more difficult to illustrate on a whole butterfly) by changing the pressure that structures are subjected to. Until the physical destruction of the latter, the effect is reversible and can easily be examined with an optical microscope.

Finally, it is possible to separate the pigment and the structure effects by making the optical measurements on an impress. However, we will see that some structural effects occur not on the surface but within the scale and thus cannot be revealed by this technique. In other cases, it allows us to distinguish between interference and diffraction effects. From a strictly optical point of view, the fact that colors proceed from a structure and not a pigment has important consequences. In particular, as there is no absorption, the incident flux is shared between reflection and transmission. In the visible, the color that is transmitted is almost the complementary of the reflected color. In reality, this is not easy to observe because of the constant presence of pigments, even in small quantity, within the scales or membrane structure.

We won't go beyond this simple explanation. The variations in certain colors of butterfly



Figure 5.4. Colors variations in *Morpho godarti* under different index liquids. On the right, the butterfly in its normal state in the open air. In the center, immersed in acetone — $n = 1.362$ —and in trichloretylen on the left hand-side— $n = 1.478$. *Morpho godarti* structural scales hardly contain any pigment and turn transparent when the index matching is reached, thus exposing the ventral side motifs.

wings can be explained with the index of the medium by the traditional theories of geometric and physical optics: scattering, interferences, or diffraction. We will call these colors structural. Others proceed from absorption and selective reflection phenomena. We will call them pigmentary. It is essential to remember that this distinction doesn't hold in reality. If there are many a butterfly colored with a pigment, I don't know any owing its color to physics only. The spectacular results always proceed from a subtle mix between the two phenomena, the two reinforcing each other, annihilating or combining.

A Few General Principles

Based on this first remark, we will examine each of these physical phenomena more closely as presented by specific butterflies. Although, they don't establish strict rules and the reader is invited to find the counter-example, here are a few principles that can help us in our choice.



Figure 5.5. Indonesian *Ebonia*—9 cm. The anterior wings of this butterfly, which belongs to the *Pieridae* family, are totally pigmented in orange. Posterior wings—yellow-white—are highly scattering. Under index liquid, they turn transparent, exposing the ventral side motifs, while anterior ones remain almost unchanged. The pigment is contained in small granules also scattering light. When not illuminated, wings look darker.

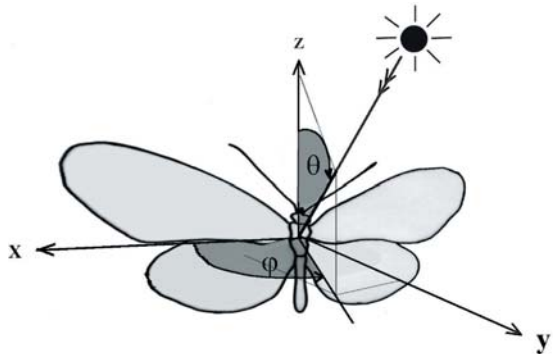


Figure 5.6. Spherical coordinates system determining the source position. The butterfly is observed according to the Oy axis normal to the dorsal-ventral plane of the insect.

Figure 5.7. The big Indonesian Papilio, *Papilio ulyse*, illuminated under two extreme angles. On the right, under low-angle from the left. The predominant wavelength is in the blue-violet range, around 475 nm, approaching purples in places. On the left, the insect is illuminated and observed under normal incidence. Its color tends toward the green— $\lambda \sim 500$ nm. In both cases, there are no significant differences between the left and right parts of the insect, suggesting there is a symmetry in the incident plane.



Let us begin with basic remarks:

Blue pigments are rare in the animal world. Most of them are metallo-protein pigments characterized by the presence of one or several metals on various protein molecules, the most common of which is haemocyanin, which derives from copper. It is usually found among mollusks, crustaceans, and some arachnids in solution coloring plasma blue.

On the contrary, red, yellow and brown pigments are widespread, especially among butterflies, either as a product of degradation (such as melanins, widespread in the animal world), or as tetrapyrrolic pigments (like hemoglobin) from which derive the vivid reds of numerous vanessas (*Inachis io*, *Aglais urticae*...).

If we now examine the wings from the point of view of the variations in colors related to the angle of incidence, we can establish a new selection:

Interferential or diffractive colors change substantially depending on the angle of observation or illumination. This is the phenomenon of iridescence, one of the most spectacular among tropical butterflies like *Morphos*, *Archeoprepona*, and *Urania*, but also, for instance, among the little common forester (*Procris Statice*) in temperate regions. The aspect of iridescence is here bright and metallic.

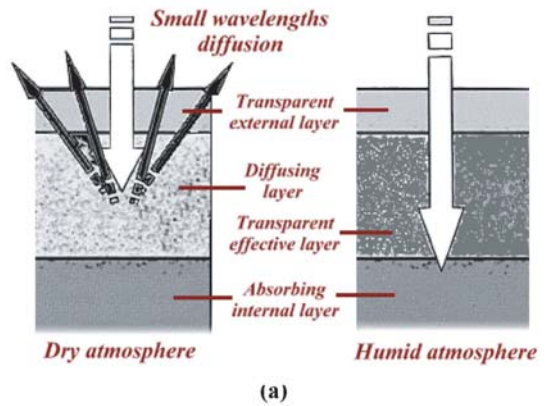
Pigmentary colors or colors proceeding from selective scattering hardly vary, whatever the angle of observation or illumination, except when angles are very high and for highly polarized light. The corresponding aspect is matte, even dull.

These experimental techniques—modification of the index or of thickness—permit us in many cases to distinguish between structural and pigmentary origin of colors. They always lead to the alteration or disappearance of colors—a real opportunity for nature and the opportunity for us to mention all the types of color alterations, of *chroma*, observed among insects. Let us only note that color alterations are quite rare among the latter. There are physiological modifications, rather quick and generally reversible, and morphological changes generally irreversible resulting in a new pigment. We will focus on the former, which are obtained through the modification of the cuticle structure or the migration of pigments.

We will call the devices leading to color variation with the generic term X-chrome, X designating the factor causing the variation, *thermo* for temperature, *gonio* for the angle, and *hygro* for humidity... Many of those phenomena don't involve color strictly speaking but rather brightness, that is why we will briefly mention them. Goniochromic structures on the contrary are the very focus of the present book.



Figure 5.8. The viewpoint is different here, but the light source remains unchanged, here in the equatorial plane at 60° on the right to the normal. The observer is in the same plane, at 30° to the normal, on its right or left. Color varies even more; from yellow— $\lambda \sim 560$ nm—it turns blue— $\lambda \sim 496$ nm. Colors also appear in the basal black pigmentary areas and in the exterior edges of anterior wings. *Papilio blumei*—10cm.



Changing Colors

Goniochromic Structures

They strictly concern iridescence. Indeed, color changes according to the viewpoint or angle (*gonio* in Greek) of light, which means that color is physical here, except for the very specific

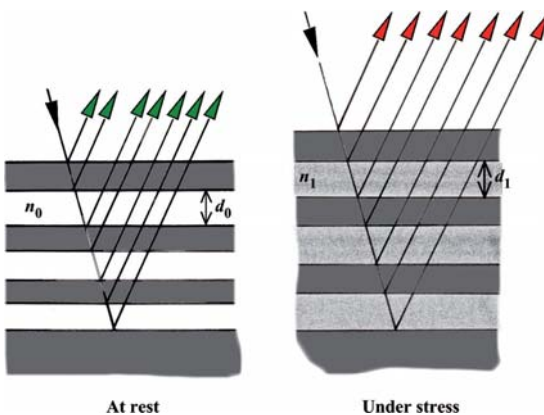


Figure 5.9. Active color change in the Australian Cassida, *Notasacanta dorsalis*. Under stress, a liquid penetrates the structure and increases the optical thickness of permeable layers.



Figure 5.10. (a) The yellow form of *Dynastes hercules*. (b) In a humid atmosphere, the naturally diffusing external cuticle gets soaked with water and becomes more transparent. Light is absorbed by deep layers.

cases of selective reflection already mentioned. The angles of observation and illumination are generally established within a system of spherical coordinates. Those effects are often spectacular and accompanied with polarization

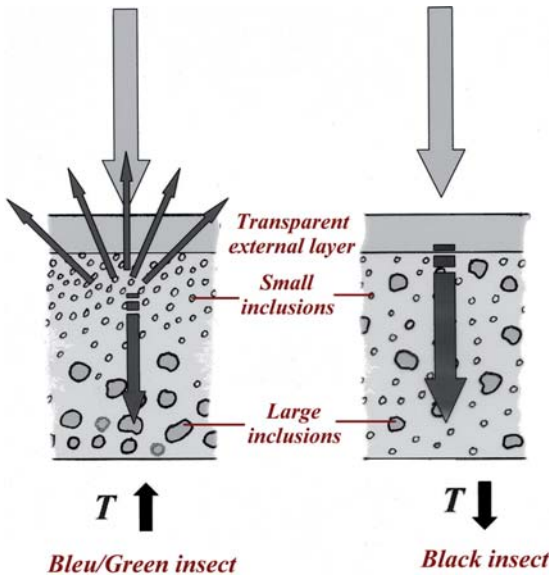


Figure 5.11. Thermic regulation in *Kosciuscola*. Under high temperature, small inclusions are on the surface and scatter light. When temperature is lower, a mix occurs and absorbs all wavelengths, the insect turning black.

phenomena. We will further study them in the chapters on physical colors.

Thermochromic, Hydrochromic, and Other Structures

We have mentioned that when the optical index of one of a components in a multilayer was changed, it could change the color of a *Morphos* from blue to green and finally to brown. This cannot occur in the reality. The only fluid a butterfly could use, water—the index of which $n \sim 1.35$ would be perfect for such a phenomenon—is yet not wet enough in order to penetrate the thin structures of scales. However, there is at least one Australian casida, *Notasacanta dorsalis*, that uses this technique. The colors are created in a multilayer, the hygrometry of which can be changed by the insect, resulting in the variation in the index and thickness of layers. This is the only known occurrence of an active change of col-

ors among insects. These variations are not related to the ambient humidity nor to the alternation of night and day, but correspond to the reaction to an aggression. This device is commonly used among other classes for camouflage or offense. This is the case of Cephalopodes (octopus, cuttlefish, and squid), some skin areas of which present a multilayer cytoplasm/water structure, the thickness of which can be quickly modified by the animal. The other color changes are strictly passive as they depend on exterior physical conditions (temperature, hygrometry...) and they more often lead to a change in the thermodynamic potential of the animal. In this case, there is no variations in color but in brightness. Among the South American big Scarabaeidae *Dynastes hercules*, the external cuticle is composed of a yellow spongy layer covered by a thinner transparent layer.

In the sun, the animal looks yellow-brown. But when hygrometry increases, the spongy layer becomes impregnated with water and turns transparent, thus letting light penetrate the deep layers where it is absorbed. The insect turns matte black. In the forest where those insects live, such hygrometry variations occur on a daily basis. Therefore, the insect looks brown during the day when it feeds under the trees and black at night, becoming invisible to its predators.

Another modification due to thermochromism: the darkening of the grasshopper *Kosciuscola* as well as many Odonata and Phasmida. During the day when the temperature is mild, *Kosciuscola* looks bluish due to the scattering of the shortest wavelengths by small inclusions consisting of leucopterines and uric acid (less than $0,2 \mu\text{m}$ high) on the surface of the integument. At night, when the temperature is falling, bigger pigmentary inclusions come up to the surface and absorb all visible wavelengths. And the insect looks black. It is assumed that these thermo-chromatic variations allow insects to regulate their temperature more rapidly.

6

Physical Colors, Chemical Colors Basics of Solid State Optics

Light—Matter Interaction, Polarization, and Optical Index

Now that we have completed our tour of butterfly colors and of their advantages for a given species and mentioned how difficult it could be to interpret them in the past, we will examine their origin in detail and try to offer a simple view of today's knowledge on this matter. We have already mentioned optical index in the last chapter, and a few basic experiments in which butterflies are immersed in various liquids. These experiments and their effects on colors are the keys for solving the problem. When one knows the optical index and the geometry of a given material, one automatically knows its color. Contrary to Raleigh and Michelson, we now have access to the geometry thanks to electronic scanning technologies—scanning and transmission electronic microscopes—and atomic force microscopes. Yet, what about the optical index?

It would go well beyond our subject to mention all the aspects of optical index theory concerning the various kinds of materials. This would leave butterflies aside and moreover, materials that concern us are all of the same type. They are insulating organic materials, so it would be pointless to study metals or semiconductors. We will therefore focus on general principles necessary to understand the physical phenomena that will be described. The index is the parameter governing the interaction of light with matter. We will first briefly describe the former and we will then move

on to the different phenomena that light produces in the material, which are characterized by the index. Under its wave aspect, a ray of light consists of the propagation of two fields: an electric field \mathbf{E} , and a magnetic field \mathbf{H} . They are perpendicular to each other and to the direction of propagation. As a consequence, the electromagnetic wave is transverse. The spatiotemporal dependencies of the fields were established in the 19th century and expressed by J. C. Maxwell in his famous equations that were named after him. We won't present these equations but only one of their simplest solutions—the harmonic plane wave (Figure 6.1) and a more complex solution that is critical for the study of Coleoptera—wave with circular polarization. Within such waves, \mathbf{E} and \mathbf{H} fields vibrate in the same plane, called wave plane, and propagate perpendicularly to this plane.

In natural light, like sunlight, no direction of vibration is imposed—the wave is said to be nonpolarized. Always perpendicular to each other, \mathbf{E} and \mathbf{H} fields can vibrate in any direction of the plane. It is yet possible to force the fields to take a specific direction of vibration or to change a preexisting direction by making the wave interact with polarizers. Polaroid films offer one of the most common examples of polarizers. If they are not as effective as the latter, Coleoptera and butterflies are also often sources of polarization. It is one of their most remarkable properties. Before studying further this aspect, let us finish presenting the magnetic field. Since \mathbf{E} and \mathbf{H} fields are not independent, it is pointless to study them both. For

Définitions	Relations
\mathbf{E} = electric field	Frequency: $\nu = c/\lambda$
\mathbf{H} = magnetic field	Wave vector: $ \mathbf{k} = 2\pi/\lambda$
\mathbf{k} = wave vector	Period: $T = 1/\nu$
W.P. = wave plane	
λ = wavelength	

both historical and physiological reasons—the eye and most of collectors are sensitive to the only electric field—optical demonstrations traditionally use the latter. \mathbf{H} variations can then be deduced from those of \mathbf{E} thanks to Maxwell's equations.

Linear Polarization

Let us first note that when a wave, even nonpolarized, falls on a surface, specific directions show up ipso facto. If one calls plane of incidence the plane defined by emergent and incident rays, whatever the direction of the incident field, it is always possible to express it as two vectors: one \mathbf{E}_s being perpendicular to the plane of incidence—(from the German term

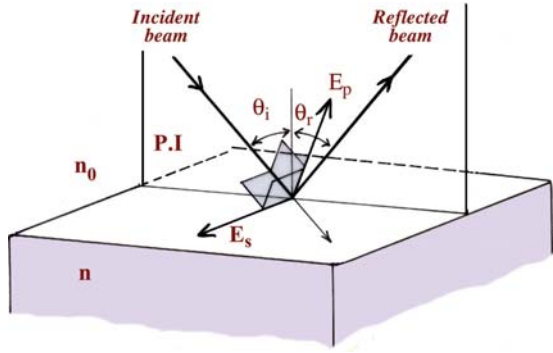


Figure 6.2. The electric fields of a nonpolarized wave falling on a dioptr. According to Descartes law, the angle of incident θ_i is equal to the angle of reflection θ_r . The electric field of s wave \mathbf{E}_s , perpendicular to the plane of incidence P.I., remains in the dioptr plane, whatever the incidence, contrary to the field \mathbf{E}_p .

senkrecht) and the other \mathbf{E}_p being parallel to the plane (*parallel*, in German).

The two fields define two perpendicularly polarized waves, which, if they follow Snell-Descartes laws establishing their propagation directions, can interact with matter in different ways. One of the most noticeable consequences is the angle dependence of their

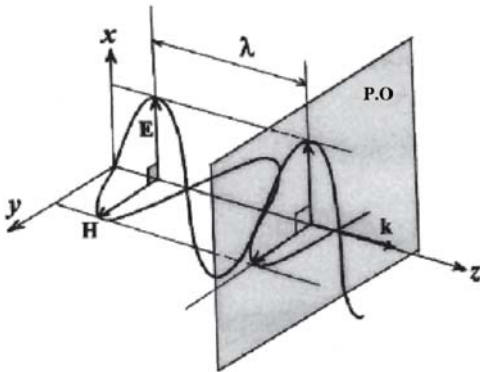


Figure 6.1. According to Maxwell equations, the \mathbf{E} and \mathbf{H} fields of an electromagnetic wave are perpendicular to each other and to the \mathbf{k} propagation direction. Under nonpolarized natural light, they can oscillate in any direction in the wave plane—W.P. Under polarized light, a vibration direction was given—Ox for the electric field and Oy for the magnetic field, on the figure above.

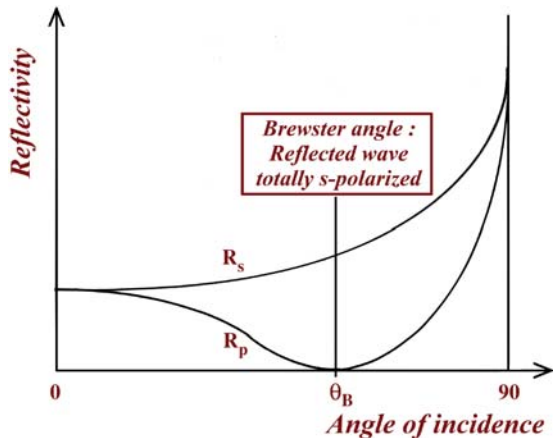


Figure 6.3. Variations in the reflection factors of s and p waves with the incident angle. For a given angle of incidence θ_b , known as Brewster angle, the reflection factor of the p wave is equal to zero; the reflected wave is totally s-polarized.

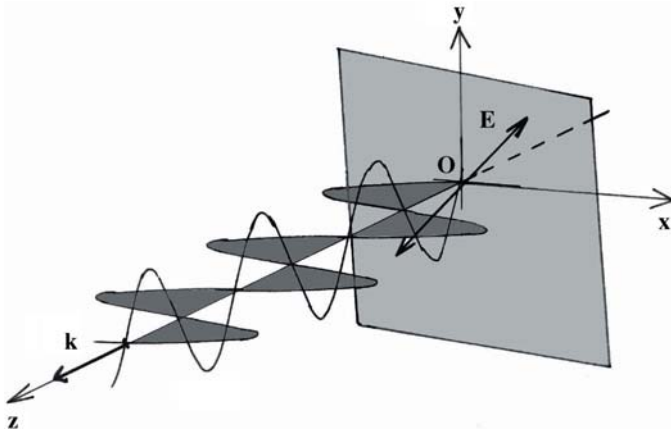


Figure 6.4. Decomposition of a wave linearly polarized into two waves in phase, E_x and E_y , before crossing any anisotropic material. In a plane perpendicular to the propagation direction, the direction of the electric field E remains unchanged during its propagation.

reflected intensity (Figure 6.3), which is often observed among butterflies.

Although that of the s wave, with its electric field remaining in the layer plane, whatever the incidence, hardly depends on the latter, that of the second wave p presents a surprising angle variation. Under a particular incidence, Brewster incidence, the p wave reflectivity is equal to zero! If one illuminates a diopter under the θ_B Brewster incidence, the reflected light is strictly s polarized. A useful consequence, which is well known among photographers, is that under this incidence, it is possible to suppress the reflections of a surface. Another consequence that directly concerns us is that under the same conditions, the light reflected by some butterflies can be highly polarized. It is well known that contrary to humans, many insects are sensitive to light polarization. Their chromatic messages are thus enriched with a new aspect! The Brewster angle only depends on the indices of the materials bathing the diopter:

$$\operatorname{tg}\theta_B = n/n_0 \quad (6-1)$$

Brewster angles of biological materials, with indices close to $n = 1,5$, put in air ($n_0 = 1$) range between 50 and 60° .

Circular Polarization

Linear polarization as mentioned above is a mere particular state of light, which is important for us since it causes interesting optical phenomena in butterflies. However, there is another state of light generated by some

Coleoptera, that we should present: circular, or more generally, elliptic polarization.

The vector nature of the electromagnetic field entails a matrix treatment of this kind of problems. We won't try to study this matrix formalism here. We will only mention it through a descriptive and intuitive approach, which will allow us to give a good overview of the different phenomena observed among insects. When one studies a single vector, like the E field for instance, it is common and convenient to orient one of the reference axes parallel to the vector. Indeed, there is no point in considering two components—which are not equal to zero—when one is enough.

However, we won't proceed this way. Let us consider a reference in which the vector E has two components: E_x and E_y (see Figure 6.4). In addition, if this field oscillates with a given frequency ω and moves in a direction k , with a speed c , so does each of its components, which thus behave like two independent waves and form the two polarization states of the electromagnetic wave. In any wave plane—a plane perpendicular to the propagation direction—the E vector extremity moves forward and back along a straight line segment. This proves that the plane wave is indeed polarized linearly.

It is well known that in vacuum, light speed is $c \approx 3 \times 10^8 \text{ ms}^{-1}$. Yet, in any other material, this speed diminishes proportionally to the optical index value of the material:

$$v = c/n. \quad (6-2)$$

In a glass block with index 1.5, light speed decreases by one third, which is quite significant. And, as will be mentioned later, many beetles elytrons consist of a very anisotropic material, roughly long sticks all oriented in the same direction. This provides the elytron with great mechanic properties and it also entails that the optical index is not the same for waves vibrating in the stick direction (slow axis) or in the perpendicular direction (quick axis) in which, according to the formula above, the wave propagates more quickly. When going out of such a material, the two waves are separated from one another by a distance d depending on the thickness of the crossed material and on the difference between the indices in the two directions. If before crossing the material, the E vector extremity of a linearly polarized wave follows a straight line segment as already mentioned, it is not the case at the exit of the medium where it in general follows an ellipse. In the specific case where the two waves have the same amplitude and are shifted from one another of exactly one quarter of wavelength—the medium is then called $\lambda/4$ slide—the ellipse degenerates into a circle; the wave is circularly polarized! We won't further study this phenomenon; we'd rather let Coleoptera illustrate it. Let us only note that making the wave cross the same $\lambda/4$ slide rotated by an angle of 90° produces the inverse process; the two waves are back in phase and rebuild linearly polarized light. This is how one can point out circularly polarized waves.

Matrix Approach to Polarization

Our purpose is not to offer a comprehensive study of the diverse polarization states of light and their transformations. Polarization effects, which are always associated with color effects produced by animal structures, represent one of the great interests of such a study and generate many industrial applications. It is therefore useful to give an overview of one of the modern approaches of light polarization: Jones' matrix representation.

In an orthonormal reference, a periodic electric field, which we have expressed in a reference formed by the diopter, and the plane of incidence can be reduced to the following

equations:

$$\begin{cases} X(t) = E_x \cos(\omega t - \Phi_x) \\ Y(t) = E_y \cos(\omega t - \Phi_y) \end{cases}$$

Where Φ is the phase difference between the two components. The vibration direction being totally determined by the two equations, they define a polarization state. In 1941, R.C. Jones found another expression, with matrix formalism this time, inspired of quantum mechanics, known as Jones vector:

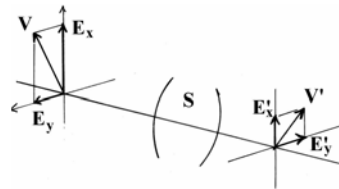
$$V = \begin{bmatrix} E_x e^{i\Phi_x} \\ E_y e^{i\Phi_y} \end{bmatrix}$$

When light travels through any optical system S , its polarization state is modified in amplitude, phase... and the outgoing Jones vector takes another form:

$$V' = \begin{bmatrix} E'_x e^{i\Phi'_x} \\ E'_y e^{i\Phi'_y} \end{bmatrix}$$

Jones matrices M express the relations between the wave polarization states before and after crossing the optical system.

$$V' = [M]V$$

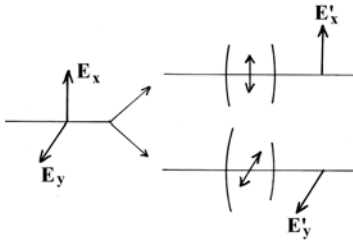


We will illustrate the few most common situations involving insects with several examples but without demonstration. We will consider the changes only in polarization direction and not in intensity. All biological media nevertheless present to various extent some absorption, thus modifying light intensities. Yet, this has little effect on color, so we will neglect this effect.

Linear polarizer. The simplest case is linear polarization, which is produced by glass reflection under Brewster incidence.

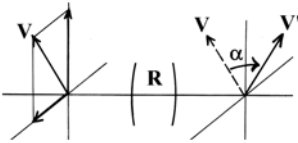
$$P_x = \begin{bmatrix} 1 & 0 \\ 0 & 0 \end{bmatrix}$$

$$P_y = \begin{bmatrix} 0 & 0 \\ 0 & 1 \end{bmatrix}$$



Rotator. Some structures, commonly found in Coleoptera elytrons, make polarization rotate. Jones matrix then takes the form of the traditional rotation matrix R .

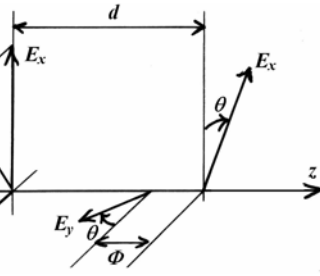
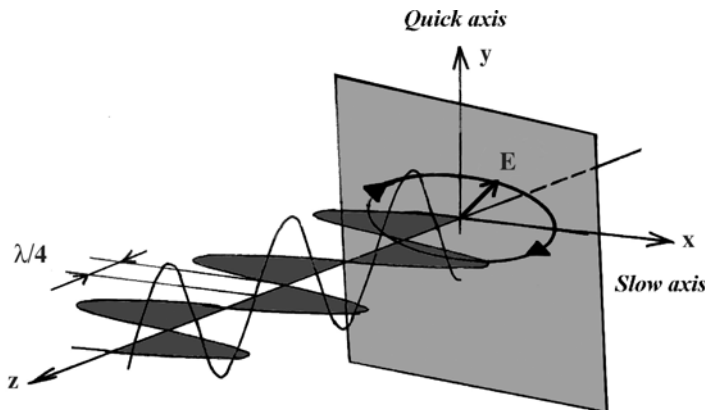
$$R = \begin{bmatrix} \cos \alpha & -\sin \alpha \\ \sin \alpha & \cos \alpha \end{bmatrix}$$



Dephasing. Finally, some anisotropic structures can produce a phase change Φ between the field components. Φ is related to the difference in the optical paths Δ of the two components by:

$$\Phi = \frac{2\pi}{\lambda} \Delta.$$

$$\Delta = \begin{bmatrix} e^{-i\Phi/2} & 0 \\ 0 & e^{+i\Phi/2} \end{bmatrix}$$



Optical Index

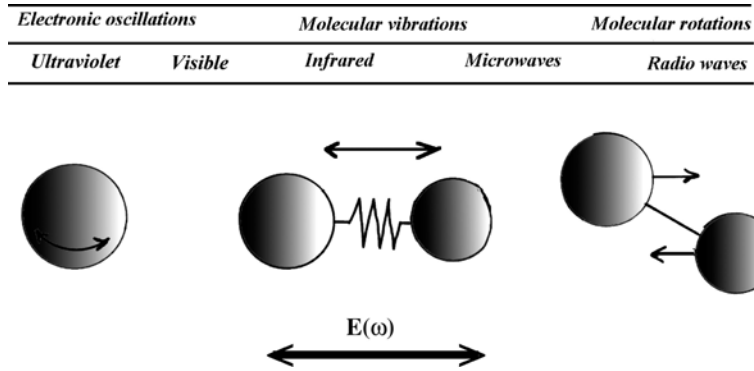
As has just been seen with the few previous specific cases, the optical index is the fundamental parameter of electromagnetic waves. We will now put waves aside for a moment in order to focus on matter and its optical properties characterized by its index.

One should first figure the various phenomena that can occur in a material when it is subject to the action of an electromagnetic wave. We will limit our field of study to material types that can be found in biological structures. We can thus exclude metals, semiconductors, and ionic crystals and focus on the electromagnetic field action. Its interaction with matter occurs through the electric charges—electrons—and produces different phenomena.

- Firstly, in every atom, the periodic electric field of the wave makes electrons move away from their initial position and deforms their orbitals, thus generating oscillating dipoles.
- Secondly, in a molecule, the field affects the links between atoms, shortening or lengthening them, changing their orientation...

Figure 6.5. After crossing an anisotropic material, the vertical component has a quarter of wavelength optical path difference with the horizontal component. The E extremity—or its projection—here follows an ellipse.

Figure 6.6. Action of a periodic electric field $E(\omega)$ oscillating on atoms or molecules in the different spectral ranges.



- The field can finally tend to orient—on average—molecules containing a permanent electric dipole in a given direction.

In any case, there is a displacement of charges. In electromagnetism, this displacement is called \mathbf{D} . As long as the applied field is not too strong—like with sunlight and traditional electric lamps—the displacement is proportional to the electric field:

$$\mathbf{D} = \varepsilon \mathbf{E}. \quad (6-3)$$

The ε proportionality constant is a characteristic of the material, or rather of its response to the action of light. Since it depends on the wave frequency, it is called “dielectric function” of the material. By definition, the optical index is the square root of ε :

$$n(\omega) = \sqrt{\varepsilon(\omega)} \quad (6-4)$$

This mere definition doesn’t tell us anything about the aspect, the value, or the frequency dependence of this index... Let us now consider the latter, with the least equations possible. It is important to note first that if the displacement \mathbf{D} (i.e., the effect), is indeed proportional to the applied field \mathbf{E} (i.e., the action), they are not systematically in phase; a field can vary very quickly, while a charge can be slowed down in its motion.

This phase difference is expressed by making ε become a complex quantity with a real part, ε_1 , and an imaginary one, ε_2 , which directly accounts for the energy provided by the wave in order to move charges, i.e., the energy absorbed by the material. Like the dielectric function, the index \tilde{n} also becomes complex and its imag-

inary part characterizes the absorption of the material.

$$\begin{cases} \varepsilon = \varepsilon_1 + i\varepsilon_2, \\ \tilde{n} = n - ik. \end{cases} \quad (6-5)$$

We won’t elaborate on the calculation of the dielectric function, which doesn’t concern us directly. A simple method consists in considering the charges in motion as small masses carrying electric charges linked to the nucleus or to neighboring charges by springs: This is the mechanistic model, basic but allowing us to understand most of phenomena. For certain specific frequencies, ω_0 , this oscillator resonates and the absorption is maximal. The model leads to the following expression of the dielectric function:

$$\begin{aligned} \varepsilon(\omega) = \tilde{n}^2(\omega) &= \varepsilon_0 + \frac{Ne^2/m}{(\omega_0^2 - \omega^2) - i\gamma\omega}, \\ \varepsilon(\omega) &= \varepsilon_1(\omega) + i\varepsilon_2(\omega) \text{ and } \tilde{n}(\omega) = n(\omega) - ik(\omega). \end{aligned} \quad (6-6)$$

N is the number of oscillators, i.e., the number of molecules or polarized atoms per unit volume, and γ is a damping term, both parameters characterizing each kind of atoms. As illustrated by Figure 6.7, the ε_2 imaginary part variation, directly linked to the optical absorption, looks like resonance peaks centered on the various ω_0 frequencies. As concerns the ε_1 real part, it tends towards the static dielectric constant $\varepsilon(0)$ of the material at low frequency ($\omega \ll \omega_0$), whereas at high frequency, it tends towards that of vacuum by decreasing. This gradual decrease of the real part of the dielectric function of insulators is important and worth mentioning. One can show that the real

and imaginary parts of the dielectric function are not independent, and that they are related to each other by integral relations: Kramers-Kronig relations.

$$\begin{cases} \varepsilon_1(\omega) - \varepsilon_0 = \frac{2}{\pi} \int_0^{\infty} \frac{\omega' \varepsilon_2(\omega')}{\omega'^2 - \omega^2} d\omega', \\ \varepsilon_2(\omega) = \frac{2}{\pi} \int_0^{\infty} \frac{\omega' [\varepsilon_1(\omega') - \varepsilon_0]}{\omega'^2 - \omega^2} d\omega'. \end{cases} \quad (6-7)$$

I decided to mention these relations here because they have an important physical meaning. First, with one component—generally ε_2 , which can be more easily determined through experiment—one can calculate the other one. Second, these relations express the index dissymmetry on both sides of a resonance, and therefore selective reflection, i.e., surface color, that was so dear to Michelson.

As has been seen, the ε_2 imaginary part of the dielectric function looks like peaks—possibly several—centered on a ω_n frequency, and between these peaks, ε_2 is almost equal to zero (6.7). The integral resulting in ω_1 as a function of ε_2 , which is a sum on all frequencies can thus be expressed as a series of integrals over the only ranges where ε_2 is not equal to zero, i.e., on the various absorption peaks:

$$\varepsilon_1(\omega) = \varepsilon_0 + \sum_n \frac{2}{\pi} \int_{\text{picn}} \frac{\omega' \varepsilon_2(\omega')}{\omega'^2 - \omega^2} d\omega'. \quad (6-8)$$

One thus notes that at high frequency ($\omega \gg \omega_n$), all of these integrals are equal to zero and ε_1 tends towards ε_0 , demonstrating that the various absorptions don't take part in the

dielectric function, but that, on the contrary, every integral has a positive value at low frequency ($\omega \ll \omega_n$) and their different contributions $\Delta\varepsilon_n$ are additive and approximately equal to:

$$\Delta\varepsilon_{1n} \approx \frac{2}{\pi} \int_{\text{picn}} \frac{\varepsilon_2(\omega)}{\omega'} d\omega'. \quad (6-9)$$

In other words, each absorption peak contributes to ε_1 at low frequency, and so does the index real part n , which is always larger in the red side of an absorption peak (low frequency) than on the blue side (high frequency). This is nothing than the mathematic expression of a well known phenomenon: The larger the mass, the more difficult to make it oscillate at high frequency. In the case concerning us, when frequency is gradually increased, molecules, atoms, and electrons stop vibrating successively. At each step, the dielectric function decreases to finally reach the value of the dielectric function of a material in which nothing vibrates: vacuum (ε_0).

Let us finally note that the index varies significantly only when it is close to resonance frequencies. Outside of these high absorption areas, within transparency windows, the index real part is not strictly constant and slightly varies with wavelength. Rather than using expression (6-6)—which still remains valid—a better account of the variation is given by an empirical expression. This polynomial expression as a function of λ , or ω , is easier to use. Its coefficients are determined by fitting the experimental variations of the index of each material.

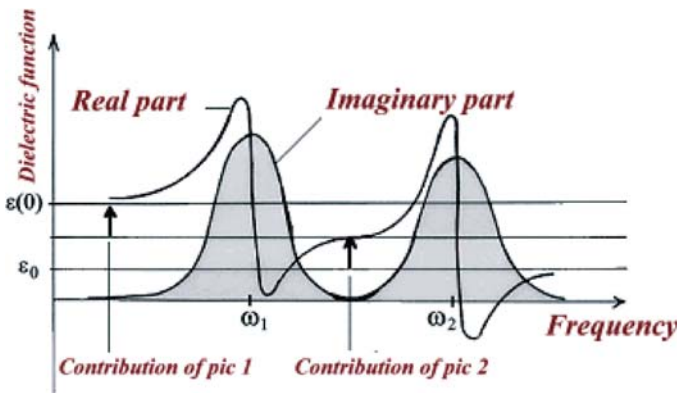


Figure 6.7. Evolution of the real part of the dielectric function of a material presenting two absorption peaks. Each peak brings a finite contribution on its “red” side, towards low frequencies. ε_1 is always larger on the “red side” of an absorption than on its “blue side.”

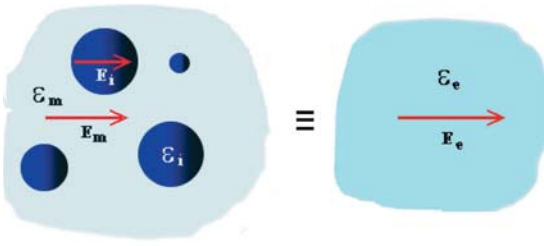


Figure 6.8. Definition of an effective medium by the mean field theory. The field in the effective homogeneous medium is the volume average of the fields in each component.

Effective Index

In what has previously been seen, the materials considered were implicitly homogeneous, i.e., containing no heterogeneity nor inclusion larger than the characteristic size of molecules. This is very rare concerning biological materials and we will later encounter media consisting of a continuous matrix containing a certain number of inclusions with various indices. In this way, we have to determine the index of such a disordered medium, after making sure that such an index has a physical meaning.

Any real medium presents heterogeneities, the typical sizes of which can vary from atomic scale (alloys, defects...) to macroscopic scale (composites, concretes...). This classification is not as simple as it seems; any such inhomogeneous medium that is scattering in the visible or ultraviolet is not scattering anymore at lower frequency, thus presenting a homogeneous behavior. Therefore, the domains are determined according to the wavelength but not in the absolute.

A homogeneous medium is indeed characterized by a rectilinear propagation of light. In an inhomogeneous medium, when light encounters inclusions, with sizes comparable to the wavelength, a scattering regime takes place. We will further describe this regime, which is widespread among butterflies. If on the contrary, inclusions are smaller than the wavelength, there is almost no scattering and the medium behaves like a homogeneous medium. One can thus try to deduce the ϵ_e average or effective dielectric function of these “homogenizable” composite materials. In the materials that we will encounter in butterflies,

inclusions are generally very small and with low concentration, so that the medium is highly dissymmetric on the one hand. And on the other hand, a matrix can be defined without ambiguity, the ϵ_m dielectric function embedding isolated and noninteracting inclusions of ϵ_i dielectric function. We will always be far from the percolation regime (which we won't mention) where inclusions, more numerous, tend to join together and form aggregates. We will focus on the simpler case where inclusions are much smaller than the wavelength, so that the electric field is—as a first approximation—uniform on the whole inclusion (in which case the regime is referred as quasi static). The method traditionally consists in expressing the E_e effective field and the D_e effective electric displacement in the composite as the volume average of the fields and displacements taking place in the inclusions with volume concentration p on the one hand, and in the matrix on the other hand.

$$\begin{cases} \mathbf{E}_e = p\mathbf{E}_i + (1-p)\mathbf{E}_m, \\ \mathbf{D}_e = p\mathbf{D}_i + (1-p)\mathbf{D}_m, \end{cases} \quad (6-10)$$

The second equation can be expressed as follows:

$$\epsilon_e \mathbf{E}_e = p\epsilon_i \mathbf{E}_i + (1-p)\epsilon_m \mathbf{E}_m. \quad (6-11)$$

Traditional electrostatic calculation allows to link the E_i and E_m fields and thus to define ϵ_e in relation to p , ϵ_i and ϵ_m . For spherical inclusions, one obtains:

$$\epsilon_e = \epsilon_m \frac{\epsilon_i (1 + 2p) + \epsilon_m (1 - p)}{\epsilon_i (1 - p) + \epsilon_m (2 + p)}, \quad (6-12)$$

This expression was established by Maxwell Garnett in 1904 and was named after him.

This average medium presents interesting properties, especially when inclusions are metallic. In this case indeed, the real part of the denominator of expression (6-12) can vanish within a specific range of frequencies, generally in the visible, leading to a high absorption generating colors. This is how stained-glass windows colors are obtained. Yet, this effect doesn't concern butterflies, so we will leave it aside. Among the latter on the contrary, the materials making the compound are often of the same type—dielectrics—and present close

index values. One can thus show that the volume average of the dielectric functions represents a good approximation of expression (6-12). This is the linear theory of mixing, which we will be able to apply to butterflies in most cases:

$$\epsilon_e = p\epsilon_i + (1 - p)\epsilon_m. \quad (6-13)$$

Maxwell Garnett's research focused on the optical properties of colloidal suspensions of metals and on the colors of stained-glass windows obtained from metal inclusions in glass. It is to this phenomenon, among others, we owe the extraordinary blues of Medieval Age stained-glass that illuminate our cathedrals. In this specific case, the quantity of metal inserted is extremely small and metal atoms, lost in a dielectric ocean, join together and form small aggregates—several tens of nanometers big—that are somewhat spherical at this stage. In order to use this approach in the framework of the biological structures concerning us, one must consider nonspherical inclusions. This development of the model was started more than half a century later. When an inclusion is subject to an electric field, a displacement of charges systematically occurs. This results in a charge accumulation on the periphery of the inclusion, which thus behaves, as a first approximation, like an oscillating dipole if the field is periodic, which is the case in optics. One can intuitively understand that the distribution of charges on the inclusion periphery and conse-

quently the dipole value depend to a great extent on the inclusion geometry. One thus introduces a shape factor, called depolarizing factor A , which modulates the intensity of the dipole generated by the field. It is generally difficult to calculate this coefficient. It leads to integral expressions with no analytic solutions, which can be determined only numerically thanks to abacus. In the more common case of spheroids and other simple geometries, these elliptic integrals are expressed by using basic functions depending on the inclusion eccentricity. We are only concerned with their graphic representations and more especially the extreme cases of long infinitely inclusions, like chitin sticks, or extremely flat inclusions, like stria lamellae. These shapes are the closest to that observed in our biological structures. The coefficient varies from the value $A = 1$ for a flat inclusion to $A = 0$ for a very elongated inclusion when the field is oriented in the direction of the revolution axis. In the perpendicular direction, it is equal to half of $(1-A)$, i.e., 0 in the first case and $1/2$ in the second. Those are the only values needed to model optical structures of insects.

A mean field calculation according to Maxwell Garnett results in the following tensor expression of the dielectric function, established by Cohen *et al.* in 1973:

$$\epsilon_e = \epsilon_m \frac{\epsilon_i [A + p(1 - A)] + \epsilon_m (1 - p) (1 - A)}{\epsilon_i A (1 - p) + \epsilon_m [1 - A(1 - p)]}, \quad (6-14)$$

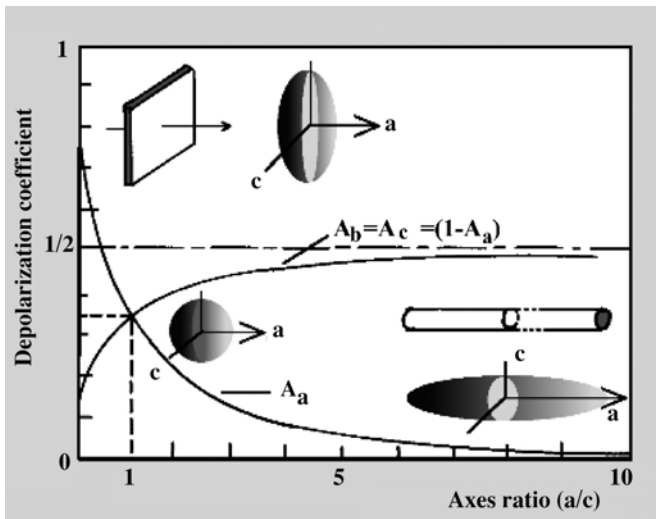


Figure 6.9. Depolarization coefficient of a spheroid in relation to the a/c axes ratio. The inductor field is parallel to the revolution axis a . Non spheroid geometries—plane and cylinder—have the same depolarization coefficients as that of very flat or elongated spheroids, respectively.

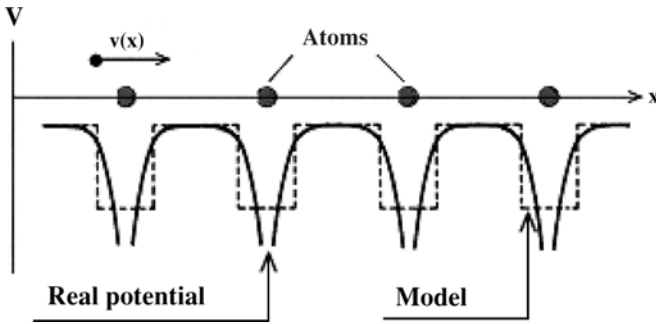


Figure 6.10. An electron moving along a 1-dimension crystal is subject to a Coulomb periodic potential that is schematically represented as a crenal potential.

This tensor expression reduces to the Maxwell Garnett's scalar expression when $\mathbf{A} = 1/3$, which is depolarizing factor of a sphere. It is important to note that for a given structure, ϵ_e wouldn't have the same value for two different orientations of the electric field. This is particularly true in *Morphos*, when the structure is illuminated with Transverse Electric or Transverse Magnetic polarized light. This anisotropy of the material index results in both colors and polarization effects observed in *Morphos*.

Structural Origin of Colors; What Kind of Logic for Structures?

The Ordered Phase; Photonic Crystals Before Time

In the traditional sense of the term, the crystal phase characterizes a periodic organization of atoms both at short and long distances. In any place on the crystal, one can observe that atoms are distributed in the same way. This strict periodicity has surprising consequences on particles trying to move within the crystal. In order to solve such a problem, quantum mechanics starts by strictly modeling the shape of the potential subjecting the particle—generally an electron—when the latter comes near atoms. This approach substantially simplifies calculations, without losing any physical meaning, and gets us closer to the optical phenomenon that are interested in here.

One then has to solve Schrödinger's famous equation, which in this case is expressed as follows:

$$\nabla^2 \psi = -\frac{2m}{\hbar^2} (E - V) \psi, \quad (6-15)$$

where ψ is the wave function of the particle and E its energy. We won't try to solve this equation, which is actually not so easy in the present case. We will rather keep in mind that its solutions are discontinuous; propagation cannot occur with any energy. Allowed energies are grouped in bands separated by energy areas—*forbidden areas*—that the particle cannot experience. The potential periodicity causes a partial quantification of energies.

Let us now come back to optics, and more precisely to butterfly structures. The particle is now a photon and its associated wave is the electromagnetic wave. What happens when the particle tries to propagate within this medium presenting a periodic alternation of index, the equivalent of the electron electric potential? Strictly the same thing happens! The equation to solve is now Helmholtz's:

$$\nabla^2 \varepsilon = -\frac{n^2 \omega^2}{c^2} \varepsilon, \quad (6-16)$$

which is expressed in the exact same way as Schrödinger's equation (the ω frequency replacing the E energy) and leads to the same type of solutions: successive bands of permitted frequencies alternating with bands of forbidden frequencies. The index periodicity causes a partial quantification of the frequency range.

The term "photonic crystal" proceeds from this analogy between electrical phenomena in a crystal and optic phenomena—also called photonic—in a structured medium.

It is in this context that we will describe the structures of the wing and the associated phenomena. From the point of view of geometry indeed, one can classify photonic crystals according to the number of dimensions in which periodicity develops.

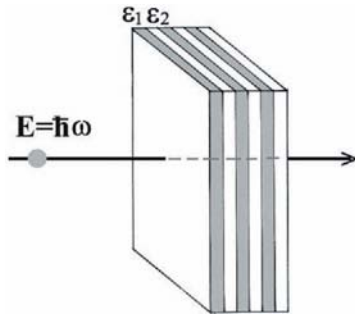
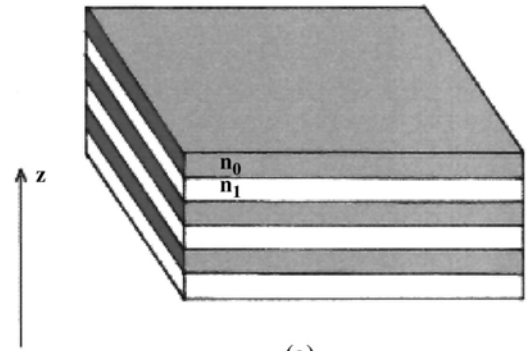
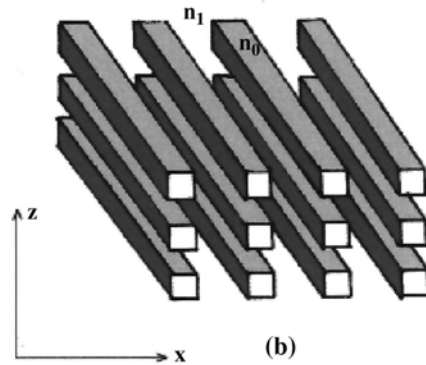


Figure 6.11. A photon with energy $E = \hbar \omega$ propagates into a stratified medium. It successively goes through high— $\sqrt{\epsilon_1}$ —and low— $\sqrt{\epsilon_2}$ index materials.

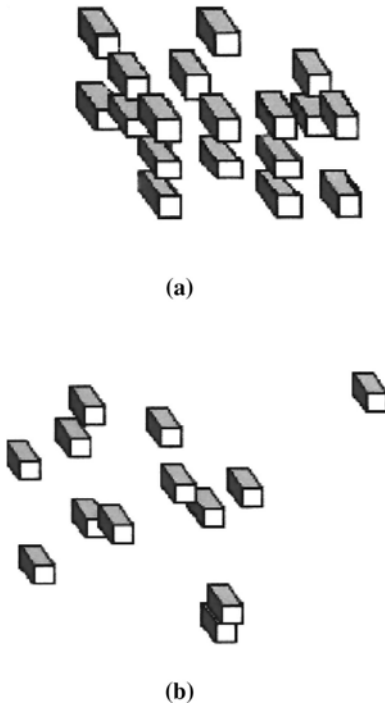
One-dimensional crystals present a periodic index following one direction, and is uniform according to the two others. It is the case, for instance, for overlapping thin layers of alternate high and low indices. One knows that such structures produce interferences, and are to a large extent—as they have been for a long time—used as dielectric mirrors, filters, and so on. In the same way, 2-dimensional and



(a)

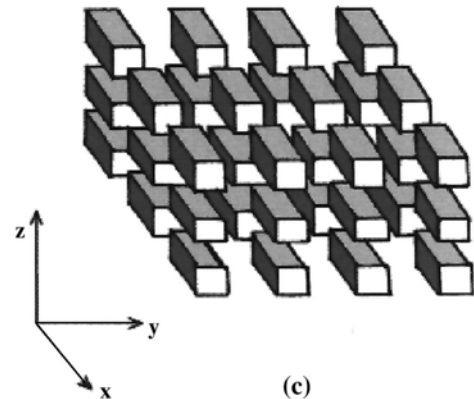


(b)



(a)

(b)



(c)

Figure 6.13. Two amorphous structures; (a) defects introduced in a periodic structure—the distances separating elements are a multiple of the crystal period. (b) The distances between elements are random.

3-dimensional crystals present periodicities in respectively two and three dimensions, corresponding in this last case the traditional geometry of mineral crystals.

These gratings are the origin of phenomena that have historically been classified as diffractive but that are actually a generalization of

Figure 6.12. Three examples of a 1-dimension (a) 2-dimension (b) and 3-dimension (c) crystalline structure.

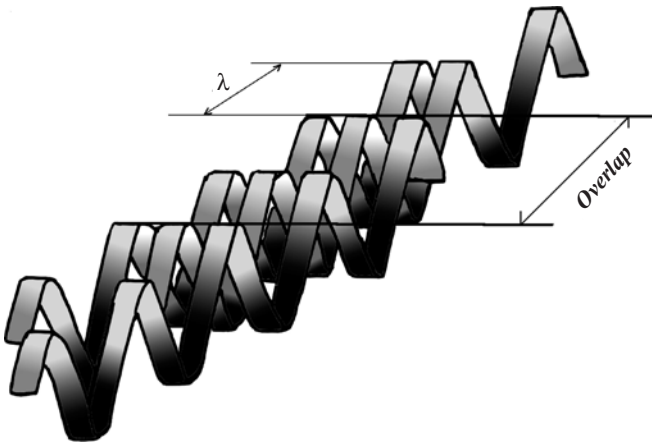


Figure 6.14. In both figures, the phase difference between the three waves is a multiple of π . (a) Their shift is inferior to the coherence length d , the overlaps are large and waves can interfere. (b) The shifts are larger than d , the waves do not overlap and cannot interfere.

interference phenomena encountered in a thin layer.

After studying ordered structures, or crystalline phases, let us now see what happens when this beautiful arrangement deteriorates, i.e., when it gets in disorder and when the phase becomes amorphous.

Amorphous Phase

All the phenomena that have been mentioned (interferences, diffraction) occur because there is a relation between the phases of the two waves diffracted by two neighboring objects, and because the periodicity of the two objects enables this relation to spread to all the waves, thus leading to a global effect that can be observed. Were the periodicity lost, the effect would vanish. Phase relations would still occur here and there, but they would not produce any global phenomenon. This is amorphous phase. Light is scattered. As the beautiful arrangement has been lost, only the sizes of the scattering objects and the compactness of the whole play a part. This is this type of structure that produces most of the blue and white colors found among butterflies in our regions. The very fine structures of *Argus* preferentially scatter blue, whereas the structures of bigger ovoid grains of *Pieridae* scatter all wavelengths, hence their whitish color.

An Important Parameter: Coherence Length

Disorder can be seen as quite an intuitive notion, but it is actually very complex and we won't tackle it. Let us only note that consider-

ing the two examples presented in Figure 6.12, disorder can proceed from two different ways. The method that may be the more intuitive consists in arranging elements at random (Figure 6.13 (b)). One can easily understand that there is no phase relation between the two waves diffracted by each of the elements. In fact, such a structure doesn't lead to any diffracting phenomenon.

One can also, as shown on Figure 6.13 (a), randomly remove elements from an ordered structure. There is no order over a short or long distance anymore. It is indeed an amorphous phase, although all the distances between elements remain a multiple of the initial crystal period. In a given direction, diffracted waves can thus very well be in phase, actually out of phase of n wavelengths the one to the others, with n varying randomly. Consequently, nothing prevents interference phenomena from taking place. Yet, this hardly occurs with natural light. The reason is quite simple: waves are not infinite but truncated. They have a beginning and an end. One thus speaks of trains of waves, and the finite length of these trains is called δ . If the distance between two objects is superior to this length, then the two resulting waves—even if they were in phase—don't superpose and therefore cannot interfere. We will call coherence length, this distance beyond which two waves in phase don't interfere anymore. Let us only remember that a periodic structure is not necessarily sufficient to produce constructive optical phenomena and that the latter can only proceed from ranges that are smaller than the coherence length.

7

1-Dimensional Structures: Interferences

Theory Recalls

Interference in Thin Layers

Interferences in thin layers are common but produce colors that are not very bright (soap bubbles, oil or gas sheets . . .). The intensity can be increased by stacking many layers. Multilayer systems are indeed commonly used in the industry but also in nature.

An optically homogeneous medium is characterized by its complex index $\tilde{n} = n - ik$ (k being equal to zero when materials are not absorbing), the physical sense of which has just been mentioned. We will follow the evolution of a plane wave from the entry to the exit interface of a thin layer. We will thus successively examine a simple interface between two different media, the front medium being usually air, with a real index $n_i = 1$. We will then study the second interface, the inferior face of the thin layer. This will be the end of our physical study, the multilayer representing a mere repetition of the same elementary problem.

The Plan Diopter

Let us consider an electromagnetic wave falling on an interface between two semi-infinite media. Part of this wave crosses the diopter—this is the transmitted wave. Another part, the reflected wave, goes back to the incident medium. On both sides of the interface, the electric and magnetic fields are not independent, as they come from the same wave. Boundary conditions impose very specific propagation directions and amplitudes, depending on

the indices of the two media separated by the interface.

The equations of continuity on the field phases indicate their propagation directions. The reflection angle θ_r is equal to the incident angle θ_i , and the angle of the transmitted wave—or refraction angle— θ_t is linked to the incident angle through the relation involving the medium indices $n_i \sin \theta_i = \tilde{n} \sin \theta_t$. These two laws are known as the Snell-Descartes relations.

As for the equations of continuity on amplitudes, they lead us to Fresnel's formulas, which link the reflection and transmission coefficients of the incident wave (s and p components) to the medium indices:

$$\left\{ \begin{array}{l} r_p = \frac{n_i \cos \theta_t - \tilde{n} \cos \theta_i}{n_i \cos \theta_t + \tilde{n} \cos \theta_i}, \\ r_s = \frac{n_i \cos \theta_i - \tilde{n} \cos \theta_t}{n_i \cos \theta_i + \tilde{n} \cos \theta_t}, \end{array} \right. \quad \text{and} \quad \left\{ \begin{array}{l} t_p = \frac{2n_i \cos \theta_i}{n_i \cos \theta_t + \tilde{n} \cos \theta_i}, \\ t_s = \frac{2n_i \cos \theta_i}{n_i \cos \theta_i + \tilde{n} \cos \theta_t} \end{array} \right. \quad (7-1)$$

Under normal incidence ($\theta_i = \theta_r = \theta_t = 0$), every wave is parallel to the layer plane, and the preceding relations become:

$$\left\{ \begin{array}{l} r = \frac{n_i - \tilde{n}}{n_i + \tilde{n}}, \\ t = \frac{2n_i}{n_i + \tilde{n}} \end{array} \right. \quad (7-2)$$

One more commonly uses the reflection and transmission factors, ratios of the reflected and

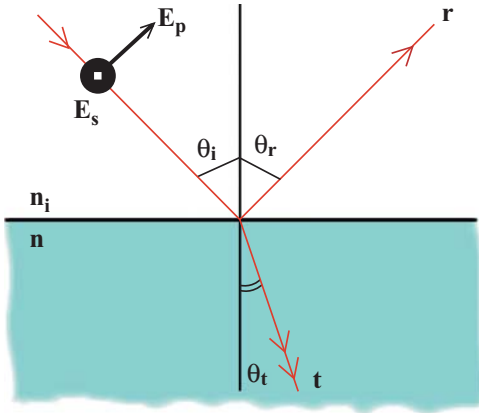


Figure 7.1. A diopter and its normal form an orthogonal coordinate system in which any wave can be split into two waves vibrating respectively in the plane of incidence (E_p) and in a plane parallel to the layer (E_s).

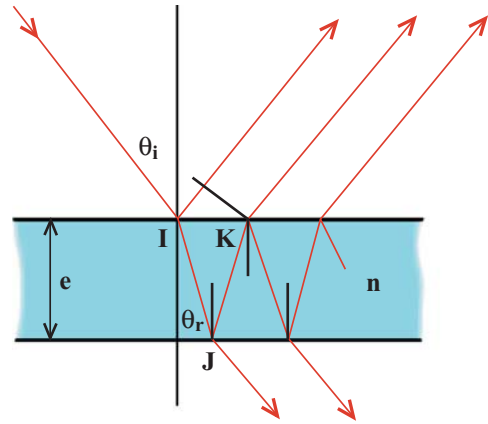


Figure 7.2. The optical path of the first rays reflected and transmitted by a thin layer. The intensities of the first two reflected rays are almost similar. The intensities of all the transmitted rays, excepted the first one, are negligible.

transmitted intensities with the incident intensity, which can be directly obtained from spectrometric measurements:

$$R = |r|^2 \quad \text{and} \quad T = \frac{\text{Re}\{\tilde{n}\}}{n_i} |t|^2 \quad (7-3)$$

In the case of butterflies in a weakly or non-absorbing medium like air, which we will often encounter, the reflection and transmission factors become:

$$R = \left| \frac{n-1}{n+1} \right|^2 \quad \text{and} \quad T = n \left| \frac{2}{n+1} \right|^2. \quad (7-4)$$

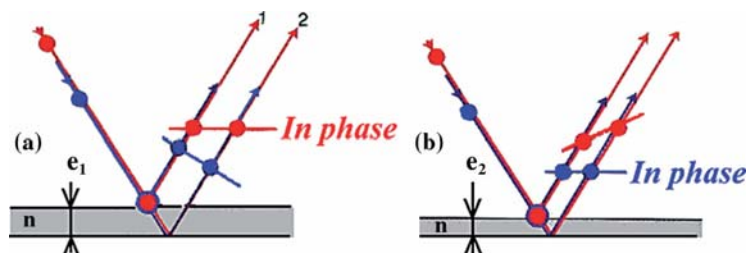
Before going further, let us note that indices of the most widespread nonabsorbing natural/biological materials (for example, water and chitin) are not very high—approximately 4% in the mentioned cases—and that most of the incident wave is transmitted. It is therefore a wave that is more affected in its propagation

direction than in its amplitude falling on the layer inferior side.

The Thin Layer

The wave reflected on the first interface is obviously not affected by the presence of the second one, but the transmitted wave now plays the role of an incident wave with a different angle θ_t . It here splits, following the same laws at the superior interface into a transmitted wave of high amplitude and a reflected wave of low amplitude. The latter, back on the upper interface, splits again into a transmitted wave and a reflected wave. Although this play of come and go between the two faces of the layer goes on infinitely, producing an infinite number of transmitted rays, it is not necessary to analyze it further. By following point by point the trajectory of the first transmitted wave and the evolution of its amplitude, one can easily observe that the first two reflected rays have

Figure 7.3. The evolution of constructive interferences according to the layer thickness. (a) For the given thickness and incidence, red waves are in phase after reflection on the two interfaces of the layer: interferences are constructive. (b) If the thickness is decreased, this behavior is followed by the blue waves.



approximately the same low intensity, whereas that of the following reflected rays are insignificant. In the same way, only the intensity of the first transmitted ray is important; interference phenomena proceeding from the reflection on thin layers can be considered as phenomena of two waves with almost similar intensities, and thus of maximum contrast. These two rays, generated by the same incident ray, are coherent and interfere. In a given direction, these interferences are constructive only for a given wavelength, which indeed gives the wanted iridescent effect in the visible.

The period difference between the two first reflected rays is:

$$\delta = 2ne \cos \theta_t + \frac{\lambda}{2}. \quad (7-5)$$

The latter are thus out of phase—destructive interferences—if d is equal to an odd number of half wavelengths:

$$(2k + 1) \frac{\lambda}{2} = 2ne \cos \theta_t + \frac{\lambda}{2} \quad (7-6)$$

For a given configuration, there is a minimal reflection for each wavelength verifying

$$k\lambda_{\min} = 2ne \cos \theta_t, \quad (7-7)$$

where k is an integer, and the reflection maximal for:

$$k\lambda_{\max} = 4ne \cos \theta_t, \quad (7-8)$$

i.e., under normal incidence, for optical thicknesses equal to a quarter of wavelength.

The Multilayer

As has been seen, the reflection factor generally remains weak. Refraction indices that are widespread in nature span from 1,34 for cytoplasm to 1,83 for guanine crystals. Under normal incidence and for an optical thickness of $\lambda/4$, such a thickness doesn't reflect much more than 8 to 9% of the incident energy for this wavelength. One can nevertheless increase quite significantly this reflection factor by multiplying the number of layers, i.e., by piling a certain number of layers of high and low indices with optical thicknesses close to $\lambda/4$.

All basic physic phenomena are contained in the treatment of the unique layer and to mathematically analyze the multilayer would not provide us with much more information. It only deprives us of the pleasure to present my teacher's, F. Abeles, delicate matrix treatment, in which every layer is represented by a matrix linking the fields at the entry and at the exit, the effect of the multilayer being obtained by multiplying matrices.

Summary

The main results, as derived from the study of the unique layer or multilayer are: (a) there is no absorption—the multilayer interferential mirror is not a colored filter in the literal meaning of the word—and nonreflected wavelengths are transmitted. The color of the transmitted light is thus the complementary of that of the reflected light. (b) As shown by the equation (7-8), the wavelength reflected by a multilayer mirror varies linearly

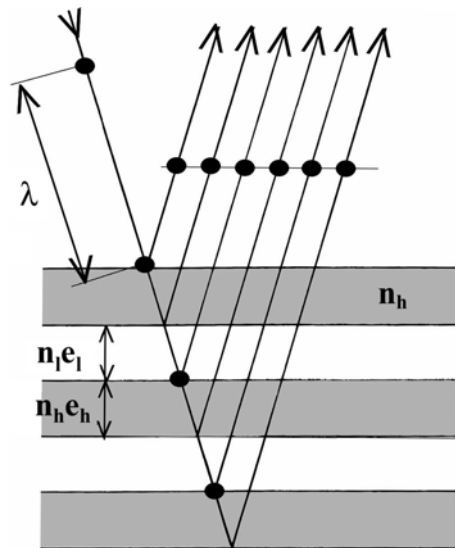


Figure 7.4. The optical path in each layer of the stack must be equal to the quarter of the incident wavelength. The waves reflected by each interface are phase synchronous. This occurs when $n_l e_l = n_h e_h = \lambda/4$. The more important the index difference $n_l - n_h$ between the two materials, the larger the amplitude of the reflected waves. Ray deviations caused by crossing each diopter are not figured here.

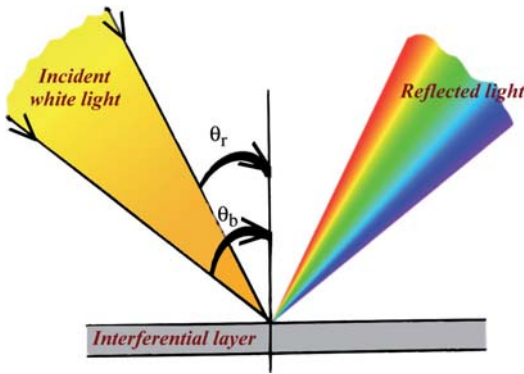


Figure 7.5. Variations of interferential colors with the angle of incident. For given thicknesses and indices, the wavelength of the reflected wave decreases when the incident angle increases; color tends towards blue.

with the cosine of the angle of incidence, and thus decreases—tending towards blue—when the latter increases. (c) Lastly, the more constant and even the thickness of the various layers, the purer the reflected color. One can almost obtain white mirrors by gradually modifying the thickness of the layers in a multilayer.

Various Types of Multilayer

In interferential phenomena, materials are involved only through their indices. They can thus occur, whatever the phase of the components—liquid, solid, or gaseous—provided the required conditions are respected. Almost every kind of combination involving at least a gaseous phase and supporting the

structure can be found in nature. The second phase can be gaseous, generally air, like among butterflies and birds, or solid among Coleoptera, fish and shell, or even but rarely liquid in cephalopods. We will also mention the possible changes in phase, a liquid replacing a gas in the structure, leading to a variation in optical thickness, and consequently of the reflected color.

Compared to pigmentary colors, and excepting colors obtained through scattering, physical colors are bright and rather pure. From the sole point of view of intensity, the messages delivered, whether sematic or aposematic, are optimized. This requires that there is no dead angle, if I may say so. However, a thin layer is a mirror, even if it selects wavelengths, as it reflects light in a specific direction. Interferential devices must therefore be associated with a system of spatial dispersion of light.

As we will see, such systems are very often present, whether on wings—Coleoptera and their convex elytrons—or on scales, or even at a smaller scale on mesoscopic structures in the scales. In any case, the diopter is deformed. Light comes under a variable incidence and the dispersion is generally associated with polarization effects. This very principle will help us classify and present interferential structures. The deformation of the diopter results in concave and convex structures, and more rarely to structures alternatively concave and convex. We will begin our study with convex structures, from the biggest ones to the smallest ones.

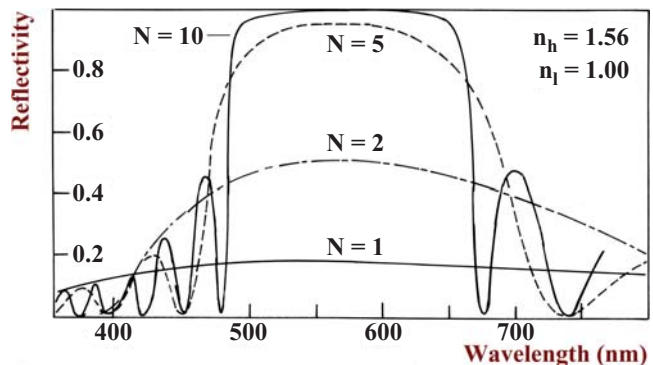


Figure 7.6. Variations in the reflected intensities with the number of layers, for a given system. Indices are approximately equal to that of air— $n_l = 1$ —and chitin— $n_h \sim 1,56$.

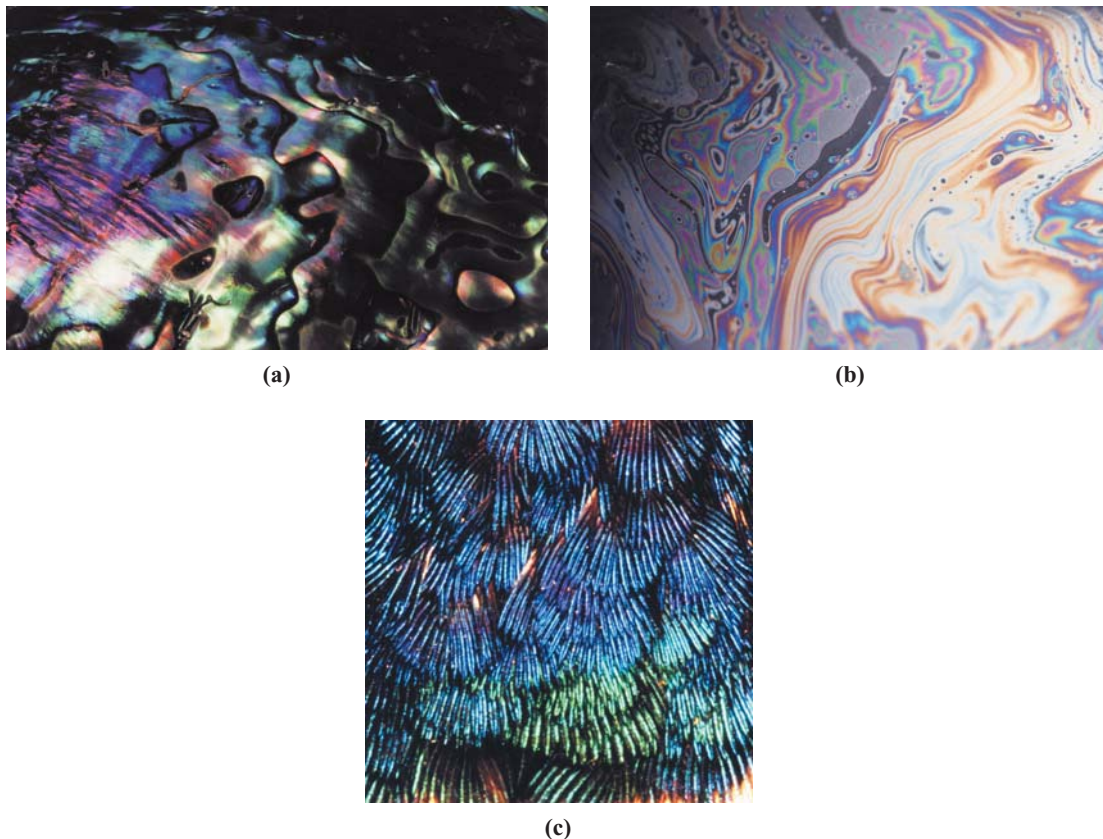


Figure 7.7. Some examples of interferential colors. (a) a solid-solid multilayer—an *Aliotis Iris* nacre. (b) a liquid-liquid multilayer; a thin layer of petrol over a water film. (c) a solid-gas structure quite similar to that of Butterflies—hummingbird feathers.

Type Butterflies with Convex Structures

Chrysidia madagascariensis, *Urania leilus*, and *Prepona*

Interferences and diffraction are the two physical phenomena leading to the most spectacular iridescent effects. They occur among miscellaneous butterfly species throughout the world, yet hardly with the same brightness as the large neotropical family of *Morphidae* and the more smaller one of *Uraniidae* represented by the Madagascan species *Chrysidia madagascariensis* and South-African *Urania leilus*.

For practical reasons, the study of colored effects has always been carried on these two families. Certain scales have even been named

after them: *Morpho* type and *Urania* type scales. Indeed, they are big butterflies presenting areas of rather homogeneous colors and are well-suited to routine spectroscopic measurements. We will comply with this convenient tradition. Yet, facility here is only apparent since at the microscopic scale, the two families do present two specific types of scales. Yet concerning *Uraniidae*, their scales are quite deformed, which makes it difficult to get a general view, and as concerns *Morphidae*, the effects produced at the smallest scale are then modulated.

We will start our study of iridescence as produced by convex structures of *Uraniidae* (mostly *Chrysidia madagascariensis*) and *Charaxinae* (*Prepona*), which provide a better basis for the interpretation at a small scale. We



Figure 7.8. The South-African *Urania*—*Urania leilus*.

will discover those butterflies by plunging into the infinitely small, according to six different orders of magnitude, and zooming out, establishing each time the principles of the optical effects are produced or suppressed.

As we have already seen, iridescence can be created either by variations in the incident angles of the light ray or by changes in the viewpoint of the observer. That is why it may be useful to specify the meaning of our notations at the beginning of this chapter. Except for contradictory cases clearly outlined, the observation of the whole butterfly as well as scales under the optical microscope is made perpendicular to the plane of the wings or the membrane. It is the light source that is mobile and its position is traditionally established by its θ azimuth and its φ declination.

Uraniidae and Charaxinae

The Uraniidae *Chrysidia madagascariensis* is a Madagascan crepuscular butterfly that lends to breeding. Its bright wings are unfortunately extensively used in handicrafts. The colors of their medial areas on both faces cover almost the whole range of the visible spectrum from



Figure 7.9. Iridescence in *Chrysidia madagascariensis*—under normal incidence (0,0) above and in low-angled incidence (90,0) below. In the anterior wings medial area, the predominant color goes from 565 nm (yellow-green) to 505 nm (green) and reaches 495 nm (blue-green) in places. What is remarkable is that effects are similar on the ventral side

green to yellow for the anterior wings and red to blue for the posterior ones. Basal and marginal areas of the dorsal side are deep black (Uraniidae warm themselves in the dorsal position), and the posterior is entirely fringed with long white scales. All those colors vary with incidence, and once dipped into trichloretylen (index: 1,478), the butterfly shows a regular brown color, which demonstrates the structural origin of colors and the systemic presence of melanin in the scales of both faces. The disappearance of black suggests that structures also

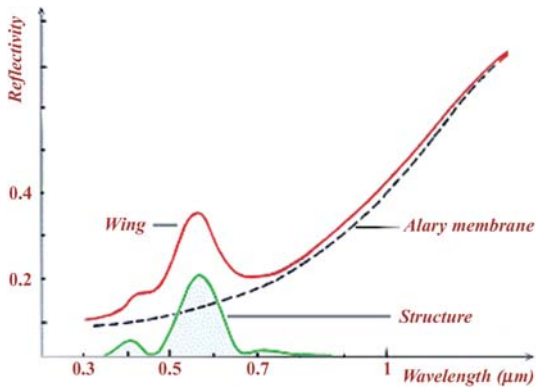


Figure 7.10. Diffuse reflection factor of the green areas of *Chrysidia madagascariensis* anterior wings—Cu1. The role of the wing membranes and of the scales themselves, which is significant in infrared, has been underlined in order to reveal that of the scales structures.

play a part, at least as important as that of pigments in the emergence of blacks, hence in visible absorption.

Reflection spectroscopic measurements carried on the green areas of the anterior wings show fringes that are characteristic of interferential effects in thin layers. The same measurements conducted on the sole alary membrane, from which the scales of the two faces were removed, allow us to point out the roles of the various components in the general reflection of the wing. We can thus confirm that scales are in charge of the visible structures, whereas most of the infrared reflection

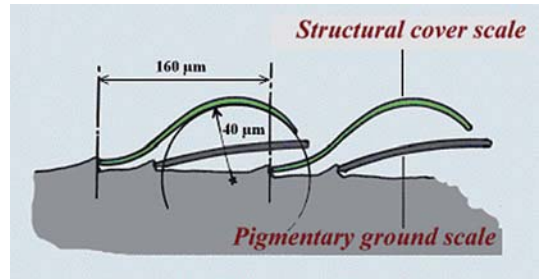


Figure 7.12. Typical arrangement and sizes of *Chrysidia* scales. Structural scales emerge almost horizontally from cupules and undergo a double curvature before covering the roots of the preceding row of scales.

depends on the membrane. These properties are quasi-constantly found among all species.

Scales are consequently the driving point of the reflecting structure in the visible field, from which colors proceed. The shift of the peaks in the visible spectrum observed under the optical microscope when varying the incidence (Figure 7.11) demonstrates that colors are interferential and thin layer-type. The high value of the reflected intensity (more than 30% at 560 nm, at the limit between green and yellow) suggests the presence of a multilayer structure given the concerned materials. Optical microscopy shows regularly implanted scales arranged in two different layers. The first layer, consisting of the bottom pigmentary scales folded longitudinally and slightly convex, form an

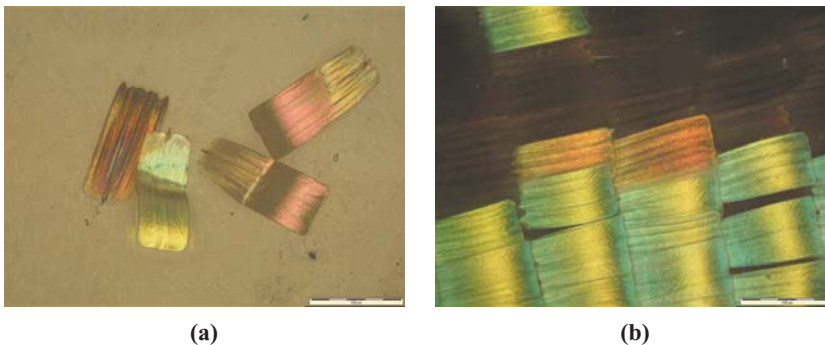
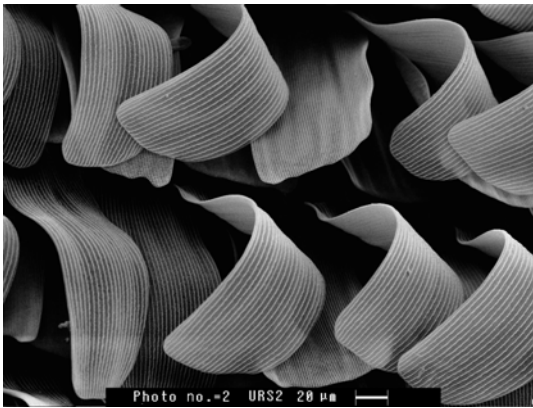
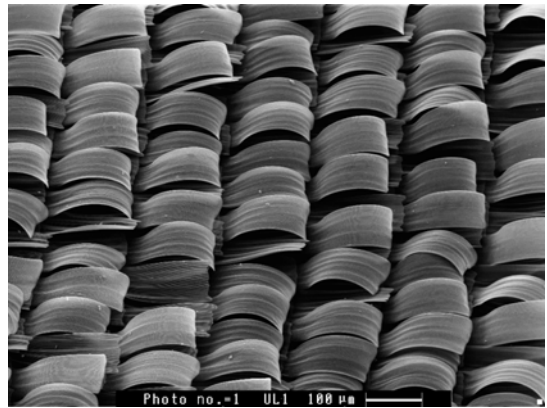


Figure 7.11. The two scales types of *Urania leilus*—in arrangement (right) and isolated (left). Ground scales form a black screen under cover structural scales that present an interferential color variation from the crest to the root.



(a)



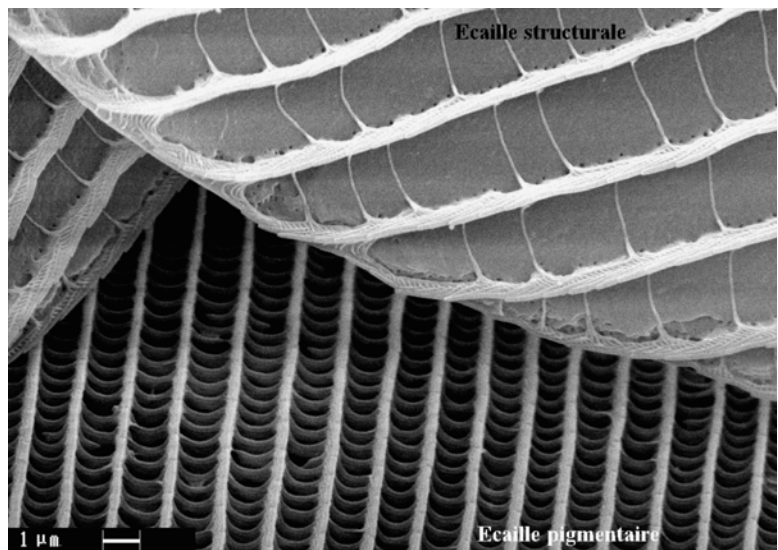
(b)

Figure 7.13. SEM views of the dorsal side of *Chrysidia madagascariensis*, (a), and of *Urania leilus*, (b). They show the general arrangement of structural scales and their significant convexity. One can distinguish pigmentary ground scales under the indented apex.

absorbing screen on which the second layer of structural scales is placed. The latter, strongly convex, slightly pigmented, and their sides adjoining, form long rolls resembling waves, on the crests of which the light is reflected, thus drawing long colored bands transversal to the wing (Figure 7.18.). An enlargement with scanning electron microscopy enables us to underline the general shape of the scales as well as their superficial structures (Figure 7.12). The

two types of scales present not very distinct longitudinal striae, with a larger spacing on the structural—about 4 μm apart—than on the pigmentary ones (1 to 2 μm). There are almost no counter-striae on the structural scales, while pigmentary scales present some that are very distinct and regular with spaces from 230 to 300 nm. It is this quite condensed alveolar structure, which is responsible along with melanin for the strong visible absorption of the

Figure 7.14. A *Chrysidia madagascariensis* structural scale above and a pigmentary ground scale below. The alveolar structure formed by striae and counter-striae shows up very clearly on the latter. It significantly increases visible absorption. Over the structural scale striae, the spacing of which is much bigger, one can note the overlap of very short lamellae inclined in a large extent on the membrane plane.



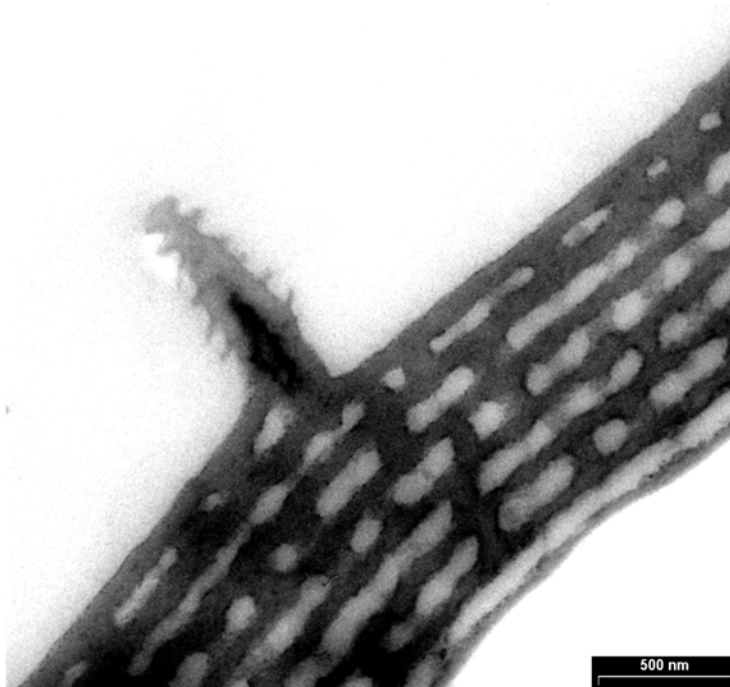


Figure 7.15. Transmission Electron Microscopy image of the cross section of a *Chrysidia madagascariensis* structural scale. The outgrowth in the center is a stria, which apparently presents a pleated structure similar to that of *Morphos*, but too small to produce any effect in the visible.

ground scales, that we will further describe in the study of the thermodynamic properties of butterflies.

Let us now observe the striae of the structural scales. They show a traditional structure composed of short lamellae that don't overlap, the length of which is almost equal to their spacing. Given their structure and spacing, they cannot be the source of the strong reflection that one can observe. One must get into the scales in order to discover the secret of the *Urania*. Transmission electron mi-

croscopy (TEM) reveals the superior membrane consisting of 13 to 15 overlapping alternate layers of air and chitin, 90 nm thick on average, and supported by microtrabeculae. TEM also reveals the external layer present's many pores. The penetration speed of the various index liquids in the scales suggests that the deeper layers should also include pores.

Between two striae (that is, on distances about 4 μm), the structure is rather flat and is easily modeled by a symmetric multilayer of

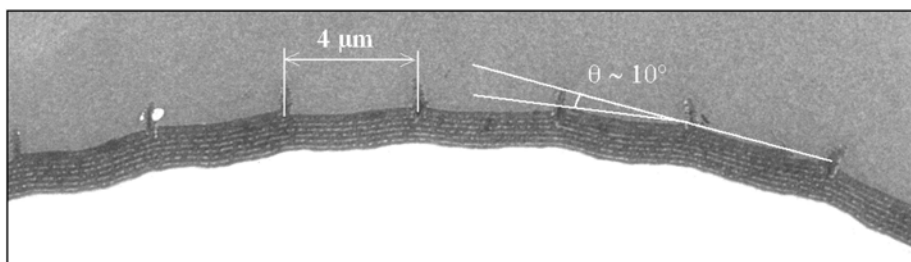


Figure 7.16. Cross section of a *Chrysidia madagascariensis* structural scale cut almost through the middle. The spacings between two striae, slightly concave, can be likened to planes tilted of about 10° in relation to each others.

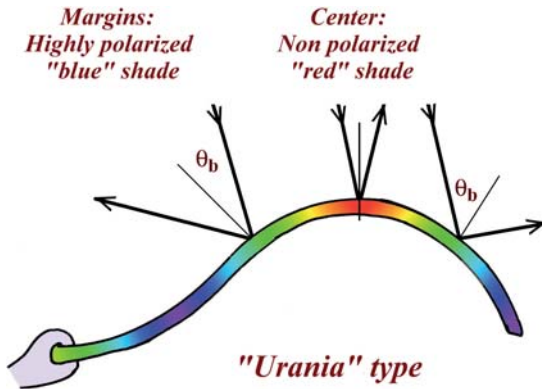


Figure 7.17. Variations of colors and of polarization (a) and schematic representation of an *Archeoprepona* structural scale. (b) A ray falling under near-normal incidence onto the center of the scale generates a non polarized color. The same ray falling closer to the apex or the root produces a bluer color (higher incidence) and more polarized (incidence close to the Brewster angle.)

chitin and air of about the same thickness and without any support. A fit of the visible reflection results in index values around 1,6 for chitin and slightly larger than 1 for the air layer, due to the presence of microtrabeculae in it. The scales being a little convex transversally, one can also assume that in this direction, it looks like a mirror consisting of 4- μm wide facets, each inclined by an angle of about ten degrees with respect to the next, slightly more in the center and less on the periphery. This tends to broaden the reflection peak, which yet remains centered on $\lambda = 560 \text{ nm}$ under normal incidence—a value corresponding exactly to what was theoretically assumed (equation 7-8) resulting in an average thickness of 87.5 nm—and to decrease the spectral purity. The same effect is produced in the longitudinal direction of course, yet substantially augmented, the scales almost forming a semicircle so that only a small area in the crest—about 50 microns—can produce interferences in the visible. Spectral purity is here again reduced.

Dispersion and Polarization

Multilayer systems can generate bright and rather pure colors, but cannot produce the

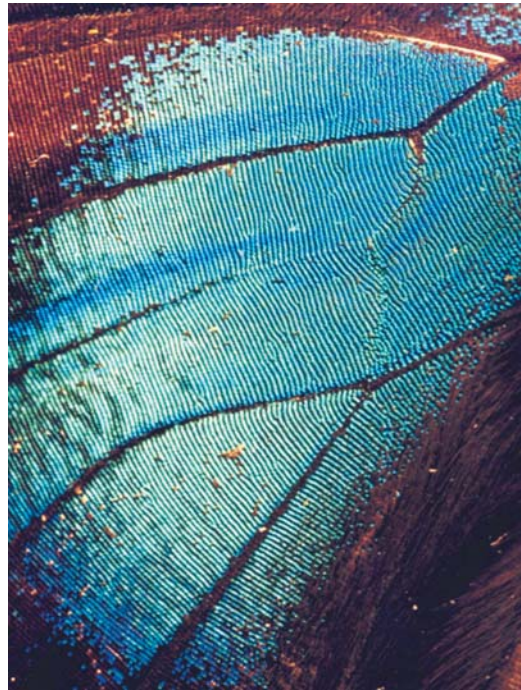


Figure 7.18. Among all butterflies with convex scales, only a part of the scale reflects light in a given direction, which results in color stripes. *Prepona* anterior wings.

spatial dispersion of light. They are consequently always associated with a dispersive system. When the convexity of scales is responsible for dispersion, as we have just seen with the *Urania*, incidence varies from the center to the edge of scales, causing the reflected light to disperse substantially with two coexisting effects. On the one hand, the incident angle increases from the center to the base of the scales apex leading to the reflected wavelength shifting towards the shorter wavelengths, hence the blues. On the other hand, certain areas are illuminated under the Brewster incidence, which makes the corresponding color highly polarized. Let us note that (Figure 7.17) the various colors are not reflected in the same direction and so don't mix. This is an iridescent effect, which is associated with a polarization effect.

Colored Effects

As we have already mentioned, structural scales are usually well organized. This is



Figure 7.19. Scattered structural scales on the *Papilio paris* black wings.

particularly noticeable in convex structures under direct light. The crests of scales illuminated under near-normal incidence create long and very bright bands contrasting with the constantly blue background formed by the base and apex of the scales illuminated under low-angled incidence.

The green color of *Uranidae* in particular is due to a mix, not pointillist, but of bands, green-yellow on crests and blue in troughs.

Concave Structures: *Papilio* and *Cincidelae*

Concave structures at the scale of scales are rather rare. If they generate wonderful colored effects, it is more of a shade effect, like in velvet for instance, than one of iridescence

strictly speaking. Iridescent concave structures are found at a smaller scale, especially—as Lepidoptera are concerned—in the big family of *Papilionidae* and among *Cincidelae* that belong to Coleoptera.

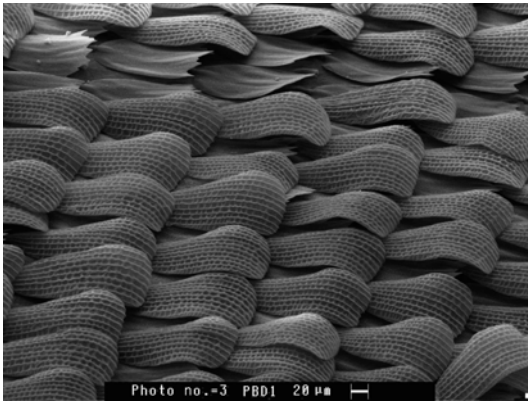
Hemispheric concave diopters belong, along with perpendicular plane mirrors, to optical structures that reflect light under its direction of incidence, whatever the incidence. It is thus not surprising that these structures produce remarkable iridescent effects, since there is no shading on scales anymore, like in the previous case. *Papilionidae* are indeed among the brightest Lepidoptera.

Papilionidae: Solid/Gas Structures

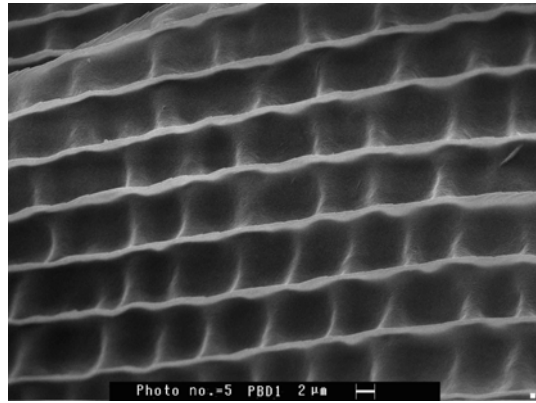
The general arrangement of scales of *Papilionidae* of the genus *papilio* is similar to those of *Urania* and *Prepona*. In colored areas, mostly green or blue, cover scales are structural and the ground scales pigmentary. Numerous species of the genus are characterized by structural scales that are scattered over the entire wings, which are very dark in addition. This produces a very beautiful effect of span-gles that are particularly perceivable under a rather high incidence.

Structural scales all present almost the same shape; slightly rectangular and convex with rounded angles. Striae are spaced (around 5 μm) and little structured. Inter-striae spacing is regularly undulated with a period and amplitude varying according to species. The striae and undulations in the membrane thus isolate basins, more or less long and deep.

Cross-sections observed through transmission electron microscopy show a stacking of layers often bigger than those of *Urania*, sometimes reaching up to 15 air/chitin series. This ensures high reflectance. The phenomenon here occurs within each basin. A light ray falling in the middle of a basin is reflected and produces a specific color, in accordance with equation (7-8), whereas another falling next to the middle will be deviated producing color slightly shifted towards the blue. There is indeed an iridescent phenomenon here, yet the



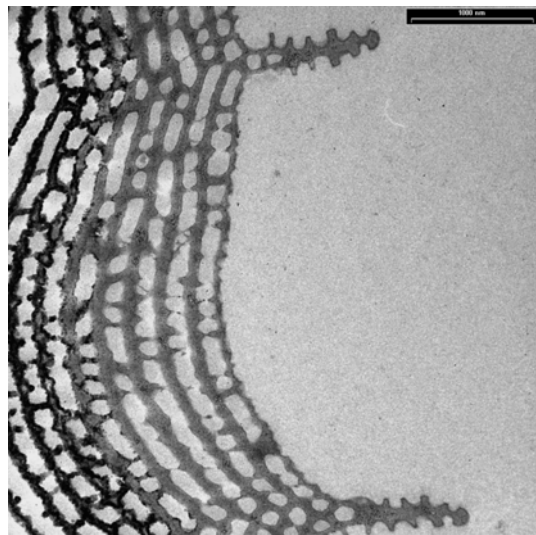
(a)



(b)



(c)



(d)

Figure 7.20. Structural organization of *Papilio*—*Papilio ulysses*. (a) cover structural scales. (b) a striated network and undulations forming a counter-striae network. Below, a section performed perpendicularly to striae next to the center of a basin and showing the (c): SEM, (d): TEM.

polarization effects are minor because of the low incidence of the wave. Even further from the center, the result is totally different. The incidence increases, getting closer to the Brewster angle (Figure 7.22). Polarization effects expand and the blue becomes more intense. A double reflection occurs, making light emerge in the incident direction. There is no iridescence anymore but a mixing of colors with the wavelength coming from the center. Here is a peculiar case of combination of structural colors. The final color, with a green predominant,

proceeds from a “pointillist effect” of the outline, blue framing green at an invisible scale. Interferential colors generated by curved structures always entail polarization effects by reflection. In the case interesting us here, these effects also occur at the scale of the thin structures of scales (basins), not always perceivable at the butterfly scale. The reason why is quite simple, as illustrated in Figure 7.24.

When a nonpolarized wavelength falls onto a basin, under normal incidence for instance, we know that in the areas that are inclined

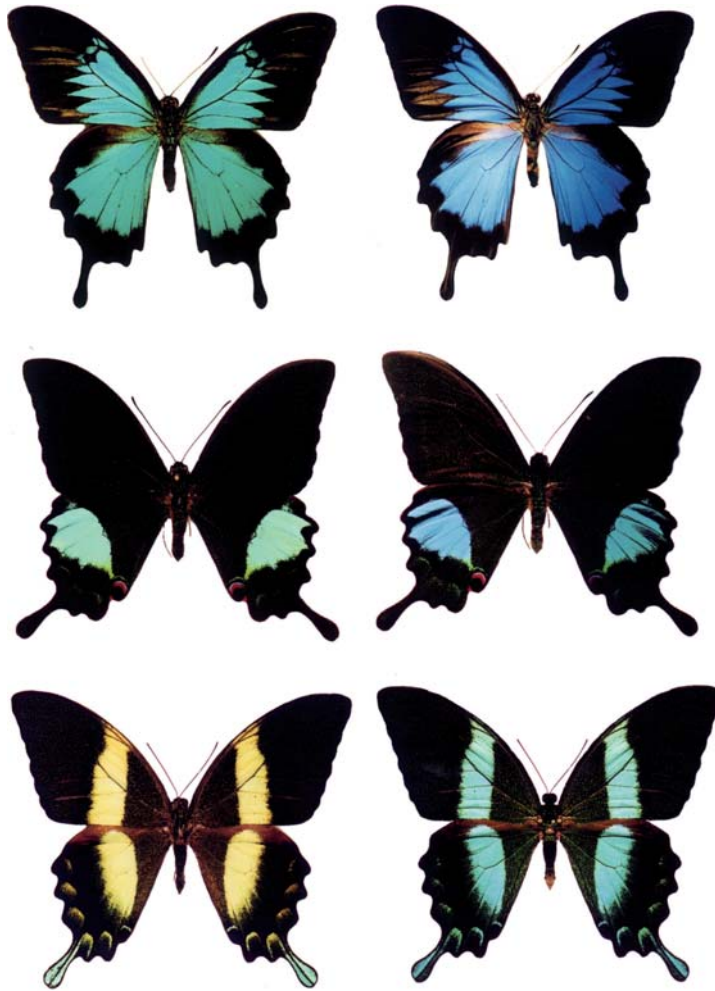


Figure 7.21. Iridescent effects on *Papilio* illuminated under grazing incidence on the right hand-side, and under normal incidence on the left hand-side. From top to bottom: *Papilio ulyse*, *papilio paris*, and *papilio blumei*.

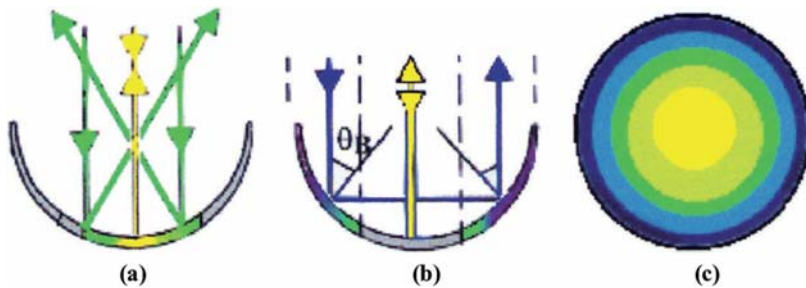
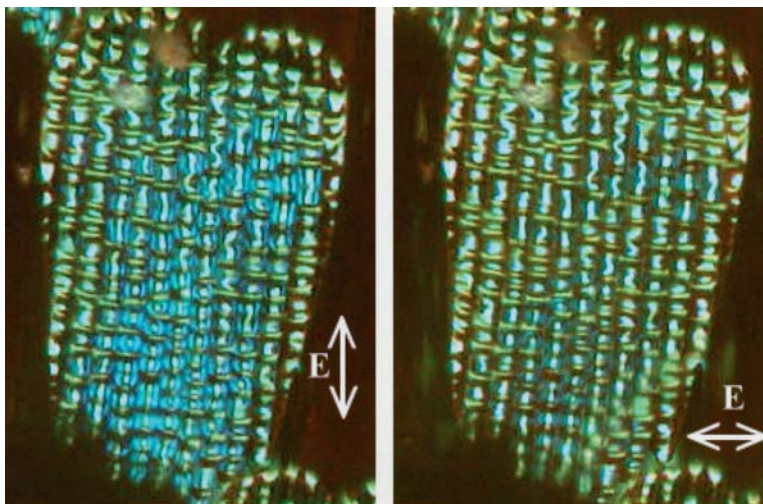


Figure 7.22. Reflection in a concave multilayer. Under low incidence (a) the center is illuminated under near-normal incidence and produces a generally yellow-brown nonpolarized color by interference. Incidence is a bit higher on margins, the color approaches green, goes out under an oblique angle, and remains weakly polarized. Closer to the basin (b) incidence is close to the Brewster angle, itself close to 45° . The reflected light is blue, highly polarized, and goes out after a double reflection, in the direction of incidence. (c) Aspect of a basin illuminated under normal incidence.

Figure 7.23. Polarization effect on *Papilio paris* scales. On the left, the polarization of the incident wave is parallel to striae. The high edges of the basin illuminated under high incidence, send back a blue polarized light in this direction. On the right, polarization is perpendicular to striae, the small edges of the basin now reflect the polarized wave. Under nonpolarized light, the elongated shape of basins leads to a reflected light that is slightly polarized in the direction of striae.



according to the Brewster angle θ_B , only the s component is reflected. If the angle is not exactly equal to θ_B , a small part of the p wave will also be reflected. Within an angle of 10° around θ_B , the p proportion doesn't exceed 10%. This case is particularly interesting, because if the Brewster angle is not exactly equal to $\pi/4$ —more around 55° —it remains still very close

to it. When the double reflection occurs with light deviating in the incident direction, there are two successive reflections both increasing the proportion of wave s over wave p, which results in a highly polarized ray, even if the angle is not optimal.

However, such a device doesn't create a polarization effect at the scale of the whole

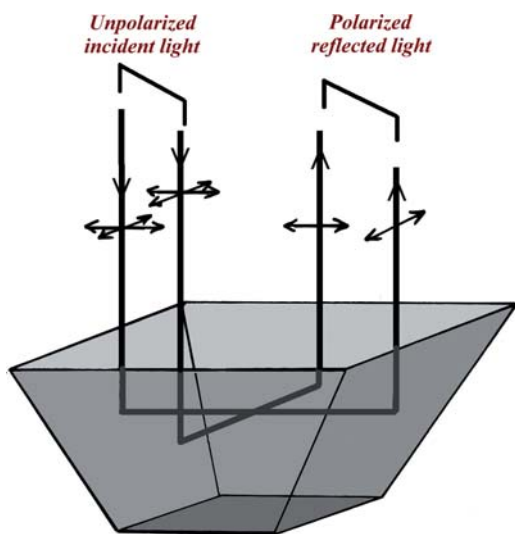


Figure 7.24. Variations of polarizations after two successive reflections under an incidence close to the Brewster angle. Emergent waves are very highly polarized, but in perpendicular directions, which generally cancels the effect.

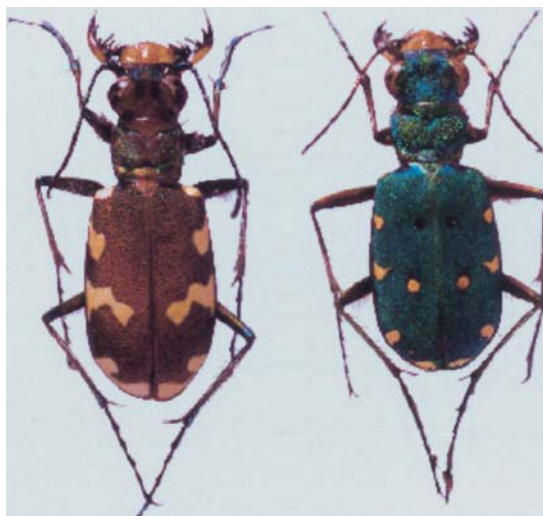


Figure 7.25. Two cincidelae of the Mediterranean regions; left, *Cincidela hybrida* Linne, and right *Cincidela campestris* Linne. (Photography and collection; Jean-Paul Leclerc—Paris).

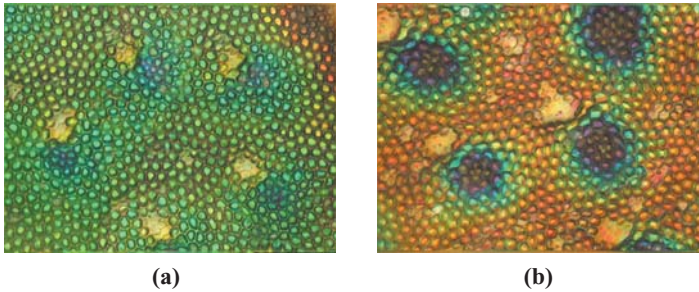


Figure 7.26. Photon microscopy views of *Cincidela hybrida* elytrons (a) and *Cincidela campestris*, (b).

butterfly, or only indistinctly in some cases. Basins present a relatively central symmetry, which makes that wave s that is reflected by the two opposite edges of the basin—let us say the left and right edges—is a wave p from the viewpoint of the two perpendicular edges (top and bottom). At the scale of the scales or of the whole wing, the reflected ray includes as many s polarized waves as p polarized waves. The *Papilio Ulysse* is a good illustration. A discrepancy can only occur when certain edges are constantly longer than their perpendicular counterparts, like *Papilio paris* for instance, in which the blue chromatic component is slightly polarized after the double reflection.

Cicindelidae: Solid/Solid Structures

Cicindelidae, or tiger beetles, are small Coleoptera belonging to the *Carabidae* with green or brown elytrons. The epicuticle surface consists of adjacent hexagonal alveoles around ten microns in diameter. Alveoles present a hemispheric section, which results in the same phenomenon observed in *Papilios* at a bigger scale and with more diverse colors.

This alveolar system includes small protuberances surrounded by some ten alveoles and presenting a color that can be quite different from the rest, sometimes violet-blue.

The cuticle has a traditional structure, fibrillated in the exocuticle and multilayered in the epicuticle. There are up to 12 stacked solid layers of 150 to 200 nm. They appear slightly contrasted under the electron microscope, hence a slight contrast in the optical index, probably minor yet sufficient to create the resulting colored effects.

All the optical phenomena described in *Papilios* can be found here, especially polarizing effects in alveoles. However, the latter don't show any lengthening in a definite direction, that is why there is no polarization including the whole insect.

Cetonia: Circular Polarization

The last interferential phenomenon to mention is that associated with optical activity. The *Cetonia* family (chafers) is well known for its extraordinary insects with bright metallic glance. It also commonly shows helicoidal structures

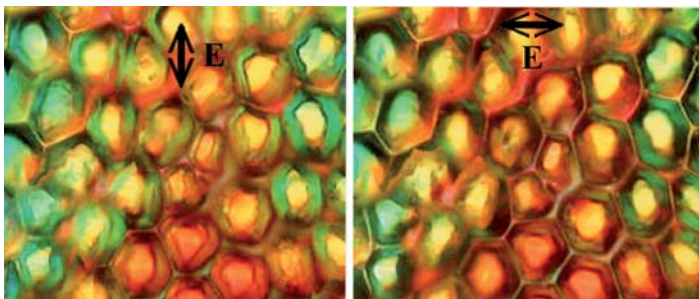
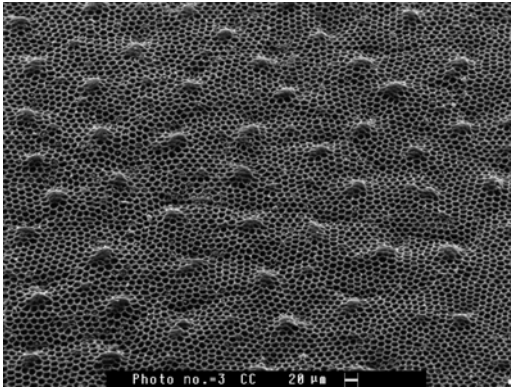
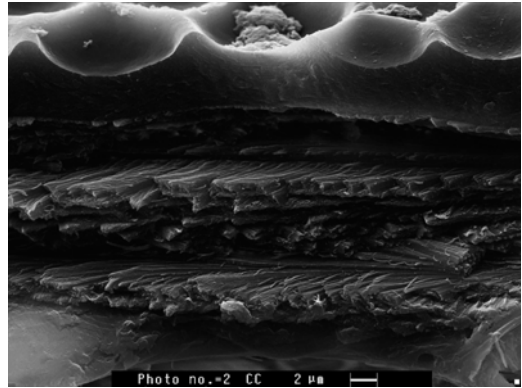


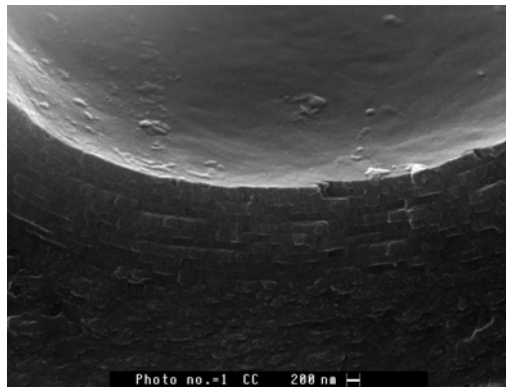
Figure 7.27. Polarization effect resulting from reflection in the basins of *Cincidela hybrida* elytrons. On the left, the polarization direction is vertical, while it is horizontal on the right. The yellow background is not polarized contrary to the green edges of basins.



(a)



(b)



(c)

Figure 7.28. SEM images of volume and surface structure of *Cincidela campestris*. (a) Surface alveolae and protuberances. (b) A section of the cuticle showing the exocuticle chitinous fibrillae and the nonfibrillated epicuticle. (c) The multilayer hemispheric structure of the epicuticle in an alveola.

that generate the peculiar polarization effects, as we have already described in the previous chapters.



Figure 7.29. The Rose chafer *Cetonia aurata* in the flying position.

This case is an anisotropic solid/solid multilayer structure with a director rotating from one layer to the other, creating a periodic gradient of index, though quite weak, in the epicuticle. This little difference in index is compensated by the large number of layers leading to the famous bright glance. It is important to note that there is no alternation of materials with low and high indices in the multilayer. Yet, the latter results from the rotation in its plane of a layer composed of a single material with two different indices in perpendicular directions. Interference occurs between layers with the same direction. It is associated with an optical activity, which can be demonstrated by using a $\lambda/4$ slide introducing a delay of



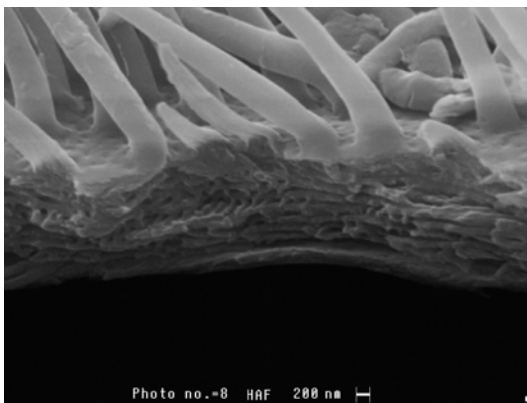
Figure 7.30. Two *Hoplia* of Europe. Left, *Hoplia argentea* and right, *Hoplia cerulea*.

130 to 135 nm—so, a $\lambda/4$ slide for a wavelength $\lambda = 550$ nm corresponding to the green color of the Rose chafer for instance—followed by a linear polarizer.

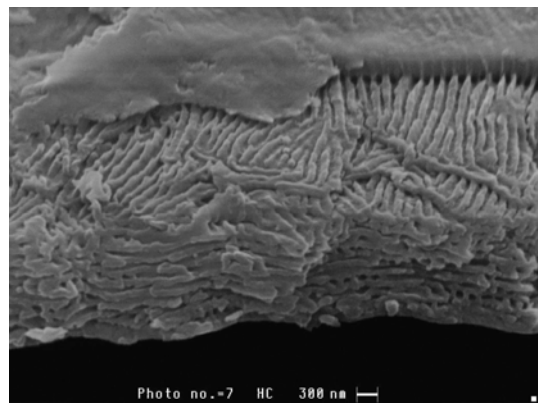
All the measurements suggest that polarization is counterclockwise on the two elytrons and that the axial symmetry of the insect is thus not respected. The origin of the layer rotation remains obscure. It could be the result of the daily alternation of illumination during the nymphal stage. It can be suppressed by keeping the insect exposed to a constant illumination.

The *Scarabeidae* family includes other members with elytrons covered with scales. The arrangement, morphologies, and structures of these scales differ greatly from one species to another. We have already mentioned in the third chapter the singular arrangement of *Hoplia cerulea* scales, resembling that of a fish, but also as singular the scales of *Hoplia argentea* that are covered with thin radicles.

In the absolute, treating such a problem is tedious, yet it is somewhat simplified in the present case, in which the coefficient of phase delay $\beta = (n_e - n_0)k_0$ is large compared to the



(a)



(b)

Figure 7.31. Cross section of *Hoplia* scales. On the left, a female *Hoplia argentea* scale and *Hoplia cerulea* on the right. Layers are well visible and set equally apart, but their individual structures are quite disorganized.

rotation coefficient α of the director given by $\theta = \alpha Z$. (n_e and n_o are the extraordinary and ordinary indices of the material, k_0 the wave vector, and Z the traveled distance measured from the surface.)

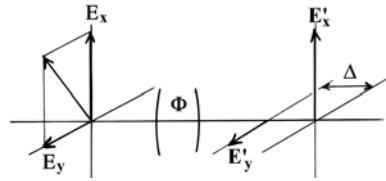
One thus demonstrates that the Jones matrix of the system giving the polarization state of the wave after a travel on a distance d can be expressed as follows:

$$\mathbf{T} = \mathbf{R}(-\alpha d) \begin{bmatrix} \exp\left(-j\beta \frac{d}{2}\right) & 0 \\ 0 & \exp\left(j\beta \frac{d}{2}\right) \end{bmatrix},$$

i.e., like the product of an optical activity and a dephaser.

After a travel on a distance d in such a material, the two components have rotated of an

angle θ and the one remaining parallel to the quick axis (E_x on the figure) is ahead with a phase difference of Φ .



A microscopic observation reveals in the scales a multilayer solid/gas-type structure without any specific orientation of fibrilles. *Hoplina argentea* radicles, whether male or female, 300 nm in diameter and 1 to 2- μm long, scatter the reflected light and weaken substantially the elytron brightness.

8

2-Dimensional Structures: Interferences and Diffraction

Theory Recalls

Diffraction by Gratings

It has been noted that butterfly scales showed on their superior faces a system of striae, often very regular, which can explain iridescence through diffraction. Many biologists in the late 20th century defended this hypothesis and Michelson again was attracted to it for a moment. We will briefly review the principle of grating and the most obvious characteristics of the color created through diffraction.

A plane grating is a system consisting of numerous diffracting elements, known as groves, and regularly spaced. Groves can be slits separated by opaque areas in transmission gratings, or mirrors in reflection gratings. As with insects, iridescence is the more often observed in reflection, so we will illustrate our study with the latter, the physics of which is the same of the former.

When an electromagnetic wave falls on such a grating, it is diffracted in all directions by each grove serving as secondary sources, so that outgoing waves—here the reflected waves—will interfere. For a given wavelength, these waves will be in phase in certain directions and they give constructive interferences, while they will be out of phase in other directions leading to destructive interferences. These directions thus only depend on the grating period and the incident angle. Under white light, each wavelength will interfere constructively in a different direction. These two aspects are characteristics of iridescence.

If one considers an incident monochromatic wave under an angle i on two groves spaced of a , the difference of period between two diffracted waves in one direction i' is:

$$\delta = a (\sin i + \sin i') . \quad (8-1)$$

The interference between the two waves is constructive when they are in phase, i.e., when the period difference d is a whole multiple of the wavelength:

$$a (\sin i + \sin i') = \pm k\lambda, \quad (8-2)$$

or also:

$$\sin i' + \sin i = \pm kn\lambda \quad (8-3)$$

where n is the number of groves per unit of length.

If a white light illuminates the grating, one concludes that for $k = 0$, all the wavelength interfere constructively in the same direction (the direction of the specular reflection $i = i'$), thus producing white light. But one also concludes that the wavelengths are separated and form spectra for all of the other orders ($k = +/- 1, +/- 2 \dots$).

For a grating of 1000 groves per mm such as one formed by the scale striae, and a blue wavelength $\lambda = 400$ nm under normal incidence ($i = 0$), equation (8-3) shows that k can only be equal to 0, ± 1 and ± 2 with corresponding deviation angles around 0, $23^\circ 30'$ and $53^\circ 6'$. In the red, at the other end of the spectrum ($\lambda = 700$ nm), k can only be equal to 0 and ± 1 and the deviation angle is around $44^\circ 30'$. The higher k and the larger the wavelength, the greater the



Figure 8.1. One of the most widespread examples of a grating; diffraction resulting from burning a compact disc.

dispersion. Contrary to prism, and in every order, red is more deviated than blue.

I described in the most simple way the principle of diffraction and the properties of the diffracted wave. Many aspects of the theory have purposely been avoided, yet what has been mentioned allows understanding the phenomena observed among certain butterflies. Yet, other phenomena cannot be explained as simply, especially those related to the polarization of the diffracted waves. We won't either address complex gratings, multiple-periodicity ones for instance, whereas they characterize those found among butterflies.

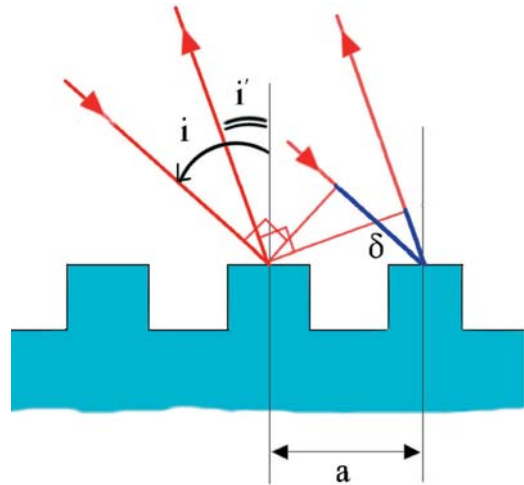


Figure 8.2. The optical path difference between two beams diffracted by two adjacent grooves depends on the angle of incidence i , the angle of diffraction i' , and the grating period " a ". The larger the period " a " and the difference between i' and i , the higher the phase difference between the two waves.

The rigor that is necessary to address such aspects would go beyond the limits of this book. The structures found among *Morphos* and their optical properties, which will be studied later, are sufficient to convey the richness and complexity of the phenomena. We can still mention them by wondering why, for instance,

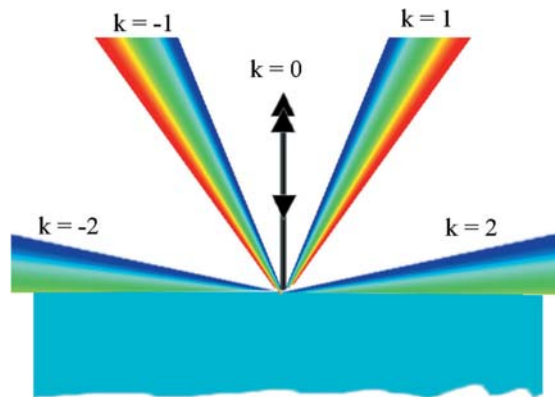


Figure 8.3. The number of orders is limited by the sine modulus ranging from 0 to 1. In the illustrated case, the period is 1000 grooves/mm, which is close to that of iridescent butterflies. Only the orders with $k = \pm 1$ are whole. When $k = \pm 2$, only the shortest wavelengths—green and blue—remain visible.

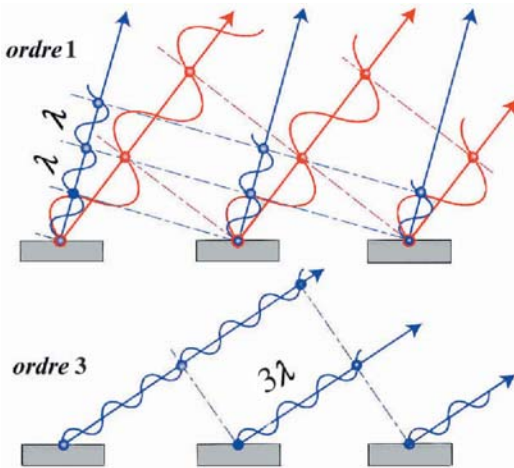


Figure 8.4. The different orders. In order 1, two waves proceeding from two neighboring motifs present an optical path difference of one wavelength, three in order 3...

the whole optical spectrum is never observed in the light as reflected by *Morphos* wings. The latter obviously present a grating structure but its color varies between only violet and blue-green. In the traditional presentation that has just been made, we have assumed that each groove interacts with each wavelength in a similar way. Although the term is not appropriate for such tiny elements, it has also been assumed that the reflection coefficient of the mirrors forming grooves was the same along the whole spectrum. Yet, one can assume that it is different and that in one way or another, only short wavelengths are diffracted, the remaining ones being transmitted and absorbed by bottom layers. Only reflected colors will be found in every order, including in the 0 order, which is not white anymore.

Another possible cause would be the presence of a period so short that no whole order can be visible and that only the smallest wavelengths of the first order, which are the less deviated, appear. Let us note that in this case, the whole of the spectrum should be in the 0 order, thus appearing white.

The reality is more complex of course, and is somewhere between the two assumptions! In fact, the periods found on scales are quite close, among certain species, to $0,5 \mu\text{m}$, which

is required to produce the second effect. Interferences, a phenomenon selecting short wavelengths, also occur within each of the striae. They are constructive for blue waves and destructive for reds. As we will now see, striae indeed show a vertical lamellate structure.

This confirms the double periodicity in two different directions: the first in striae in the plane of scales (and slightly wings), and the second in the striae lamellae perpendicularly to the scales. Here lies all the complexity of *Morphos*, and the origin of their beauty.

Gratings are commonly used in many laboratory materials. In spectrophotometers, for instance, they are used to separate the various wavelengths of a light beam, but also in many other applications, like CD players. Everyone has at least once looked at the iridescent colors of light rays reflected on a microgroove and even more on compact disks possessing a higher reflection factor. They are yet much rarer in nature, as the detailed study of *Morphos* will demonstrate. Diffraction partly generates the colors of the coleopter *Serica sericea*, and of certain arachnids like *Cosmophasis thalassina*. Yet, it is often difficult to distinguish the respective roles of interference and diffraction in the colors resulting from these structures, as they tend to be interwoven. In the case of surface gratings, a rather simple technique is to take a replica of the surface and to examine its color. In this way, one gets rid of interferential structures that are 3-dimensional, and only the colors generated by gratings remain.

Let us finally note that contrary to interferences, diffraction produces color, but also scatters it spatially. In this way, this function doesn't depend on scales anymore, which are usually quite flat, as we are going to see now.

Type Butterflies with 2-Dimensional Structures

Morphidae

Morphidae is slightly more complex. The *Morpho* genus (there are two others in the family: *Antirrhoea* and *Caerois*) includes more than

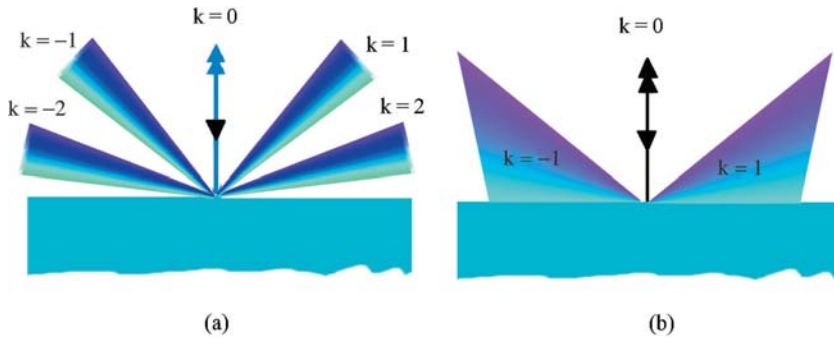


Figure 8.5. (a) Selective diffraction. Long wavelengths are either transmitted or absorbed. Only short ones can be found in each order, including in order 0. (b) High dispersion. Under normal incidence, a 2000 groves/mm grating diffracts only the wavelengths shorter than 500 nm—blue-green—in the first order, while they are all present in the 0 order.

30 species and many sub-species, all presenting a strong sexual dimorphism. That is why it is not an easy task to choose a species for our study. Our predecessors tended to choose one more because of some opportunity rather than based on rigorous scientific reasons.

All male *Morphos* show marked iridescent effects with a predominant blue. Some are very dark, of a deep blue, while others are almost white with only a slightly bluish touch. Many present marked bright colors, whereas others have a matte surface that seems to extensively diffuse light. One could thus classify them very basically in a plane according to two criteria: brightness being the first coordinate and ranging from 1 for a mirror to 0 for a perfectly scattering surface, while the second coordinate representing spectral purity ranging from 1 for a monochromatic color to 0 for white. This is merely a subjective classification, which isn't based on any measurements. We have chosen our standard *Morpho* (*Morpho menelaus*) among the species classified in the center of this plane, eventually selecting the more common ones in order to study them morphologically and optically, and to widen our study with some other species of the plane by focusing more on differences.

Morpho Menelaus: Characterization and Modeling

Our choice proved relevant, *Morpho menelaus* revealing average in every way as it seemed

a priori. It is also a *Morphalidae* widespread in the Amazonian basin and even in Bolivia. The male is entirely blue on its dorsal side, excepting the abdominal and costal edges, fringed with black. It is cryptic on its ventral side with three ocelli on posterior wings and two on the anterior, all little developed. As has already been shown in Chapter 5, these colors vary with the exterior medium index, demonstrating without any ambiguity their structural

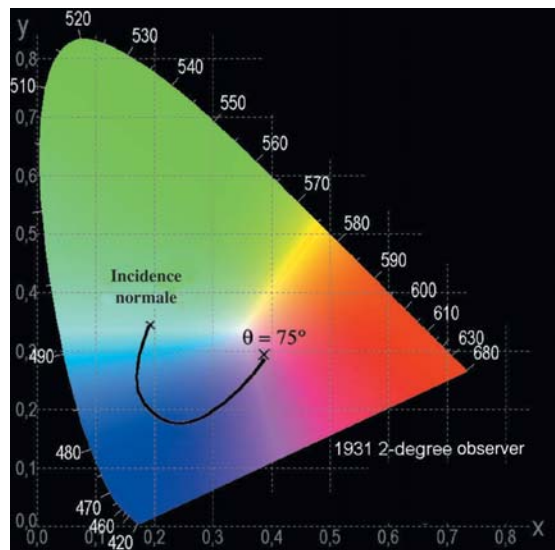


Figure 8.6. Iridescence curve of a *Morpho menelaus* in the CIE chromatic diagram from normal incidence to grazing incidence. The curves are interpreted in chapter 13.

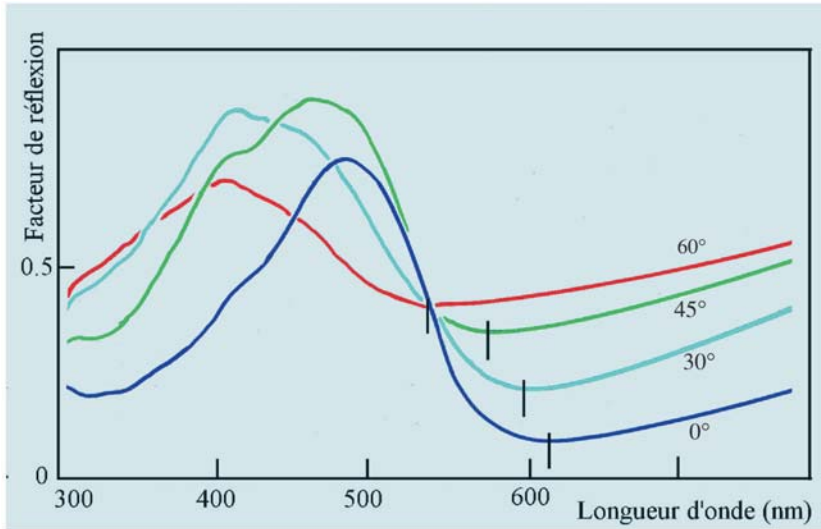


Figure 8.7. Reflection factor of a *Morpho menelaus* whole wing for different negative incidences, (from the base to the apex). Angles have been measured from the normal to the wing plane. One must add 10.5° in order to obtain incidence on the interferential structure.

origin. Immersed into a medium with a rather high index, close to that of chitin, and when colors have totally vanished, the butterfly looks extremely dark, revealing concentrated pigments on either face.

Iridescence is particularly marked, as shown by the series of pictures in Figure 8.8. The evolution and characteristics of colors will be studied further, but let us now first focus on the aspect of the butterfly under various illuminations. What is the most remarkable initially is the important dissymmetry of colors in the wings when illuminated under the same angle from the right or the left. This suggests that reflecting structures on the wings are inclined. An obvious fact that Michelson missed, yet he had then to assume that the structure existed. Visible and near-infrared spectrometric measurements, performed on the big homogeneous areas of cells M3, Cu1, Cu2, and discoidal, confirm this initial visual impression.

Indeed, through measurements performed from the apex towards the base or the reverse, one can observe a shifting in the spectral structures towards blue when the incident angle increases, with maxima and minima in various places for a given incidence. In addition,

amplitudes differ, as can be seen on the chromatic lines obtained from spectral measurements and which, contrary to an isotropic thin layer, do not overlap. This observation questioning Michelson's interferential hypothesis could, on the contrary, confirm it. As has been seen in the last chapter, the reflection minima of an electromagnetic wavelength on a thin layer are given by:

$$k\lambda_{\min} = 2ne \cos \theta_t$$

This equation can be rewritten by involving, not the θ_t refracting angle, which we don't a priori know, but the θ_i incident angle. Snell's law allows to modify this variable and results in the following apparently more complex expression:

$$\sin^2 \theta_i = -\frac{k^2}{4e^2} \lambda_m^2 + n^2 \quad (8-4)$$

Nevertheless, under this form, one notes that $\sin^2 \theta_i$ varies in a linear way with the square of the wavelength λ_m . The slope of this straight line gives the thickness of the layer and the abscissa at the origin its index. In pre-computer times, this simple graphic method allowed us to determine indices and thickness layer. Subjected to spectral measurements performed on

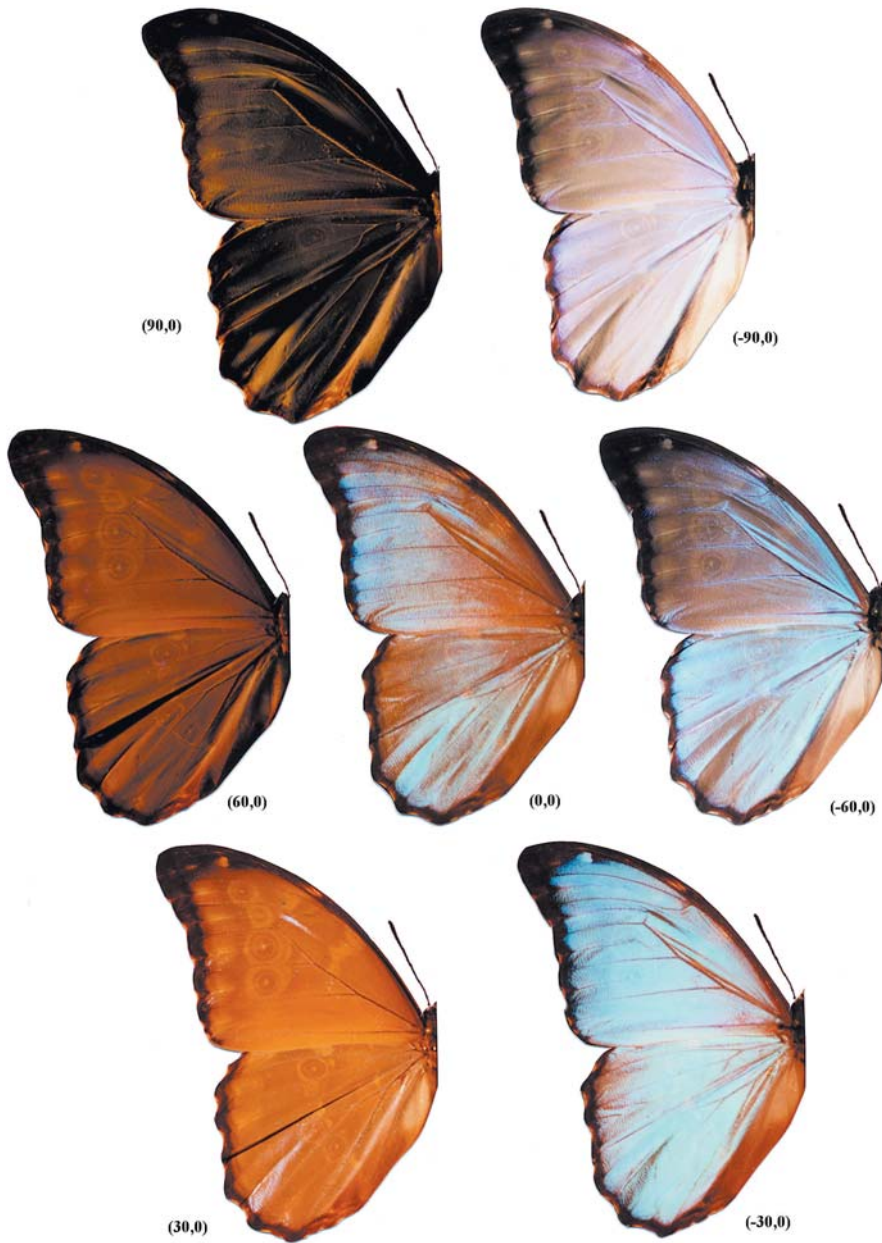


Figure 8.8. Iridescence effects on *Morpho godarti* exposed to collimated illumination. One can note that colors vary quite substantially depending on the illumination direction—from base to apex or the opposite.

M. menelaus, one notes that, like Michelson, this linear variation isn't respected, and by far. Experimental points form large arcs of circle: concave for positive incidences and convex for negative ones.

The dissymmetrical colors made us conclude that the structure was inclined. It is therefore necessary to correct every incidence angle of a constant angle ϕ . Once done, all the points of the two arcs of circle converge towards their

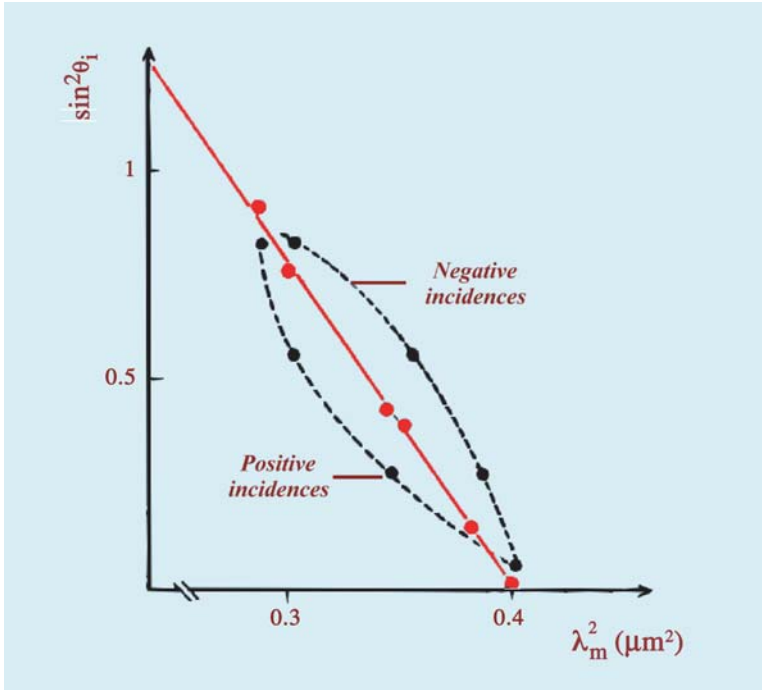


Figure 8.9. Positive incidences (apex—base) Negative incidences (base—apex) Wavelengths of minima of reflection of *Morpho menelaus* wings in relation to the incidence measured from the normal to the wing plane (---•---) and after correcting the angle θ_s of the structures on the plane (—•—). The best alignment is obtained when θ_s is equal to 10.5° . The thickness of the corresponding layer leading to these interferences, given by the slope of the straight line, is $e = 0.186 \mu\text{m}$ and its index $n = 1.68$.

common chord, giving thus the index, thickness, and angle of the reflecting structure, here about 10° . Measurements performed in the visible and the near infrared on zones of complete wings or on wings deprived of the scales of the dorsal side, and then of the ventral, allow one to underline the influence on the total reflection of each layer. Dorsal scales are responsible for the visible structure of spectra and thus color, whereas the alary membrane and pigmentary scales are in charge of infrared reflection,

as has been seen in higher proportions among *C. madagascariensis*.

Structures of Wings and Scales

Let us discover this structure by zooming in by six orders of magnitude. By using optical microscopy, one observes that scales are here again arranged in two layers, yet structural ones are in the bottom. Cover scales are thus

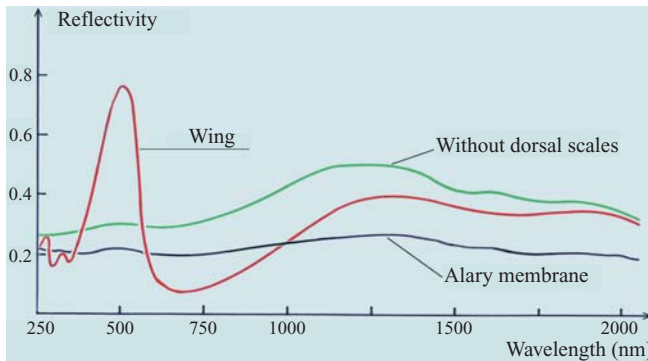
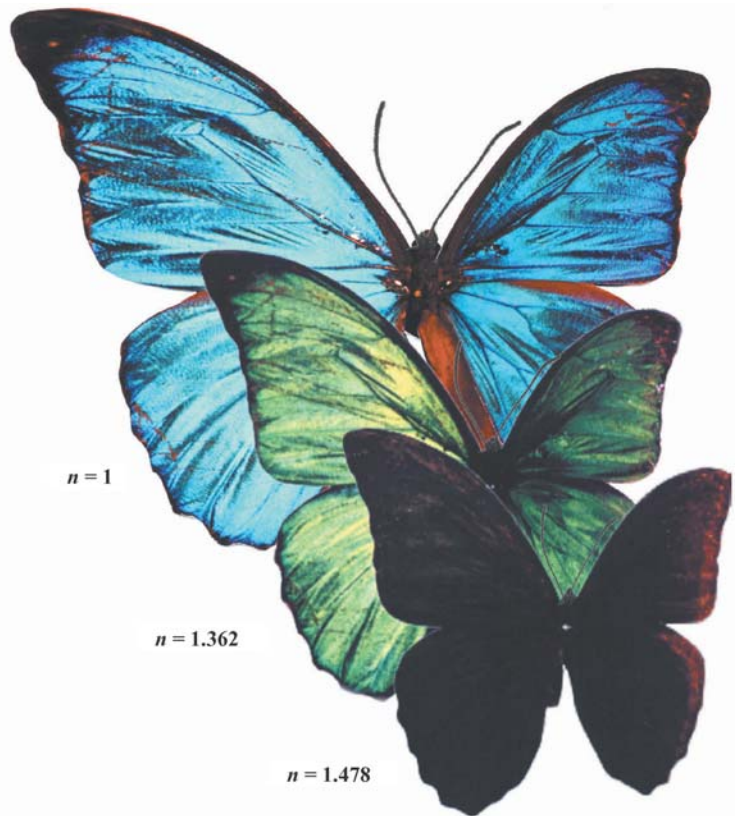


Figure 8.10. Diffuse reflection factor under normal incidence of a whole wing of *Morpho menelaus*, then of the wing from which the dorsal scales were removed, and finally of the only membrane.

Figure 8.11. *Morpho menelaus* in the open air and under index liquid. Colors vary similarly to *Morpho godarti*, yet the layer of the dorsal pigmentary scales and to a lesser extent, the pigments of the dorsal structural scales are highly absorbing, and the butterfly turns almost black when immersed in a liquid of high refraction index.



deprived of pigment so that light can come and play on the structures of the ground scales that are partly covered. Immersed into a liquid of adequate optical index (Figure 3.22), the latter

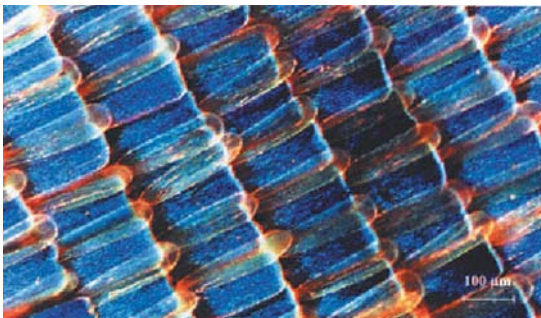
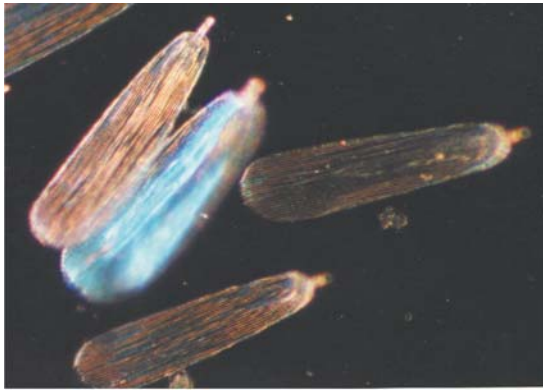


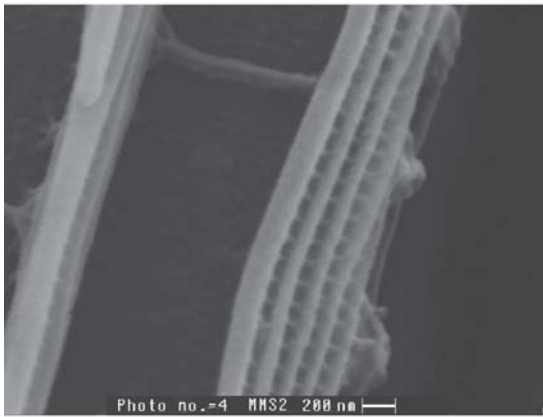
Figure 8.12. Optical microscope view in reflection of *Morpho menelaus* dorsal scales. Long and narrow, cover scales are almost invisible in transmission or in reflection under normal incidence. Immersed in an index liquid—Figure 3.22—structural scales look brown. They contain pigments and take part along with ventral scales, in the formation of an opaque screen that absorbs the wavelengths that are not reflected by the structure.

disappear completely and one can note that ground scales, if they have lost their colors, still serve as a dark screen. From different origins among *C. madagascariensis*, the two structural and pigmentary effects here on the contrary proceed from the same scales. The influence of cover scales is minor and it is possible to observe them by using reflectance optical microscopy only under grazing incidence, where a slight scattering effects makes them appear whitish by diminishing the brightness of covered areas.

Scanning electron microscopy reveals the same dense arrangement of structural scales that form a regular background all over the wing almost without overlapping. Structural scales are flat, rectangular ($80\ \mu\text{m} \times 200\ \mu\text{m}$) and slightly rounded and fringed at the apex. The cupule axis from which scales issue, is strongly inclined on the wing plane, thus forming a layer parallel to the alary membrane. Striae are also dense (1600 to 1800 per mm) and seem very deep—some even tend to join in places. Cover scales are slightly longer and



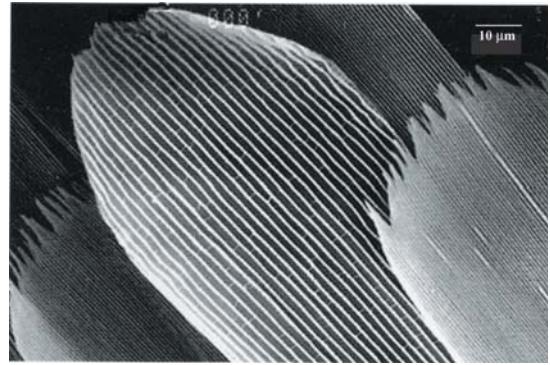
(a)



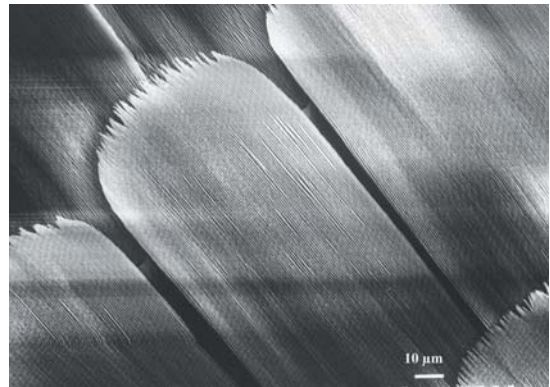
(b)

Figure 8.13. (a) Photonic microscope image of *M. menelaus* cover scales observed in reflection. The reflected color is extremely rarely visible. Its intensity is weak and very directional. (b) Striae and interstria space of a *M. menelaus* cover scale. The number of lamella is limited and the period is large.

narrower ($50\ \mu\text{m} \times 250\ \mu\text{m}$) and their striae much more spaced (around $2\ \mu\text{m}$) and linked together through some bridges. If one examines striae more closely, the two types of scales still appear quite different at this scale. The lamellae of structural striae overlap in a large part, the ratio between their spacing and length sometimes reaching up to 10 or 11. This leads to a structure of around 20 to 22 alternated air/chitin layers, every lamella looking slightly plane when covered, but becoming cylindrical at their ends. Finally, they are inclined on the plane of scales under an angle of about 10° , as it could be assumed with the adjusted arrangement of minima. Cover scales are simi-



(a)



(b)

Figure 8.14. *Morpho menelaus*. SEM images of a cover scale, (a) and of a structural ground scale, (b).

lar to ground ones from a structural point of view. However, they differ on three aspects, which undermine their effects on the wing color (1). They are—this is true for all the species that are observed—deprived of pigments. Non-reflected wavelengths are transmitted to the ground scales on which they lie (2). Spacing between striae is much more important. Striae form a scarcely dispersing grating with a period of 2 to $4\ \mu\text{m}$ (3). The number of lamellae is limited, four in average among *M. menelaus*; this substantially reduces the general reflection factor of the scales. Cover scales actually hardly contribute to the wing color and to spatial dispersion of light. This function is fulfilled by ground scales, whereas cover scales let light enter them without hindering it in any way. As will be seen later, it is not always the case. Nevertheless,

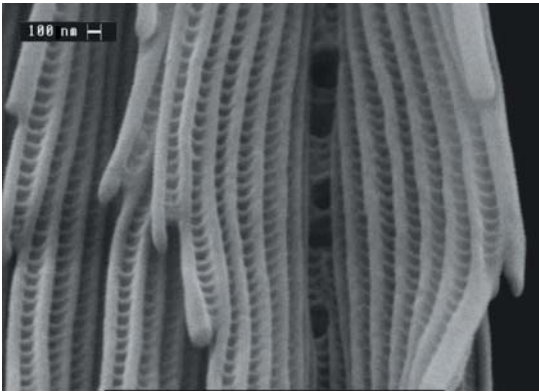


Figure 8.15. *Morpho menelaus*. On this image, one can distinguish between two striae of a structural scale up to 8 overlapping lamellae linked by a tight network of vertical microtrabeculae.

in order to play a critical role in coloration, their arrangement and structure must be modified.

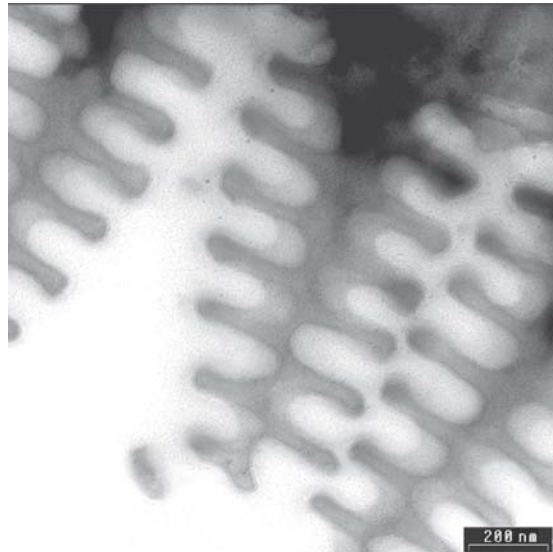
Observed by using transmission electron microscopy, a transversal cross-section of these scales shows the real shape and arrangement of lamellae at last, which are alternately arranged on both sides of the stria median axis.

The modeling of optical properties of *M. menelaus* proves much more complex than that of *Uranidae*. Scales are certainly flat and almost parallel to the alary membrane, contrary to the latter. Yet, two aspects make it more complicated:

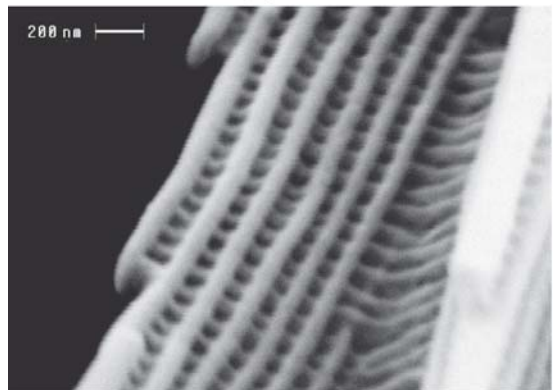
In relation to the longitudinal axis of scales on the one hand, lamellae, with a finite length, are tilted on the membrane plane from which they spring. Therefore, it is not merely a multilayer that is infinite in every direction and, the inclination of which would have been modified, but in reality a supported and truncated multilayer.

According to a transversal axis on the other hand, the stacks of lamellae are translated to one another by a half-period.

Between the two obstacles, the first is the most obstructing; yet they don't really influence the physics of the phenomenon. The inclination and translation of lamellae can therefore be neglected and let us figure in the most basic way each stria as a horizontal overlapping of lamellae presenting rectangular sections. The



(a)



(b)

Figure 8.16. (a) Above, a cross section of striae showing the arrangement in staggered rows of lamellae on both sides of the central axis. (b) Below, on the lateral view of the same striae one can note the angle formed by lamellae and the scale membrane, around 10 to 15°.

width of lamellae, l , is constant in most cases. The distance d between the edges of two neighboring lamellae can also be considered as constant. Vertically, each stria consists of alternating air/chitin layers, the thickness of which slightly varies along the stria averaging 100 nm. Under near-normal incidence, each stria behaves like the groove of a grating with a high reflection/reflectance/reflecting coefficient in blue, while the whole forms a selective grating

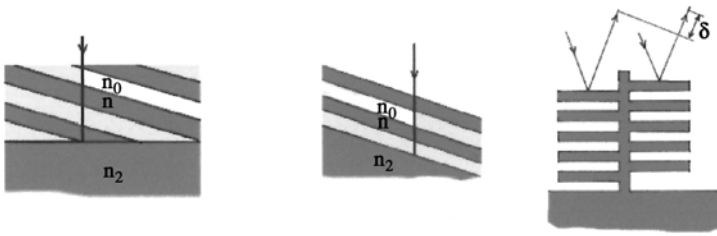


Figure 8.17. The two schematizations for the structure modeling. Longitudinally, the stack of lamellae (a) is assimilated to a tilted infinite multilayer (b). Transversally, the two edges are shifted from one another by the thickness of one lamella. The reflected rays on one side or on the other are thus not systematically in phase.

composed of 1600 lines per mm on average, thus only including three orders ($-1, 0, +1$) in which, as has been mentioned, the smaller wavelength are less deviated than larger ones.

More generally, and if striae are very dense ($d \ll e$), the whole behaves like a quasi-continuous multilayer generating thin layer interferences. And when one exposes the insect to a diffuse light (falling under all incidences), more short wavelengths will be observed under a high angle of incidence than large ones. The two phenomena are antagonist and unless one is predominant, this results in color mixing and thus to a reduced spectral purity.

Despite the good flatness of the *Morpho menelaus* scales, their orientations prove too anarchical and the wing distortions are such that it is illusory to expect to observe the diffraction orders from the entire wing. It then becomes possible to represent the wing of *Morpho* as a stack of alternated layers of low and high indices. High-index layers that contain lamellae mostly consisting of chitin with a few air, while low-index ones are quasi-symmetrical. These layers are thus basically composed of compos-

ite materials and the definition of the index of the components requires a rather complicated modeling, which won't be fully presented here, as well as a theory of effective medium. Maxwell Garnett's theory as mentioned in Chapter 6, with a depolarizing coefficient A corresponding to the elongated shape of inclusions, is well adapted to the present problem. It leads to an anisotropic solid phase index—chitin and protein—which means that it shows a different value depending on the direction, that of striae, or the perpendicular one. It is interesting to note that the two index curves intersect in the 450 nm–500 nm spectral range; that is, the blue-green part of the spectrum that corresponds to the maximal reflection of *Morpho*. This certainly explains why researchers have so far missed this anisotropy, as they used to define indices through immersion techniques. As has already been described, the method consists in dipping the wing into diverse index liquids and seeking the perfect match revealed by the disappearance of colors. This merely matches the index with the wavelength of the color. In the present case, it is isotropic.

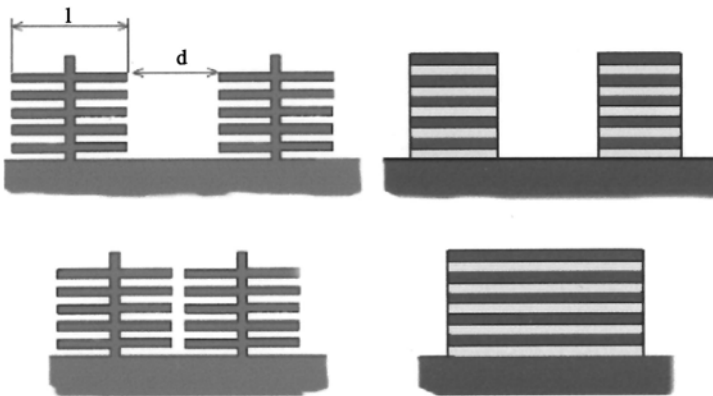


Figure 8.18. When the spacing between striae decreases, the diffraction effect is restricted to low-incidence rays and is supplanted by a multilayer interferential process. It is the case with *Morpho menelaus* where striae are almost adjacent and the optical properties of which can be determined thanks to a simple multilayer model. In both cases, one can take into account the effect of air inclusions or of chitin trabeculae on the layer indices by using an effective medium theory.

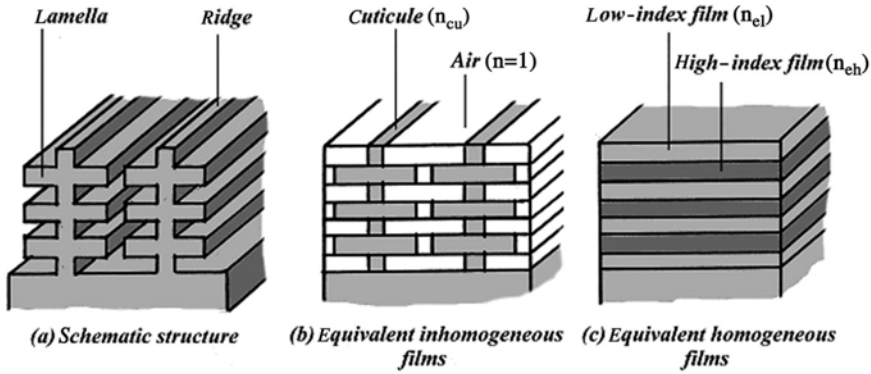


Figure 8.19. The three stages in the modeling of *Morpho* structures by using an effective medium theory. (a) Definition of a schematized structure model. (b) Determination of effective heterogeneous films. (c) Homogenizing of films by using the effective medium theory.

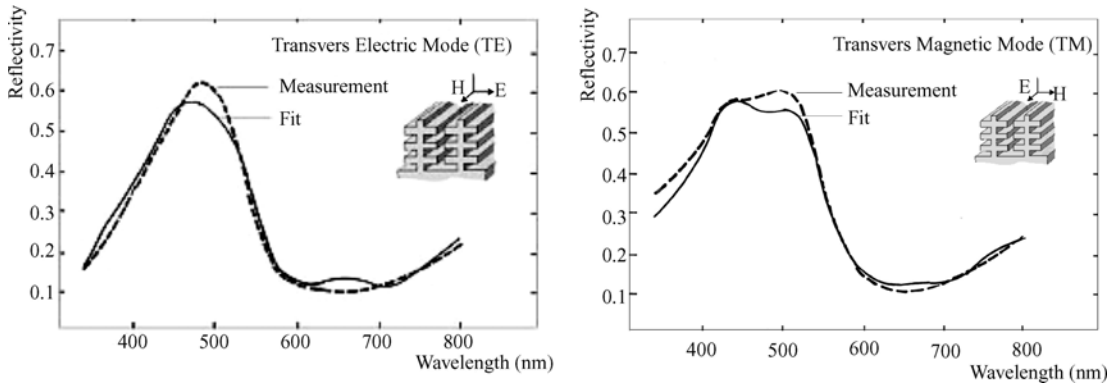


Figure 8.20. Modeling of the reflection of *Morpho menelaus* wing under normal incidence by a stack of 14 alternated air/chitin layers. Thicknesses are in fairly good agreement with those deduced from TEM observations.

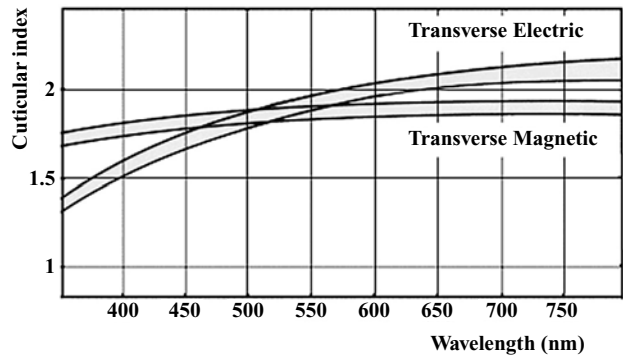


Figure 8.21. Opposite. Variations of the anisotropic index of the cuticle scales deduced from the model (see Figure 8.19).

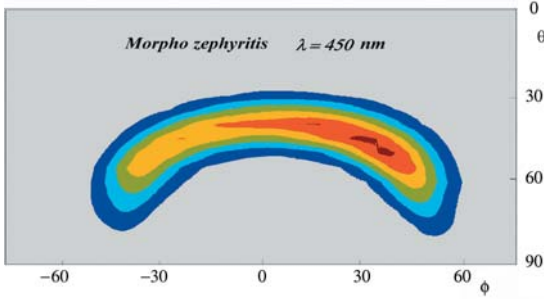


Figure 8.22. Diffraction chart of *Morpho zephyritis*. The insect is illuminated under an incidence of 20° in the normal plane $-\theta = 20^\circ$, $\Phi = 0^\circ$. Light is scattered laterally over more than 100° , but only over some 20° in the incident plane.

Dispersion and Polarization

Contrary to interferential structures, diffracting/diffractive systems are dispersive in

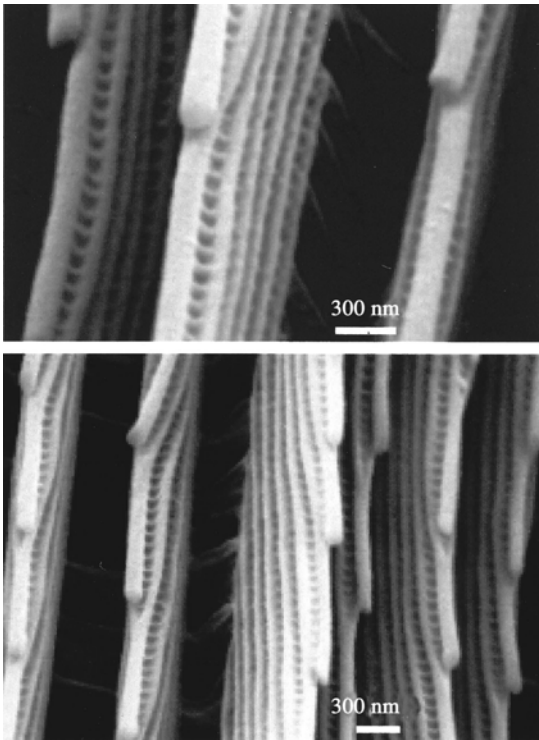


Figure 8.23. *Morpho menelaus* striae above and *M. godarti* below. Structures are strictly similar. *M. godarti* can sometimes present even more overlapping layers, but its blue color looks much paler.

essence. That is why they are so frequently used in laboratories or in industry. They are very efficient in *Morphos* and enough to largely disperse light. One actually notes that most of the scales of *Morphos* are perfectly flat. We have established a diagram of the light intensity diffracted by one of the brightest *Morphos* (*Morpho zephyritis*) at its reflection maximum of the spectrum, in the blue, at $\lambda = 450$ nm. It is meaningful. Falling onto the axis of the object, under a relatively low incidence of 20° , light is dispersed laterally on more than 100° , and only of 20° in the plane of incidence. This remarkable arrangement, associated with a high reflection factor, provides the butterfly with an excellent visibility in the full space, which is essential for *Morphos*. Indeed, sexual dimorphism is strong in this category. Females are cryptic, but sexes are also separated geographically, the latter living around the canopy, whereas males can be found in the first strata of the forest. Their recognition is essentially visual, hence the importance of this high visibility, even if it can also attract predators... or hunters.

We will now tackle intraspecific communication and focus more on differences than similarities, because it is as crucial for *Morphos* to be able to distinguish themselves as to recognize between males and females. These differences lie in the relative arrangement of cover scales and their thin structures. Before making an overview of the main species, let us review the blue *Morpho menelaus* and the light *Morpho godarti*, the chromatic variations of which have been described in the previous plates.

From the most to intense blue to the purest white, from the brightest to the matest

Even if the modeling of the optical properties of *Morpho menelaus* wings is still to be perfected, this butterfly allowed us to evaluate the numerous phenomena that play a part in its colors. Our knowledge is certainly incomplete concerning the precise place of scales, and their index—especially in ultraviolet and infrared—as well as the quality and arrangement of possible pigments. Yet our present knowledge is precise enough to be used as a reference and guide the way for research. We don't know if one could develop a convex micrograting

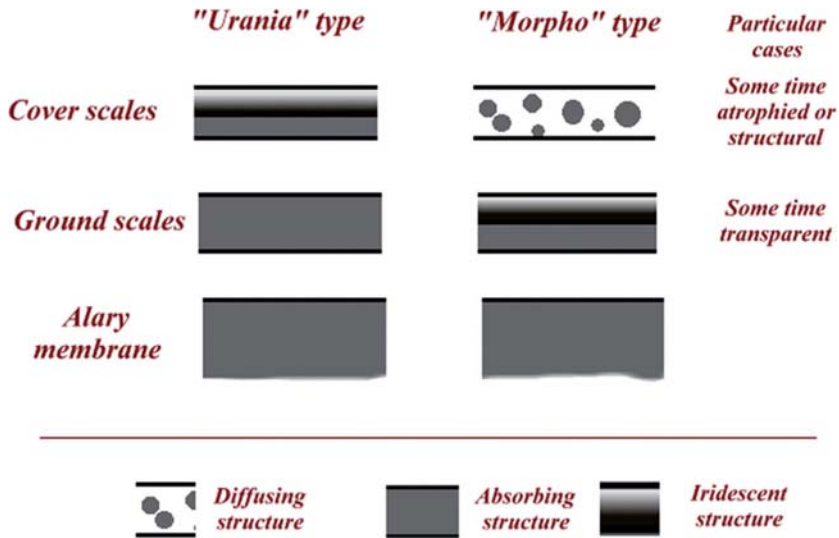


Figure 8.24. The basic structure of iridescent butterflies. First, a scattering layer formed by cover scales. Its efficiency depends on the covering ratio ranging from 0 in *M. cypris* to 80% among *M. godarti*. *Urania* are deprived of scattering layer. Second, a reflecting layer formed by structural scales, which are cover scales among *Urania* and ground scales among *Morphos*. Its efficiency depends on the number of layers, the spacing between striae, and the scale shape. Finally, an absorbing layer formed by ground scales, the alary membrane, and the ventral side. Its absorption factor depends on the pigment concentration but also on the structure of pigmentary scales.

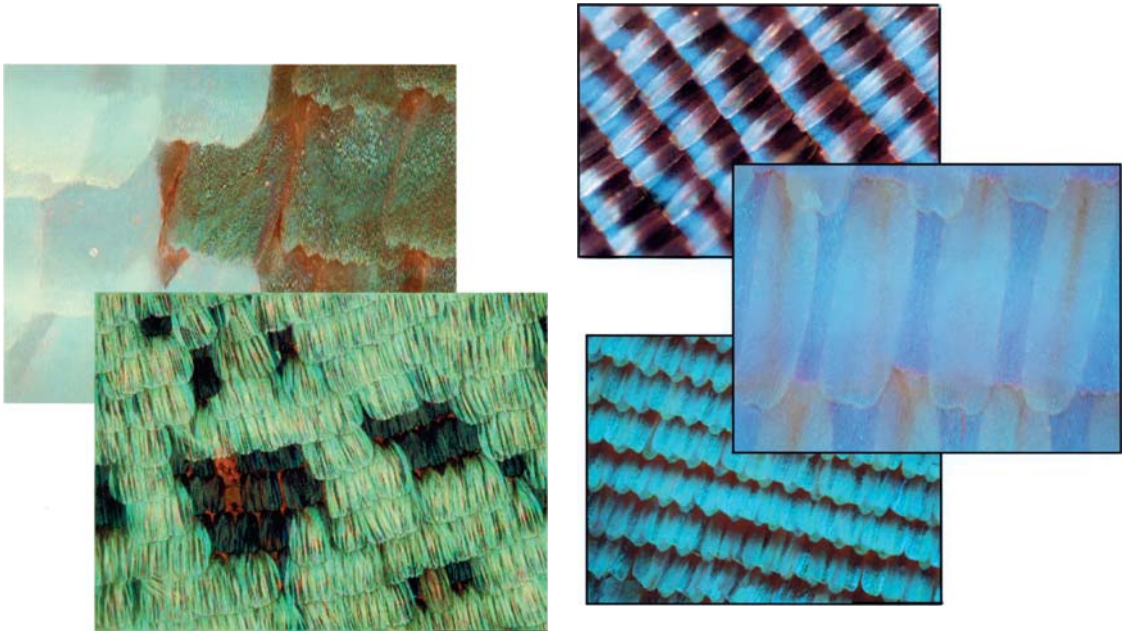


Figure 8.25. The covering ratio of ground scales by cover scales varies with the species. It is almost 100% among *M. helenor* and *M. adonis*.

Figure 8.26. In most species, the covering ratio ranges from 80% to 50%, exposing ground scales to a large extent. (above: *M. anaxibia*, center: *M. didius*, below: *M. godarti*.)

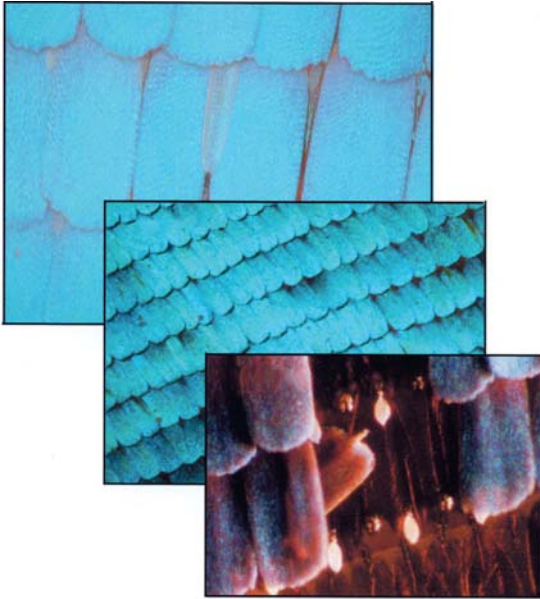
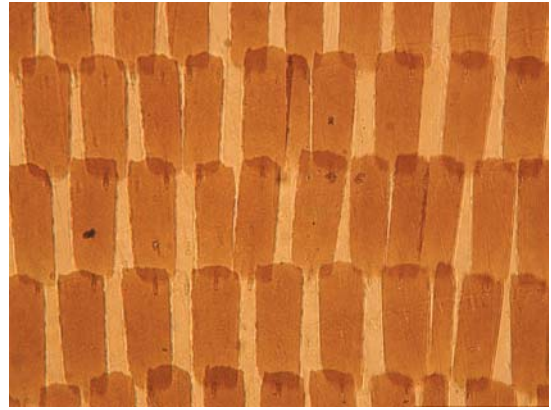


Figure 8.27. Among certain *Morpho*, cover scales are very atrophied and almost invisible. (above: *M. aega*, center: *M. rhetenov*, below: *M. cypris*)

engraved in a Bragg mirror, or even if it is worth it; yet we know that it exists and that its properties can be defined. Let us begin by studying the variations of predominant colors. *Morpho menelaus* is a rather deep-blue butterfly. Its predominant wavelength varies with incidence from the blue-green ~ 495 nm) to the violet ($\lambda_m \sim 460$ nm) with a maximal purity of 40% in the blue ($\lambda_m \sim 480$ nm) for an incidence close to 30° . If *Morpho* can hardly be bluer, it is often whiter. *M. polyphenus* breaks the record as it appears totally white. However, it is quite rare, so we chose a more widespread one that is less white: the Bolivian *Morpho*, *M. godarti*, which enabled us to illustrate how the medium index influences structural colors.

This experiment gives us a first key to decipher this evolution towards white; that is, a decreasing purity. In an index liquid close to that of chitin, wings look almost transparent, exposing the ocelli on the ventral side. The wing contains very few pigments and the same experiment, by using photonic microscopy, allows us to locate them in the ventral side scales only, dorsal ones becoming totally invisible. Contrary to *Morpho menelaus*, there is no dark



(a)



(b)

Figure 8.28. (a) *M. zephyritis* scales immersed in an index liquid, $n = 1.478$. Cover scales have completely vanished and do not include any pigment. Among *M. Sulkowskyi*, (b) ground scales do not contain any pigment either and they also vanish when immersed in an index liquid.

screen here, which makes interferential colors appear. Still through photonic microscopy, or SEM at low magnification, cover scales appear flat and slightly scattering. They are shorter, yet much wider than those of *M. menelaus*, thus almost entirely concealing structural scales, the covering ratio approximating 80%, while it is only 40% among *M. menelaus*. It is in these two aspects—lack of a dark screen, and occurrence of a scattering layer on the frontal face—that lies the main cause of the loss of spectral purity among *M. godarti*. A decrease that is partly due to the arrangement and structure of striae. The



(a)

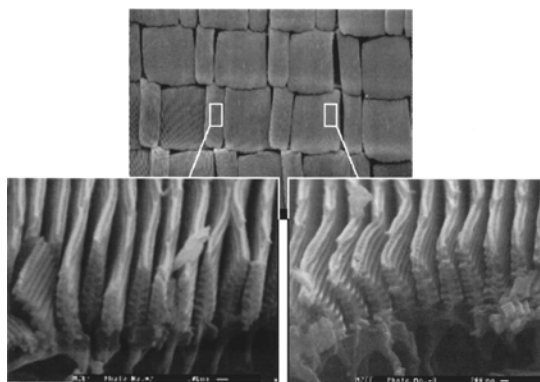


(b)

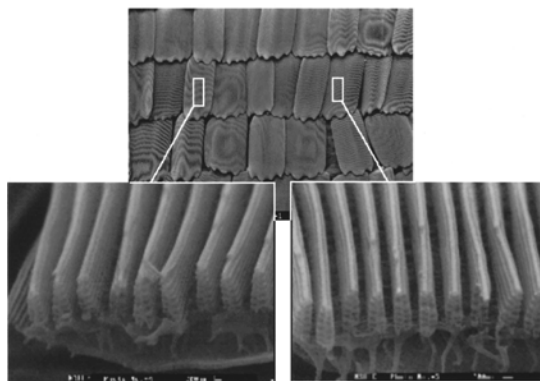
Figure 8.29. Among the two species, *M. zephyritis*—above—and *M. Sulkowskyi*, the two scale types are juxtaposed and iridescent.

spaces separating the latter are slightly wider (1200 striae per mm on average instead of 1800 among *M. menelaus*). The multilayer effect is diminished and more intertwined with the antagonist effect of the grating. Iridescence is less marked, and more due to variations of reflected intensity than to real color changes.

Let us now mention brightness variations. Among the numerous very bright *Morphos*, including *M. aega* as studied by Michelson, we selected *Morpho cypris*. This butterfly is characterized by long white streaks on the medial areas of its wings. These streaks rigorously confirm the conclusions of our previous study and we won't elaborate on them. This butterfly highlights particularly well the influence of the absorbing sub-layer. As has been seen,



(a)

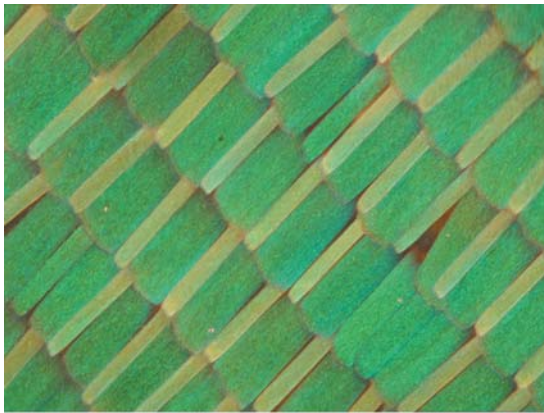


(b)

Figure 8.30. The structure of *M. zephyritis* scales, above, and *M. Sulkowskyi*, below. Cover scales on the left and ground scales on the right. Structures are almost similar.

the two membranes of the wing develop independently at the nymphal stage, so that the motifs on the two faces of scales of different structures do not show any similarity. It is the case of *M. cypris* that presents, like most of the other members of the genus, cryptic colors ranging from brown to black on the ventral side, precisely excluding the dorsal white spots. This perfect correspondence doesn't proceed from the simultaneous development of the faces, but from the relation of cause and effect.

Concerning the brightness of *M. cypris*, high magnifications are not necessary to find its cause. Photonic microscopy instantaneously offers it. Cover scales are completely atrophied and expose the total surface of structural scales



(a)



(b)

Figure 8.31. Polarization effect of the incident wave on the color of *M. zephyritis*. On the right, the incident wave is polarized in the Transverse Electric Mode, whereas it is Transverse Magnetic on the left picture.

to light. Like those of *M. menelaus*, the latter are also slightly absorbing and very flat. Besides, their striae are particularly dense (more than 2000 per mm) and composed of a great number of layers (between 10 and 12 lamellae). All these elements further the mirror effect.

If there are many a bright *Morphos*, there is but one that is matte, the *Morpho anaxibia*, which will enable us to complete our demonstration. It is little iridescent and is complementary to *M. cypris* in all of its aspects. Cover scales form a quasi-continuous scattering front layer. However, the principal characteristic of the butterfly lies in the fact that the two kinds of scales are convex. This doesn't affect much

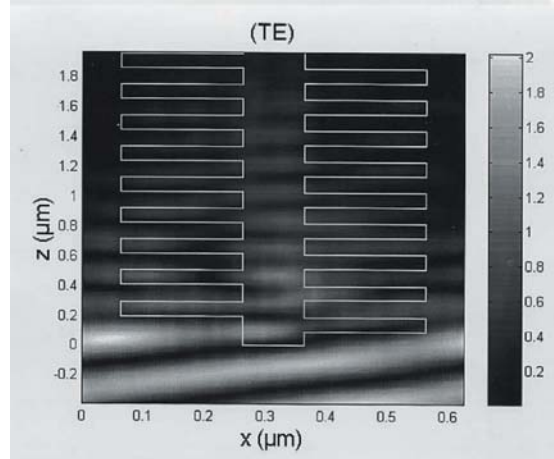
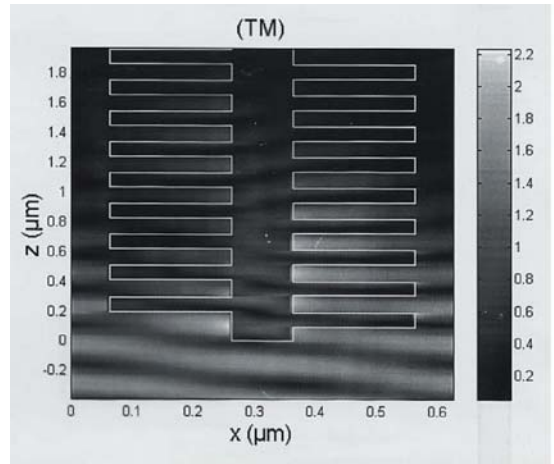


Figure 8.32. Diffracted fields as calculated from a schematized structure of striae. The incident wave is not represented here. Its incidence is normal in both cases. The TE wave diffracts in the R_{-1} order—on the right—and the TM wave in the R_1 order, on the left.

the properties of cover scales, but enable them to perfectly adapt to structural ones. As for the latter, the curve of the mirror makes wavelengths that interfere in a given direction mix, hence leading to a slight iridescence. Only a few species among an approximate total of 30 composing the genus have thus been described. However, the remaining will be classified according to the four poles revealing the variations observed, which will be illustrated in the following plates. Thanks to them, we have at least been able to define the evolution of colors and brightness among *Morphos*



(a)



(b)

Figure 8.33. Reflection factor. The same effect as the previous, yet it is less distinct among *Morpho godarti asarpai*—TE on the right, TM, left.

or *urania*, which must also occur among others with slight differences. Three elements contribute to the production of color in general among iridescent butterflies. They can sometimes be combined in the same structure:

1. An absorbing sub-layer that can either consist of scales of the ventral side, ground scales of the dorsal side—whether structural (like among *Morpho*) or not (like *Urania*)—or finally of the alary membrane itself. It includes dark pigments, mostly melanin. Absorption is amplified by the alveolar structure trapping light.
2. A partially reflecting structure composing the intermediary layer, in which through in-

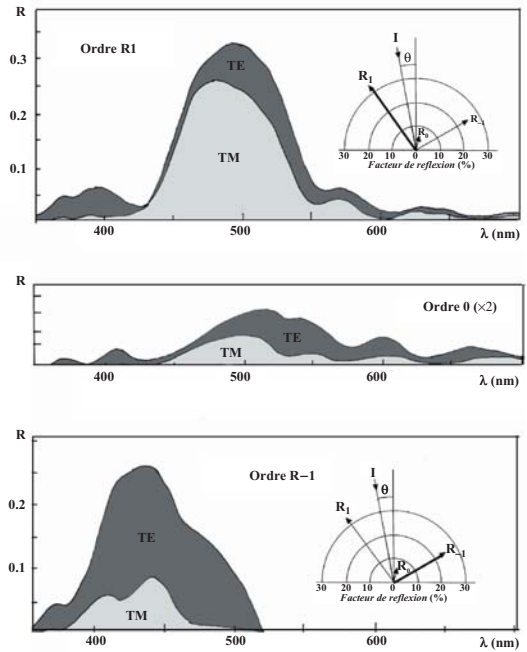
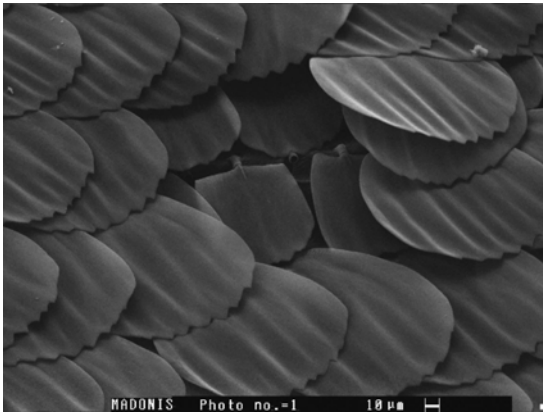


Figure 8.34. The reflected spectra in the different orders calculated from the same schematized structure, showing the chromatic shift between the R_1 and R_{-1} orders and their various polarization states. The central order R_0 is very weak and hardly polarized. The inset indicates the diffraction direction of the order maximum.

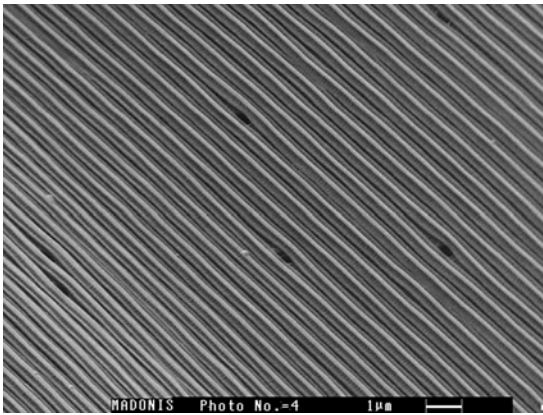
terferences or diffraction, wavelengths deviated forward are selected. Here is the origin of color and iridescence.



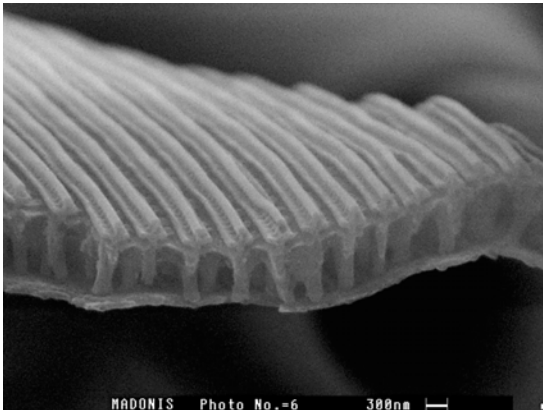
Figure 8.35. Reflection photonic microscope image of a male *Morpho adonis* cover scales, on the right, and ground scales on the left. Cover scales overlap on several layers.



(a)



(b)



(c)

Figure 8.36. SEM image of *Morpho adonis*. (a) some large cover scales have been removed in order to expose ground scales. In the (b) picture, the very regular striated network of cover scales. (c) a lateral image showing the single-lamella structure.



Figure 8.37. The bright *Morpho cypris* and *Morpho rhetenor* and the very mat *Morpho anaxibia*. The reflecting structures of the former are inclined to a large extent on the wing plane and the specular component of the reflection is significant, so that under collimated light, one cannot see color on both wings at the same time. *M. anaxibia* presents convex and very numerous cover scales, whereas the former are deprived of them.

3. A possible scattering front-layer that more or less covers the intermediary layer and alters the brightness of the color resulting from the latter.

Evolution of the Structures

This great diversity is also encountered at a microscopic scale in the thin structures of each scale. Among the few species that have been presented and actually among most of others, cover scales are scattering as has been seen (except for *M. adonis*, perhaps) and brightness

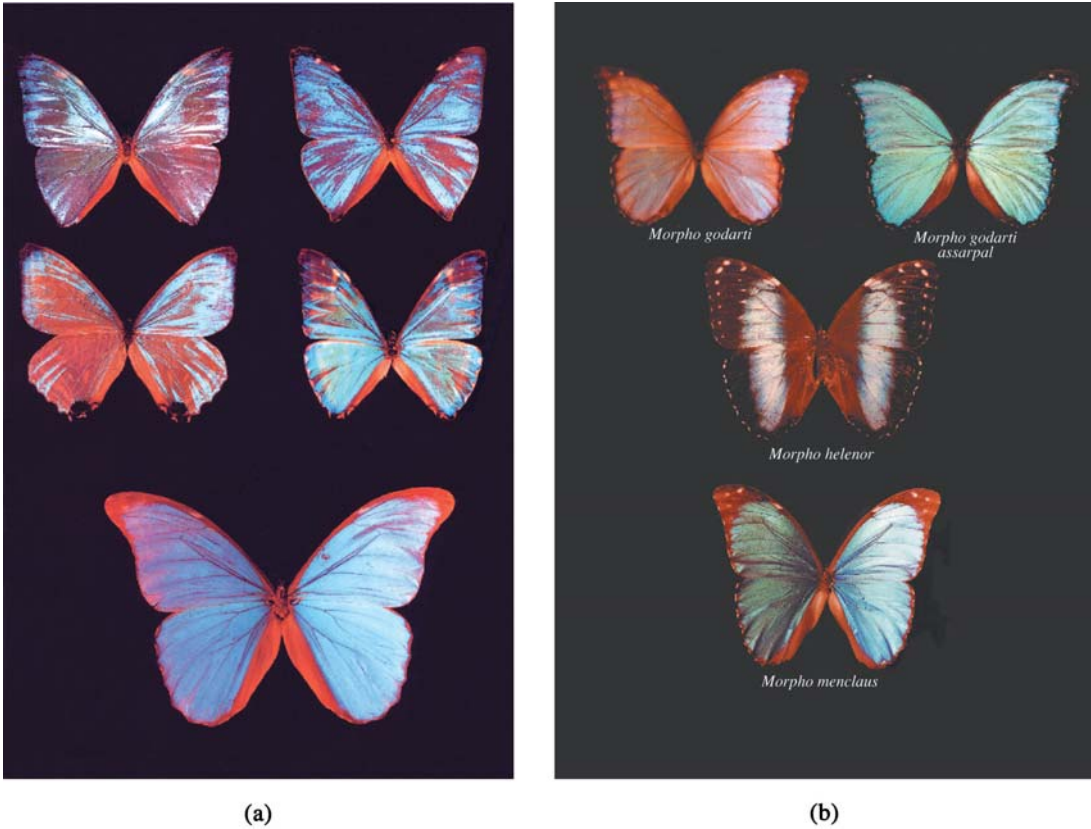


Figure 8.38. (a) and (b) The various *Morpho* species examined. The genre includes some 30 species, most of which are iridescent. Yet, the micro structural study of the latter is incomplete.

can be modified by affecting their covering ratio. However, more original solutions based on the structures of these scales this time exist. Among two species at least, *M. sulkowskyi* and *M. zephyritis*, cover scales become structural and take part in the coloration of the insect. There is no scattering layer on the surface and the two butterflies show an extremely bright aspect. The distinction between cover/ground scales becomes meaningless here since scales are arranged side by side. Surface structures that are very dense, are almost identical. It seems that cover scales tend to be deprived of pigments and that they vanish once immersed into a index liquid. This is not a perfect test though, because a certain number of ground scales are also deprived of pigments (*M. sulkowskyi*).

Polarization Effects

The polarization effects generated by complex 2-dimensional structures still remain somehow obscure and it is difficult to locate some of them experimentally. In this way, calculations will show the way.

These effects are first colorimetric. Reflection spectra are shifted from one another depending on whether the incident polarized wavelength is Transverse Electric or Transverse Magnetic. This is easily perceivable by using photonic microscopy, and the effect seems to be systematic, yet with variable intensity depending on the species. A butterfly illuminated by a Transverse Electric (TE) polarized wave always appears bluer than the same one illuminated by a Transverse Magnetic (TM)

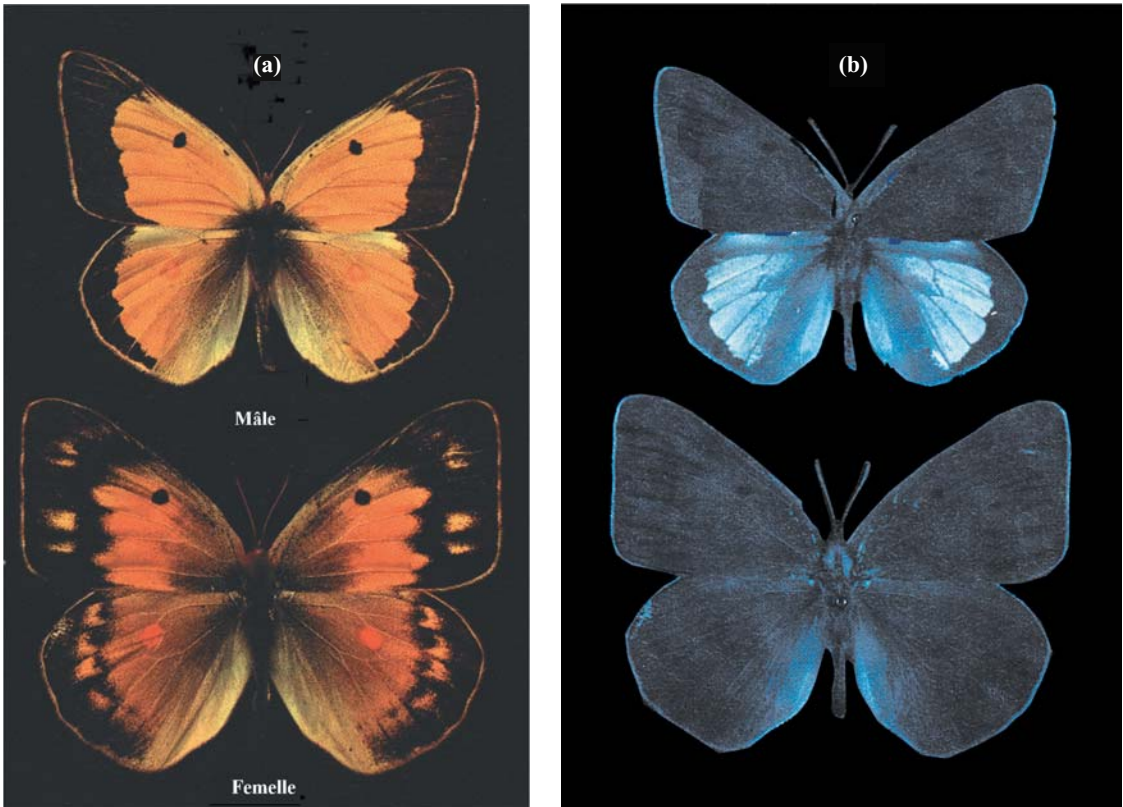


Figure 8.39. *Colias crocea* in the visible (a) and in ultraviolet (b). The wings of the female uniformly absorb in the ultraviolet spectrum, whereas the male posterior wings reflect it partially.

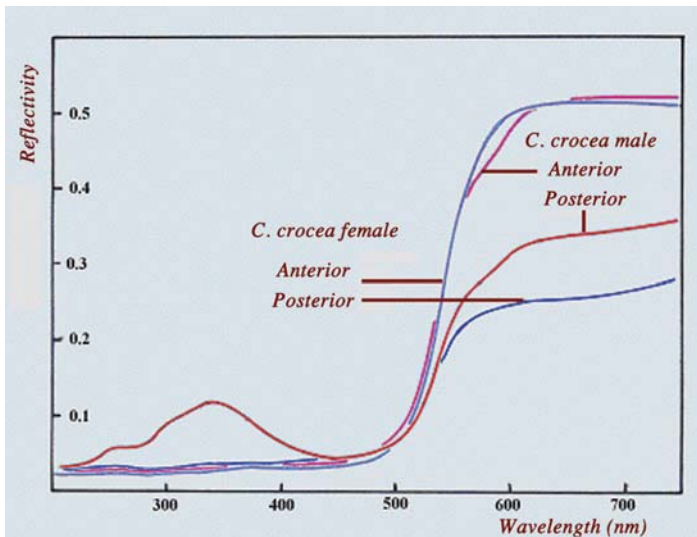
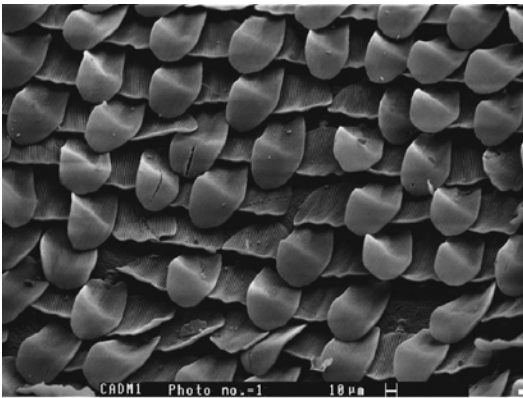
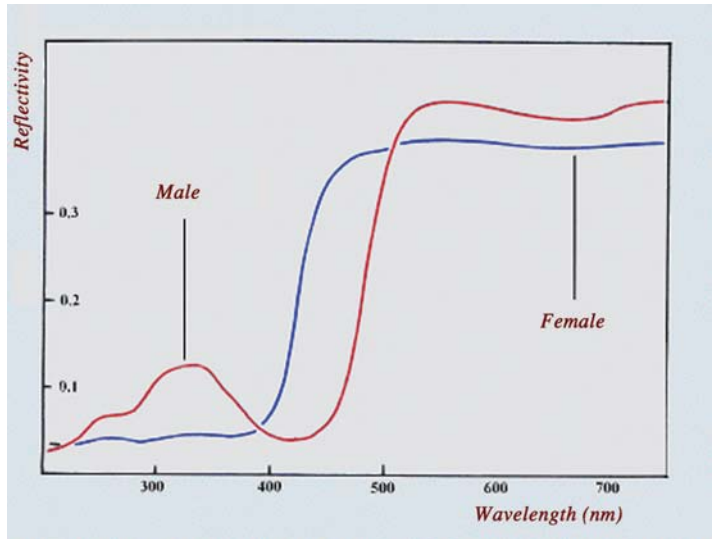
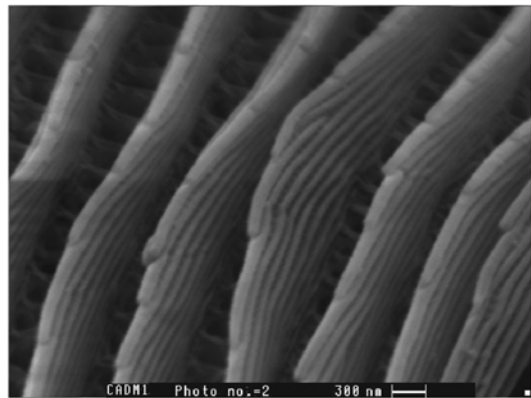


Figure 8.40. Diffuse reflection factor of male and female *Colias crocea* anterior and posterior wings. Anterior wings behave strictly similarly throughout the studied range, whereas posterior ones behave differently in ultraviolet. While male ones are weakly reflecting, female ones totally absorb these radiations.

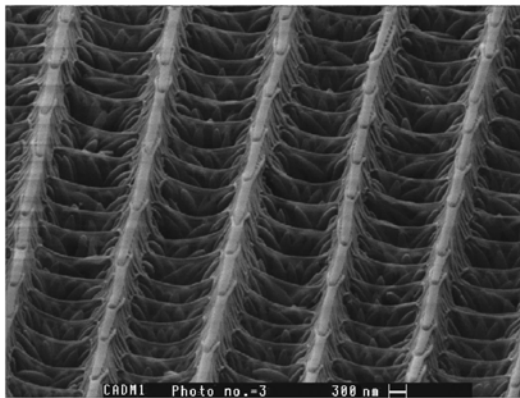
Figure 8.41. Diffuse reflection factor of male and female *Gonepteryx cleopatra* anterior wings – (5 cm). Male anterior wings show reflection in ultraviolet, contrary to its posterior wings and to female wings.



(a)



(b)



(c)

Figure 8.42. SEM image of *Gonepteryx cleopatra* Anterior wings. (a) General view showing the two scale types, very distinct here. (b) Multilayer structure of cover scales. They are responsible for iridescence in ultraviolet. (c) Ground scales contain numerous pterinosomes and generate the orange-yellow color in the insect.

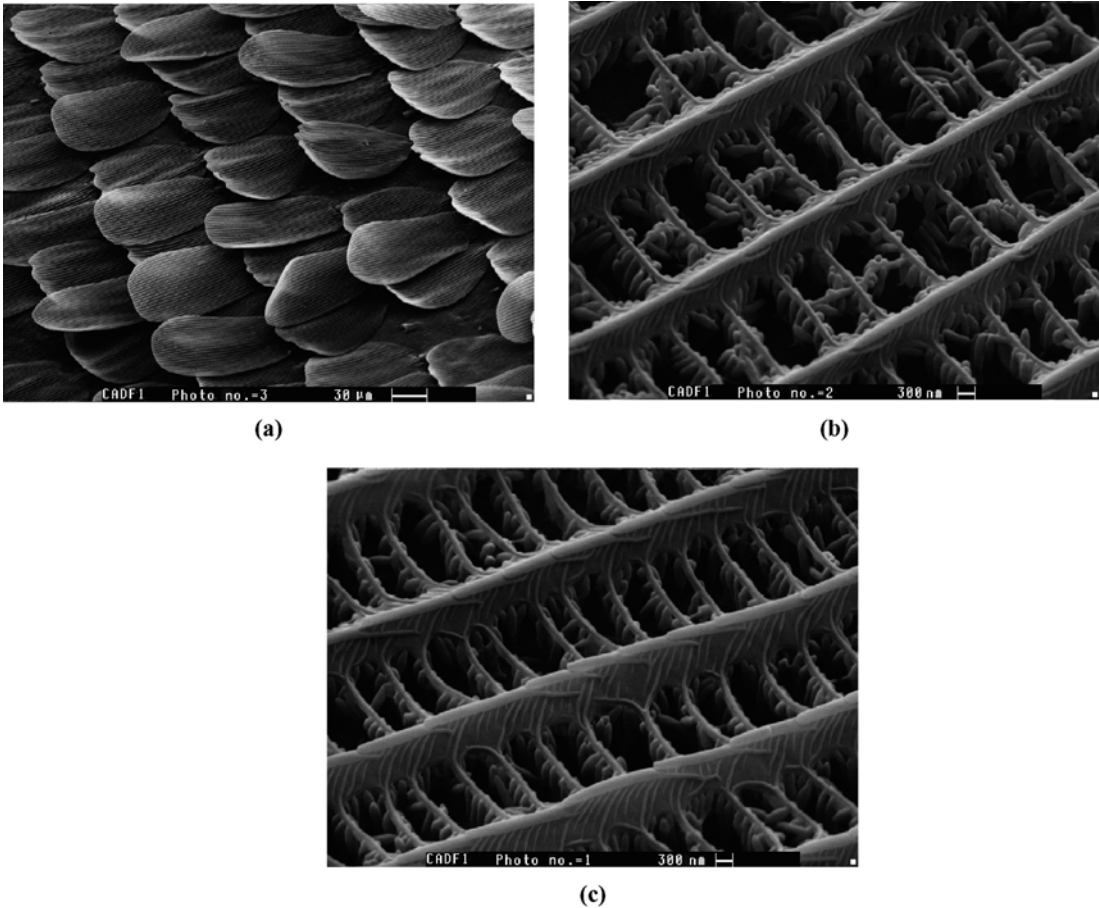


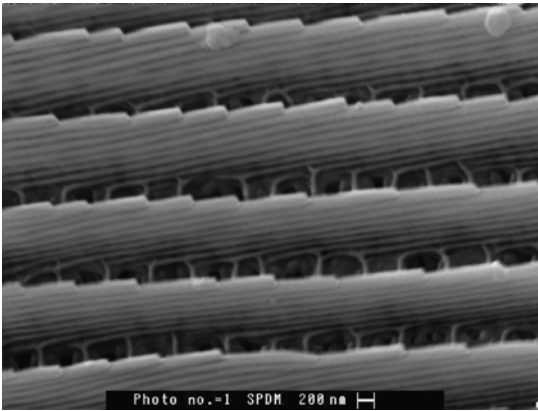
Figure 8.43. The same arrangement among females (a) yet structures are identical in both types of scales (b) and (c). Lamellae are short and do not overlap and both scales contain pterinosomes.

wave, making it turn green. This corresponds to theoretical assumptions, yet it goes further. In fact, this diffracting structure polarizes light, even (and especially) under near-normal incidence, which is quite singular! In other words, diffraction orders are polarized in very different ways when the structure is exposed to a natural non-polarized light. This is clearly revealed by the calculated spectra. The order R_1 is mostly Transverse Magnetic (TM) polarized, whereas the opposite order R_{-1} is Transverse Electric (TE) polarized. As for the specular order R_0 , not only is it little polarized, but it also shows a very low intensity. The calculations and maps of diffracted fields offer a different vision. Exposed to a polarized TE

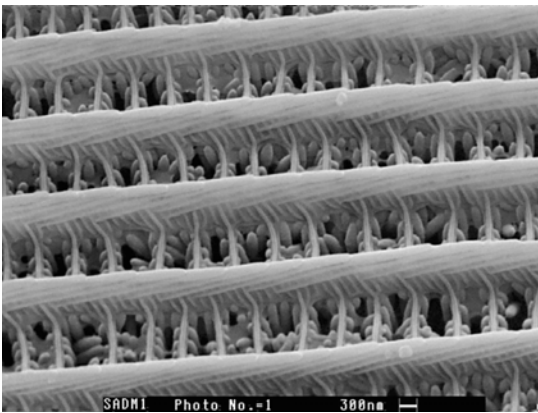
light, the wavelength is diffracted on one side and in TM polarized light on the other side. Although it is accepted that *Morphos* distinguish the two polarization states, the advantage of the phenomenon for them remains unclear, so is its origin. One can at least argue that it is due to the arrangement in staggered rows of the lamellae on both sides of the striae vertical axis, since the effect vanishes on a symmetrical structure.

Mysterious *Adonis*

Every family has its lame duck. I would like to complete this presentation by mentioning the particular case of the beautiful *Morphos adonis*.



(a)



(b)

Figure 8.44. Male *Colias crocea*. (a) Posterior wing scales show the multilayer structure of striae. (b) Anterior wing scales with lamellae presenting a restricted overlap. In both cases, one can note the presence of pterinosomes in inter-stria spacings, which generate the orange-yellow color.

It looks quite similar to *M. sulkowsky* or *M. zephiritis*. And yet, its scales structure is completely different and the origin of its brightness remains unclear.

As has been seen on Figures 8.35 and 8.36, cover scales are very large, covering the whole wing so that one must remove them to reveal ground scales. They vanish totally in an index liquid and don't include any pigment. Ground scales on the contrary are smaller and highly pigmentary. Nothing extraordinary so far, yet it is the striae structure that is remarkable. Contrary to what has just been described,

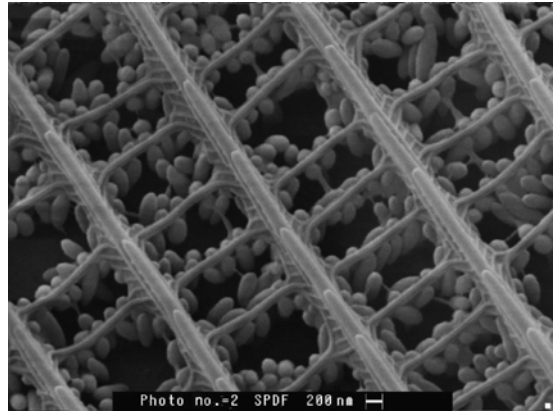


Figure 8.45. SEM image of posterior wing scales of female *Colias crocea*. The structure is similar to that of male posterior wings. Lamellae hardly overlap and numerous granules of pigment can be found between striae, like in the male.

and whether from bottom or cover scales, striae include only one long lamella along the whole scales. The periods of these striae are different according to scales. It is 300 nm long for ground scales and 600 for cover ones, but sections show a rigorously identical structure. The optical study of this butterfly might have surprises in store. It is indeed hard to believe that the bright reflection of the wings only result from dielectric layer thickness. It could rather proceed from a general effect of the cover scales, which sometimes overlap three or four times. However, no interferential effects can occur anymore since the various thicknesses are separated.

Iridescence in Ultraviolet

Iridescent effects in ultraviolet are widespread among Lepidoptera, especially in the *Pieridae* big family, the colors of which commonly derive from pigments or scattering. We are here approaching the limits of human vision, thus of colors. Yet, as has been seen, the sensitivity spectrum of butterflies extends on a large part of ultraviolet, an advantage they use. The structures responsible for these effects are surprisingly close to that of *Morphos* and should therefore be classified as 2-dimensional structures. They are here always associated with pigments and scattering structures in the

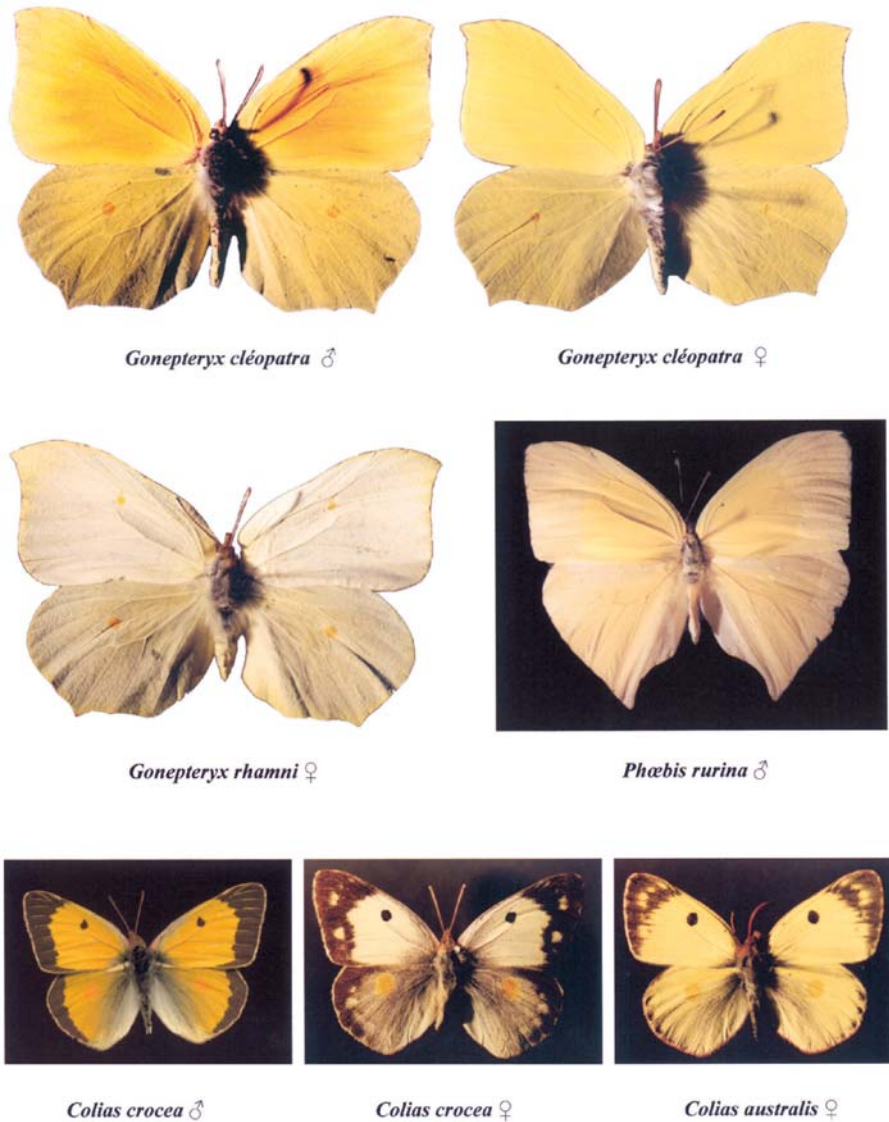


Figure 8.46. A few examples of butterflies showing iridescence in ultraviolet. They are all widespread in France, excepting *Phoebis rurina* from Brazil.

visible, which makes these butterflies particularly interesting, yet complex. To be able to display characteristics that predators cannot see presents at least two advantages. On the one hand, it results in a better sexual recognition between partners of a same species showing the same colors and motifs, whether cryptic or mimetic, in the visible. The differences between males and females are generally found on large areas of wings or whole wings, ante-

rior, posterior, or even both. On the other hand, it insures a certain distinction between mimetic species, which could otherwise be taken in by each other, hence hindering reproduction.

This is true concerning both Batesian and Müllerian mimicry and can affect males as well as females.

Spectrometric measurements performed on the anterior and posterior wings of female and male *Colias crocea* underline the different

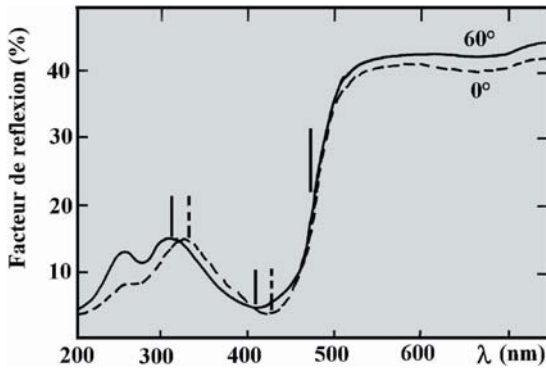


Figure 8.47. Reflection factor. Shift of the reflection maxima and minima of *Gonepteryx cleopatra* anterior wings with the angle of incident. The pigimentary reflection reaches a plateau in the visible, the amplitude of which slightly varies, but not its position.

optical properties in ultraviolet. The male posterior wings show a broad reflection peak centered on 350 nm in ultraviolet and are slightly more reflecting than female ones in the visible. This peak is neither encountered on male anterior wings, nor on any female wings. *Gonepteryx cleopatra* is the opposite, the male anterior wings being reflecting in ultraviolet.

The origin of the motifs in ultraviolet can be diverse. We will see in Chapter 10 that the common blue *Polyommatus icarus* shows a scattering peak centered on 380 nm, which marks the limit of our perception spectrum and extends well into ultraviolet. It thus includes motifs from this spectral field. But, one can note that the peak in *Colias crocea* shifts ac-

ording to the angle of incidence, which reminds us of *Morphos* and suggests that the origin must be interferential. Depending on the method used, the adjustment of the shift according to Bragg law leads to 105 ± 15 nm layer thicknesses inclined of 20° on the wing plane.

This is strengthened by scanning electron microscopy. Among two species, the male iridescent wings contain *Morpho*-type structural cover scales, the striae of which consist of 8 to 9 lamellae ($L/1 = 8 - 10$) overlapping one another and substantially tilted ($\theta \sim 20^\circ$) and remarkably regular, especially in *Colias*. Their average thickness is around 90 nm. On anterior wings, lamellae are much shorter ($L/1 \sim 2$), and almost don't overlap. In both cases, the cavities formed between striae include pterinosomes, ovoid small vesicles of pigment that generate visible coloration.

Among females, the structures of anterior and posterior wings scales, whether ground or cover, is similar to males *Gonepteryx cleopatra* anterior ones and *Colias* posterior ones. They all present a very low ratio of the covering of striae and numerous granules of pigment in inter-striae cavities.

The species possessing visible motifs in ultraviolet must be widespread, yet their study is incomplete. Most of them belong to the *Pieride* family and some to *Lycenide*. Flowers, which depend on insects to reproduce, also use visible motifs in ultraviolet to distinguish themselves and attract pollinators.

9

3-Dimensional Structures: Crystalline Diffraction

Theory Recalls

The structure now presents a periodicity in the three spatial directions, and it is under this form that the analogy with classical photonic crystals is the most obvious. Such photonic crystals are naturally present in the mineral world (they are opals), and also in the animal world among some butterflies, but especially among certain Coleoptera (*Curculionidae* and *Eupholus*, among others). Those Coleoptera possess thick resisting scales—3 to 3,5 μm —that are irregularly arranged on the elytrons, limbs, and head. When individually examined with optical microscopy, these scales present an extraordinary opalescence, producing bright green or blue colors. A section of some broken scales show a very regular 3-dimensional alveolar structure with an approximately 200 nm-long period. As a crystal diffracts X-rays, this structure diffracts certain visible wavelength in different spatial directions, resulting in the iridescence of the insect.

We have followed a historical distinction between interference and diffraction so far. Diffracting 3-dimensional gratings or crystalline diffraction perfectly illustrate the fundamental equivalence between the two phenomena. A simple way of addressing the problem has been to assimilate the crystal to its reticular planes and to treat the wave diffraction by atoms as the interferences of the reflected wave in all directions by these planes. Calculations are quite similar to those mentioned in Chapter 7 concerning interferences produced by thin films, so we won't repeat them here. However, for historical reasons, the result is in

a slightly different form, known as Bragg relation and which is based on the complementary of the angle of incidence, that is here angle Φ between the incident ray and the reticular plane:

$$2 d \sin \theta = k\lambda \quad (9-1)$$

This approach is simple and speaks for itself. And yet, if it succeeds in expressing the directions and colors of diffracted wavelength, it doesn't mention their intensity, which depends on the nature and arrangement of atoms in the planes. That is why we will briefly describe, without elaborating on a demonstration, a more modern and comprehensive approach.

Whatever the object observed—thin layer, grating, or crystal—the physical phenomenon is fundamentally the same. An electromagnetic wavelength falling on a point object is diffracted in all directions. Depending on the way the punctual secondary sources are related spatially, these diffracted wavelengths interact differently and can either be reinforced or destroyed, thus causing interferences in the first case or diffraction in the other. Nevertheless, the common origin of all these phenomena obviously lies in the initial emission of a point source. So, the first thing to specify is the amplitude emitted by the source in any point in space. The problem can be simplified by moving away from the source, which is justified when one studies butterfly colors produced by molecules or by structures of size around several tens of nanometers.

One shows that at infinity, or in the image focal plane of a lens, the amplitude emitted by

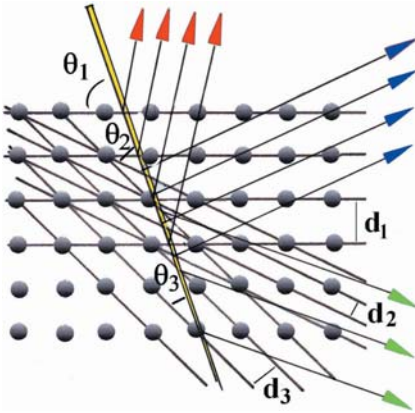


Figure 9.1. Bragg model. If the incident wavelength is smaller than or equal to the grating period, an interferential approach allows to determine the color and direction of the diffracted waves.

a punctual source M is the Fourier transform of a δ function—if the source is situated in the object focal plane.

$$f(u, v) = \iint_T e^{iK(u\xi + v\psi)} d\xi d\psi \quad (9-2)$$

We won't elaborate on the study of Fourier transforms. Undergraduates are familiar with it, yet it won't much affect people who aren't! Let us just say that the only advantage of such

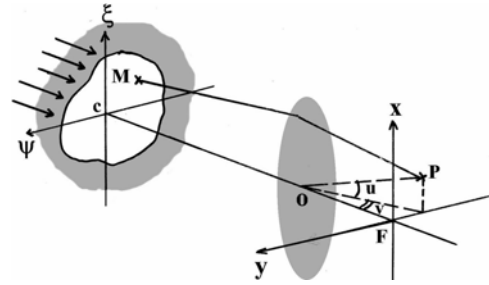
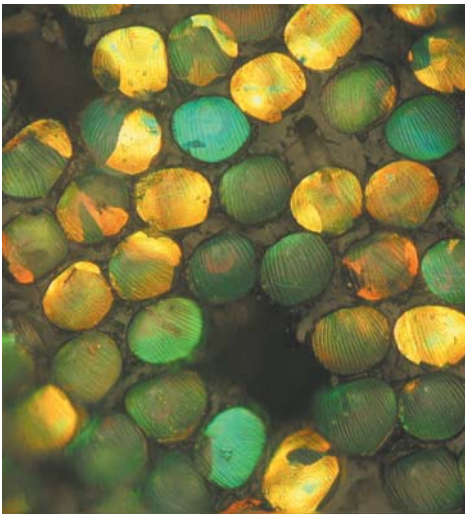


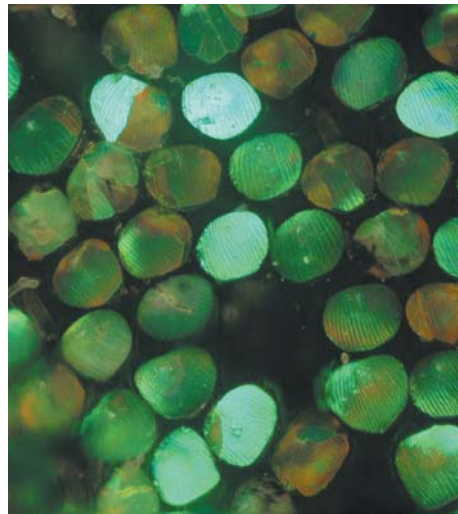
Figure 9.2. Diffraction at infinity—or to a lens focus. The diffraction phenomenon observed in the image plane is obtained by the Fourier Transform of the distribution of amplitudes in the object plane.

a formalism when studying crystalline diffraction lies in several simple properties of Fourier transforms. In particular, that the Fourier transform of a linear combination of functions is the linear combination of the Fourier transforms of each function. In other words, the calculation of the diffraction by a grating, whatever its dimension, can be reduced to that of the diffraction of its basic motif; the latter function has just then to be convoluted with one or several periodic functions—known as combs—indicating repetition in the motif space.

To finish with this introduction, let us show now the calculation of the diffraction figure of a



(a)

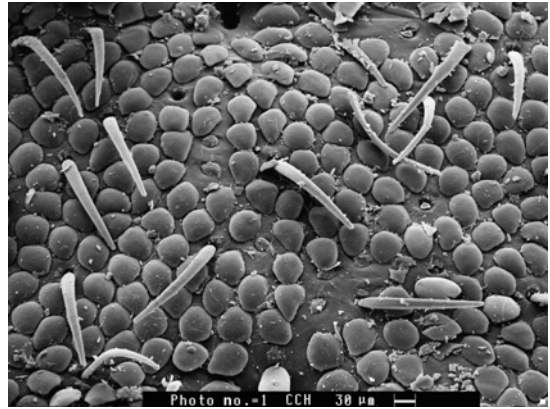


(b)

Figure 9.3. Polarization effects observed on *Curculionidae* scales, under natural light (a), and polarized light (b).



Figure 9.4. The South African *Curculionidae* *Cyphus hancocki* – 2cm. The insect colors are not very bright, contrary to its isolated scales.



(a)

complex motif crystal reduces to the following operations:

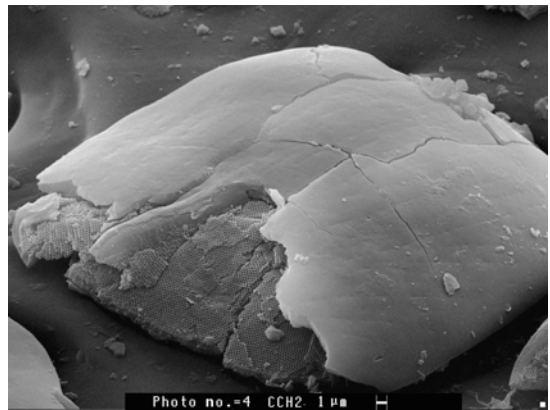
Fourier transform of a single atom

×

Fourier transform of the delta functions indicating the atom positions in the molecule

×

Fourier transform of the delta functions indicating the positions of the molecule in the crystal.



(b)

Polarization Effects

The rigorous treatment of the polarization of wavelengths refracted by a grating or a crystal

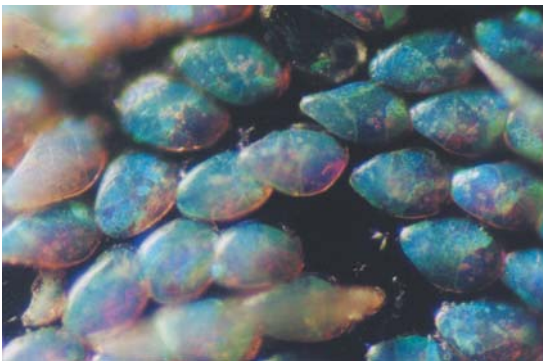
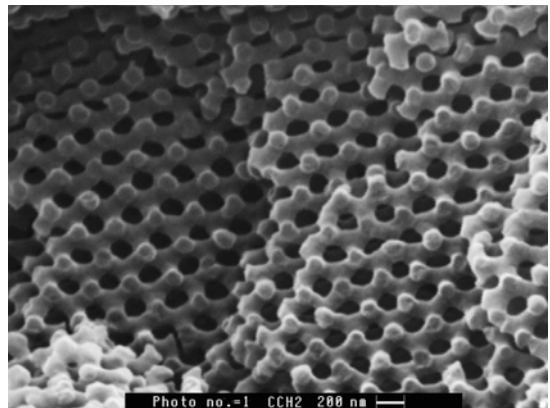


Figure 9.5. Photonic microscope image of opalescent colors in *Cyphus hancocki*. The various colors of a scale correspond to areas that are oriented in different directions within the structure.



(c)

Figure 9.6. Organization and structure of *Curculionidae* *Cyphus hancocki* scales. Like in butterflies, one can distinguish two types of scales that unevenly cover the elytron surface (a). A broken scale exposes the internal structure. One can very clearly distinguish reticular planes (b). The grating is tetraedricatetrahedral (c).

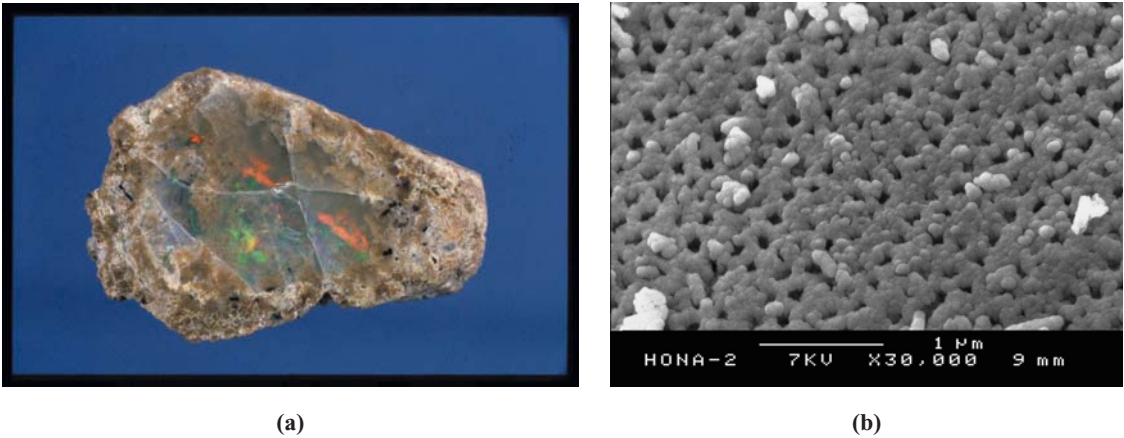


Figure 9.7. A natural Australian opal and its crystalline structure, left. It is less ordered than in *Curculionidae* scales. Photo and collection E. Fritsch and A. Barreau, Institut des Matériaux, Université de Nantes.

is generally intricate, and won't be tackled here. One can convey an idea of it, in terms of quality at least, by keeping a Bragg interferential approach and reminding one that on a diopter, the s and p components of a wavelength are reflected differently. In a similar way, when a crystal is illuminated more or less diffusely, the color observed in a given direction results from the colors created through interferences of reflected wavelengths under various incidences, and thus differently polarized. Some chromatic components—as reflected under an incidence close to that of Brewster angle—are thus more

polarized than others and can be suppressed by using a polarizer. Chromatic effects are sometimes quite impressive locally. And yet it is more often difficult to distinguish them at a macroscopic scale, since natural light is little polarized and the scales orientations are quite anarchical.

Insects and Photonic Crystals

The formalism that Bragg developed in order to analyze the diffraction of X-rays by a crystal dates back to the early 20th century, whereas passion for photonic crystals is a very recent phenomenon. One should be wary of too-simple transpositions and make sure that basic hypotheses remain unchanged. Here, the initial hypothesis is that structures are actually periodic on rather long distances and that the period of the grating and the incident wavelength present approximately the same size. As the following illustrations will show, these conditions are met at the scale of the insect scales, but not at the scale of the insect itself. Although colors are beautiful locally, the insects tend to look quite dull.

A good illustration of this is provided by certain members of the *Curculionidae* big family, as represented by weevils in our regions. They can actually show quite nice blue or green colors in other regions. The whole body,



Figure 9.8. Two *Curculionidae*. *Eupholus sulcicollis* from New Guinea, on the left, and *Eupholus humeralis* from Papua, right. Like the rest of the family, they are entirely covered with scales.

including legs, head, antenna . . . , is covered by thick and hard scales that seem to be scattered in an anarchical way. Two types of scales can be distinguished: on the one hand, rather flat scales plating the elytrons surface and on the other hand, rare ones that are pilliform and bristled. The former present various shapes—spherical, more or less rectangular or oblong—and can also include an indistinct surface structure. They seem to be striae rather than undulations and they don't take part in the coloration of the insect. When they are mechanically broken after freezing, they reveal a quasi-perfect tetrahedral crystalline structure, actually very close to that of opals, and often leading to the same iridescent effects. Though rarer, similar structures were found among certain butterflies such as *Parides seostris* by Pete Vukusic and Roy Samble from Exeter University in England.

Amorphous Structures: Scattering

Theoretical Recalls

Scattering by Particles

The scattering of an electromagnetic wave by particles is a major source of color in nature. The color of eyes, sky, snow, of certain feathers, and of course, numerous butterfly wings show that the phenomenon can occur on hundreds of kilometers as well as only a few micrometers.

Obviously, there are various regimes of scattering depending on the size and concentration of the scattering particles. Many refer to famous physicians. Very small particles, little concentrated but at a large scale are linked to Raleigh senior, who has already been mentioned, whereas important concentration at a very small scale relates to Thyndall. The wide range of characteristic lengths of the phenomenon will be further described. At a microscopic level, i.e., at the scale of the scattering particle, one must consider the interaction between the incident wave and an object of variable index, size, and shape. At a macroscopic level, the static aspect of the problem comes into play, which entails the number and distribution of particles, and their possible interactions.

The first aspect was rigorously treated by Gustav Mie in 1908 for a sphere of any size and index, immersed in a nonabsorbing medium. This treatment has been gradually extended to other geometries. It allows us to underline the various parameters involved in the phenomenon. The second one requires more calculations, is still being developed, and allows us to distinguish the different scattering regimes.

Single Scattering, Multiple Scattering

For very weak particle concentrations, i.e., if particles are small and very far from one another, one can rather accurately consider that each of them is illuminated by the only incident flux. Indeed, a particle scatters a certain amount of the incident light in all directions. The further one moves away from the scattering particle, the weaker the influence of scattering, as it is spread over a larger surface. Thus, beyond a certain distance γ , the scattered wave can be neglected, and a second particle situated beyond γ won't be affected by the former. The problem is in this way substantially simplified, since one has only to "multiply" the calculation performed for each of them by the number of particles and thus find the optical response of the whole scattering medium. This is known as single scattering.

The probability that a wave scattered by a particle doesn't meet a second one decreasing with distance, one can easily understand that such a simplification is valid provided that the thickness of the scattering medium be not too large compared to the particle spacing. If it is not so, i.e., if the concentration in particles increases or if the thickness of the medium is too important, the scattering becomes multiple. One will always be able to treat a single particle, yet the flux incident on it becomes more complex; it proceeds from both the main source and the other particles behaving as secondary sources.

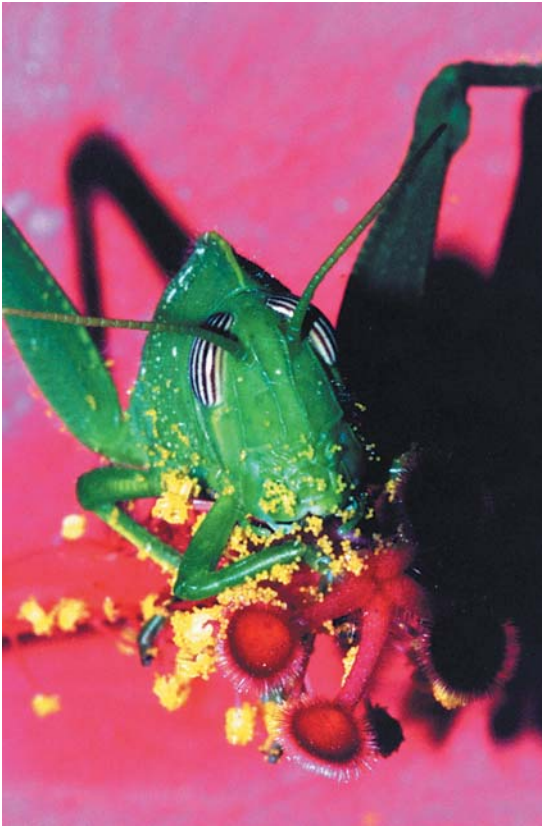


Figure 10.1. The green color of this grasshopper is a complex color due to scattering and to absorption by pigments.

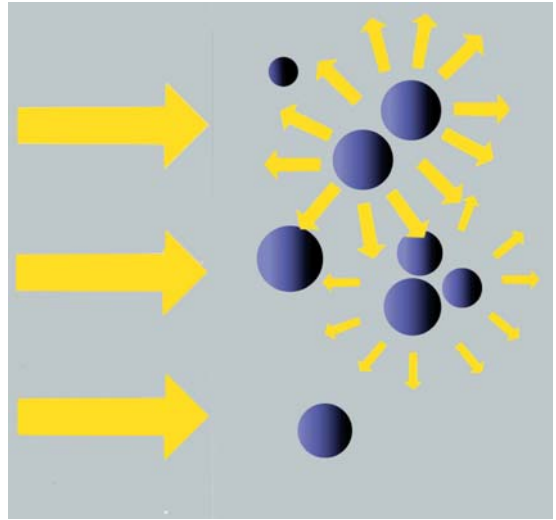


Figure 10.3. Dependent scattering: particles are next to each other and their individual response is no longer that of a sphere.

Dependent Scattering I, Independent Scattering

In the cases previously mentioned, scattering being either single or multiple, the individual properties of each inclusion were implicitly determined by their shape and index, independently from the presence of neighboring inclusions. The only incident flux on the particle

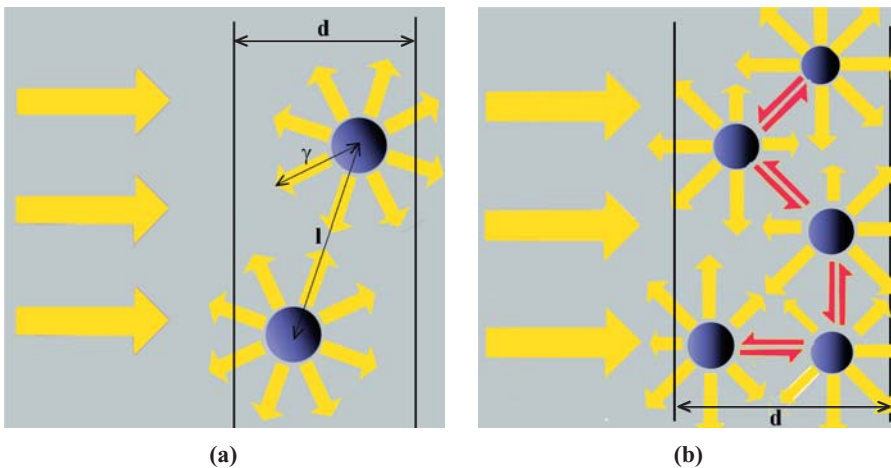


Figure 10.2. Single scattering (a). Particles are far away from one another and the thickness of the scattering medium is weak; each particle receives only the main incident beam. Multiple scattering (b). The particle concentration is higher. Their response is still that of a sphere but they are also subjected to the field scattered by neighboring inclusions.

could in these cases be affected and undergo variations. This case is known as independent scattering. Such an approximation is obviously not always applicable. The borderline case in which inclusions touch each other is enough to demonstrate this. The aggregate thus formed scatters as an individual entity that is all but spherical. The radiative characteristics of each particle are modified by the presence of neighbors that are too close. This is known as dependent scattering, the latter occurring mainly when particle concentrations are high, independently from the size of the scattering medium.

The physical process and the treatments used for modeling such media are very different from one regime to the other, mostly by taking into account the phase of the scattered waves. If configurations are such that interference phenomena can occur between two neighboring inclusions, i.e., if distances between particles are approximately equal to the wavelength, or smaller, one must take into account the phase difference between the various waves and apply a coherent treatment. If not, a more basic calculation, defined as incoherent, involving only the field intensities, represents a good approximation.

Scattering by a Particle

Mie's Treatment

Whatever the scenario, one is brought to consider the interaction of a wave with a particle at the microscopic level. This problem has been treated by Lorentz as early as 1890, and rigorously formalized by Gustav Mie in 1908 for a spherical inclusion of any size and index, immersed in a nonabsorbing medium with real index. We won't introduce Mie's calculations here, which are more complex in their form than in their content because of their obvious dissymmetry; the incident wave is plane and the inclusion is spherical. As for studying the interaction, one must introduce one—forcefully!—in the location of the other, i.e., here, to split the plane wave into an infinite series of spherical waves. All the rest is technical . . . and allows us to determine the amplitude of the scattered fields in all directions, i.e.,

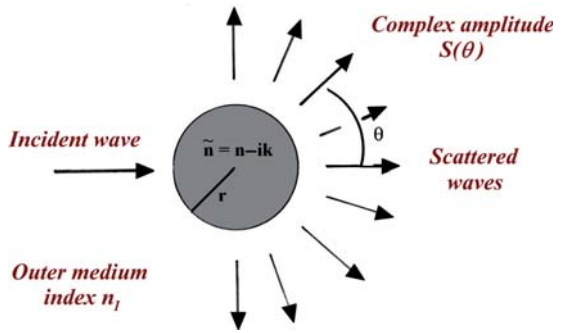


Figure 10.4. The basic concepts of the Mie Theory. The spherical inclusion with radius can present a complex index, but it is immersed in a nonabsorbing medium with real index n_1 . The relevant parameters are the ratio of \tilde{n}/n_1 and the Mie parameter $x = 2\pi n_1 r/\lambda$. It allows us to calculate the complex amplitudes scattered in a $\theta : S(\theta)$ direction.

the indicator of scattering. The fundamental parameter of Mie's theory is the size parameter x linking the incident wavelength λ in a medium of index n_1 to the radius r of the particle:

$$x = 2\pi n_1 r/\lambda. \quad (10-1)$$

Calculations thus allow us to determine the electromagnetic fields in every point in space, i.e., the fields absorbed by the particle as well as those scattered outside. One can also deduce from these calculations energy quantities cross-sections, which are better indicators of the scattering amplitude than the very fields. This is how one defines the absorption cross-section



Figure 10.5. The human eye iris is another example of a complex color proceeding from absorption—by melanin—and scattering.

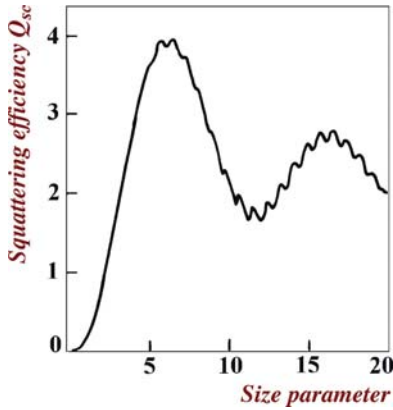


Figure 10.6. Scattering efficiency of a non-absorbing sphere in relation to the size parameter $x = 2\pi r/\lambda$. Scattering reaches its maximum for $x \sim 6$, i.e., for the radius of a particle immersed in vacuum approximately equal to the wavelength.

C_{abs} and scattering cross-section C_{sca} as the ratios of the electromagnetic energies absorbed and scattered by the sphere and the energy of the incident wave respectively:

$$\begin{cases} C_{\text{sca}} = W_{\text{sca}}/I_{\text{inc}} \\ C_{\text{abs}} = W_{\text{abs}}/I_{\text{inc}} \end{cases} \quad (10-2)$$

These cross-sections directly depend on the size parameter x and thus allow us to evaluate the relative influence on scattering of the incident wavelength, of the particle size and index within the various regimes studied. Divided by the geometric cross-section, these cross-sections allow us to at last define the scattering

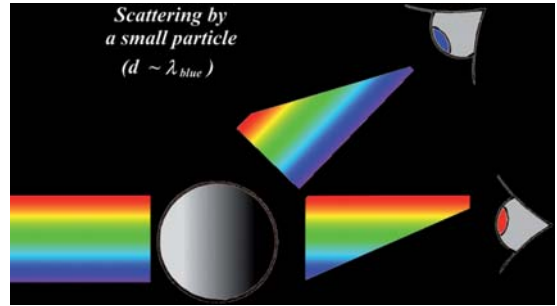
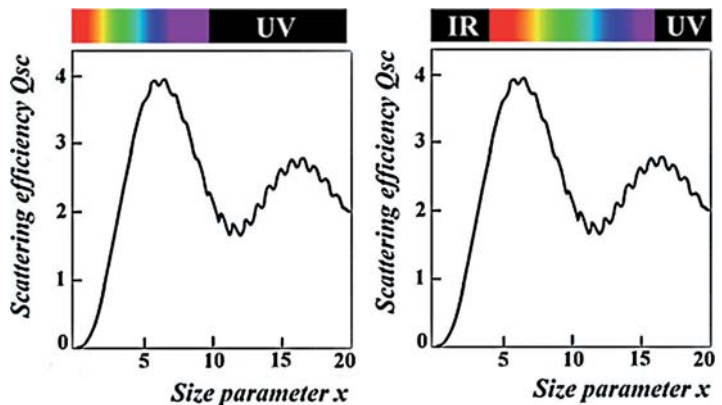


Figure 10.7. Selective scattering. Particles with radius approximately equal to the blue wavelength tend to scatter the latter to a large extent, while hardly scattering long wavelengths—or red ones. The transmitted light is predominantly red, whereas light that is scattered in all directions is predominantly blue.

or absorption efficiency Q , which is the quantity representing the phenomenon the best ($Q = C/\pi a^2$ in the case of spherical particles).

As is often the case when using spherical coordinates, the expressions of these efficiencies are formally complex and to present them would be pointless. It is nevertheless possible, if x is small i.e., when inclusions are small compared to the wavelength, to expand these expressions as power series of x . This is much more relevant and allows us to demonstrate how scattering can generate colors. If the product $|m| x$, where m is the relative index of the particle in its surrounding medium, is small compared to 1, only the first terms of each

Figure 10.8. It is hard to obtain red through scattering because of the dissymmetry of the scattering efficiency. When the radius of particles is close to blue wavelengths – size parameter : $x = 2\pi \sim 6$ —(a) blue is highly scattered, as well as UV, which doesn't affect color. (a) The other colors are very little scattered. If the radius of particles is close to red wavelengths—the size parameter remaining close to 6—red is highly scattered but the other colors also exist, and the color therefore tends to white (b).



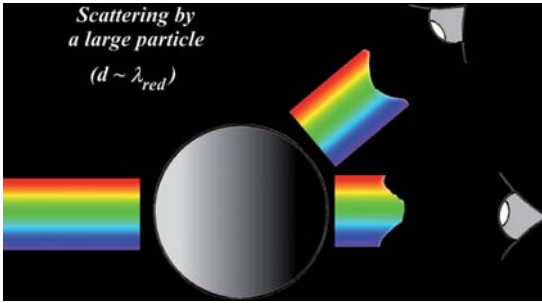


Figure 10.9. Scattering by particles of size close to red wavelengths. The latter are highly scattered, and so are the others, but to a lesser extent. The aspect is whitish in the forward—transmission, as well as in the scattered directions.

of these developments are significant and are equal to:

$$\begin{cases} Q_{\text{sca}} = \frac{8}{3}x^4 \left| \frac{\varepsilon_1 - \varepsilon_2}{\varepsilon_1 + 2\varepsilon_2} \right|^2 \\ Q_{\text{abs}} = 4x\text{Im} \left(\frac{\varepsilon_1 - \varepsilon_2}{\varepsilon_1 + 2\varepsilon_2} \right) \end{cases}, \quad (10-3)$$

where ε_1 and ε_2 are respectively the dielectric functions of the particle and of the surrounding medium. In this way, if these dielectric functions don't vary very much in the studied spectral range, the scattering and absorption efficiencies vary respectively like $1/\lambda^4$ and $1/\lambda$. We here come across again with Rayleigh's theory, which shows that the blue wavelengths on one end of the spectrum ($\lambda \sim 400$ nm) are 16 times more scattered than reds on the other end ($\lambda = 800$ nm). The largest wavelengths (red dominant) are thus encountered in the direc-

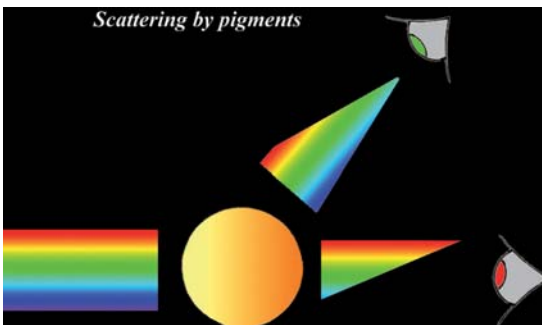


Figure 10.10. Scattering by pigments. In the transmitted and scattered spectra, pigments absorb some wavelengths, thus changing color to a large extent.

tion of the incident wave, while the shortest ones (blue dominant) are more present in the direction of the scattered light. When still neglecting the spectral variations of indices, with constant scattering efficiency, an increase in the size of particles leads to an increase in the scattered wavelengths; the scattered light thus tends towards white.

When the size of the particles increases, most of the largest wavelengths are successively scattered, yet the resulting colors are never as bright as in the blue. This is due to the dissymmetry of the scattering cross-section, which quickly tends towards 0 when the wavelength increases (or when the particle radius decreases), but tends towards a finite value (and not insignificant: 2) when the wavelength decreases. If one considers particles with a radius equal to that of the wavelength ($x \sim 6$, close to the cross-section maximum), only the blue wavelengths are scattered by small particles in the visible. Ultraviolet is also scattered but it doesn't take part in color. In the reverse case of bigger particles, of size comparable to the red wavelengths, the latter are highly scattered. And yet, so are all the others—to a lesser extent—and the resulting color tends towards a slightly colored white.

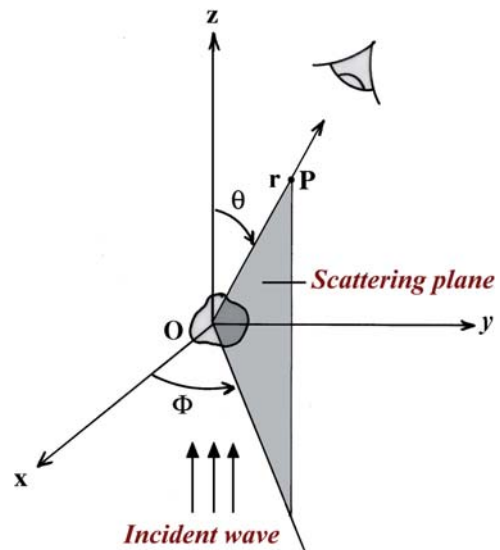


Figure 10.11. The scattering plane is determined by the directions of incidence and observation. It is equivalent to the plane of incidence for the reflection on a diopter.

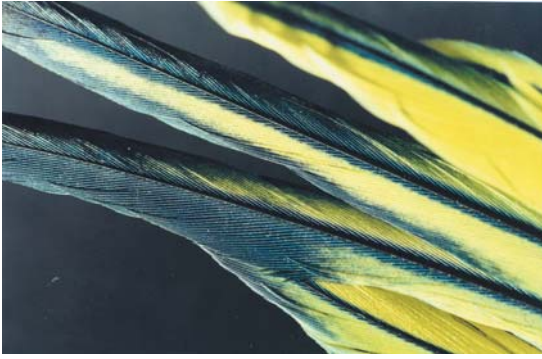


Figure 10.12. The feathers of the parakeet *Melopsittacus undulatus* are blue due to scattering and yellow due to the presence of pigments. There are green areas when the two sources of color overlap.

Scattering with Pigment

In nature, scattering particles are rarely deprived of pigments. A widespread case is melanin, which often appear as granules, like in the iris in the eye, for instance. As will be shown, melanin is a pigment ranging from black-brown to yellow, i.e., absorbing the smallest wavelengths, and mostly the blue. If the size of granules is such that it produces scattering, the scattered spectrum as well as the transmitted one are here deprived of any blue wavelength. Usually containing a lot of blue wavelengths, the former thus turns more green. The second one, which was already deprived of blue wavelengths, is not altered much and remains red. This combination of effects gives birth to many green colors, such as that of lizards, grasshoppers, and many others.

Polarization Effects

Polarization effects generated by these scattering phenomena are important in many regards. They can be found in both the light scattered by insects, which gives them their colors, and also light that sometimes illuminates them sunlight, for instance. The directions of polarization of a scattered wave are marked within the scattering plane formed by the direction of the incident wave and that of observation.

My calculations that have only been briefly mentioned allow one to determine the scattered intensities in a given direction for a polarization state of the incident wave. For a given

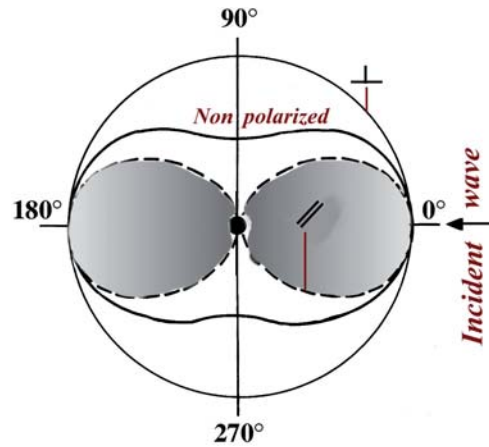


Figure 10.13. Scattering maps of waves polarized parallel (----) and perpendicular (.....) to the scattering plane, and the result for a nonpolarized wave.

wavelength, they are as follows:

$$\left. \begin{aligned} i_{//} &= \frac{9 |a_1|^2}{4k^2 r^2} \cos^2 \theta, \\ i_{\perp} &= \frac{9 |a_1|^2}{4k^2 r^2}, \end{aligned} \right\} \Rightarrow i = \frac{1}{2} (i_{//} + i_{\perp}). \quad (10-4)$$

where k is the wave vector, r and θ are the polar coordinates of the measurement point in a location, the center of which is occupied by the scattering particle, and a_1 is a scattering coefficient depending on the size parameter and the particle index. Let us only note without elaborating that when the incident wave is polarized perpendicularly to the scattering plane, scattering is isotropic, but that it varies like the square of the cosine of the scattering angle when polarized perpendicular. This



Figure 10.14. The common Pieridae, *Pieris brassicae*, female.

implies that even when the incident wave is not polarized, part of the scattered wave is polarized and always perpendicularly to the scattering plane. The P polarization ratio, defined as the following product:

$$P = \frac{i_{\perp} - i_{//}}{i_{\perp} + i_{//}}, \quad (10-5)$$

becomes, according to the previous equations:

$$P = \frac{1 - \cos^2 \theta}{1 + \cos^2 \theta}, \quad (10-6)$$

which demonstrates that at right angle of the incident direction, the scattered wave is even totally polarized. This effect is similar to the total polarization obtained in reflection at the Brewster angle. The scattering diagrams of waves polarized perpendicularly and parallel to the scattering plane are shown on Figure 10.13, as well as their result when the incident wave is not polarized.

Type Butterflies with Scattering Structures

Pieridae and Lycaenidae

White or Blue

Scattering as a source of colors is widespread in nature. Although it may seem quite laborious, the presentation we have just made of the phenomenon enables to convey its intricacy. After this long chapter on thin layer interferences and the fact that theoretical predictions and experimental conclusions correspond, the present chapter may appear quite short and disappointing. Yet, it will be justified by the following study of the wing—according to the same zooming in approach. Whether it is from the microscopic point of view, from that of each scattering particle, or the macroscopic and static point of view of their distribution on wings and their interactions, formalism is much more complex than what has been seen so far. As cross-sections observed by electron microscopy will show so wonderfully, one is here confronted with an extraordinary accumulation of mathematical and calculation complexities, these butterflies thus proving impossible to model so far. Let us come back from the beginning. Contrary to interferences and

scattering that can both substantially split colors, scattering is relatively little selective. This is easily understood when one remembers that a particle of a given size will highly diffuse the radiations of wavelengths that are shorter to itself, whereas it won't diffuse much that of longer wavelengths. Consequently, scattering by itself cannot produce a color situated at the center of the visible spectrum or at its red end. Very small particles can indeed diffuse blue wavelengths but hardly others. Nevertheless, when one increases their sizes, they won't diffuse just a greater wavelength, but more and more wavelengths, from green to yellow . . . the superposition of which leads to an increasingly pure white. This process implies a mixing rather than selection of colors, and the resulting colors are not very pure. More marked colors will appear, provided scattering be combined with a more selective phenomenon, which is pigmentary absorption.

We will illustrate this phenomenon with two species that live in our temperate regions and that are situated at the two ends of the spectrum, as has just been mentioned: the male Common blue *Polyommatus iracus* and *Celastrina argiolus* on the one hand and the white Pieridae *Pieris brassicae* on the other hand. As has been already said, those are the only colors that can be obtained through scattering. But the two species also happen to illustrate the two possible ways of scattering: a high index particle immersed in air or, on the contrary, an air inclusion in a material with a higher index.

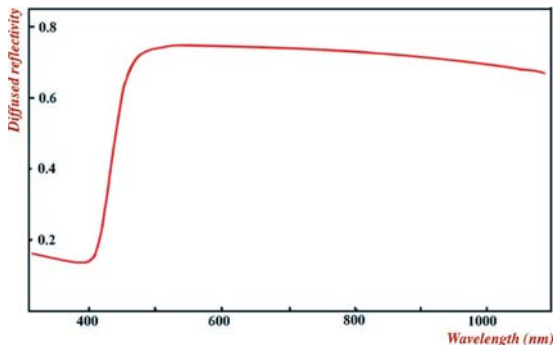


Figure 10.15. Diffuse reflection factor under normal incidence of a *Pieris brassicae* anterior wing. Reflection is strong throughout the visible spectrum. UV and part of the blues are absorbed, hence the slightly yellow color of the wing.

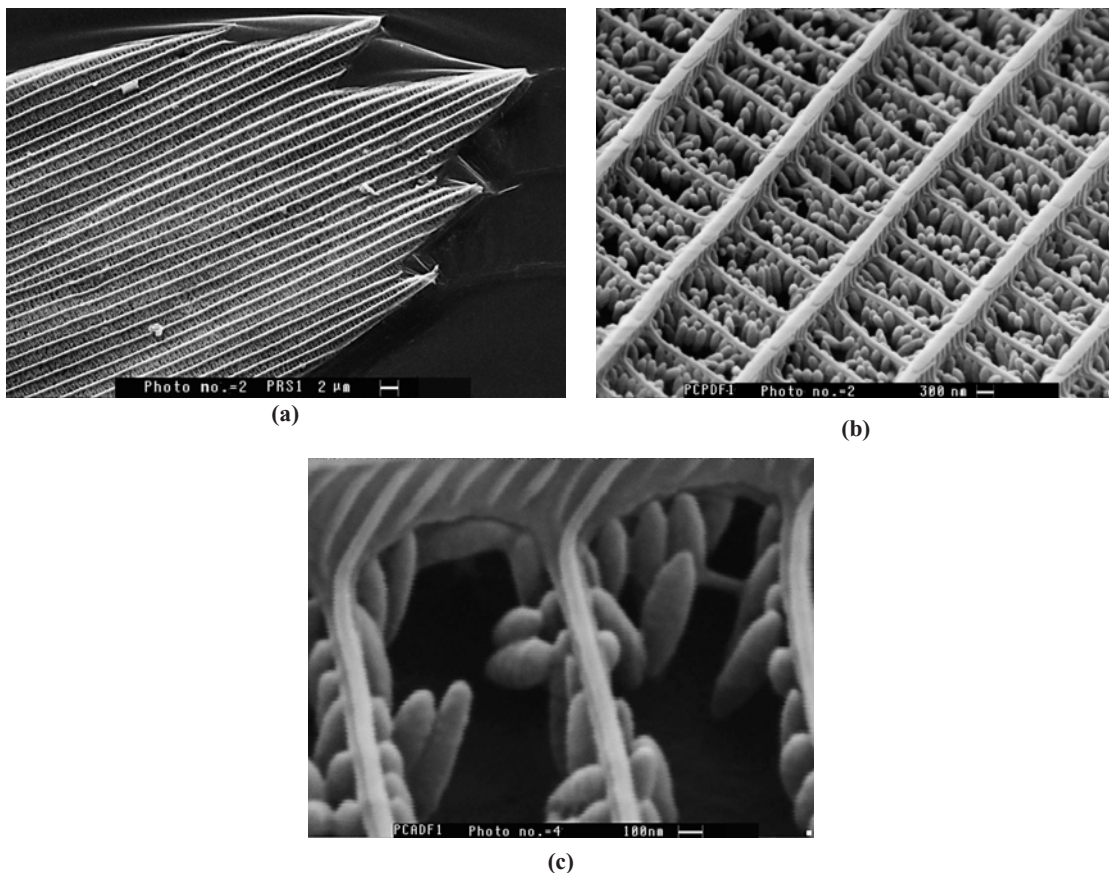


Figure 10.16. (a) SEM image of the extremity of a *Pieris brassicae* scattering scale. (b) view of the center of the scale approximately showing a non-covered area and the neighboring scales. In covered areas, striae are denser, counter-striae are thicker, and inclusions are fewer. Pieride scales also present traces of leucopterine, mostly on the ventral side of posterior wings, which gives them a slightly yellow color. Pterinosomes: (c).

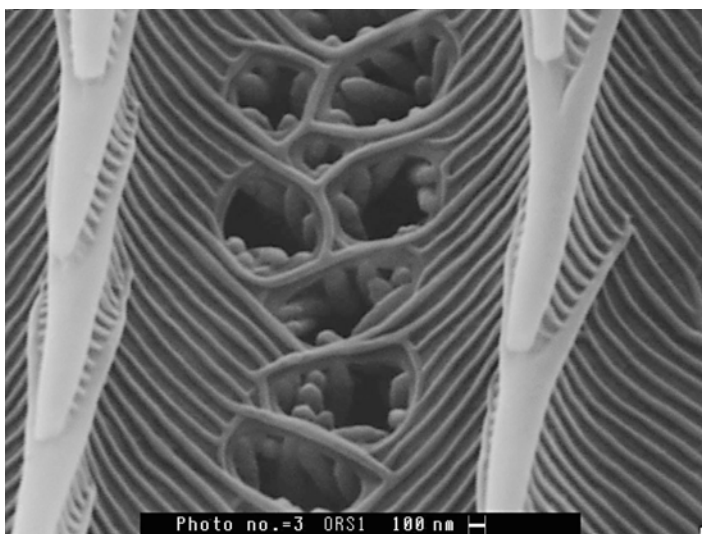


Figure 10.17. Scale roots covered by the extremity of preceding scales. Roots contain fewer Pterinosomes.



Figure 10.18. The male blue Argus *Polyommatus icarus* and the Argus *Celastrina argiolus*. The colors of both mainly proceed from scattering of the shortest wavelengths. The ventral side of *P. icarus* is pigimentary, more bluish at the base.

White

The scales of *Pieris rapae* are long, narrow, indented, and highly inclined on the wing plane. It is hard to distinguish between the bottom and cover scales, all being evenly white,

whether in reflection or in transmission and showing quite similar shapes. The whole appears rather disorganized and scales largely overlap.

By using scanning electron microscopy, striae look little developed, with an average spacing of 1,5 μm . Lamellae are very short, do not overlap, and therefore cannot produce any interference effect. They include remarkably developed counter-striae, which are regularly spaced—approximately 600nm—the whole creating a surprising square pattern on the wing formed by parallel rows of rectangular compartments. The latter contain scattering particles, around 20 per compartment. The particles are tiny pterin granules, known as pterinosomes, and present a regular and slightly ellipsoidal shape, all oriented vertically over the surface of the wing. The small axis is 100 to 150 nm long and the largest is around 350 nm, although it is quite difficult to estimate since its base is not always visible.

In this case, we are confronted with ellipsoidal scatterers that are arranged on a plane, parallel to each other and almost touching. Given a pterines estimated index of about 1,6 in the visible spectrum, the parameter of the sizes of isolated particles ranges from 3.5 in blue to 1.6 in red, which doesn't allow us to obtain maximal scattering. And yet, particles touching each other, we are here obviously confronted with an extreme case of dependent scattering, which experimentally leads to an overall substantial reflection on the whole of

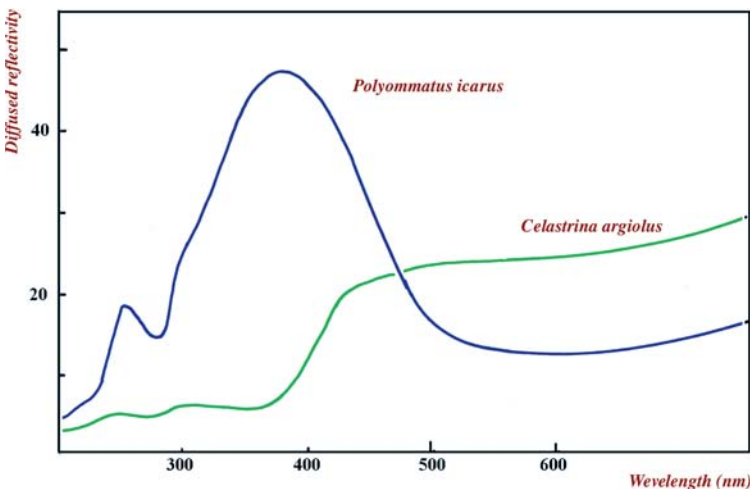


Figure 10.19. Diffuse reflection factor of *P. icarus* and *C. argiolus* Argus. The former shows a strong reflection factor centered on the blue/ultraviolet limit. While the second, presenting bigger inclusions, scatters more in the visible and has a weak spectral purity.

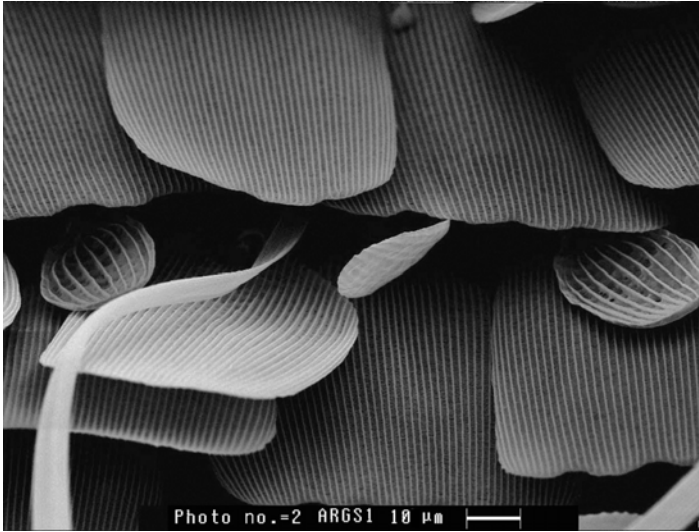


Figure 10.20. Superior side of *Polyommatus icarus* wing showing flat and highly striated scattering scales, as well as the root of a long thread-like scale—over 500- μm long—and small androconies in interstice.

the visible spectrum, yet the modeling of which remains to be established.

Blue

The common blue appears like the negative of *Pieris brassicae*. Most of the scales, with a more geometrical shape, prove quite disorganized, while some very long threadlike scales are scattered on the whole. Spacing between striae is well marked, lamellae are short and not covered, and counter-striae are well developed.

There is no inclusion here. The bottom of compartments is lined with an air spongy structure. It is difficult to evaluate the structure thickness by using Scanning Electron Microscope (SEM) images. Yet one can roughly estimate the average size of pores, here below 100 nm. The efficiency of scattering diminishes very substantially for long wavelengths, which makes short blue and violet wavelengths become more visible. The intensity remains weak and the purity much lower than that of *Morphos* obtained by interference.

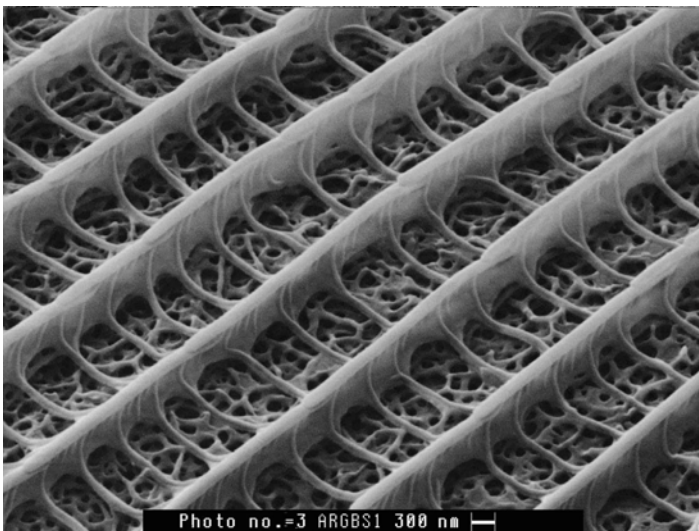


Figure 10.21. Spongy structure of the scattering layer of *Polyommatus icarus*. The structure is highly permeable and by using an optical microscope, one can observe how after absorption of an index liquid, color disappears.

Pigments and Pigmentary Colors

If the present book is mostly dedicated to physical colors, they are still a minority in nature. Most of animal colors derive from a pigment, and although these substances don't produce iridescence or very little in the usual observation conditions, they still have their place in a book dedicated to butterfly colors. We will mention them along two distinct lines, first the physicochemical aspect, which will include an overview of some important and distinct families of pigments as well as the physical process causing color: selective absorption. Since butterfly colors are observed in reflection, this aspect of the problem, generally less known, will be further studied. Secondly, we will tackle the physiological aspect of pigmentation, as well as its origin and from the point of view of evolution.

Selective Absorption and Colors of Pigments

Absorption is a transfer of energy between the incident electromagnetic wave and the atoms or molecules composing the illuminated object, or more precisely, the electrons of these atoms that are distributed on various orbitals, each characterized by one energy level.

Transitions between the different levels proceed from absorption or emission of the corresponding energy. In the case that concerns us here, the energy that is absorbed comes from the incident light, which will thus be deprived of certain wavelengths and its color will be consequently changed if the latter are situated in the visible part of the spectrum. When a photon interacts with an atom, it can transfer its

energy to the latter—and thus disappear—if the energy corresponds to the difference of energy between two levels of the atom. After a photon is absorbed, the atom is in an unsettled state—known as excited—and goes back to its fundamental state. Several processes allow this. Symmetric to the previous, the first one, is radiative relaxation. The atom goes back to its fundamental state by emitting its excess energy under the form of a photon. An exterior observer won't notice anything: A photon enters and another, identical to the first, goes out. The incident light is not modified and no color appears. However, such relaxation can be non-radiative. Surplus energy can, for instance, make a crystalline grating or its neighboring molecules vibrate, thus leading to an increase in the temperature of the object. Yet, there is no emitted light anymore. The incident photon is indeed absorbed during such a process. Yet, for the observer, this or these photons have disappeared from the incident light spectrum, and the color of the body somehow corresponds to the complementary of the absorbed color.

In order for such a phenomenon of coloration to occur, the difference of energy between the two levels must correspond to a frequency that is perceivable by the human eye. For us, this corresponds to wavelengths ranging from 380 to 680 nm. It is generally the case for isolated atoms in a gas, but not atoms that are linked to each other. In this latter case, the absorption bands of electrons forming covalent bonds are usually situated in the ultraviolet. Pigments and dyes belong to a very singular category of substances, in which the distribution of electrons is such that absorption bands are brought

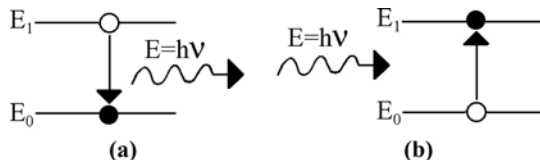


Figure 11.1. Transition between two energy levels of an atom with absorption and emission of a photon.

back to the visible. This category is that of π orbitals. Relaxation on the inferior levels occurs in a non-radiative manner through heat transferring, phosphorescence or fluorescence, or during a chemical reaction with the surrounding medium, in which case pigment is decomposed and loses its initial coloration. The function, or elementary group, responsible for light absorption is called chromophore. Its color can be modified by linking with other chemical

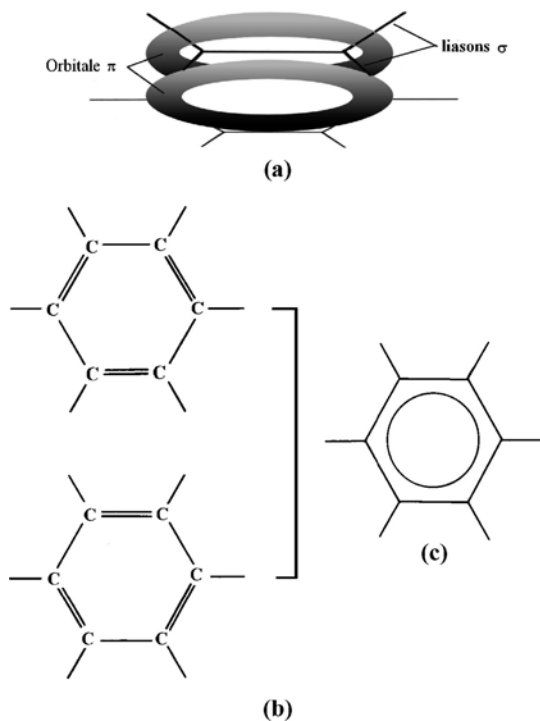


Figure 11.2. Different schematizations of benzene cycle. The two (a) and (b) cycles are symmetrical and equiprobable. (c) is a more appropriate representation. Below, the schematized representation of π orbitals.

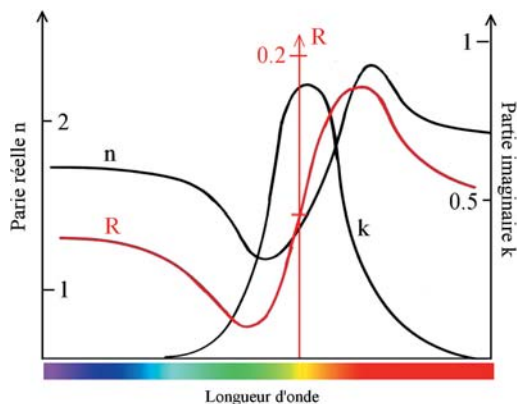


Figure 11.3. Optical index of a material— n real part and k imaginary part—due to electronic polarization. Other polarization phenomena occurring when frequency is lower, make the real part dissymmetric on both sides of the absorption peak. The reflection factor is thus also different. Absorption in the yellow makes an object look red in reflection.

groups receiving or giving electrons; they are auxochromes.

Organic chromophores always present a series of carbon atoms that are alternatively linked by single or double bonds. The simplest example of this is the benzene cycle. The two representations with localized bonds are of course strictly identical and equiprobable, and the electron pairs forming them should only absorb ultraviolet radiations. However, none of these representations is adequate. The most realistic one consists in linking atoms with single bonds, the supplementary three atomic pairs being divided and distributed on the whole molecule in delocalized orbitals (orbitals π). Here again, the excited states of these orbitals correspond to ultraviolet radiations. The energy of π orbitals decreases and their absorption bands come back into the visible only if molecules of the type mentioned above gather and form long polymers. The resulting colors are altered or intensified by the presence of auxochromes on the polymer margins. The auxochromes' role is to increase the mobility of chromophore electrons π , thus the wavelength of absorption. Contrary to that of isolated atoms, the energy levels of molecular orbitals are relatively high. One could almost designate them as energy bands, each

containing many vibrational sub-levels. Their number varies with the complexity of the molecule: the more complex the molecule, the more the vibrational sub-levels. Absorption bands are thus also broadened and the colors obtained are generally not very pure. The energy diagrams of pigmentary molecules consequently present wide bands, centered in the visible range of the spectrum or next to it. When the pigment or the pigmentary solution is illuminated by white light, all the wavelengths contained in the incident light and corresponding to a transition energy between two levels (the fundamental and an excited level in general) are absorbed, and the corresponding energy is the more often turned into heat. The transmitted spectrum is therefore deprived of this range of wavelengths and the resulting color is the complementary of the absorbed one. And yet, butterflies are hardly observed in transmission, but more in reflection. In this case, the reflected color is not the complementary of the absorbed one anymore: This is selective reflection, a phenomenon so dear to Michelson, which will now be described.

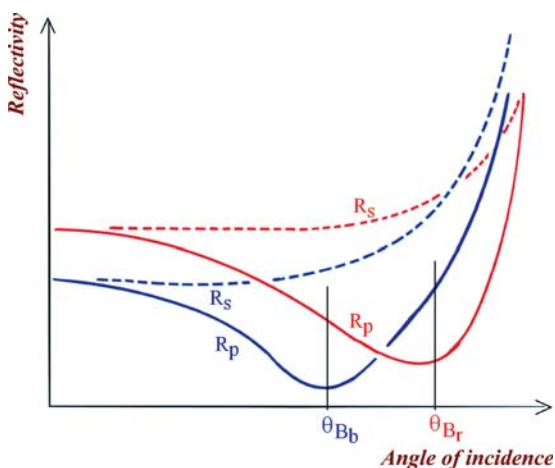


Figure 11.4. Variations of the reflection factor with the angle of incidence, for two radiations situated on both sides of an absorption peak. The optical index is weaker in the blue than in the red of the spectrum, and so is the θ_b pseudo Brewster angle. Under a light polarized parallel to the incident plane, the reflection factor of the blue wave R_p is weak for incidences close to θ_{Bb} and the object looks red. The reverse occurs when incidence is higher and the object turns more blue.

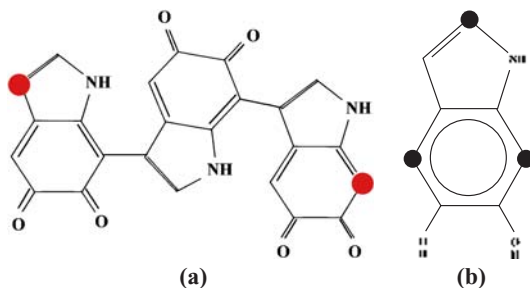


Figure 11.5. The dihydroxy-5,6 indole monomer and its three possible insertion points. (a). A portion of a eumelanin skeleton (b).

Substances presenting selective absorption such as pigments in the visible also show a selective reflection phenomenon that is due to the asymmetrical refraction index on both sides of a large absorption band. As has been mentioned, unless other processes come into play, the refraction index n indeed tends to be higher on the red side of the band, thus producing a higher reflection, compared to the blue side (Figure 11.3).

The colors created due to their dominant reflection factor on one side of a pigment absorption band, also depend on the angle of incident. Yet, this phenomenon can only be clearly perceived under polarized light parallel to the plane of incident. In this case indeed, the Brewster angle of long wavelengths radiations, an angle for which the reflection factor goes through a minimum, is approximately higher than that of blue radiations. Thus, the latter, mostly responsible for color under normal incidence, are here almost not reflected under high incidence (from around 60 to 70°), which cause a shift of the observed color towards blue, i.e., an effect similar to that of an interferential layer. Hence the controversy between Michelson and Raleigh. This phenomenon is of course undermined in non or weakly polarized light and cannot totally explain the important iridescent effects as observed in butterflies in natural light.

Lepidoptera Pigments

Among diurnal butterflies, excluding melanins that form the alary pattern motifs and that are

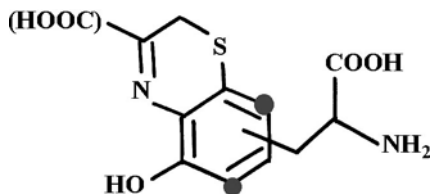


Figure 11.6. The pheomelanine monomer and its extension points.

present in all species, each family characterizes itself by a given type of pigment. They are mostly ommochromes among *Nymphalides*, papillochromes among *Papilionides*, and pterines among *Pierides*, while flavonoïdes and biliary pigments can be found in various species.

Melanins

Melanins form a large family of miscellaneous pigments, widespread in both vegetal and animal realms. They certainly represent the most common, yet most complex, pigments. They are polymers, the biological precursor of which is tyrosine. Their colors range from yellow to brown and black. In the animal world, there are two distinct kinds: phaeomelanins (yellow to reddish) and eumelanins (yellow to reddish) and eumelanins



Figure 11.7. Melanism examples among *Melanargia galathea*.

Above, left—normal individual.

Above, right—suffusion of black scales in the white. Below, left—melanian individual extension of black motifs.

Below, right—generalized melanism; black motifs still remain visible.

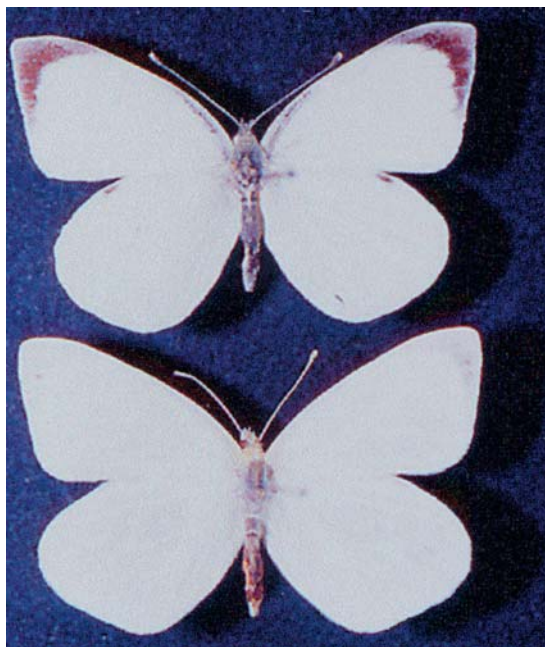


Figure 11.8. Albinism occurs when melanin is not synthesized.

Here, *Pieris brassicae*. Above, the fellow individual is normally pigmented, white areas are colored by pterines and the apex by melanins. The individual illustrated below, presents normally synthesized pterines, but the apex scales are depigmented due to the incapacity of synthesizing pterines. (11.7 and 11.8 Photo and collection H. Descimon)

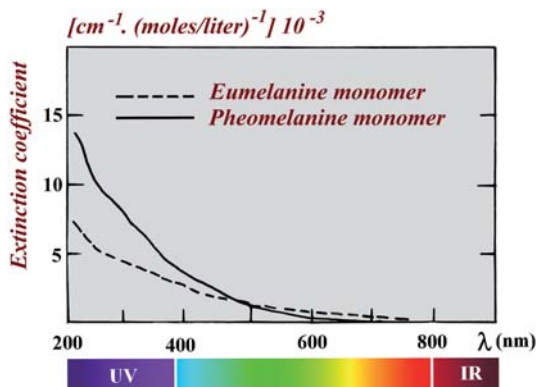


Figure 11.9. The absorption spectra of the monomers of the two animal melanins. They usually cover ultraviolet to a large extent, reaching the green-yellow range in the visible.

(brown to black), while Allomelanins are only found in Plants, Mushrooms and some Bacteria. Phaeomelanins and eumelanins are often associated and generate a great diversity of pigments. All the reactions causing melanins are catalyzed by a unique enzyme: phenoloxylase. Yet the latter are very sensitive to environmental conditions like temperature, humidity, or CO₂ rate. Variations in these parameters can lead to cases of melanism or albinism, as has been mentioned, directly affecting the survival of the species or some of its members.

A key element of human pigmentation, optical properties of eumelanin and phaeomelanin solutions are well known. However, the structure of the polymer has not been precisely established yet. The extinction coefficient of the monomer always shows a maximum in ultraviolet and then rapidly decreases in the visible, hence the yellow-brown colors that are generally observed. Yet it is established that the lengthening of the polymer chain and the presence of auxochromis increase absorption in the visible, sometimes leading to deep black. In addition to their role in the alary pattern, melanins often serve as an opaque screen under or within structural scales. As has already been seen, butterfly wings often contain several layers of scales of different kinds and the alary membrane itself is not optically inactive. In the cases of colors generated by the dorsal side scale pigments, for instance, and observed in reflection, the transmitted light can be partially reflected by the alary membrane or ventral side scales. It thus once again goes through pigmentary layers almost without any color alteration, since it has already been deprived of the absorbed colors, and thus contributes to the globally reflected light by weakening its purity. This phenomenon surprisingly scarcely occurs with structural colors. With a few exceptions like *Morpho godarti* and *Morpho polyphenus*, the affected butterflies always present a layer of highly absorbing pigmentary scales (*Archeoprepone* type) or structural scales containing pigments themselves (*Morpho menelaus* type) and creating a dark screen, hindering any parasitic reflection that would undermine the purity of the reflected color.

Pterines

Pterines are well known components. One pterine is contained in a major vitamin, folic acid, and others are coenzymes. Their biosynthesis chain is also well known, mostly thanks to experiments performed on butterflies (*Pieris* and *Colias*). They proceed from the molecular redistribution of nucleotide, the triphosphate guanosine (TGP)—the TGP purine nucleus and the ribose merge into a double heterocyclic nucleus; that, is pteridine. Secondary enzymatic reactions generate pterines with varying lateral chains. Among them, one can distinguish leucopterine and isoxantopterine, which are white, xanthopterine and sepiapterine (yellow), and erythropterine (orange red). The deep red of certain *Appias nero* is due to a pterine dimer, that is pterorhodine. All of these pigments almost only concern *Pieridae* and they are situated in scales as microscopic granules, called pterinosomes.

Ommochromes

Yellow, red, orangey, tawny, or brown. They are quite complex molecules deriving from the polymerization of cyclic amino acids—mostly tryptophane—that are found in the eyes of a majority of insects and on the scales of numerous *Nymphalides*. One owes its study to the German A. Butenandt and his group. As they were mostly chemists, their work lacks a zoological study of the distribution of these components among butterflies. In this way, the determination offered here, based on elementary criteria, remains to be proven.

The simplest components are soluble in water. It is the case of the initial component of ommochromics biosynthesis chain; that is, the yellow fluorescent 3-hydroxycynurenine. One can find it on wings of some *Heliocoenurus*. The same butterflies present xanthommatine that is orangey and the red dihydroxanthommatine. Vanesses show the latter, but also D ommatine (red-brown) and rhodommatine (dark red). The only difference between these components is their lateral chain. Yet, the origin of the bright red pigment of *Melitaea didyma* and of certain *Cymothoe* or *Callicore* remains a mystery.

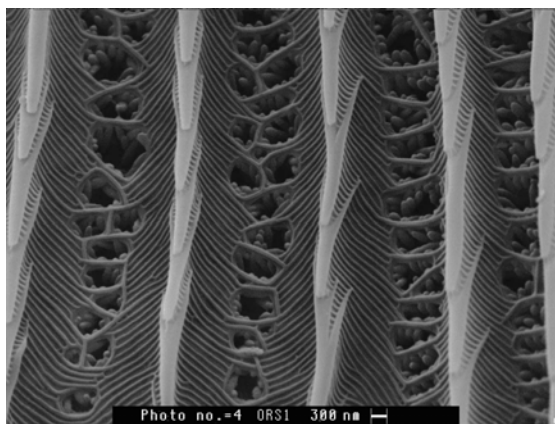
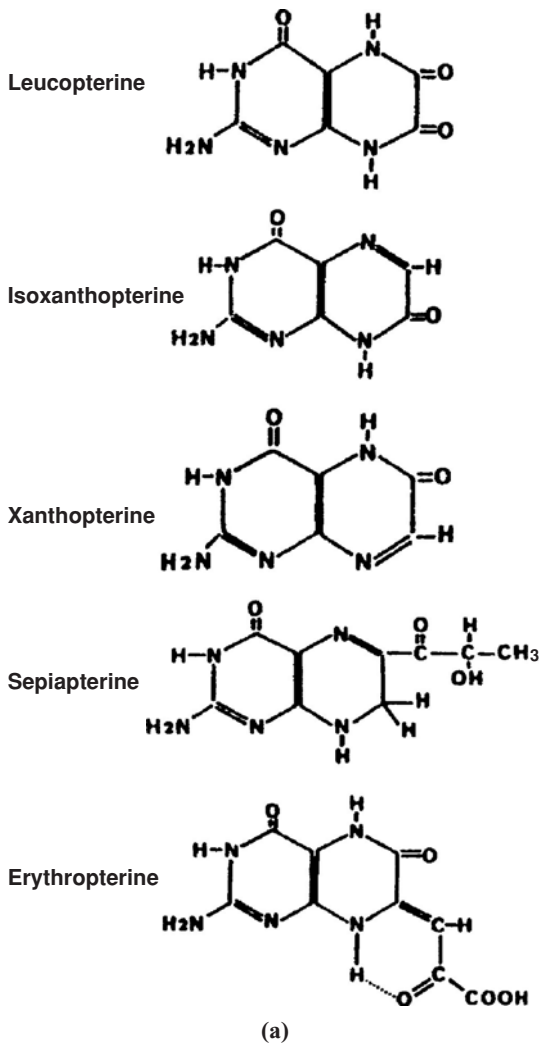


Figure 11.10. Pterinosomes between the striae of a *Hebonia glaucippe* Pieridae.

Ommes are little soluble in water and it is quite difficult to study them from a chemical point of view. They are mostly found in eyes. Other pigments, red and highly insoluble, that can be observed in Nymphalides (*Precis coenia*), prove to belong to the same chemical family since they derive from tryptophane. It was established through blending it with tryptophane—¹⁴C.

Papiliochromes

They are close to ommochromics and derive from cyclic amino-acids, tryptophane (via kynurenine) and from phenylalanine (via

dopa) for the simplest ones. The structures of other more complex ones are little known and only the structure of papiliochromic II has been discovered. Their coloration ranges from light yellow to red, and as their names suggest, they are present in *Papilionides*. A polymorphism determined by one gene and opposing a light yellow pigment to an orangey one has been researched among *Zerynthia*. The Greek species, *Z. polyxena*, thus includes an orangey type, *Ochracea*, present in both males and females. Among *Z. rumina*, it is the *canteneri* type characteristic of Southern Spain and Maghreb, which is dominant and tends to only occur in females.

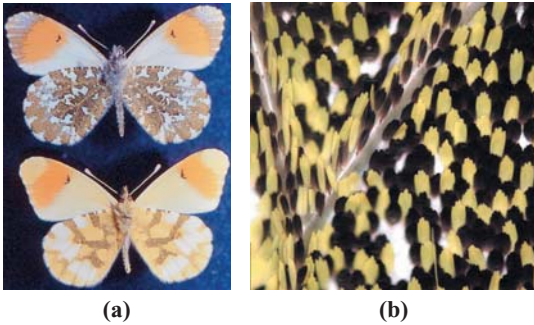


Figure 11.11. Left: two *Anthocaris* Pieride, *A. cardamines* and *A. euphenoides*, colored by pterines. White proceeds from a mix between leucopterin and isoxanthopterin, orange to the two previous ones mixed with erythropterine. Green is due to the "pointillist" juxtaposition of pterine yellow scales and structural bluish black scales.

Flavonoids

Flavonoids or anthoxantines rank among the rare vegetal pigments found among adult insects. They are absorbed by the caterpillar, then stocked and fixated in wings during nymphal stage. When mixed with ammoniac, they turn bright yellow, which allows to easily detect them. They are widespread among diurnal butterflies—*Hesperiidae*, *Lycaenidae*, *Pa-*



Figure 11.12. Nymphalide from the center of Africa, *Cymothoe sungaris*—male, 5 cm—one of the very few entirely red butterflies. Its ventral side is cripteous.

pilionidae (*Graphiini*, *Parnassius*), and *Prieridae Dismorphiinae*—where they are associated with pterines—*Nymphalidae Satyrinae*—like *Melanargia*, which reacts extremely well to the detection technique mentioned above.

Biliary Pigments

These pigments are unique as their coloration tends to be green or even blue. They are components deriving from tetrapyrrolic

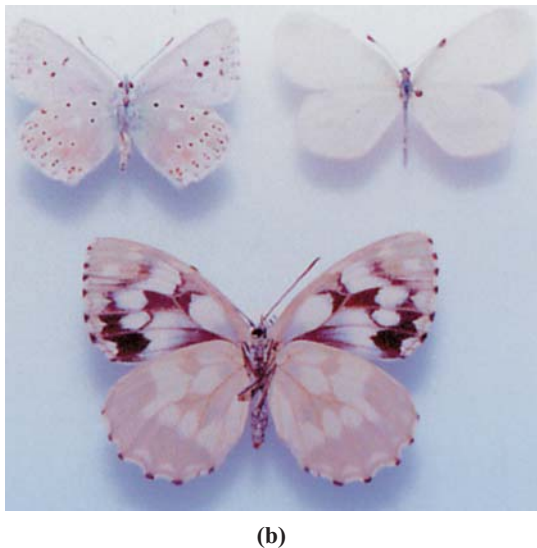
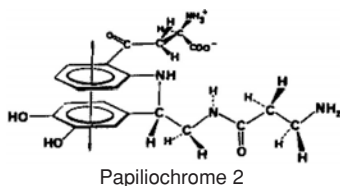


Figure 11.13. Flavonoids among various butterflies from different genus. *Lyсандra coridon*, *Leptidea sinapis*, *Melanargia galathea*. Above, normal aspect. Below, insects immersed in ammoniac vapors—characteristic reaction of flavonoids.



(cf. hemoglobin or cytochrome). Pterobiline that is usually found in the alary membrane, makes the latter turn green in female *Gonepteryx*, in the Cabbage Pieride or even more in *Graphium* (*papilionidae*), and *Actias*... They are very unsettled pigments and become altered very rapidly especially in *Eurotides celadon* from Cuba, the extraordinary blue of which turns greenish when it dies...

The pigments of diurnal butterflies are rather well known, whereas those of Heterocers are very little known. They could have many surprises in store if studying them became as common as it used to be in the past. Even among diurnal butterflies, red pigments remain obscure.

Y. Umebachi and H. Descimon have independently tried to characterize the red pigment of the Papilionide *Atrophaneura horishanus*—most probably a papiliochromic—yet their analysis was hindered by extraction, as was also the case for ommochromic. The same author isolated the pigment that confers the extraordinary bright orange of Coppery among *Lycaena phlaeas* (Figures 5.1 and 5.2). It is a component deriving from the acid 3-hydroxyanthranilique (Umebachi, 1982). And yet, one may have assumed that such a color was physical as it is so bright. This discovery is all the more interesting since some pigments presenting the same chemical nature and colors that are close are common among mushrooms—in Agaric, whether imperial mushroom or fly agaric.

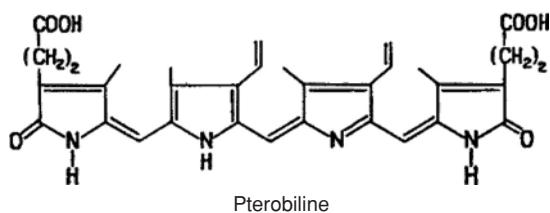


Figure 11.14. The green spots of this *Graphium weiskei* are due to a biliary pigment, a pterobilin. The light purple also proceeds from a pigment, which has still not been identified to my knowledge.

The study and characterization of butterfly pigments are far from being complete. In addition to the fact that they are quite neglected nowadays, these studies are often confronted with major technique difficulties. Indeed, many of these substances are hardly soluble, thus difficult to extract. We will only offer an overview here based on a study by Pr. Henri Descimon, which includes a comprehensive bibliography on the subject.

The big families of pigments as described above come from two different origins. They can be the result—or residue—both of a synthesis or an excretion. In most cases, these components are toxic in high concentration and must therefore be eliminated or stocked. Paradoxically, wings, which make butterflies look so beautiful, serve as containers for these toxics. Wings are indeed a dry and sclerotic organ in adults that can thus stock toxic substances without any risk. It is also worth noticing that their coloration is a mere secondary effect, even if it becomes a key element for the survival of insects.

Thermoregulation and Spectral Selectivity

Imperatives

As in the animal world, the body temperature or that of some parts of the body of insects—is one of the principal parameters of their vital balance. It is indeed directly linked to mobility thus affecting feeding, reproduction, and reactions to threats in butterflies . . .

During flight, it is essentially the six pairs of tergosternal muscles, situated in the mesothorax, that make anterior wings flap, whereas posterior ones are equipped with a mechanic frenate coupling. These muscles are not directly attached to wings but permit the thorax to contract longitudinally, flapping resulting only from a mechanic reaction. The efficiency of such a device is surprisingly weak. An estimated 80% (on average) of the energy used during flight is converted into heat.

The overheating of muscles is not only the harmful result of muscular activity, but also a requirement for flying. During takeoff, wing abductor and inductor muscles must quickly—and in alternation so they don't collide with each other—contract, the resulting optimal temperature reaching 40°C. This heterothermal animal, which must reach a temperature of 36 to 38°C to be able to take off, is equipped with a flying device that is not only energetically little profitable, but that would also not withstand a temperature over approximately 42°C. However, after taking off, and in a usual situation, a dynamic balance is found with a lower temperature ranging from 30 to 35°C. In this way, butterflies must be able to quickly heat their muscles when at rest and then during flight, efficiently eliminate calorific

energy. The wing optical and infrared properties more or less contribute to each of the processes.

Let us first consider the heating phase. All diurnal butterflies have two techniques in different proportions, enabling them to make their thorax muscles reach the critical temperature necessary to get off. The first process is endothermal, as the muscles themselves maintain the optimal temperature by stimulating their metabolism. This situation is more often observed when the insect is resting in the shade and is characterized by quick trembling that resembles human shivering. Inductor and abductor muscles contract quickly and in phase, i.e., in an antagonist way, thus preventing any flapping and saving the entire energy to rise the thorax temperature.

The second process, which concerns us more directly, is designated as exothermal. It picks up solar energy, thus involving the wing optical properties but also that of the insect body. The alary membrane proves to conduct heat poorly and lymphatic circulation is weak, so it has been assumed that it is essentially the body or basal area—which represents less than a third of the total wing surface—that picks up energy. The way wings are situated in relation to solar flux depends on their optical properties and varies according to species. Butterflies with wings presenting dark colors on either side directly pick up solar energy by spreading the latter to the sun or pressing them vertically above the body.

The latter position is adopted by butterflies with cryptic colors, both allowing camouflage and thermal regulation. White species or

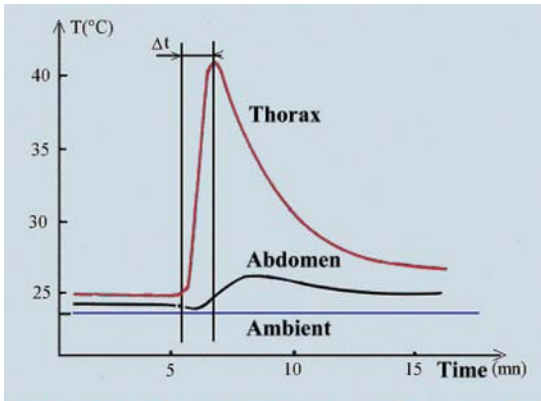


Figure 12.1. Endotherm heating of thorax and abdomen of a Lepidopteron. It takes a little more than a minute for the insect to reach the thorax temperature that is critical for taking off. The slight increase in abdominal temperature during the cooling off phase suggests that the insect evacuates energy through trachea from its thorax towards its abdomen. (after B. Heinnick, *Sciences* 185 (1974), 797)

light-colored ones make their temperature rise indirectly by concentrating solar flux on their dorsal side, which is black in this case. Facing the sun, wings are more or less open above the body at an angle determining the amount of energy picked up by the body.

As concerns cooling that is only required during flight, most of it proceeds from convection and conduction of the environment air, and also from tracheal exchanges between the thorax and the abdomen. Another smaller part derives from the thermal radiance of the body and wings. If one considers the average temperature of 40°C, this radiance occurs in near infrared reaching its climax around 9,5 μm. Before further studying the thermo-optical properties of the “butterfly collector,” we will now briefly present the few principles involved.

Energetic Balance

A Few Definitions

Endothermal sources of heat aside, as concerns the Q energetic balance of a solar collector, solar energy incident on the whole collector surface represents the credit, whereas the debit is the convective, radiative or optical loss: reflected

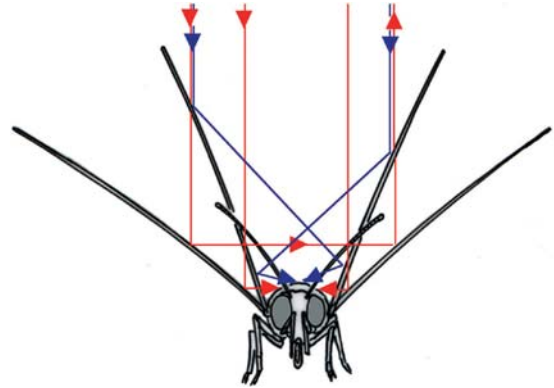


Figure 12.2. Solar flux concentration on thorax and abdomen. In wide open position, only a small part of energy is concentrated on the body. The smaller the wing angle, the larger the energy concentration.

or transmitted flux. We get:

$$Q = S_c \alpha E_i - O_p - A_0 (T_a - T_0) - S_a \varepsilon \sigma (T_a^4 - T_0^4) \quad (12-1)$$

where S_a is the collector surface, S_c the surface that is really exposed to radiation—they are equal when one considers wings only— O_p the total optical loss, E_i incident light, T_0 and T_a the temperatures of the environment and of the collector, and finally α and ε absorptivity and emissivity of the collector.

Scales actually prove to be a great insulating coating, which is why convection and conduc-

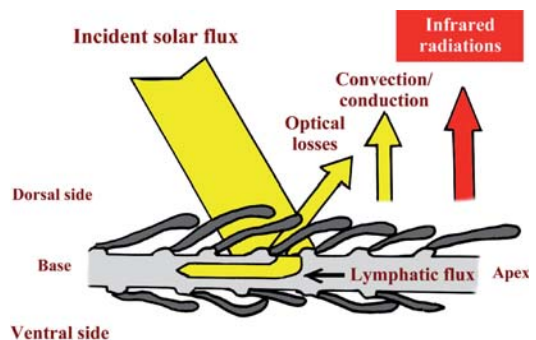


Figure 12.3. Photothermal collector losses. Optical losses are due to light being reflected on wings. They are very small in black butterflies. Losses proceeding from convection and conduction are small when the insect is at rest, but can be substantial yet useful during flight in order to get rid of surplus heat. Losses due to radiation are predominant.

tion loss for a resting animal can be neglected ($A_0 = 0$). One can therefore determine a radiative efficiency allowing to study the influence of the optical properties of butterfly wings or body:

$$\eta_r = \alpha - \frac{\varepsilon \sigma (T_a^4 - T_0^4)}{E_i} \quad (12-2)$$

One can notice that in a given environment, the greater the efficiency, the greater the absorptivity and the weaker the emissivity—for a given body temperature. Let us study these two quantities. In a given configuration, the absorptivity of a material is the amount of incident energy that it absorbs. One distinguishes between the directional absorptivity $\alpha'(\theta)$ when the radiation specularly falls onto the wing under an angle θ (clear sky) and α hemispheric absorptivity when the incident radiation is diffuse (cloudy sky), the latter being the integral over all the irradiating space of the former. As a first approximation, these two magnitudes do not depend on temperature.

As concerns emissivity, it is defined as the ratio between the energies radiated by the material and by the black body at the same temperature and in the same configuration. In a given direction, one measures the directional emissivity $\varepsilon_T(\theta)$ which, integrated over the whole open space, gives the total emissivity ε_T . Determined in this way, ε_T and α represent global energetic magnitudes in which the absorbed and emitted spectra do not show up precisely. They can nevertheless be deduced from the $\varepsilon_{T,\lambda}(\theta)$ and $\alpha'_\lambda(\theta)$ monochromatic quantities by integration on the wavelengths and dividing by the irradiance of the incident spectrum and the black body emission spectrum, respectively:

$$\begin{cases} \alpha'(\theta) = \frac{\int_0^\infty \alpha'_\lambda(\theta) L_\lambda(\theta) d\lambda}{\int_0^\infty L_\lambda(\theta) d\lambda}, \\ \alpha = \frac{1}{\Omega} \int \alpha'(\theta, \varphi) \cos \theta d\Omega, \end{cases} \quad (12-3)$$

and

$$\begin{cases} \varepsilon'_T(\theta) = \frac{\int_0^\infty \varepsilon'_{T,\lambda}(\theta) M_\lambda(T) d\lambda}{\int_0^\infty M_\lambda(T) d\lambda}, \\ \varepsilon = \frac{1}{\Omega} \int \varepsilon'(\theta, \varphi) \cos \theta d\Omega, \end{cases} \quad (12-4)$$

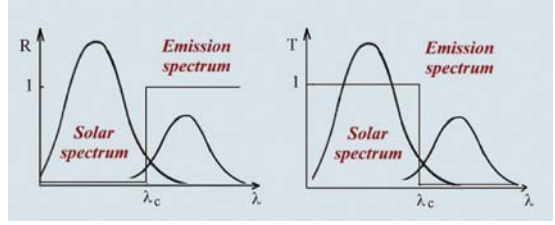


Figure 12.4. Reflection and transmission curves of a selective collector and an ideal selective window. As concerns the former, absorption is maximal until the cut off wavelength λ_c and is equal to zero beyond it. As concerns the latter, the transmission is equal to zero beyond λ_c , preventing thus radiative losses.

where L_λ is the monochromatic luminance of the incident flux—the solar spectrum as far as we are concerned—and $M_\lambda(T)$ the monochromatic emittance of the black body at temperature T . These relations tend to be complex, but not independent. Indeed, if the body is at thermal equilibrium, a conservation law—Kirchhoff's second law—determines that for a given direction and wavelength:

$$\alpha'_\lambda(\theta) = \varepsilon'_\lambda(\theta) \quad (12-5)$$

Absorptivity is directly related to the transmittivity $\tau'_\lambda(\theta)$ and the reflectivity $\rho'_\lambda(\theta)$ according to the law of energy conservation:

$$\rho'_\lambda(\theta) + \tau'_\lambda(\theta) + \alpha'_\lambda(\theta) = 1 \quad (12-6)$$

Energetic quantities involved in the radiative balance can therefore be obtained through reflection and transmission optical spectrometric measurements.

Ideal Selective Collector

If the aim is to increase the efficiency of the collector to reach thermodynamic balance, the optimal solution is therefore to realize an absorptivity α maximal over the whole solar spectrum and an emissivity ε minimal in the spectral domain emission corresponding to the temperature reached. For an opaque object ($\tau = 0$), this comes back to ideally have a reflection coefficient equal to zero in the visible and equal to 1 in infrared. Equations (12-5) and (12-6) highlight that in this case, α is maximal in the visible and ε minimal in infrared. The transition from visible to infrared occurs for a wavelength—called



Figure 12.5. *Archaeoprepona menander* (Charaxinae) iridescent medial areas present an *Urania*-type scale arrangement, with convex structural cover scales and multi-lobed pigmentary ground scales. Dipped into trichlorethylene, its colors vanish totally and the black areas of both sides turn dark brown.

cut-off wavelength λ_c —depending on the temperature reached by the body and which is about $4\ \mu\text{m}$ in the present conditions, $T_c \sim 50^\circ\text{C}$.

This is how most of plane solar collectors—designated as selective, i.e., with marked transitions between their visible and infrared optical properties—are produced nowadays. According to the same principle, we have to mention transparent coating or selective glass. In this case, visible reflection is equal to zero ($\rho = 0$) and transmission to 1 up to λ_c . Beyond, τ is equal to zero and ρ to 1. Equations (12-5) and (12-6) thus reduce to:

$$\alpha'_\lambda(\theta) = \varepsilon'_\lambda(\theta) = 1 - [\rho'_\lambda(\theta) + \tau'_\lambda(\theta)] \quad (12-7)$$

and an ideal selective glass is characterized by:

$$\begin{cases} \alpha_\lambda = 0 \text{ et } \rho_\lambda \approx 0 \text{ soit } \tau_\lambda = 1 \text{ for } 0 < \lambda < \lambda_c, \\ \varepsilon_\lambda = 0 \text{ et } \tau_\lambda = 0 \text{ soit } \rho_\lambda = 1 \text{ for } \lambda > \lambda_c. \end{cases} \quad (12-8)$$

An Example: *Archaeoprepona*

These two cases are extreme, since the condition that is necessary and sufficient to decrease radiative loss, as defined by Kirchhoff's second law, doesn't imply any of these solutions. Butterflies favoring direct absorption of solar energy through their wings have generally developed a third alternative. It is the absorption by the black areas situated at the wing base that provides the body with the most part of the incident energy. The absorption is very high over the whole solar spectrum—absorption approximates 98%—but becomes insignificant in the

infrared due to the combined action of reflection and transmission. As can be seen in Figure 12.5, the basal areas of the wings turn lighter black to dark brown when the insect is immersed into an index liquid. This demonstrates that absorption doesn't depend on pigments only, but also partly results from a structural effect.

Solar collectors indeed commonly use the surface roughness in order to increase visible absorption and sometimes even to obtain a higher spectral selectivity. The technique consists of creating a roughness big enough so that short wavelengths—the entire visible spectrum—get trapped on the absorber surface, whereas longer wavelengths—corresponding to the thermal emission spectrum of the collector—are reflected.

In the industry of solar collectors, this is obtained by producing dendritic structures over metal surfaces, providing them with a high intrinsic infrared coefficient. The manufacturing process, mainly chemical, only produces roughness with random shapes and sizes, which doesn't make them a good support for rigorous modeling. They are determined by the statistical distribution of heights in relation to the average level and by an autocorrelation function transposing the distribution of the roughness in the absorber plane: roughness spacing.

This static aspect of the system is therefore opposed to precise calculations of the optical properties of the rough surface and the many models developed to determine them can only do so based on drastic simplifying assumptions. We won't mention the formalism of such models since they are quite close to scattering models as far as their principles are concerned. We will only focus on their qualitative predictions, which for lack of rigorous calculations on butterflies will enable us to evaluate the role of structures in butterfly thermal balance. The most basic models allow to compare the reflection R of a rough surface as characterized by σ the average height of roughness and T the average period, to the reflection R_0 of a smooth surface of the same material, for a given wavelength λ . The ratio R/R_0 is a function of the only three parameters: λ , σ ,

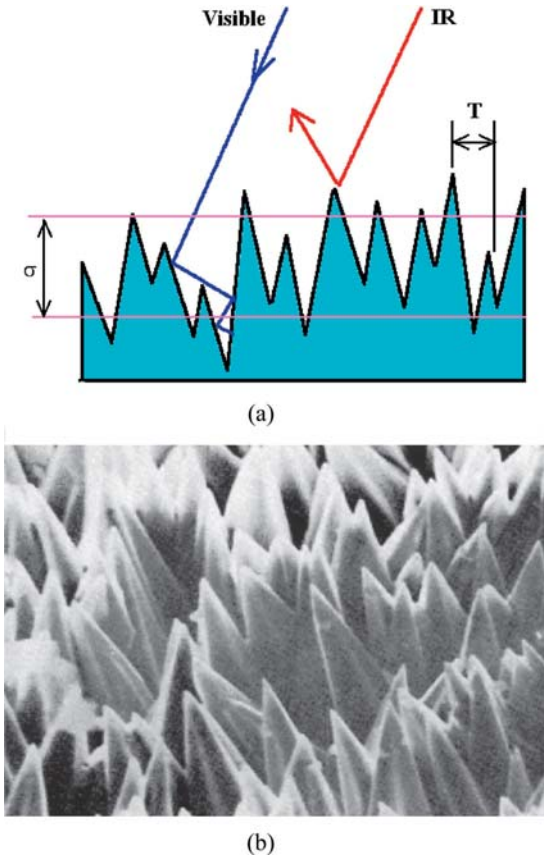


Figure 12.6. The dendritic selective surface of a solar absorber. (a) Radiations of the short wavelength radiations penetrate into the roughness where they are absorbed, while long wavelengths are reflected. (b) rhenium dendrites. (after B.O. Seraphin, 1974)

and T . As a first approximation, one can distinguish a specular, or R_c coherent component and an incoherent R_d diffuse component in the reflection. As expected, the various models demonstrate that the coherent part has a significant influence only in the long wavelength range larger than the height of roughness ($\lambda > 5\sigma$), which is not “seen” by the radiation anymore and thus hardly affect the reflection. On the contrary, the diffuse part prevails at small and medium wavelengths ($\lambda \geq \sigma$), its intensity greatly depending on the ratio T/σ . The smaller the ratio, i.e., the deeper and the denser the roughness, the higher the absorption. Finally, if the average height σ is increased, the cut-off wavelength λ_c shifts towards infrared. What about the butterfly? We

will neglect structural scales—which, as we have seen, sometimes contain pigments and therefore contribute to the overall absorption—to focus on scales that are strictly pigmentary. According to species, they can form two quasi-continuous layers, one on the ventral side and the other on the dorsal. Their structures as well as their shape are characteristic. Contrary to structural scales, pigmentary ones tend to be lanceolate or multi-lobed, rather long and substantially overlapping.

Among *Archaeoprepona menander*, which has been studied more fully from this point of view, the pigmentary scales striae present a very regular spacing of $1 \mu\text{m}$, while that of counter-striae averages 300 nm with a higher dispersion. They form rows of alveoles, approximately elliptic, over $1 \mu\text{m}$ -high and opening on the bottom on the scale alary membrane. If one considers an average period $T = 1,3 \mu\text{m}$ and an average height $\sigma = 1 \mu\text{m}$, the structure leads to a ratio R_c/R_0 , thus to a specular component that is high beyond $7 \mu\text{m}$ in the infrared, and to a total reflection, mainly diffuse, below 30% in the visible. A significant amount of the incident energy is therefore trapped into an alveolar structure which, as has been mentioned, consists of pigments that are efficient in this part of the spectrum although it does not take part in the infrared emission because of its weak absorption in this spectral range. Both structures and pigments combine their efforts in order to actually absorb over 95% of the incident light over the whole visible spectrum, even reaching 98% at 550 nm , the maximum of the solar spectrum.

Infrared properties are even more remarkable. Absorptivity reveals two strong peaks of absorption at $3 \mu\text{m}$ and $6 \mu\text{m}$ and remains more or less constant at a rather high value approximating 0.4 , up to $\lambda = 50 \mu\text{m}$, which marks the limit of our measurements. From the strict point of view of efficiency, this situation is not optimal. A rather high absorption hence, emissivity—covering the whole spectrum of the thermal emission is implying substantial radiative loss. This is ignoring the double constraint subjecting the insect, to raise its body temperature, yet not by too much. As concerns this matter, this situation

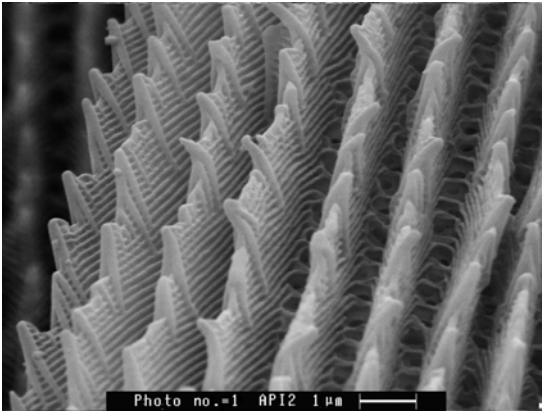


Figure 12.7. SEM image of *Archaeoprepona* pigmentary scales.

approaches perfection and contains the outline for a remarkable self-regulation phenomenon of the radiative balance, allowing the stabilization of temperature in the survival area of the butterfly.

The first absorption peak, centered on $3\ \mu\text{m}$, i.e., between the solar radiance and the thermal emission spectra, is not involved in the radiative balance at these temperatures. However, the second one, on the edge of the emission spectrum, plays a key role as a thermal regulator. Its marginal situation is such that according to the wing temperature, it overlaps or not the

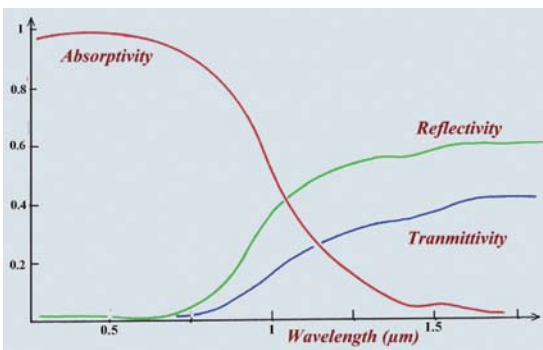


Figure 12.8. Reflection, transmission, and absorption factors of *Archaeoprepona* black areas—Cu1 and Cu2 base—showing the strong spectral selectivity of wings near the thorax and the combined action of reflection and transmission that weakens the absorption in the infrared.

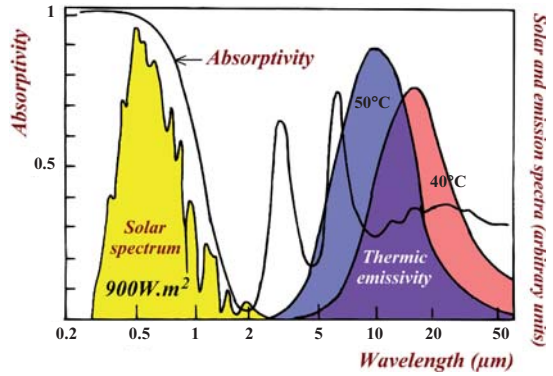


Figure 12.9. Absorptivity of the base of *Archaeoprepona* wings between 0.3 and $50\ \mu\text{m}$, spectrum of solar irradiance and of the emission of a black body at 50 and 40° . The second absorption peak overlaps with the emission spectrum at 50° , but it does not at 40° , leading to a quick change in the emission regime according to temperature.

emission spectrum, modifying the collector efficiency, and thus its temperature.

When after exposure to the sun, the temperature raises, the emission spectrum shifts towards short wavelengths and overlaps the absorption peak. According to Kirchoff's second law, this leads to a higher emissivity, hence lowering the radiative efficiency and decreasing the temperature. On the contrary, when there is no sun, the temperature is lower, the emission spectrum shifts towards infrared and

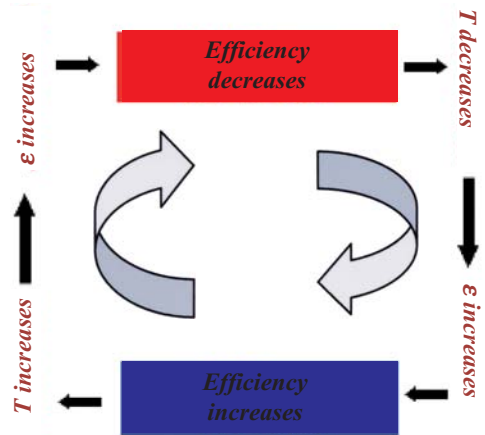


Figure 12.10. Temperature stabilization cycle of a butterfly black wing. When temperature increases, the captor efficiency decreases and the way round.

thus long wavelengths and the absorption peak lies outside of the emission spectrum. In this case, the emissivity is lower, the radiative efficiency increases, and the temperature raises. The real efficiency of this stabilization cycle is not easy to precisely determine when one does not know the temperatures that wings reach when exposed to the sun. One can still evaluate the emissivity for the extreme cases of wing temperature; for instance, 50° and 30°C. In the first case, the peak totally overlaps the emission spectrum, while it is outside of the spectrum in

the second case. The radiated energy is here proportional to the surface common to the absorption peak and the emission spectrum. At 30°C, when the peak does not take part in the thermal emissivity at all, radiative losses reach 275 W.m⁻², but go over 500 W.m⁻² at 50° temperature. The temperature of a butterfly warming itself in the sun remains quite inferior to these extremes, yet the previous rough calculations demonstrate that this auto-stabilizing system can play a substantial part in the insect thermodynamic.

13

Vision and Colorimetry

Color Perception

The colored perception of an object is a complex and totally subjective phenomenon involving numerous parameters, physicochemical as well as psychological. As has been seen, butterflies prove quite talented at drawing attention or hiding themselves. We will now consider the fellow creature, the predator, or more generally, the observer viewpoint. We will briefly introduce the physiology of the human eye and focus on the techniques to characterize colors, the stimulus, and the nervous message and its corresponding image in the brain.

As has been mentioned, physiological and psychological phenomena involved in the perception of colors are complex and interwoven. They are also specific: Insects, particularly Lepidoptera, perceive colors in a slightly different way from us, as is also the case of many of predators. Thus, the question why Butterflies are so vividly colorful, entails two answers depending on the point of view. First, the point of view of physics—: What are the physicochemical processes, elements, or structures producing such a color? Secondly, the point of view of biology: What is the point of color as concerns evolution? Indeed, if butterflies survived with such colors, it implies that they are not harmful to their evolution. Apart from these two points of view, it will only remains for us to go into raptures on how ingeniously and delicately butterflies use physical phenomena to meet their goal.

It is difficult to precisely determine the perceived color of an object, as it involves three

fundamental components, among which the eye and the interpretation of the nervous message by the brain is physiological and psychological, and thus varies with the observer.

The light signal $P(\lambda)$ that reaches the observer's brain can be described as a spectral convolution of the light source irradiance $E(\lambda)$, the object reflectance—butterflies are usually observed in reflection, but the approach would be similar for transparent objects observed in transmission—and the spectrum of the sensitivity of the eye to the different colors composing the signal $V(\lambda)$:

$$P(\lambda) = E(\lambda) \cdot R(\lambda) \cdot V(\lambda). \quad (13-1)$$

It is easy to quantify these various factors, especially the first two. We will briefly recall the spectral characteristics of the sun, which is the source that has traditionally been used to observe “in vivo” diurnal butterflies. We will here only overview the basic principles of colorimetry.

As colorimetry allows us to define a color in a nonambiguous way, as well as its possible faithful reproduction, we will consider the standardization of all the physiological and psychological parameters involved in visual perception; in other words, the definition of a standard source and average observer—the reference observer CIE 1931 (International Commission for –Lighting: 1931)—to be a prerequisite. This definition is based on the statistical study of normal human vision, which is very different from that of a lizard or a butterfly.

The color perceived by an observer can be defined as the result of a measurement per-

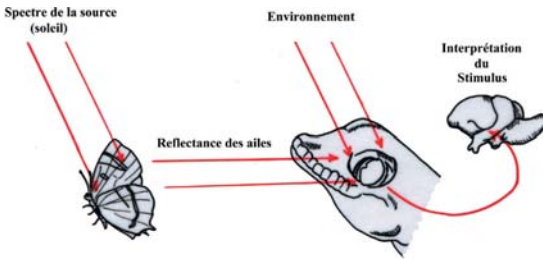


Figure 13.1. The color perceived by an insectivore depends on the spectrum of the light coming from the insect and reaching the retina photoreceptors, i.e., both from the source—usually solar, specular, or diffuse light—and from the wing reflection coefficient. It can sometimes depend on the close or distant environment of the insect, on the adaptation state, and even on the predator experience.

formed by the eye, i.e., its various collectors, and interpreted by the brain. The result of this process is the perception, by order of the more obvious to the less, of three elements. First, a predominant color or shade, we tend to say a dominant wavelength in physics (blue, green, yellow...); secondly, an intensity—strong, intense, or weak light—determined by the amount of energy in the color spectrum. The larger the intensity, the lighter the color. One can thus establish a scale of intensities ranging from 0 (black) to 1 (white). And finally, a purity that determines the amount of energy emitted to the predominant wavelength com-

pared to the whole energy emitted by the source. An atomic emission ray that is quasi-monochromatic has a purity of 1, while that of white is equal to zero. All of this can actually be more or less independent of the spectral composition of the wave coming in the eye, since it does not perform a spectroscopy of the wave but rather a non-univocal translation. We will now describe more or less in detail each of the stages involved in the process of color perception as illustrated in Figure 13.1. A distinct chapter has indeed been dedicated to the study of the optical properties of solids.

Sources and Illuminants

In nature, the universal source of light is the sun, the radiance of which is perceived directly or diffusely during the day and sometimes by reflection on the moon at night. The monochromatic distribution of solar radiance is complex, combining emission spectrum and ray spectrum. Beyond atmosphere, the spectrum somehow looks like a black body at 5 800° K, yet it is very altered when it reaches the earth ground after a more or less long trip—depending on the time and latitude—across terrestrial atmosphere, one says traveled “air mass,” where a significant part of energy is absorbed by ozone, mostly in the blue, and by water vapor in the infrared, before being scattered in the blue again.

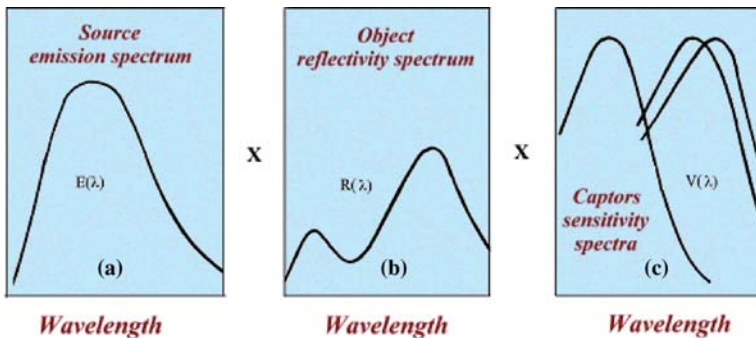


Figure 13.2. The physical components of a visual stimulus—arbitrary units. Light perception depends on the spectral composition of the source, (a) on the reflectance—or transmittance for transparent objects—of the observed object, (b) and on the sensitivity of the various eye receptors to different wavelengths (c). The corresponding brain representation is more complex to quantify, for instance, as coordinates within a color space—and is the goal of colorimetry.

Whatever the atmospheric conditions, the solar spectrum always presents a lack in blue when it reaches the ground.

Illuminants are theoretical radiations determined by their energy spectral distribution and used as references for real sources. In our colorimetry calculations, we use a D65 illuminant, the spectral distribution of which in the visible and in the ultraviolet corresponds to a daylight time with a color temperature of 6 504 K.

Colorimetry Notions

The Perception of Colors by Humans

Let us now study the aspect of the color perception process that is certainly the most complex; the eye response $V(\lambda)$ and its interpretation by the brain.

The human eye contains two kinds of receptors with very different properties. Cones, which possess a high resolution yet weak sensitivity resolution power/capacity, are mainly concentrated in the retina central area: the fovea centralis. They are both photometric and chromatic receptors allowing photopic vision and colored diurnal vision. Moving away from the retina center, one then encounters rods that are very dense at the periphery. Rods allow nocturnal scotopic vision. Those photometric receptors are highly sensitive, but do not perceive colors and only give an image in

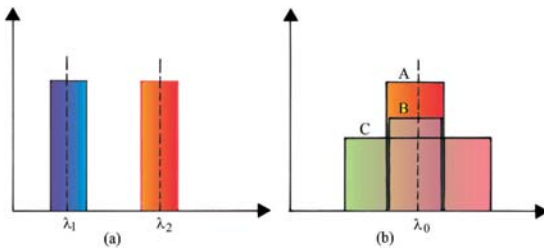


Figure 13.3. A color corresponds to a dominant wavelength: λ_1 or λ_2 . This does not necessarily entail that the wavelength is really present within the received spectrum, since two wavelengths can combine and thus produce the effect of a third one (a). For a given dominant λ_0 wavelength, light intensity can be more or less strong (A and B) and color more or less pure (C) according to the spectrum height and width respectively (b).

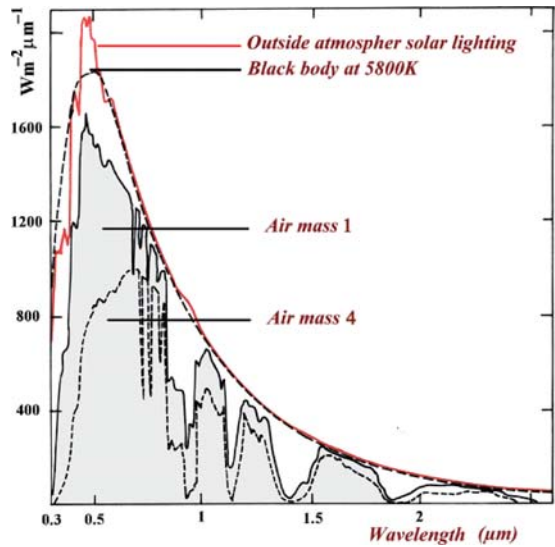


Figure 13.4. Monochromatic solar illumination in relation to the wavelength. Outside of the atmosphere, the solar spectrum can be modeled as the emission spectrum of a black body at 5800 K. At ground level, and according to the crossed air mass, it is slightly shifted towards red and presents numerous absorption bands by the atmosphere components. For an air mass of 4, spectrum intensity is substantially weakened and it is shifted towards red.

grey levels. The sensitivities of the two collectors differ by more than three orders of magnitude (and their spectra are shifted); the maximal sensitivity of cones peaks around 550 nm approximately (yellow-green), while that of rods peaks around 500 nm (at the limit between green and blue). Since the latter don't take part in color perception, the definition of the reference observer involves the response curves of the various cones only. There are three types of cones, each containing a pigment presenting a maximal sensitivity in a specific part of the spectrum: long (L), medium (M), and short wavelengths (S). Sensitivity maxima are situated respectively at 560 nm in the red, 540 nm at the yellow-green limit, and at 420 nm in the blue. These cones are sometimes designated by their predominant color: red (R), green (G), blue (B). These different types of cones are not distributed evenly on the retina, especially the blue ones that do not represent more than 2% of the fovea cones.

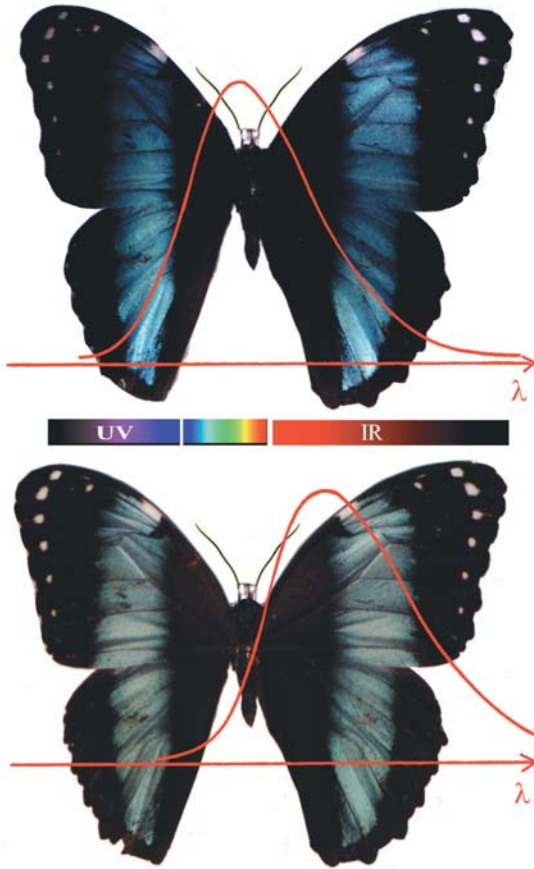


Figure 13.5. Influence of the source (spectral) distribution on colors; *Morpho helenor* 10 cm under daylight – air mass 1 – and illuminated by a tungsten lamp color temperature ($T \sim 2580$ K). The source irradiances have been normalized. The blue radiation decreases to a large extent and the big spots that slightly reflect other colors are gray and weakly bright.

Colorimetry Bases, Trichromy

It is almost possible to reproduce all spectral colors by superposing with adequate proportions three monochromatic radiations; it is the principle of additive trichromy. The colors established by the CIE are the red at 700 nm, the green at 546,1 nm, and the blue at 455,8 nm. The “RGB” system is based on them, but it is not the only possible combination.

Once the base has been determined, an appropriate unit system has been adopted, a visible electromagnetic radiation—determined by its whole spectrum in physics—can be, con-

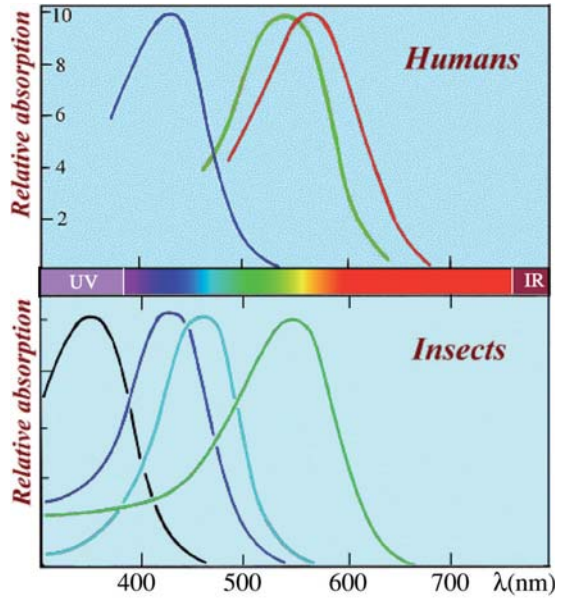


Figure 13.6. Cones relative absorption among humans and insects—normalized responses. Among humans, the green and red cones sensitivity curves overlap to a large extent, which suggests they are not mere chromatic captors. A red cone, for instance, cannot differentiate between a weak stimulation in the red and a stronger one in the green, because the signals transmitted to the brain can be of equal intensity depending on its sensitivity to the various wavelengths. It is by comparing the signals coming from red and green cones that the brain can make a distinction. The same phenomenon occurs among insects with blue and purple cones. They also possess a fourth type of cone that is sensitive to ultraviolet rays.

cerning its resulting color (Q), defined by the following relation using only three variables (R), (G), and (B):

$$(Q) = R(R) + V(V) + B(B) \quad (13-2)$$

where R , G and B are the amounts of primary colors contained in the mix, which also determine the stimulus chromacity and its intensity. These two last quantities are usually separated by normalizing the trichromatic components, i.e., by defining the proportion of each primary color in the mix.

$$\begin{cases} r = R/(R + V + B) \\ v = V/(R + V + B) \\ b = B/(R + V + B) \end{cases} \quad (13-3)$$

with:

$$r + v + b = 1 \quad (13-4)$$

The ratios r , v , b , are the trichromatic coordinates of color. As they depend on each other, a color can very well be defined by two coordinates and its luminosity or intensity.

The same approach applied to the energy of the monochromatic radiation $E(\lambda)$:

$$E(\lambda) = \bar{r}(\lambda)(R) + \bar{v}(\lambda)(V) + \bar{b}(\lambda)(B) \quad (13-5)$$

where r , g and b are the colorimetric coefficients, all the values of which for the various visible wavelengths are the base of the colorimetric functions of the RGB system. However, certain very pure colors sometimes prove impossible to reproduce through additive combinations of the three key colors. That is why the CIE suggested a new base in 1931: the (XYZ) system CIE 1931. Thus, the colorimetric functions $x(\lambda)$, $y(\lambda)$, and $z(\lambda)$ in the new system are always positive and the $y(\lambda)$ curve precisely fits the human vision curve. As in the RGB system, the $x = X/(X + Y + Z)$ and $y = Y/(X + Y + Z)$ reduced coordinates define the chromaticity of the color in a (x,y) plane, known as chromaticity plane, whereas the Y value, which is proportional to the visual intensity perceived, defines its intensity. For a given source defined by its spectrum $E_0(\lambda)$, the chromatic coordinates of an object with a reflectance $R(\lambda)$ are as follows:

$$\begin{cases} X = \int_{\lambda} E_0(\lambda)R(\lambda)x(\lambda)d\lambda \\ Y = \int_{\lambda} E_0(\lambda)R(\lambda)y(\lambda)d\lambda \\ Z = \int_{\lambda} E_0(\lambda)R(\lambda)z(\lambda)d\lambda \end{cases} \quad (13-6)$$

In a plane of equal intensity, the trajectory of monochromatic colors, purity equal to 1 (included in 380 to 780 nm, the theoretical limits of human vision) describes a horseshoe curve, the *spectrum locus* closed by a straight line, the *purple colors line*, characterizing the mixing between the two extreme colors of the visible spectrum. The coordinates of the perfect white (point O) are $x = y = 1/3$.

Any nonmonochromatic color is thus characterized by its position C in the chromaticity diagram.

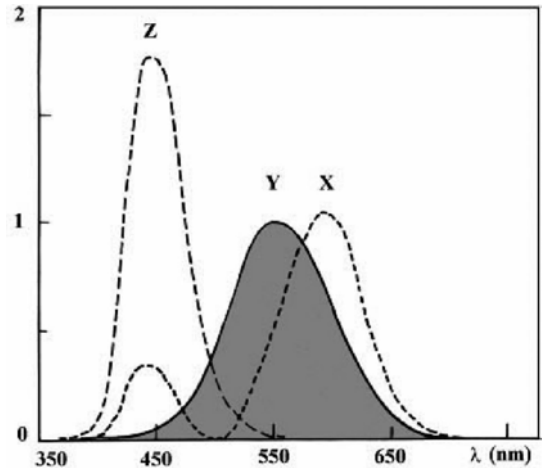


Figure 13.7. The 1931 CIE system X, Y, and Z components. The Y curve is equal to the average sensitivity curve of human eye.

- The color depends on the dominant wavelength λ_e , the value of which can be found by prolonging the straight line starting in the white and intersecting the (x,y) color coordinates up to the *spectrum locus*. Prolonging it in the opposite direction indicates the complementary color, if the intersection is on the *purple colors line*, the color determined by the predominant wavelength λ_e preceded by a sign.
- The purity is defined by the ratio $OC/O\lambda_e$.

Butterfly Vision

The anatomy of the extraordinary diverse photosensitive organs in animals is rather well known today. Yet, it proves more tedious to determine precisely the sensitivity of the cells composing these organs. One can still mention several established general ideas on the vision of butterflies and of reptiles and birds, their main predators.

Anatomy of Compound Eyes

Butterfly compound eyes consist of a great number—several thousands—of functional units: the ommatidia, which are hexagonal and arranged on hemisphere.

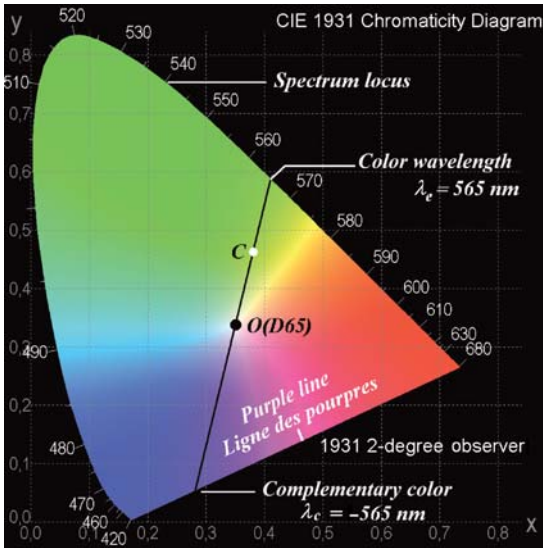


Figure 13.8. Chromaticity diagram. The color corresponding to a C point is determined by a dominant wavelength $\lambda_e = 563$ nm, a purity of 75%, and a complementary color, that is here situated in purples ($\lambda_c = -563$ nm). The Y tristimulus curve strictly corresponds to the eye sensitivity curve, and the Y value is directly proportional to intensity.

Ommatidia include three elements, listed here from the exterior to the interior. First, the corneal lens, a superficial dioptric device that is a small plane lens either convex or biconvex. Second, a conic crystalline lens fringed by pigmentary cells, which is extended by a third element, the rhabdom, a deep nervous device fringed by 6 or 8 visual cells, the retinula. Each cell presents a nervous fiber that transmits the nervous message of the excited pigment to the brain.

In apposition eyes of most of diurnal insects, each ommatidium receives the incident light under a very little solid angle only, oblique rays being absorbed by pigmentary cells, which also prevent light from entering next ommatidia. Resolution is high, but sensitivity is quite low. The compound eyes of many Lepidoptera, particularly *Papilionidae*, show on the corneal lens surface a quasi-periodic structure consisting of rather conic micro roughness, a hundred of nanometers in diameter and 200-nm high. The size of the latter being somehow inferior to visible wavelengths, with a size parame-

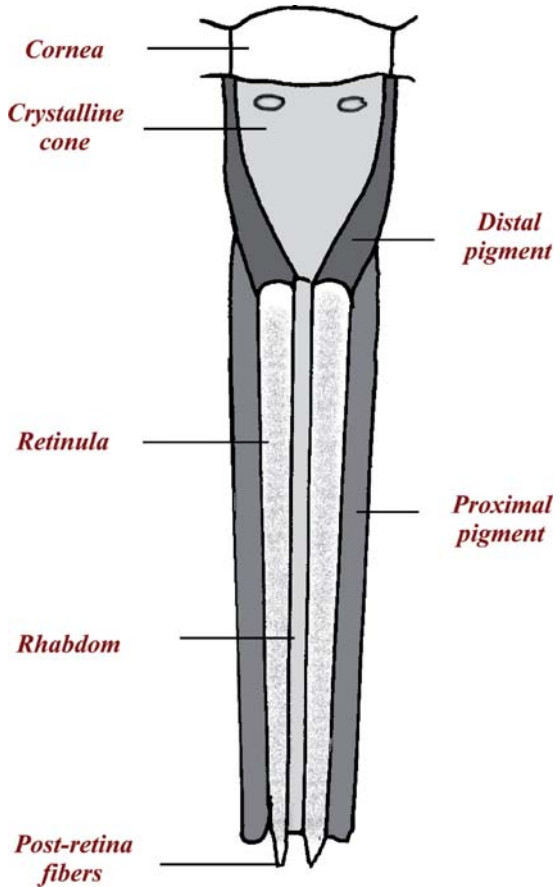


Figure 13.9. Schematized representation of an eye ommatidium by apposition.

ter around 1, are little scattering in this spectrum. We here enter the typical field of application of effective medium theories. This rough layer behaves, as concerns visible light, like an homogeneous layer with an index n_e that is

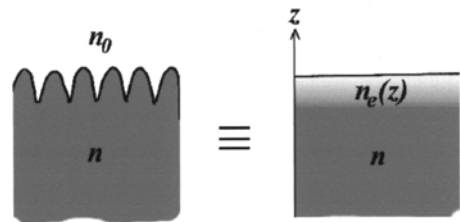


Figure 13.10. The corneule surface roughness create an index gradient serving as an anti-reflection coating at the air/corneule crossing.

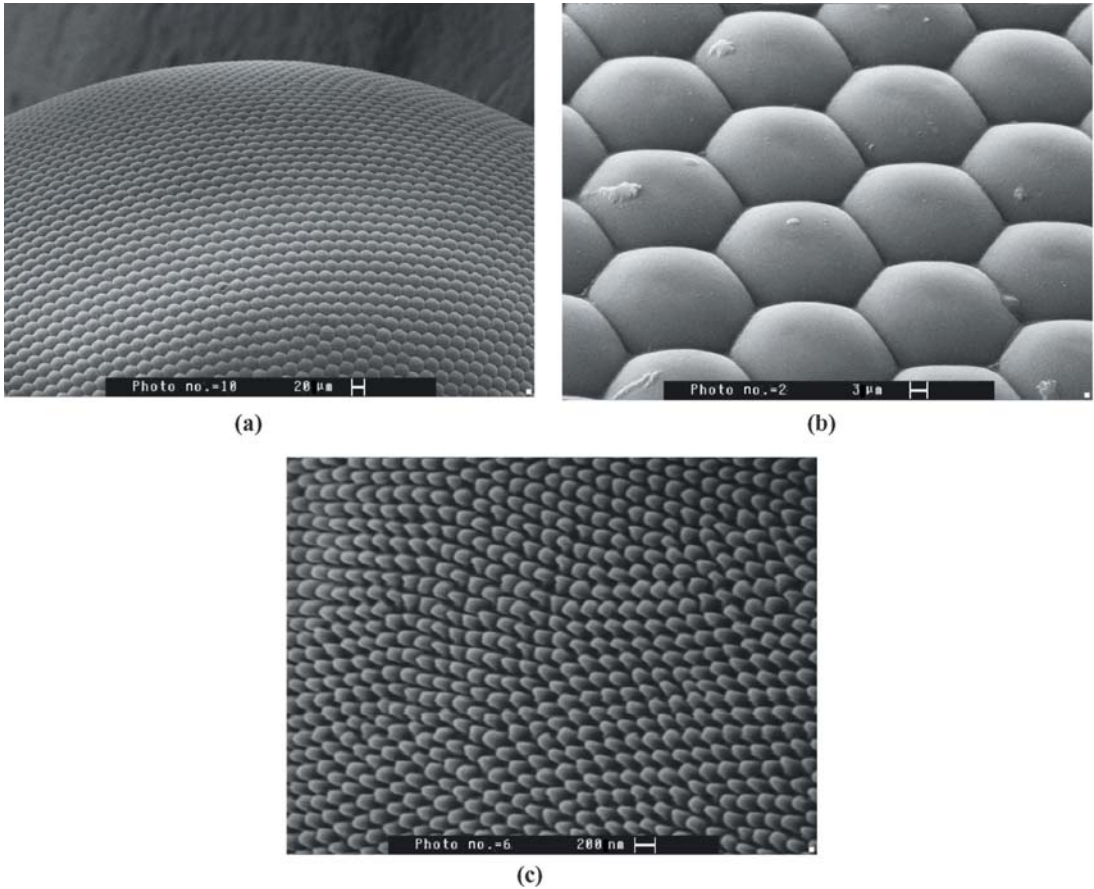


Figure 13.11. SEM general image and details of *Parnassius apollo* compound eye.

intermediary between that of air ($n_0 = 1$) and of the corneal lens ($n \sim 1,5$). This index, approximating 1,2, can be evaluated thanks to Maxwell Garnett's theory or through its approximation to neighboring indices. This effective layer behaves like an anti-reflecting coating, both allowing to reduce optical loss at the ommatidium entrance and to avoid reflections

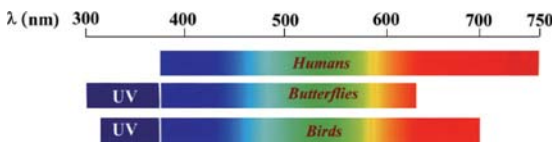


Figure 13.12. Comparison between the photoreceptors sensitivity spectra of humans, Lepidopterons, and Birds. The butterfly spectrum goes far beyond that of its main predators in ultraviolet.

that could reveal the presence of the insect to predators. These devices, known as “moth eyes structures,” are also used in the space industry.

How images are formed through such an optical device is complex and varies according to species. The apposition eyes, in each compound of which rays enter and give an independent signal, are distinguished from the superposition eyes of generally nocturnal species, in which rays can be combined on the same receptor. These eyes do not allow any focalization but are highly sensitive to motion. A fact that concerns us more is that butterflies can perceive colors well and that their sensitivity spectrum is shifted towards ultraviolet as compared to ours. They can therefore perceive on their fellow creatures motifs that are invisible to predators.

If the range of their spectral sensitivity is rather well known, the capacity of distinguishing colors among insects has only recently been established and precisely only on a small number, mostly bees. Studies applied to other categories are incomplete, not introducing any dramatic change. It is accepted that these species can perceive colors, yet the perceived color remains to be determined.

The majority of the observed Lepidoptera show four types of receptors (Figure 13.6) with rather wide sensitivity band (around 100 nm) respectively centered in ultraviolet (350 nm), blue (450 nm), blue-green (500 nm), and green-yellow (540 nm). At 350 nm, the UV peak is always narrower than the peaks observed in the visible. The visibility spectrum is thus on average shifted towards ultraviolet by around 100 nm in comparison to the human spectrum, a little less in comparison to that of birds, reptiles or arboreal amphibians, their main predators.

This gives them many advantages, among which for some of them is the ability to display—in spite of a similar cryptic or mimetic aspect in males and females in the visible—a strong sexual dimorphism in ultraviolet, thus allowing them to better recognize each other without any risk.

Some flowers, which are pollinated by insects, show also in the ultraviolet very bright distinctive marks due to the presence of flavones, which attract insects searching for nectar.

Perception of Polarized Light

As has been seen in the previous chapters, whatever the physical phenomenon involved, colors produced by structures are partially polarized. They are even more polarized when incident light is polarized. There are two important aspects involved in this problem: (1) Is natural light polarized? If it is, the polarization effects generated by the insect are amplified. (2) Are insects sensitive to this effect; in other words, can they distinguish between different polarization states?

(1) As has been seen in Chapter 10, the scattering of a wave leads to a partial polarization of light, except for the direction of incidence—

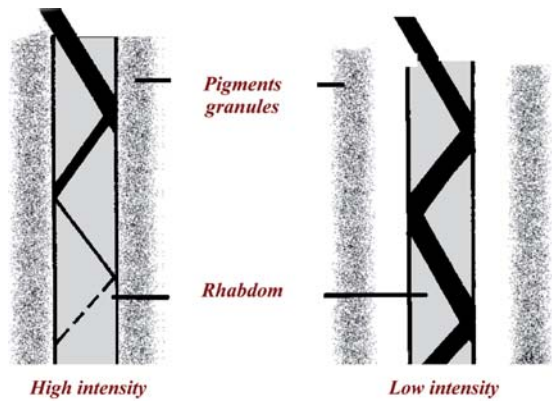


Figure 13.13. Axial or longitudinal pigmentary migrations along the rhabdome enable to adapt to various intensities. In the case of axial migrations, pigment granules are lining the rhabdome inner surface and absorb light during the different reflections. They get away from the surface when the intensity decreases.

transmitted and retro-scattered light—and the polarization direction is always perpendicular to the scattering plane. In this way, light coming from a clear blue sky, is always partially polarized, excluding certain neutral points—Babinet

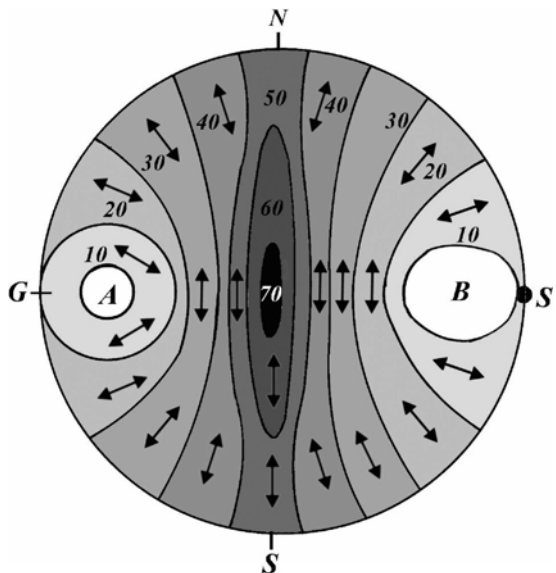


Figure 13.14. Isopolarization map of the sky at sunrise (S). The two nonpolarized areas above the sun and its image (G), are respectively known as Babinet point (B) and Aragon point (A). Arrows show the polarization direction of light.

point and Arago point—that are not always visible.

This has two important consequences. First, when the sky is clear, diffuse light falling on an object or an insect is polarized mostly perpendicularly to the scattering plane. The polarization rate can reach about 70% at 90° from the sun direction. According to the orientation of the insect or of the structure in relation to this plane, polarization effects by reflection on wings can be amplified, thus increasing the contrasts.

This also entails that a measurement of sky polarization can reveal the direction of the sun, even if it is hidden. It has been established that bees actually use this property to find one's bearings, and perhaps also by some big migrants like *Danaus plexippus*.

(2) Even if the study of insect sensitivity to light polarization is still far from being com-

prehensive, it is accepted that a great number of them can perceive polarization states. This perception is based on the variations in absorption of the electric field with its orientation. Indeed, it has been discovered that the absorption of some materials depends on the polarization states of the incident light, either rectilinear or circular. Known as dichroism, the phenomenon is caused by the shape of absorbing molecules, which are either elongated in a single direction or in spiral. A linear dichroism has indeed been discovered in the visual cells of rhabdomes in some insects, and orientation maps have even been established. It has thus been proved—even if their meaning remains obscure—that all polarization effects generated by the complex structures previously mentioned—can be perceived by most insects and therefore represent one more vehicle for visual communication.

Conclusion

Since its creation, the laboratoire d'optique des Solides, a CNRS-Pierre et Marie Curie University unitté mixte, has focused on the study of optical properties of inorganic solids, first on metals, and later on semiconductors, dielectrics, and inhomogeneous materials. Nothing to do with butterflies indeed. And yet, the further we study wings, the more similarities we find. Or rather, we realized how much butterflies were ahead of us concerning optical phenomena. They in fact proved to conceal all that concerned us: dielectric multilayer, scatterers, selective materials, disordered media—and that only concerns wings: all subjects that we were studying. In this way, butterfly wings became quite naturally part of our research. Materials are new, yet structures are traditional. Our research resulted from a passion dating back to my childhood and a definite industrial request.

Within the framework of a prospective research on the fabric of the future, we were asked about the origin of iridescence among butterflies and its possible application to textiles. The answer to the first question is the topic of this book. It didn't reveal more complex, yet it proved to be more diverse than expected. As concerns the application to fibers, and even garments, represents a real challenge, even independently from any technical creation. It is worth mentioning the method. As the introduction was dedicated to the butterfly, so the conclusion has to be. One thus starts by defining precisely the optical properties of a plane multilayer. It is then rather easy to optimize the system, based on the materials available for textiles, in order to obtain a greater iridescence.

Let us first describe the traditional structure of a fabric. Its basic component is fiber—synthetic in the present case. It is a long fiber, usually about 10 nanometers in diameter, composed of various more or less long polymer chains, the nature and arrangement of which determine the mechanical properties of the fiber. It is on this fiber that the optical structure generating iridescent colors are produced. These fibers are then gathered in a varying number—usually 60—and form the thread that is woven or knitted to create fabric. During the various stages, one can notice that the basic element supporting the very irregular optical structure is subjected to numerous distortions at extremely different scales. The fiber curving rays, for instance, can be measured in tens of micrometers when twisted into a thread, and some millimeters once woven. Finally, the creases in the finished garment present distortions measured in centimeters.

The main difficulty is then to model, or at least evaluate, the evolution of the optical properties at these various scales. Physical phenomenon involving elements occurring at different scales are among the most complex. In fact, it is to them that one is confronted when one wants to evaluate the visual effects of a garment, the iridescent colors of which—generated at the smallest scale and imposing a strict order—are modulated by local entropies of increasing scales. The solution we chose is directly inspired by *Urania* scales. It consists in distributing over the fiber as it is being woven, a certain number of thickness and index layers corresponding to a given color. Calculations show that this number actually does not need

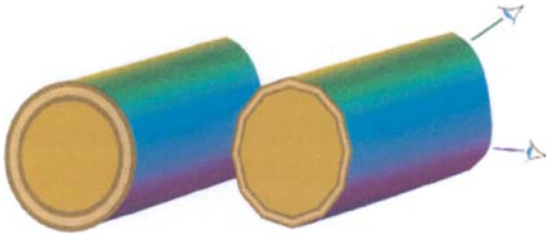


Figure C.1. Transition from a plane multilayer to a cylindrical multilayer. One actually models a polygonal-section fiber. If the number of facets is big enough, their width is inferior to the eye resolution limit.

to be excessive. Manufacturing process and other various constraints impose a minimal thickness—around 100 nm—and specific materials. The optical index that are available are included between 1.4 and 1.7. One can therefore determine the multilayer parameters—thickness and index—which generate an optimal iridescence centered on a given color. By modifying these parameters as well as the number of layers, one can increase or decrease as one wishes the luminosity, color purity, and iridescence amplitude. It proved that a mere piling of two or three layers can produce the effect that is wanted.

Difficulties start at this point. The first is geometric and consists in passing from the plane multilayer on which calculations were based, to the same multilayer arranged on a cylinder, i.e., the fiber. The simplest way is to assimilate/compare the fiber circular section to a polygonal section. The fiber thus doesn't consist of a continuous cylindrical surface anymore, but of facets. For a 11,5- μm total diameter—fiber + multilayer—we divided the section into 5° angular sectors; that is 72, 0,5- μm wide facets. If one considers an isotropic diffuse lighting, one can determine the light spectra reflected into a given direction by each facet and also the characteristics of the observed color, by taking into account shadowing effects and possible multiple reflections proceeding from neighboring facets. Simulations reveal that passing from plane to cylinder doesn't affect much the iridescence amplitude, nor the purity of the resulting colors.

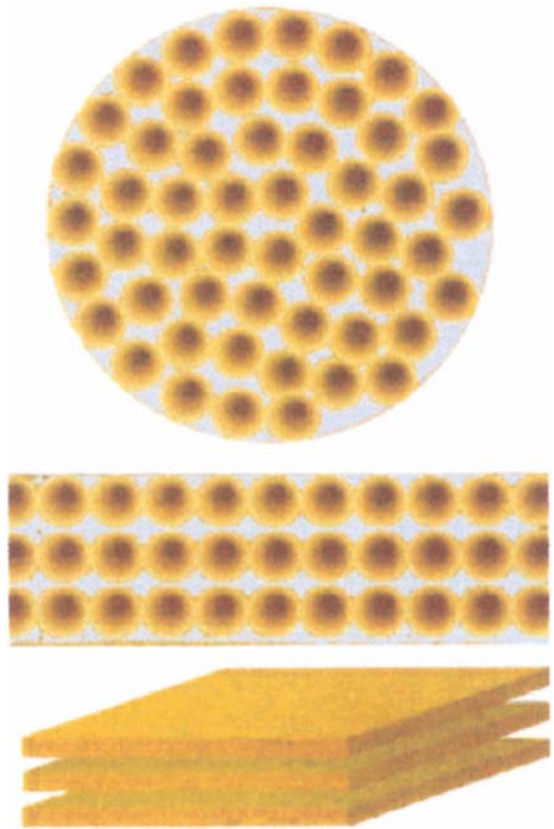


Figure C.2. Modeling of a thread. Fibers that are randomly disposed in the thread are arranged as planes in the model. These “inhomogeneous” planes are then assimilated to continuous planes.

One then has to determine and characterize the effects that can occur when fibers are twisted to form a thread. The resulting disorder and the system geometry require drastic simplifications, the consequences of which are difficult to evaluate. With an approach quite similar to that adopted to model *Morphos* optical properties, one can model the thread as a regular piling of fibers lining on one plane and separated from the other pilings by a very thin layer of air. Calculations thus predict a dramatic increase in intensity—which has yet to be somehow relativized—due to the perfect piling of fibers, which is produced only locally in a real thread. If the amplitude of iridescence is little affected from one scale to the other, the second predicted phenomenon—a significant decrease in color purity—is less encouraging. The effect

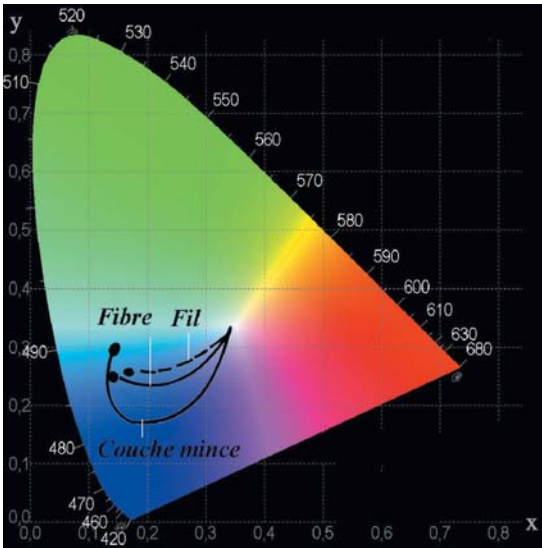


Figure C.3. Iridescence variations during the first stages of modeling of cloth. Iridescence amplitude hardly varies, but the purity systematically decreases, especially as concerns central colors.

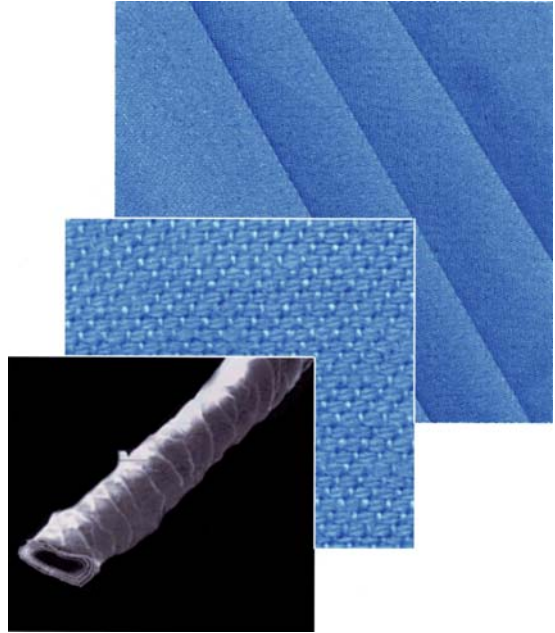


Figure C.4. From the structured fiber to cloth, passing through meshes . . .

of the weaving and knitting of threads has not been modeled, yet one can also expect a loss in purity as far as it is concerned.

Are these approximations relevant, and is it worth it in the end? In order to answer such questions, one needs a reference, which butterflies can provide. Indeed, the comparison between wing and garment is more relevant than it seems. One thus finds quite precisely the same size scales and the same structures in both of them. As has been seen among *Morphos*, for instance, the optical structure is present on striae, covering the scale surface in hundreds, the typical size of which approximates some micrometers—like fiber. Among other butterflies, the optical structure is situated on the very scales surface. Like in a thread, scales average 100 μm and are regularly distributed on the alary membrane just like in weaving. Moreover, the membrane can be measured in cm^2 and includes various creases, undulations, and irregularities typically measured in millimeters. Since the structures and size hierarchies are similar in both cases, one can expect that colored effects will also be similar.

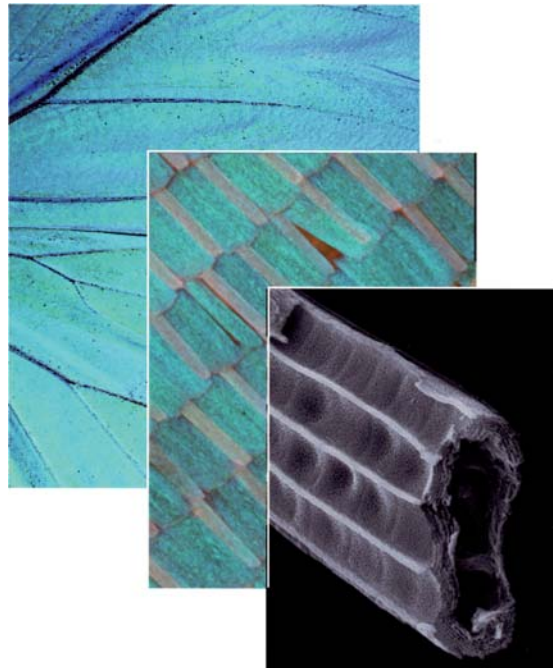


Figure C.5. Steps and scales are similar among butterflies, from their structured scales to their wings.

When one compares the experimental iridescence curves of a *Morpho* and the calculated ones of an iridescent fabric modeled as above, they appear quite similar. Butterfly colors which seem so bright to us, are in fact not so pure. Therefore, a purity equal or little inferior to that of butterflies would be quite acceptable for fabric.

The technical difficulties have been partially overcome in Japan, for instance, where such iridescent fabrics are starting to be produced. Another question and another debate would be to what extent one would be ready to wear these changing colors.

Another example of biomimetic transfer is the production of colored effects due to polarization. One of the main applications would be the marking of bank notes, cards, and so on in order to identify them and guarantee their authenticity. The inspiration now comes from *papilio* and *Cincideles*, which is to say insects presenting concave interferential structures on their wings. As has been seen, in such structures, the interferential color observed is a compound color resulting from the mix of the little polarized one produced by the basin bottoms and that generated by the inclined edges, which reveals highly polarized after being polarized twice. In this way, there should be a way of modifying color by suppressing the second component thanks to a mere polarizer. This is almost impossible to perceive on insects because structures are generally symmetric. There are as many horizontal as vertical edges and the colors reflected by these edges are polarized perpendicularly to one another, which implies that there is no global polarization of the component. Yet, one just has to break the symmetry by producing grooves rather than basins in order to maximize the effect.

One must have a few notions on bank note protection in order to fully understand this approach. Each bank note consists of a certain number of elements ensuring protection at three different levels corresponding to three types of users. Level 1 protections must make anybody in the street or in a shop be able to recognize without any equipment the authenticity of the bank note. This involves various motifs,

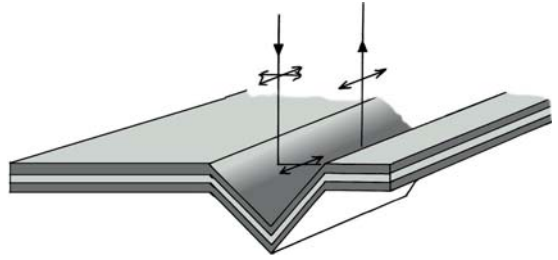


Figure C.6. Evolution of the polarization of a wave subject to a double reflection in a groove under an incidence close to the Brewster incidence. The emergent wave can be Transverse Magnetic polarized over more than 80%.

colors, papers, watermarks, and holograms. The second level of protection requires quite simple equipment and concerns shopkeepers and cashiers. It implies concealed properties, such as ultraviolet ones or even polarization ones like in the case concerning us. Level 3 protection involves all the physicochemical properties of the bank note, which can only be demonstrated in a laboratory by using cumbersome equipment and therefore only concerns central bodies.

Once their symmetry broken, the effects produced by *Papilio* and *Cincidele* structures can bring an original answer to the problems that the first two levels entail. One can on the one hand generate bright iridescent colors fulfilling the level 1 protection requirements and on the other hand, create chromatic effects depending on polarization that correspond to the level 2 protection.

One can roughly imagine the process as follows. Colored motifs are composed of grooved and flat areas that are juxtaposed and form a drawing or a sign. All the areas contain in their thickness a multilayer structure producing a high iridescence. As they are not illuminated under the same incidence, the grooved and flat areas generate different interferential colors. Under near-normal incidence, the light reflected by flat areas is hardly polarized, whereas that of grooved areas is highly polarized. The groove period must be inferior to the eye resolution in order that these areas appear perfectly homogeneous. For an observer standing some 20 cm away from the bank note, it

requires a width of 60 μm , which one can easily create.

One can then calculate the colorimetric properties of these areas, as well as their iridescence and polarization states under various incidences by considering the shadowing effects proceeding from grooves. The approach is quite similar to that adopted for fabric; so we won't describe it further. Let us only mention that one should not expect to obtain a totally polarized light with such a process and that the contrasts between areas won't be maximal. The Brewster angle, which, as has been seen, depends on the two dioptric materials index, is not determined by one multilayer anymore—as indices and incidences vary from one layer to the other. The p polarized light still presents a minimum for a “pseudo” Brewster angle for which the reflected wave is highly polarized—sometimes up to 80%. Different visual effects can be imagined thanks to this device. Here are a few examples. The one resembling *Papilio*s and *Cincideles* the most is the succession of grooves and alternated planes of the same width. This results in a compound color, one of the components of which can be suppressed to modify the color by using a polarizer. The motif color can thus vary from green to yellow by either suppressing or letting enter the blue component reflected by multilayer grooves that reflect yellow under normal incidence. Another original method consists in using only grooved areas that are perpendicular to one another. Without a polarizer, they show the exact same color, but when perpendicularly polarized, only one or the other appears, thus making concealed motifs emerge by observing them with a polarizer.

Let us now put aside the potential applications of the present research and introduce a completely different matter. In the past and more or less successfully, butterflies inspired poets, and now engineers. In fact, after striving to invent everything from scratch for decades, we are now coming back to nature to show us new paths. We were in the present book only concerned with optical properties of wings—gratings, Bragg mirror, diffractive optics, spectral selectivity, disorder—and butterflies proved to be real high-tech laborato-

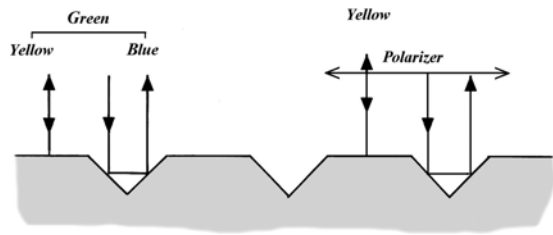


Figure C.7. A colored effect linked to the polarization of one of the components. By suppressing a large part of the blue component with a polarizer, one can make the general green color turn yellow.

ries in this field! And our brief remarks outside the main track, especially compound eyes, showed that such elements have many surprises in store.

Yet above all, butterflies proved to be great a vehicle for teaching physics, and as concerns us, optics. This new and quite unusual theme

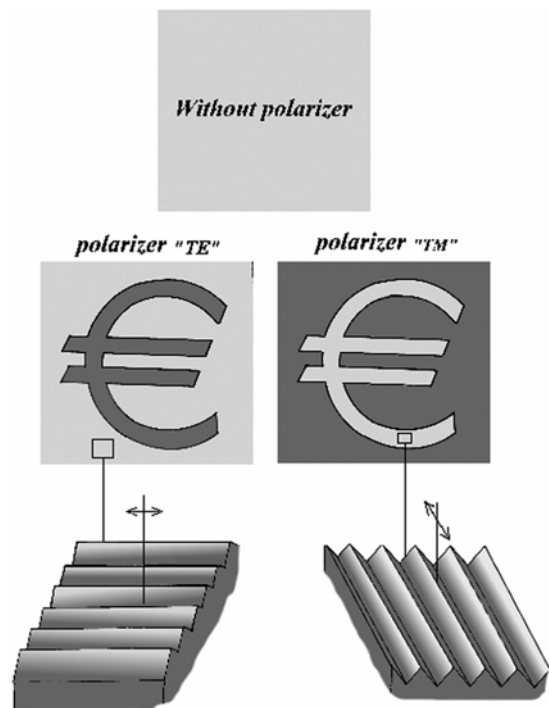


Figure C.8. When one uses grooved areas only, they present the same color under natural light and it is impossible to distinguish motifs. They can become apparent by using a polarizer. TE and TM are relative to the central motif structures.

was started prudently, yet pupils quickly took an interest in it—from middle school interns, who thought it was impossible to work seriously with this material, to high school science juniors and seniors, who discovered (better late than never) a totally different aspect of physics. They would thus attend conferences on butterflies, sometimes several hours long, without showing impatience, and I would even say with a certain enthusiasm...and at the end, they would realize they had actually studied physics for four hours. The interdisciplinary study of butterflies proved a success in high school, and a great way of introducing physics. We wished these bridges between different subjects could be implemented in universities—this modest first experiment in high school being quite encouraging. This is in fact worth describing it. Launched between biology and physics via butterflies, the experiment could very well be applied to any other organism that is a little popular according to me—shells, beetles, and, during spring months, grasshoppers, maybugs, or flowers—and between any subjects: thermodynamic, mechanics, chemistry, mathematics, and even arts or music. I had the good fortune to meet a biology and a physics teacher who agreed to adapt classes and dedicate some time to implement the project together. It entailed changing the traditional schedule of one-hour physics class and a break followed by a one-hour biology class. So, we asked pupils to resolve a complex interdisciplinary problem: How and why do butterflies present such colors? This requires quite simple experiments that anybody can carry out: a piece of red wing is dipped into acetone (nothing happens), a piece of *Morpho*

blue wing (it immediately turns green, then blue again when dry). The same experiment performed on a blue Argus results in the disappearance of blue without the green stage! The three main sources of colors in the living world have thus been experimented. Then, a group observes and carries out the same experiments by using an optical microscope, modifying incidence, while another group researches the various origins and properties of light. These classes went out, to discover in museums how it works among birds, shells, stones, and so on. When they realized that iridescence could not be generated by the striae they had observed with the optical microscope and that they had to change the scale once again, we organized several scanning electron microscopy sessions at the university. The resulting pictures were then studied in high school: to have a class count the diffusing particles of a Cabbage Pieride is worth any image-processing software...

In the end, these pupils who tend to consider physics as one of the most boring subjects discovered physics and basic optics notions via a more appealing subject like biology. Notions that they will be less reluctant to study further in class. For instance, they “saw” a wavelength and evaluated its length for the first time. Better still, the experiment showed them the advantages of interdisciplinary studies, how interfaces enrich one another, but also how jargons could represent a barrier between two communities. May they persevere in this path, and always remember this “new butterfly effect.” And may this book guide them. I would be very proud. It would be my best achievement.

Subject Index

Cetonia aurata, 44
Charaxes jasius, 19f
Chrysidia madagascariensi, 72, 73

Danaus plexippus, 150
Dynastes hercules, 55

Eupholus humeralis, 115f
Eupholus sulcicollis, 115f

Hoplia argentea, 84

Melitea phoeba, 15f
Morpho cypris, 101, 102
Morpho menelaus, 89

Morpho menelaus, 91, 94, 95, 101, 102
Morpho sulkowskyi, 105
Morpho zephyritis, 101, 102, 105

Notasacanta dorsalis, 55

Ornithoptera priamus poseidon, 18f, 30f

Papilio blumei, 54f
Papilio paris, 80f, 81f, 82
Papilio ulyse, 53f, 82
Parnassius apollo, 20f, 24f
Phaleanae Biston betularia, 09

Urania leilus, 72, 73

General Index

- 2-dimensional structures
 - type butterflies with, 88
- adult butterfly
 - body of, 19
- alary cells
 - median axis of, 26
- alary membrane, 31, 33, 92, 93, 95
- amorphous phase, 67. *See also* development of butterflies
- androconia scale, 34
- angle of incidence, 53, 71
- aniline
 - thin films of, 03
- anisotropic material, 59
- apetetic colors, 10
- archaeoprepona, 27, 138, 139
- archoeprepona, 36, 53, 131
- arthropods, 40, 42
- articulated legs
 - pair of, 18
- atomic force microscopes, 56
- auxochrome, 128
- batesian mimicry. *See* camouflage
- biliary pigments, 130, 133
- biotypes, 07, 23
 - infinite diversity of, 07
- Biston betularia*, 09
- blue pigments, 04, 53
- brewster incidence, 58, 59, 77
- butterflies
 - absorption of solar energy by, 06
 - biomimetic applications of, 05
 - development of, 15
 - diurnal and nocturnal, 14
 - high reproductive rate of, 04
 - interior temperature of thorax, 08
 - optical phenomena in, 42
 - repelling taste of, 10
 - vision, 146
- camouflage, 4, 8, 9, 10, 15, 55
- caterpillars, 9, 15, 18, 40
 - ingestion of soot by, 09
- cathedrals, 64
- cephalopodes, 55
- Cetonia aurata*, 44, 48
 - circular polarization, 82, 85
- Charaxes jasius*, 19f
- chirality, 43
- chitineou layers, 31
- cholesteric phase, 43, 44
- chrysalis development stage, 15, 30
- Chrysiridia madagascariensi*, 72, 73
- Cicindelidae*, 40, 44
- circular polarization, 82
- Cithaeria menander*, 30f, 31f
- Coleoptera, 40, 41
 - cuticle of, 40
 - life cycle of, 41
 - scales of, 41
 - study of, 56
- colors, insects, 26
 - color perception, 142–143
 - colored effects, 77
 - colored motifs, 28
 - cryptic colors, 135
 - palette of, 07
 - protection provided by, 08
- compound eyes
 - anatomy of, 146
- crystalline material
 - intra-band transitions of, 04
- Curculionidae*, 48, 112, 115. *See also* Coleoptera
- cuticle
 - structure of, 41
- Danaus plexippus*, 150
- de effective electric displacement, 63
- dephasor, 85
- depolarizing factor A, 65
- development of butterflies, 15
- dielectric function, 63, 64
- diffraction
 - hypotheses of, 03
- diopter, 68
- Dynastes hercules*, 54, 55

- ecologic context, coloration, 07, 08
 edible butterflies, 08
 effective index, 63
 electromagnetic field
 vector nature of, 58
 electronic microscopes
 scanning and transmission, 56
 elliptic polarization. *See* circular polarization
 elytron wings, 71
 embryonal stage, 15
 endocuticle, 44
Eupholus humeralis, 115f
Eupholus sulcicollis, 115f
 exocuticle, 83f
- fluorescence phenomena, 49
 frenulum, wings passive device 19
 frivolous symbolism, 01
- goniochromic structures, 54
Grapium weiskei, 16f
- haemocyanin, 53
 haemolymph messages, 22
 hard sciences, 01
 hatching, 26
Hebonia gloeippe, 52f
 helicoidal structure, 42
 heterotherm insects, 08
Hoplia argentea, 84
 hydrochromic structures, 55
 Hymenoptera, 14
- imago, 15, 18
 incidence
 angles of, 03
 industrial melanism, 09
 insects
 classification of, 05
 electromagnetic properties of, 06
 photonic crystals, 115
 standard bearers of, 04
 integument
 surface of, 55
 interstriae spacing, wings, 38
 intra-band transitions, 04
 ionic crystals, 60
 iridescence, 54
 isochromy, 10
- Jones vector equation, 59
- Kosciuscola*, grasshopper, 55
 Kramers-Kronig equations, 31
- Larval/nymphal stages, 15
 Lepidoptera, 14, 16
 pigments, 129
 protective strategies of, 12
- leucopterines, 55
 linear polarization, 57, 59
Lycaenidae, 03, 133
- mandrills
 muzzle of, 03
 Maxwell equations, 57f
 Maxwell, J. C., 56
 melanins, 129
 melanism phenomena, 09
Melitea phoebe, 15f
 metallo-protein pigments, 53
 metals
 colloidal suspensions of, 64
 metamorphosis, 01. *See also* development of
 butterflies
 earth to ether, 01
 passage, 01
 Michelson, A. A., 2, 3, 56, 62, 86
 Mie's treatment, 119
 mimicry
 basic principles of, 11
 modalities of, 10
 mullerian mimicry, 110
Morpho cypris, 101, 102
Morpho diffraction maps, 2, 4, 36, 38, 39, 50, 51, 55, 65, 72, 88
Morpho menelaus, 89
Morpho menelaus, 91, 94, 95, 101, 102
Morpho sulkowskyi, 105
Morpho zephyritis, 101, 102, 105
Morphos Adonis, 108
 mullerian mimicry, 110
 multilayer, structural scales, 49
 various Types of, 71
- N-acetylglucosamine
 monomers of, 42
Notasacanta dorsalis, 55
 nymph, development stage
 diapause, 18
 shedding, 30
- oligopod, 40
 olympic gods, 01
 ommochromes, 131
 one-dimensional crystals, 66
 optics
 optical index, 63
 optical properties
 study of, 60
 optical recognition, 07
Ornithoptera priamus poseidon, 18f, 30f
 orthonormal reference, polarization, 59
- Papilio blumei*, 54f
Papilio paris, 80f, 81f, 82
Papilio ulyse, 53f, 82
 papiliochromes, 132

- papiliochromis, yellow, 27
- Papilionidae*, 79, 81, 134, 147
- parasemantic colors, 10
- parasitism, 12
- Parnassius apollo*, 20f, 24f
- peduncle, 48
- pheromones, 07
- photonic crystal, 65
- physico-chemical origins, 10
- Pieridae*, 67, 100, 109
- pigment, 4, 7, 16
 - scattering with, 04
- pigmentary effects, 93
- pigments
 - interference/diffraction effects, 51
- Plan Diopter*, 68
- plane grating, diffraction, 86
- polarization, 83
 - matrix approach to, 59
 - polarization effects, 114
 - polarization of light, 149
 - measurement of, 150
 - polaroid films, 56
- polymorph mimicry, 13
- polynomial expression, 62
- polypod, insect larvae, 40
- predators, 13
- Prepona*, 72, 78
- procuticle, cuticle structure, 41
- pseudo-semantic, colors, 10
- pterobiline pigment, 134
- pterotecae wings, 30
- pupal stage. *See* chrysalis development stage

- Raleigh, Lord, 03
- relative immunity, 12
- rotator structure, 60

- saturnides*, 14
- scales
 - morphologies, 29
 - nomenclature attempt, 29
 - structures, 29
- Scarabeidae*, 48, 84

- scattering structures
 - butterflies with, 123
- selective reflection hypothesis, 03
- semantic colorations, 10
- sexual recognition, 08
- solar spectrum, 08
- solid state optics
 - notions of, 06
- specular reflections, pigments, 49
- structural origin, colors
 - defenders of, 03

- tetrapyrrolic pigments, 53
- thermochromic structure, 55
- tiger beetles. *See Cicindelidae*
- tillard's system, 24
- tissues
 - differentiation of, 15
 - reconstruction of, 15
- toxic compounds, 07
- tropical butterflies, 53

- ultraviolet
 - iridescence in, 109
- Urania leilus*, 72, 73
- Uraniidae*, 14, 72, 73

- vegetal cellulose, 42
- venation, 22
- visible spectrum
 - splitting of, 04
- visual camouflage
 - the art of, 08

- Walter, B., 03
- wings
 - anterior wings, 10, 19, 31
 - extensors and abductors of, 08
 - macroscopic level, 22
 - odoriferous roles, 29
 - posterior wings, 10, 13, 14
 - radiation qualities of, 06

- X-chrome, 53
- ω 0 frequencies, 61